Dissertation zur Erlangung des Doktorgrades
der Fakultät für Chemie und Pharmazie
der Ludwig-Maximilians-Universität München

Investigations on Oxygen Rich Materials as Possible High Energy Dense Oxidizers

Sebastian Franz Rest
aus
Bad Tölz

2015

Erklärung

Diese Dissertation wurde im Sinne von §7 der Promotionsordnung vom 28. November 2011 von Herrn Prof. Dr. Thomas M. Klapötke betreut.

Eidesstattliche Versicherung

Diese Dissertation wurde eigenständig und ohne unerlaubte Hilfe erarbeitet.

München, 21.08.2015

Sebastian Franz Rest

Dissertation eingereicht am 21.08.2015

1. Gutachter: Prof. Dr. Thomas M. Klapötke

2. Gutachter: Prof. Dr. Konstantin Karaghiosoff

Mündliche Prüfung am 14.10.2015

„I love when a plan comes together“

Hannibal Smith

Dedicated to

my whole family

Acknowledgements:

First and foremost I would like to express my thanks to Professor Dr. Thomas M. Klapötke, for giving me the opportunity to work on my PhD thesis within his group.

I am indebted to Professor Dr. Konstantin "Conny" Karaghiosoff for being available as the co-referee of this thesis. I am very thankful for numerous evenings which he spent at the X-ray measuring the endless numbers of half spheres.

I'm also indebted to Professor Dr. Wolfgang Beck, Prof. Dr. Andreas Kornath, Professor Dr. Ingo-Peter Lorenz and Professor Dr. Manfred Heuschmann for being available as examiners in my defense.

I would also like to thank Ms. Irene S. Scheckenbach for being the best secretary in the world, for her help with every kind of forms and bureaucracy.

In detail I would like to express my thanks to:

- Dr. Burkhard Krumm for the great support, all over the years, correcting my papers, the great time in the „Ionen-Lotto" courses, for checking this dissertation and for the supply with "Mirabellen". I hope we could improve his skills in the native Bavarian language during my time in the group.

- Dr. Xaver Steemann for introducing me into the chemistry of explosives, being a great friend and for his wise advises prior to the start of this dissertation (e.g. stress reduction in the basement of the department), which helped me to finish this work successfully with adequate effort.

- Dr. Niko Fischer (Finch) for the continuous support with Bavarian specialties („Wurst" and „Geräuchtertes") and for one of the most challenging mountain tours I've ever made.

- Dr. Richard Moll for a unforgettable time in the Lab D 3.100, being a great collegue and friend all over my time in the group and for taking care of our lab mates with the "BAM-Schnaps".

- Dr. Anian Nieder, Dr. Alexander Dippold, Dr. Marcos Kettner and Dr. Karina Tarantik is thanked for the gorgeous help with the distillery project which

meanwhile bears great fruits.

- The great team of D3.100 Quirin Axthammer, Regina Scharf Michael “Hasi” Weyrauther, for the all time great atmosphere in our lab, the many interesting discussions, coffee & cake breaks and for keeping the “Rat”-lab tidied up.

- My F-students and Bachelor students Anna Erbacher, Veronique Sproll, Andreas Baumann and Martin Reynders for their enthusiasm, interest, many great results and a very great time.

- Dr. Camilla Evangelisti for all her help with theoretical calculations, the great espresso powder and Salami from Italy and for her authentic Italian temperament.

- Stefan Huber for measuring sensitivity values of countless samples and for the supply with weird chemicals.

- The whole work group and all the friends in the chemistry department. Thank you all for a very great time! Above all, I would like to say “thank you” to my parents, my family and my girlfriend Patricia who never stopped believing in me and for their continuous support in every aspect of my life.

I can’t describe in words how grateful I am!

Table of Contents

List of Schemes ..... **V**

List of Figures ..... **VII**

List of Tables ..... **XI**

1. Introduction

1.1. Definitions & Background 1

1.2. Gun Propellants 3

1.3. Rocket Propellants and Motors 4

1.4. High Energy Dense Oxidizers 8

1.5. Motivation and Objectives 13

1.6. References 14

2. Multiply Nitrated High-Energy Dense Oxidizers derived from the Simple Amino Acid Glycine

2.1. Abstract 15

2.2. Introduction 16

2.3. Results and Discussion 17

2.4. Conclusion 35

2.5. Experimental Section 36

2.6. Acknowledgement 46

2.7. References 47

3. The Energetic Nitrocarbamate $O_2NN(H)CO[OCH_2C(NO_2)_3]$ Derived from Phosgene

3.1. Abstract 51

3.2. Introduction 52

3.3. Results and Discussion 53

3.4. Conclusion 68

3.5. Experimental Section 69

3.6. Acknowledgement 74

3.7. References 75

4. Asymmetric fluorodinitromethyl derivatives of 2,2,2-trinitroethyl N-(2,2,2-trinitroethyl)carbamate

4.1. Abstract 77

4.2. Introduction 78

4.3. Results and Discussion 80

4.4. Conclusion 93

4.5. Experimental Section 94

4.6. Acknowledgement 101

4.7. References 102

5. Polynitro containing energetic materials based on carbonyldiisocyanate and 2,2-dinitropropane-1,3-diol

5.1. Abstract 105

5.2. Introduction 107

5.3. Results and Discussion 109

5.4. Conclusion 119

5.5. Experimental Section 120

5.6. Acknowledgement 126

5.7. References 127

6. Fluorodinitroethyl Orthocarbonate and Formate as Potential High Energy Dense Oxidizers

6.1. Abstract 131

6.2. Introduction 132

6.3. Results and Discussion 134

6.4. Conclusion 144

6.5. Experimental Section 145

6.6. Acknowledgement 150

6.7. References 151

7. (2-Fluoro-2,2-dinitroethyl)-2,2,2-trinitroethylnitramine, a possible high energy dense oxidizer

7.1. Abstract 155

7.2. Introduction 156

7.3. Results and Discussion 158

7.4. Conclusion 169

7.5. Experimental Section 170

7.6. Acknowledgement 175

7.7. References 176

8. Summary 179

9. Appendix

9.1. Supporting Information for Multiply Nitrated High-Energy Dense Oxidizers derived from the Simple Amino Acid Glycine 183

9.2. Supporting Information for Asymmetric fluorodinitromethyl derivatives of 2,2,2-trinitroethyl N-(2,2,2-trinitroethyl)carbamate 185

9.3. Supporting Information for Polynitro containing energetic materials based on carbonyldiisocyanate and 2,2-dinitropropane-1,3-diol 188

9.4. Supporting Information for 2-Fluoro-2,2-dinitroethyl 2,2,2-trinitroethylnitramine, a possible high energy dense oxidizer 193

List of Schemes

2. Multiply Nitrated High-Energy Dense Oxidizers derived from the Simple Amino Acid Glycine

Scheme 2.1 Reaction sequence for the synthesis of compounds **4** and **5** as described by Feuer et al. 17

Scheme 2.2 Synthesis of compounds **6–10** 17

3. The Energetic Nitrocarbamate $O_2NN(H)CO[OCH_2C(NO_2)_3]$ Derived from Phosgene

Scheme 3.1 Synthesis of 2,2,2-trinitroethyl chloroformate (**1**) 53

Scheme 3.2 Synthesis of 2,2,2-trinitroethyl carbamate (**2**) and 2,2,2-trinitroethyl nitrocarbamate (**3**) 54

4. Asymmetric fluorodinitromethyl derivatives of 2,2,2-trinitroethyl N-(2,2,2-trinitroethyl) carbamate

Scheme 4.1 Synthesis of the compounds **2–3** *via* **1** 80

Scheme 4.2 Synthesis of the compounds **4–5** 81

5. Polynitro containing energetic materials based on carbonyldiisocyanate and 2,2-dinitropropane-1,3-diol

Scheme 5.1 Polynitro containing compounds based on carbonyldiisocyanate 109

Scheme 5.2 Polynitro containing materials based on 2,2-dinitropropane-1,3-diol 110

6. Fluorodinitroethyl Substituted Orthocarbonate and Formate as Potential High Energy Dense Oxidizers

Scheme 6.1 Synthesis of orthocarbonate **1** and formate **2** 134

7. 2-Fluoro-2,2-dinitroethyl 2,2,2-trinitroethylnitramine, a possible high energy dense oxidizer

Scheme 7.1 Synthesis of 2-fluoro-2,2-dinitroethylamine (**1**) 158

Scheme 7.2 Synthesis of compound **2** and **3** from 2-fluoro-2,2-dinitroethylamine (**1**) 158

List of Figures

1. Introduction

Figure 1.1 Structures of hexogen (RDX), octogen (HMX), nitroguanidine (NQ) and triaminotrinitrobenzol (TATB) 2

Figure 1.2 Classification of gun propellants 3

Figure 1.3 Classification of rocket propellants 4

Figure 1.4 Cutaway of a Space Shuttle SRB segments, showing a solid rocket motor including the nozzle 6

Figure 1.5 Loop of a complete STS mission 8

2. Multiply Nitrated High-Energy Dense Oxidizers derived from the Simple Amino Acid Glycine

Figure 2.1 ORTEP of compound **3** 22

Figure 2.2 ORTEP of compound **4** 23

Figure 2.3 ORTEP of compound **5** 24

Figure 2.4 ORTEP of compound **6** 26

Figure 2.5 ORTEP of compound **7** 27

Figure 2.6 ORTEP of compound **9** 28

Figure 2.7 ORTEP of compound **10**, disorder not shown 29

3. The Energetic Nitrocarbamate $O_2NN(H)CO[OCH_2C(NO_2)_3]$ Derived from Phosgene

Figure 3.1 ^1H NMR resonance of the NH_2 group of **2** at variable temperatures in DMSO-D_6. 56

Figure 3.2 Molecular structure of 2,2,2-trinitroethyl carbamate (**2**) 60

Figure 3.3 Molecular structure of 2,2,2-trinitroethyl nitrocarbamate (**3**) 62

4. Asymmetric fluorodinitromethyl derivatives of 2,2,2-trinitroethyl N-(2,2,2-trinitroethyl)carbamate

Figure 4.1 Molecular structure of **1** with two independent molecules 84

Figure 4.2 Molecular structure of **2** (showing disorder) 85

Figure 4.3 Molecular structure of **3** 86

Figure 4.4 Molecular structure of **4** 87

Figure 4.5 Molecular structure of **5** 88

5. Polynitro containing energetic materials based on carbonyldiisocyanate and 2,2-dinitropropane-1,3-diol

Figure 5.1 Molecular structure of **1** 113

Figure 5.2 Molecular structure of **2** 114

Figure 5.3 Molecular structure of **3** 115

6. Fluorodinitroethyl Substituted Orthocarbonate and Formate as Potential High Energy Dense Oxidizers

Figure 6.1 Molecular structure of ***β*-1** 137

Figure 6.2 DSC measurement for **1** from –100 to 240 °C 140
with a chilling/heating rate of ±5 °C min^{-1}.

7. 2-Fluoro-2,2-dinitroethyl 2,2,2-trinitroethylnitramine, a possible high energy dense oxidizer

Figure 7.1 ^{15}N NMR spectrum of **3** in acetone-D_6 160

Figure 7.2 Molecular structure of **2**. 162

Figure 7.3 Molecular structure of **3**. 164

8. Summary

Figure 8.1 Abridgement of the most promising compounds of chapter 2–7 179

9. Appendix

Figure 9.1 Dimer of **3** with strong hydrogen bonds 183

Figure 9.2 Disordered trinitromethyl moiety of **10** 184

Figure 9.3 Molecular structure of Bis(2,2,2-trinitroethyl) carbonyl-N,N-dicarbamate (**1**) 192

List of Tables

2. Multiply Nitrated High-Energy Dense Oxidizers derived from the Simple Amino Acid Glycine

Table 2.1 IR and Raman bands of the carbonyl and nitro groups for **1–5** 20

Table 2.2 IR and Raman bands of the carbonyl and nitro groups for **6–10** .. 20

Table 2.3 Crystal and structure refinement data for **3–7**, **9–10** 30

Table 2.4 Physical and chemical properties of **1–10** 32

Table 2.5 Predicted detonation and combustion parameters 33
(using the EXPLO5 code) and sensitivity data for **1–10**

3. The Energetic Nitrocarbamate $O_2NN(H)CO[OCH_2C(NO_2)_3]$ Derived from Phosgene

Table 3.1 Multinuclear NMR resonances of **1–3** (ppm) in Acetone-D_6 55

Table 3.2 Characteristic IR and Raman vibrations [a] /cm^{-1} of **1–3** 57

Table 3.3 X-ray data and parameters of **2** and **3** 58

Table 3.4 Hydrogen-bond distances (Å) and angles (deg.) of **2** 61

Table 3.5 Hydrogen-bond distances (Å) and angles (deg.) of **3** 63

Table 3.6 Physical and chemical properties of **2** and **3** 64

Table 3.7 Cell parameters of **2** and **3** at 25 °C 65

Table 3.8 Predicted detonation, combustion parameters 65
(using EXPLO5 V5.05) and sensitivity data for **2** and **3**

Table 3.9 Predicted specific impulse I_s of mixtures with aluminum 67
(using EXPLO5 V5.05) and sensitivity data for **2** and **3**

4. Asymmetric fluorodinitromethyl derivatives of 2,2,2-trinitroethyl N-(2,2,2-trinitroethyl)carbamate

Table 4.1 IR and Raman bands of of carbonyl and nitro groups for **1**–**5** 82

Table 4.2 Crystal and structure refinement data for **1**–**5** 89

Table 4.3 Physical and chemical properties of **1**–**5** 91

Table 4.4 Predicted detonation and combustion parameters (using the EXPLO5 code) and sensitivity data for **1**–**5** 92

5. Polynitro containing energetic materials based on carbonyldiisocyanate and 2,2-dinitropropane-1,3-diol

Table 5.1 IR and Raman bands of carbonyl and nitro groups for **1**–**4** 112

Table 5.2 Crystal and structure refinement data for **1**–**3** 116

Table 5.3 Physical and chemical properties of **1**–**4** 118

Table 5.4 Predicted detonation and combustion parameters and sensitivity data for **1**–**4** 118

6. Fluorodinitroethyl Substituted Orthocarbonate and Formate as Potential High Energy Dense Oxidizers

Table 6.1 IR and Raman bands of **1** and **2**, characteristic vibrations and their assignments 135

Table 6.2 Crystal and structure refinement data for **β-1** 138

Table 6.3 Physical and chemical properties of **1** and **2** 141

Table 6.4 Predicted detonation and combustion parameters and sensitivity data for **1** and **2**. 142

7. 2-Fluoro-2,2-dinitroethyl 2,2,2-trinitroethylnitramine, a possible high energy dense oxidizer

Table 7.1 IR and Raman bands of of carbonyl and nitro groups for **1**–**3** 161

Table 7.2 Crystal and structure refinement data for **2**–**3** 165

Table 7.3 Physical and chemical properties of **1**–**3** 167

Table 7.4 Predicted detonation and combustion parameters (using the EXPLO5 code) and sensitivity data for **1**–**3** 168

8. Summary

Table 8.1 Properties of the most promising compounds of chapter 2–7 180

9. Appendix

Table 9.1 Hydrogen bonds of S-ethyl N-(2,2,2-trinitroethyl) thiocarbamate (**1**) 185

Table 9.2 Hydrogen bonds of 2,2,2-trinitroethyl 2,2,2-trinitroethylcarbamate (**2**) 186

Table 9.3 Hydrogen bonds of 2-fluoro-2,2-dinitroethyl 2,2,2-trinitroethylcarbamate (**3**) 186

Table 9.4 Hydrogen bonds of 2,2,2-trinitroethyl 2-fluoro-2,2-dinitroethylcarbamate (**4**) 186

Table 9.5 Hydrogen bonds of 2-fluoro-2,2-dinitroethyl 2,2,2-trinitroethyl carbonate (**5**) 187

Table 9.6 Hydrogen bonds of bis(2,2,2-trinitroethyl) carbonyl -N,N-dicarbamate (**1**) 188

Table 9.7 Hydrogen bonds of bis(2-fluoro-2,2-diinitroethyl) carbonyl-N,N-dicarbamate (**2**) 190

Table 9.8 Hydrogen bonds of 2,2-dinitropropane-1,3-diyl bis(2,2,2-trinitroethylcarbamate) (**3**) 191

Table 9.9 Hydrogen bonds of 2-fluoro-2,2-dinitroethyl 2,2,2-trinitroethylamine (**2**) 193

Table 9.10 Hydrogen bonds of 2-fluoro-2,2-dinitroethyl 2,2,2-trinitroethylnitramine (**3**) 194

1. INTRODUCTION

1.1 DEFINITIONS & BACKGROUND

In the literature, there are three ways to define an explosive or nowadays called energetic material.[1]

- 1) An energetic material releases a large amount of heat and pressure during a very fast exothermic decomposition with a generated temperature in the range of 3000–5000 °C. The gaseous products formed produce a volume 12000–15000 times greater than the original volume in a few microseconds accompanied by a shockwave and loud noise.
- 2) An explosive is a chemical substance or a mixture of chemical substances, which decompose readily under release of a large amount of energy and volume of gases when exposed to thermal or mechanical stress, detonation or catalysis.
- 3) An explosive is a substance or device, which releases its potential energy and in addition a sudden large amount of gases accompanied with a high pressure affecting its surroundings.

The first known explosive, discovered in the seventh century, was black powder. It is a mixture of charcoal, potassium nitrate and sulfur. The Chinese used black powder as explosive, propellant and even for fireworks. Usually an explosive contains a fuel and an oxidizer in a metastable state. After initiation the starting materials decompose rapidly with release of energy into small gaseous products without the need of atmospheric oxygen for the reaction. Modern explosives were designed to contain fuel and oxidizer within the same molecule. The initiation of an explosive can be achieved with mechanical, thermal or electrostatic sources.[1]

To classify the large variety of explosive compounds or mixtures, energetic materials are classified nowadays according to their use and properties into primary explosives, secondary (high) explosives and pyrotechnics. Also macromolecules with energetic properties, used as binders, should be mentioned and therefore an additional fifth class may be discussed.[2]

The class of primary explosives is labeled by the high sensitivities of the materials against thermal or mechanical stress or even electrostatic discharge. Initiation of a primary explosive is accompanied with a fast deflagration to detonation transition. This leads to a propagating shockwave, which is used to initiate a usually better performing and more stable secondary explosive, resulting in a powerful detonation. Typical examples of primary explosives used as initiators are mercury fulminate and lead(II) azide. Common high performing secondary explosives, initiated with the aid of primary explosives are RDX, HMX, NQ and TATB (Figure 1.1).[2]

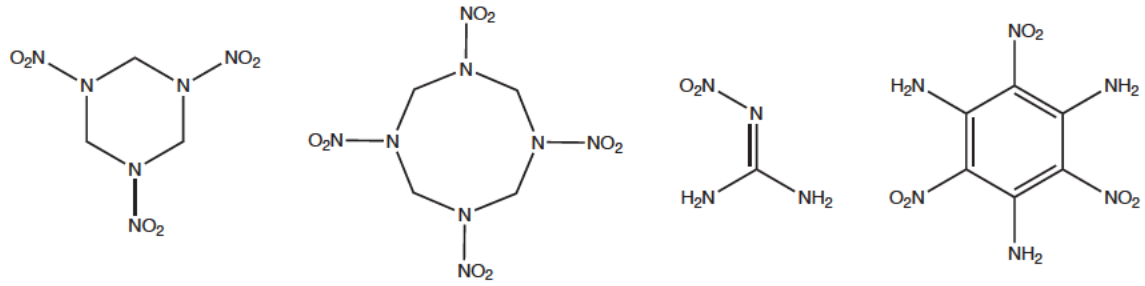

Figure 1.1. Structures of hexogen (RDX), octogen (HMX), nitroguanidine (NQ) and triaminotrinitrobenzol (TATB).

In contrast, compounds or mixtures from the class of propellants are not meant to detonate. Propellants differ from explosives with their decreased combustion rate, which should burn at uniform rates after ignition without requiring atmospheric oxidizing material.[2] Propellants are usually a mixture of different components, including a fuel and energetic oxidizer. To accelerate objects, a relatively high pressure over a long period of time during combustion of the propellant is desired. Furthermore, in some cases a lowered combustion temperature is needed to reduce erosion of the propulsion device. Due to the applications of propellants, this class is divided further into the two subclasses of gun propellants and rocket propellants.[2-3]

1.2 GUN PROPELLANTS

Propellants used for ammunition charges in all kind of weapons from pistols to artillery guns need lowered combustion temperatures to prevent severe erosion of the gun barrel by decreasing the formation of iron carbide. Gun propellants consisting of nitrocellulose (NC) are classified as single-base propellant. A composite of NC with nitroglycerine (NG) is called double-base propellant (Figure 1.2). These propellants show increased performance compared to pure NC propellants. Unfortunately, the increased performance comes along with higher combustion temperatures and therefore an accelerated gun barrel erosion is observed. Double-base propellants are mainly used for mortars due to the higher performance. To overcome the problem of the high combustion temperature of double-base propellants, nitroguanidine (NQ) is added and a triple-base propellant consisting of NC, NG and NQ is built. Despite the fact that triple-base propellants show decreased performance compared to double-base propellants, they are applied in large caliber weapons. In addition, further triple-base propellants containing hexogen (RDX) instead of NQ are used to increase the performance, although higher combustion temperatures are produced. A further problem of the used propellant systems is the appearance of a muzzle flash due to the partial combustion of the gaseous decomposition products when exposed to air at the muzzle. Modern propellants containing nitrogen rich materials might overcome the problem of gun barrel erosion as well as of the muzzle flash because of the formation of the inert decomposition gas N_2 instead of carbon monoxide.[2-3]

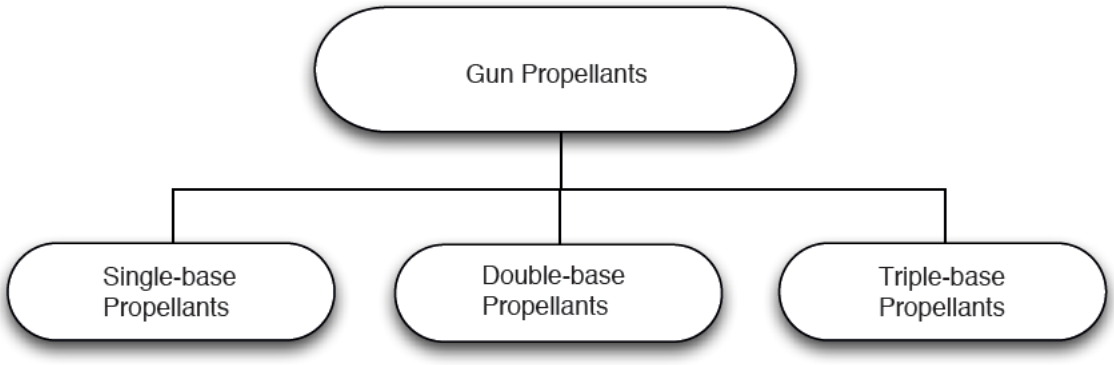

Figure 1.2. Classification of gun propellants.

1.3 ROCKET PROPELLANTS AND MOTORS

The main difference between rocket propellants and gun propellants is the lower burning rate of rocket propellants, the higher temperatures of combustion and the decreased chamber pressure formed in the combustion chamber of rocket motors (approx. 50 bar).
A typical rocket motor simply consists of the combusting propellant inside a combustion chamber, which directs and ejects the hot gaseous products formed into the direction of the nozzle at high speed. Thereby, the rocket itself moves in the opposite direction. The same principle is used in all kind of jet engines, where the jet fuel is burned continuously within the engine using air as oxidizing agent and the velocity of the hot decomposition gases makes the jet moving forward. In contrast, running a rocket motor successfully, both the fuel and the needed oxidizer have to be inside the combustion chamber. Due to their applications, two different types of rocket propellants can be distinguished: liquid and solid rocket propellants (Figure 1.3). Additionally, hybrid propellants are investigated to combine the advantages of both propulsion systems. A sever problem is the mixing of the solid fuel with the liquid oxidizer in an accurate way during combustion. Therefore, there is still a lack of application purposes for hybrid propellants.[2-3]

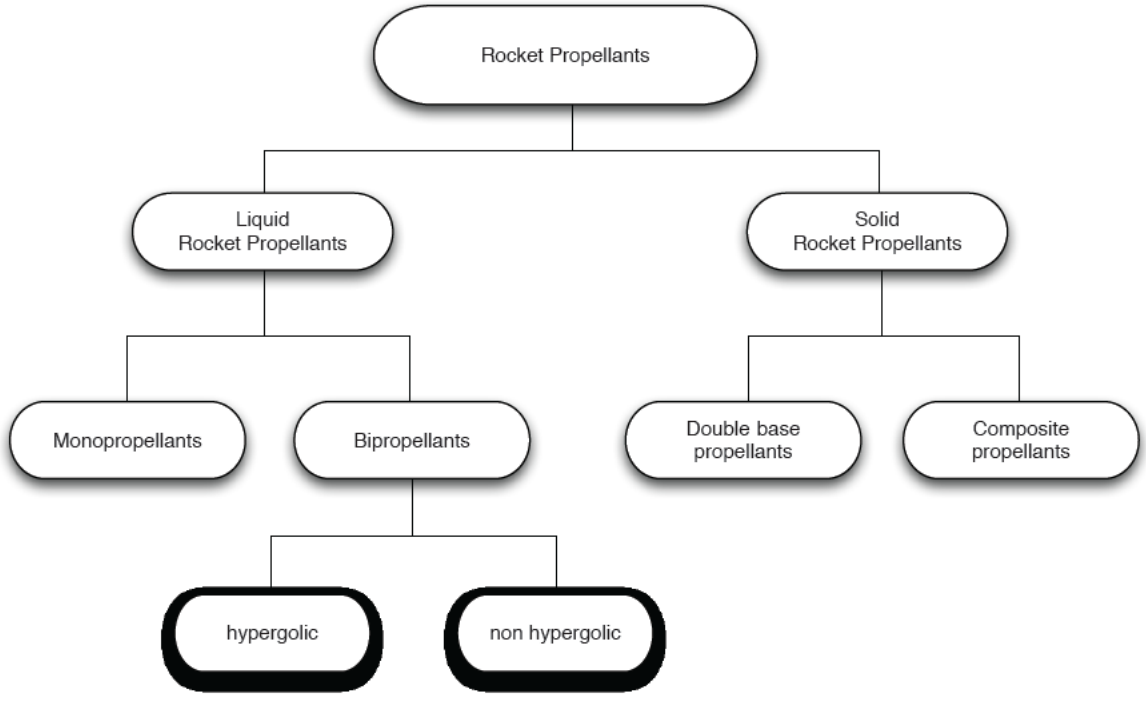

Figure 1.3. Classification of rocket propellants.

1.3.1 SOLID ROCKET PROPELLANTS

The simple constructed and easy to store rocket motors containing a solid rocket propellant are engineered to provide the thrust for launching a carrier system from the ground into space, e.g. equipped with a satellite. However, the mixed up fuel and oxidizer can be stored in the booster system easily, the once started burning can not be turned off or regulated before the fuel has been converted completely. Normally a solid rocket motor is made of up to several hundred tons of a composite propellant consisting of a heterogeneous mixture of ammonium perchlorate (AP) as solid oxidizer and aluminum as fuel. If required, additional additives like polymeric binders, plasticizer, catalysts or burn rate modifiers are added to the composite. The burning of such a motor releases enormous quantities of carbon and nitrogen oxides as well as hydrochloric acid gas and gaseous water, which push the carrier system into space or orbit. Moreover, homogeneous mixtures of macroscopic ingredients are called homogeneous propellants. These propellants are usually based on nitrocellulose (NC), accompanied with nitroglycerine (NG) and/or nitroguanidine (NQ), comparable with gun propellant systems.

The usual burn out time of a solid rocket can be as much as 100 s to 120 s with a chamber temperature between 2400 K and 4400 K, which is a great challenge for the materials used to build the combustion chamber and the nozzle. In addition, these materials should be low in weight to reduce the dead weight of the carrier system. Solid rockets are however considered to be simple, reliable and cheap and therefore solid propulsion is still used in the booster stage of orbital launch vehicles.[1] The most prominent use of ammonium perchlorate as oxidizer in a solid propulsion system was during the NASA Space Shuttle program (1981–2011), officially called SPACE TRANSPORTATION SYSTEM (STS). The in this case used SOLID ROCKET BOOSTERS (SRBs) consisted of 69.83 % AP, 16 % aluminum, 0.17 % iron oxide as catalyst, 12 % of a polymeric binder and 2 % of an epoxy curing agent (e.g. bisphenol-A ether).[4] The whole composition was named as *Ammonium Perchlorate Composition Propellant* (APCP). The total amount of propellant of one SRB with a weight of approx. 500 t provides a thrust of 11790 kN and is therefore the largest solid rocket motor ever flown successfully. During all 135 STS missions this composition was used to provide over 80 % of the needed thrust for the lift-off of a Space Shuttle with its whole weight of approx. 2000 t (fully equipped Orbiter Vehicle, external tank, two SRBs).[3-4] The remaining thrust was produced by the internal liquid propellant rocket motor of the Orbiter Vehicle. For launch purposes, fuel and oxidizer for this internal engine are stored in the external tank connected to the Orbiter.[3-4] For illustration

purposes, a cutaway of a Space Shuttle SRB is shown in Figure 4. The used SRBs as well as the external tank are disconnected from the Orbiter vehicle during the staging phase of a STS launch (Figure 1.5). The SRB's are separated at an altitude of 44 km. The SRBs can be reused up to 20 times for further launches after equipping with a new solid rocket motor.[4]

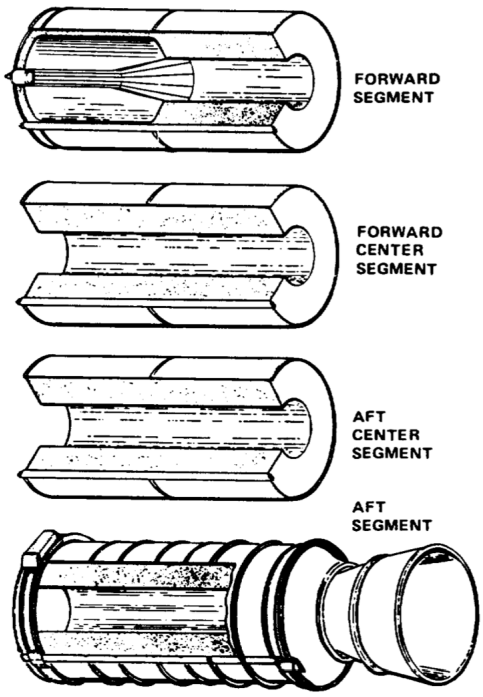

Figure 1.4. Cutaway of a Space Shuttle SRB segments, showing a solid rocket motor including the nozzle.[4]

1.3.2 LIQUID ROCKET PROPELLANTS

Liquid propellants are distinguished into mono- and bipropellants according to the number of different ingredients. The class of bipropellants can be further divided into hypergolic and non-hypergolic propellants, due to their capability to be self-igniting or non-self-igniting, respectively. In the case of liquid propellants the temperature of storage leads to a further possible differentiation into cryogenic and storable propellants.

Monopropellants are normally endothermic compounds, which can decompose exothermic without the presence of an external oxidizing agent. The most common monopropellant is hydrazine. It decomposes exothermic into nitrogen and hydrogen. Further examples for monopropellants are hydrogen peroxide, nitrous oxide or ethylene oxide.

The more common liquid propellants are bipropellants. For this system, oxidizer and fuel have to be injected into a combustion chamber continuously in a controlled manner. Therefore, two storage tanks are required for bipropellant systems to separate the fuel from the oxidizer to avoid uncontrolled combustion. The fuel and the oxidizer are only injected into the chamber when the motor is fired. Therefore, it is possible to control or even to shut off the propulsion by manipulating the flow system. In the case of hypergolic propellants various combinations are known using hydrazine, or its derivatives monomethyl hydrazine (MMH) and unsymmetrical dimethyl hydrazine (UDMH), combined with nitric acid or even dinitrogen tetroxide (NTO), sometimes containing a small percentage of nitrogen monoxide, called mixed oxides of nitrogen (MON).[1,3] The most common and mostly used hypergolic mixture consists of MMH as fuel and NTO as oxidizer.[1] It was used for propulsion in the Orbital Maneuvering Subsystem of the NASA Orbiter Vehicle.[4] Hypergolic engine systems have many application possibilities for upper stage engines, deep space rockets or controlling systems, due to advantages like long-term stability of the single components at reasonable temperatures as well as the reliability and the improved repetition rate of ignitions. However, the single compounds used are difficult to handle due to the extreme toxicity and the known corrosiveness.[1]

Cryogenic bipropellants usually provide a higher specific impulse. The most common cryogenic bipropellant system is liquid hydrogen (LH_2) and liquid oxygen (LOX). Due to the low boiling temperatures, both chemicals are stored in special facilities and are filled into the rocket only shortly before the launch. If a launch has to be postponed for a longer period of time, the rocket tanks must be emptied to avoid potential explosive danger. The Space Shuttle Main Engine (SSME) was equipped with this system. Due to the high specific impulse of 363 s at sea level and 455 s in vacuum, the fluid-engines of the Space Shuttle Orbiter were running already at lift-off.[3-4] A complete loop of a standard STS mission is illustrated in Figure 1.5.

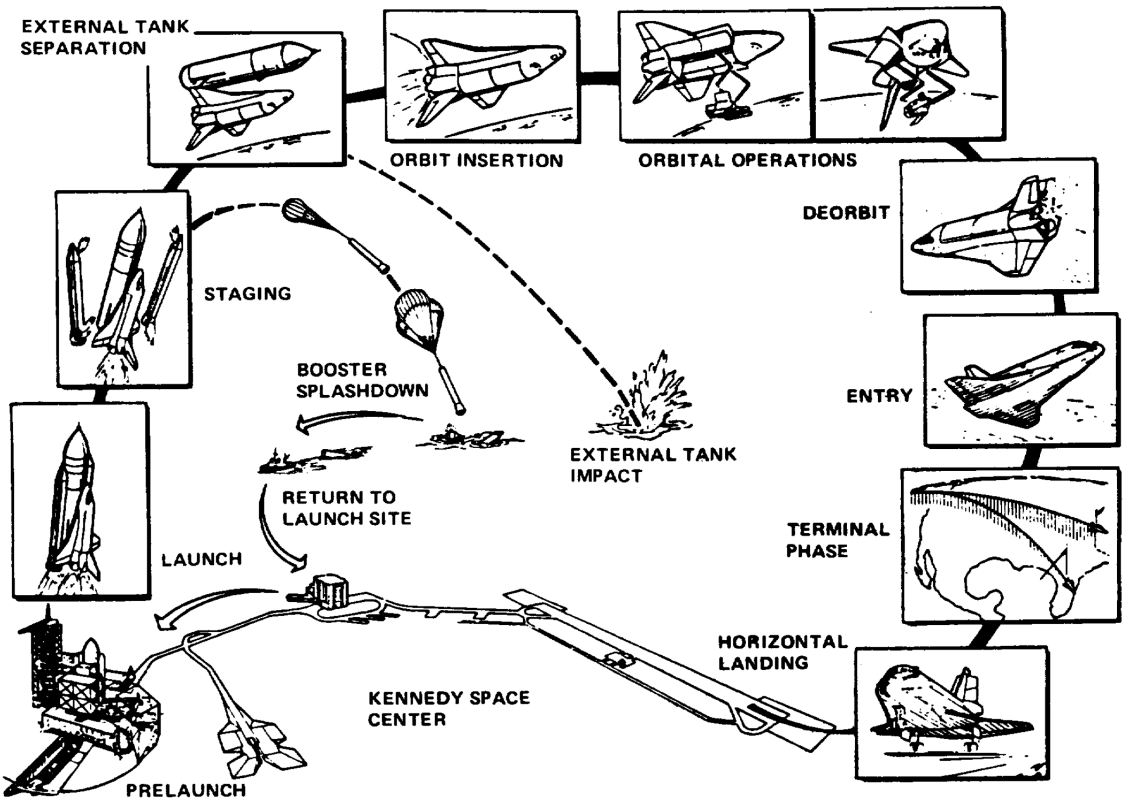

Figure 1.5. Loop of a complete STS mission.[4]

1.4 HIGH ENERGY DENSE OXIDIZERS

The most important point to get a rocket motor running properly is the supply of an adequate amount of oxidizer to a definite amount of fuel. In contrast to a jet engine, which uses atmospheric oxygen as oxidizer for a successful combustion of the fuel kerosene, a rocket motor has to carry its own oxidizer, owing to the lack of oxygen in the upper earth atmosphere and in outer space for an ideal combustion. The modern definition of materials as High Energy Dense Oxidizer (HEDO) refers to substances with special properties in terms of chemical, physical and energetic facets. New compounds should be developed referring to several minimum requirements in terms of energetic performance, costs, environmental aspects and safety with the goal to replace the widely used oxidizer ammonium perchlorate (AP) in solid rocket motors. New compounds should have superior performance to increase the load capacity and simultaneously less incriminating the environment.

1.4.1 OXYGEN BALANCE AND SPECIFIC IMPULSE

One of the key factors and the most basic requirement for an oxidizing material, is the oxygen balance. It is defined as the relative amount of oxygen provided (positive balance) or needed (negative balance) during the combustion of the material without the presence of external oxygen. The oxygen balance is simply calculated from an empirical formula, assuming a full conversion of the carbon content into carbondioxide (alternatively carbonmonoxide) and the hydrogen into water. Furthermore, components like fluorine or nitrogen, which are not decomposing into oxygen containing products, affect the oxygen balance in several ways. Fluorine atoms of a considered material for example are assumed to decompose into hydrogen fluoride and therefore decrease the amount of hydrogen. Nitrogen atoms on the other hand increase the molecular weight of the compound and decrease the oxygen balance indirectly. The oxygen balance of a CHFNO compound can be calculated according to Equation 1.

$$\Omega[\%] = \frac{M_O}{M}\left(\sum O - a\sum C - \frac{1}{2}\left(\sum H - \sum F\right)\right)\times 100 \qquad \text{(Equation 1)}$$

M_O = molecular mass of an oxygen atom

M = molecular mass of the CH(F)NO compound

ΣO = number of oxygen atoms in the sum formula

ΣC = number of carbon atoms in the sum formula

ΣH = number of hydrogen atoms in the sum formula

ΣF = number of fluorine atoms in the sum formula

a = 1 for Ω_{CO}, assuming CO as decomposition product

a = 2 for Ω_{CO2}, assuming CO_2 as decomposition product

The numbers of carbon atoms (ΣC) with the right factor a, depending on whether CO or CO_2 is the assumed decomposition product, is subtracted from the number of oxygen

atoms (ΣO) per molecule. Additionally, half the number of hydrogen atoms (ΣH) is subtracted after correction with the number of fluorine atoms per molecule (ΣF) and the resulting excess or deficit of oxygen atoms is multiplied with the molecular mass of an oxygen atom. To achieve the oxygen balance given in percentage, the result is divided by the molecular mass of the compound multiplied by 100. Obviously, besides a high amount of oxygen atoms per molecule, a small molecular weight of the compounds leads to an increased oxygen balance compulsorily.

For an example calculation we choose 2-fluoro-2,2-dinitroethanol (FDNE, M = 154.05 g mol^{-1}), an often used starting material of several compounds described in this work. FDNE theoretically decomposes into the following decomposition products (assuming the formation of CO):

$$C_2H_3FN_2O_5 \rightarrow 2CO+H_2O+HF+N_2+O_2$$

Under these circumstances, one molecule of oxygen is formed during the combustion of FDNE and therefore a positive oxygen balance of $\Omega_{CO(FDNE)} = +20.77\ \%$ can be determined referring to Equation 1.

$$\Omega_{CO(FDNE)} = \frac{16}{154.05}\left(5-1\times 2-\frac{1}{2}(3-1)\right)\times 100 = +20.77\%$$

For a analogous calculation assuming CO_2 as decomposition product, a total oxygen balance $\Omega_{CO2(FDNE)} = \pm 0\ \%$ will be received, which means, that the compound is converted into its fully oxidized decomposition products without any release of oxygen. Though, an exothermic decomposition is accompanied with elevated temperatures of combustion, CO is formed besides CO_2, as mentioned in the BOUDOUARD EQUILIBRIUM. An almost counterbalanced oxygen balance is preferred for CHNO based secondary explosives, to gain the maximum release of energy of explosion.

For high energy dense oxidizers, the main parameter referring to the performance of a rocket propellant equipped with the investigated compound, is the specific impulse I_s.[5-6] Owing to the guided release of gaseous products formed during combustion of the propellant within the combustion chamber, a recoil force (thrust *F(t)*) into the opposite direction is generated. Therefore, the specific impulse I_{sp} in m s^{-1} is defined as the integral of the thrust *F(t)*, per definite unit weight of material (m), over the period of combustion (Equation 2). [2,6-7]

$$I_{sp}\left[\frac{m}{s}\right]=\frac{\int_0^t F(t)dt}{m} \qquad \text{(Equation 2)}$$

Usually, the specific impulse is corrected with the earth gravitation at main sea level g, denoted in seconds. Besides the measurement of the produced thrust over a fixed period of time, the specific impulse of a propulsion system can be estimated according to Equation 3, containing the force of gravity g (9.81 m s^{-2}), the ideal gas constant R (8.3145 J mol^{-1} K^{-1}), the isochoric temperature of combustion inside the combustion chamber T_C [K], the average molecular weight of the gaseous products M [kg mol^{-1}] and the ratio of the specific heat capacities γ. [2]

$$I_{sp}[s]=\frac{1}{g}\sqrt{\frac{2\gamma RT_C}{(\gamma-1)M}} \qquad \text{(Equation 3)}$$

$$\gamma=\frac{C_p}{C_v}$$

Therefore, after summarizing all constant values, the specific impulse is proportional to the square of the combustion temperature and the reciprocal of the averaged molecular mass of the decomposition gases (Equation 4).

$$I_{sp}\propto\sqrt{\frac{T_C}{M}} \qquad \text{(Equation 4)}$$

Referring to Equation 4, a higher specific impulse can be achieved by increasing the combustion temperature, which comes along with a high heat of reaction, or lowering the average molecular mass of the decomposition gases.[8] Despite the fact, that the specific impulse is dependent on T_C and M, also the engineered shape of the propellant system is of great importance for the real obtained impulse.[1] An increase of the specific impulse by 20 s, leads empirically to a doubling of the load capacity of the carrier system.[2]

1.4.2 MOTIVATIONS AND REQUIREMENTS FOR NEW HIGH ENERGY DENSE OXIDIZERS

The widely used oxidizer in solid rocket formulations ammonium perchlorate (AP) has a great variety of civil and military applications. The extensive use in the past and nowadays as oxidizer and as ingredient in agricultural fertilizers causes a wide distribution of AP over the surface and even in the ground water system, owing to the high solubility and the chemical persistence. It was investigated, that the incorporation of perchlorate anions may cause a malfunction in the thyroids gland of vertebrates affecting the normal growth and development of the organism, owing to a biochemical rivalry between the iodine and the perchlorate anion, which is comparable in shape and size.[2,9] In addition, the normal pigmentation of amphibian embryos is disturbed due to the negative influences of AP. Furthermore, the combustion of AP containing propellants release a huge amount of hydrogen chlorine gas, which causes also sever problems for the environment in terms of acidic rain and acidification of fertile topsoil grounds.

The replacement of ammonium perchlorate (AP) as oxidizer is urgently needed in terms of more environmental friendly and less toxic substituents. In addition, the performance of the new compounds should be at least in the range of AP compositions. Highly nitrated organic compounds decompose completely into more environmental gaseous products and might be one option for the development of AP replacements and became therefore more and more an important matter of energetic researches. The development of new suitable high energy dense oxidizers (HEDOs) is controlled by many different factors like, cost, hazards, performance or safety aspects.

The general requirements for a new potential HEDO are the following: [2]

- High oxygen content (Ω_{CO} > 25 %)
- High density (approx. 2.0 g cm^{-3})
- Melting point greater than 150 °C
- Decomposition temperature above 200 °C
- Sensitivities not worse than PETN (Impact: 4 J, Friction 80 N, ESD: 0.1 J)
- Low vapor pressure
- High enthalpy of formation
- Compatibility with binders
- Synthesis with a minimum number of synthesis steps
- Economic or bulk starting materials

1.5 MOTIVATION AND OBJECTIVES

This dissertation has the objective to investigate molecules, which contain a high amount of oxygen. These compounds were investigated for the future use in High Energy Dense Oxidizer (HEDO) purposes. Therefore, the new compounds should have chemical, physical and energetic properties, which at least achieve as much minimum requirements for new potential High Energy Dense Oxidizers as possible. In addition, the research for new especially highly nitrated precursors and building blocks in terms of synthesis, characterization and investigation of the chemical behavior is of interest in the course of the development of new HEDOs. Owing to the influence of intra- and intermolecular interactions affecting the energetic properties, an additional analytical and theoretical investigation of the compounds made is recommended. The introduction of polynitrated building blocks, especially the 2,2,2-trinitro(m)ethyl and the 2-fluoro-2,2-dinitro(m)ethyl moieties, with the aim to dramatically increase the oxygen content of appropriate starting materials is the main concept of this work.

Various compounds using this principle were synthesized, characterized and their possible application in future applications as HEDO were discussed. This work consists of seven chapters, whereas each chapter represents a completed and published research project including their discussed results, abstracts, introductions and conclusions as well as their experimental sections. Available supplementary information for the corresponding chapters is provided in the Appendix of this dissertation.

1.6 REFERENCES

[1] J. P. Agrawal, *High Energy Materials Propellants, Explosives and Pyrotechnics*, 1st Ed., Wiley-VCH, Weinheim, **2010**.

[2] T. M. Klapötke, *Chemistry of High-Energy Materials*, 2nd Ed., de Gruyter, Berlin, **2012**.

[3] R. Moll, *Dissertation* **2013**, *Ludwig Maximilian University of Munich*.

[4] NASA, *Space Shuttle News Reference*, 2–20–22–21, http://de.scribd.com/doc/17005716/NASA-Space-Shuttle-News-Reference-1981.

[5] J. Köhler, M. R., *Explosivstoffe*, 9 Ed., Wiley-VCH, Weinheim, **1998**.

[6] G. A. Olah, D. R. Squire, *Chemistry of Energetic Materials*, Academic Press, Boston, **1991**.

[7] N. Kubota, *Propellants and Explosives*, 2nd Ed., RSC Paperback, Cambridge, **2004**.

[8] H. H. Krause, *Energetic Materials*, Wiley-VCH, Weinheim, **2005**.

[9] R. E. Tarone, L. Lipworth, J. K. McLaughin, *J. Occup. Environ. Med.* **2010**, *52*, 653.

2. MULTIPLY NITRATED HIGH-ENERGY DENSE OXIDIZERS DERIVED FROM THE SIMPLE AMINO ACID GLYCINE

Andreas Baumann, Anna Erbacher, Camilla Evangelisti, Thomas M. Klapötke*, Burkhard Krumm, Sebastian F. Rest, Martin Reynders and Véronique Sproll

As published in: Chemistry A European Journal **2013**, 19(46), 15627–15638.

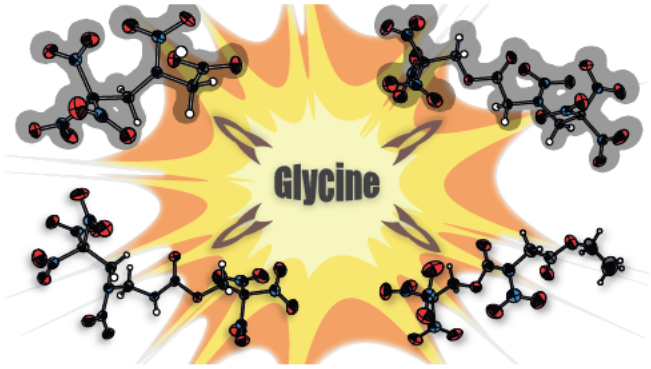

2.1 ABSTRACT

Various energetic polynitro esters, carbamates, and nitrocarbamates that were derived from the amino acid glycine were fully characterized by single-crystal X-ray diffraction, vibrational spectroscopy (IR and Raman), multinuclear NMR spectroscopy, elemental analysis, and differential scanning calorimetry (DSC). Owing to their positive oxygen balance, the suitability of these compounds as potential oxidizers in energetic formulations was investigated and discussed. In addition, the heats of formation of the products were calculated by using the Gaussian 09 program package at the CBS-4M level of theory. From these values and the calculated densities (from the X-ray data), several detonation parameters, such as detonation pressure, velocity, energy, and temperature, were computed by using the EXPLO5 code. Furthermore, their sensitivities towards impact, friction, and electrostatic discharge were tested by using a drop hammer, a friction tester (both BAM certified), and a small-scale electrical-discharge device, respectively.

2.2 INTRODUCTION

Compounds that were derived from 2,2,2-trinitroethanol have been found to be useful in the research of high energetic oxidizers because of their high oxygen content.[1] Chlorine-free, highly nitrated CHNO compounds might overcome the problematic formation of hydrogen chloride during the use of ammonium perchlorate as an oxidizer in formulations for rocket propellants. In addition, the development of new chlorine-free energetic oxidizers that decompose into volatile small molecules is a promising way of increasing the specific impulse of solid-state rocket boosters.[1a, 2] The specific impulse (I_s) is one of the main parameters for specifying the performance of a solid rocket booster. The specific impulse is proportional to the temperature inside the combustion chamber (T_c) and to the reciprocal of the average molecular mass of the decomposition products (M), according to Equation (1). An increase of the value for I_s by 20 s empirically leads to a doubling of the usual payload.[2a] Feuer et al. were among the first to investigate the suitability of amino acids for MANNICH-type reactions with 2,2,2-trinitroethanol.[3] The synthetic strategy in Feuer's work with glycine ethyl ester is shown in Scheme 1.

Herein, potential high energetic oxidizers with improved sensitivity towards external stimuli, such as impact or friction, were prepared based on the work by Feuer et al. Various esters, carbamates, and nitrocarbamates were synthesized from the starting materials glycine ethyl ester, 2-(nitro-(2,2,2-trinitroethyl)amino)acetyl chloride (**4**), and 2-(nitro-(2,2,2-trinitroethyl)amino)acetyl azide (**5**). Furthermore, additional analytical data were provided for the (in most cases) poorly characterized compounds **1**–**5**.

2.3 RESULTS AND DISSCUSSION

Synthesis

The valuable precursors that were derived from glycine, that is, carbonyl chloride **4** and carbonyl azide **5**, were synthesized as outlined in Scheme 2.1.

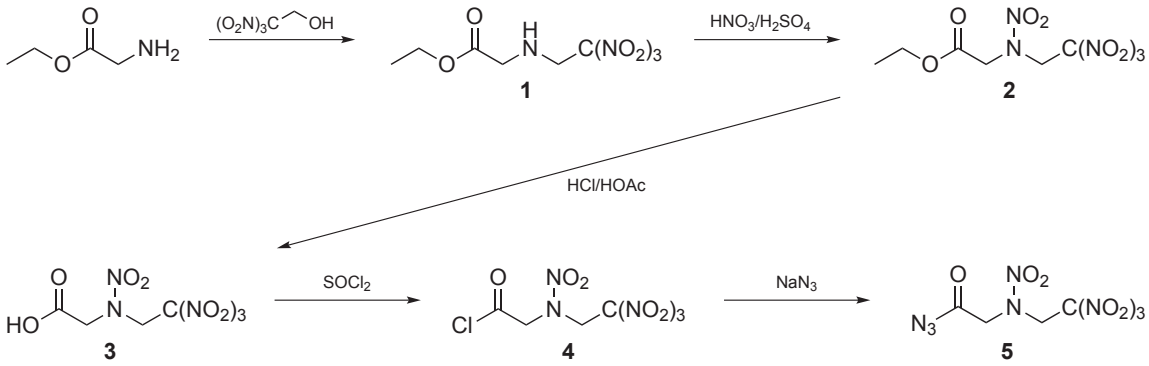

Scheme 2.1. Reaction sequence for the synthesis of compounds **4** and **5** as described by Feuer et al.[3a]

Esterification of compound **4** with 2,2,2-trinitroethanol led to the new corresponding acetate (**6**, Scheme 2.2). The reaction of azide **5** with 2,2,2-trinitroethanol proceeded through an *in situ* Curtius rearrangement and afforded carbamate **7** (Scheme 2.2). Nitration of compound **7** at the NH position resulted in the formation of the target molecule, nitro carbamate **8** (Scheme 2.2). Furthermore, glycine ethyl ester was reacted with 2,2,2-trinitroethyl chloroformate[4] to afford acetate **9**, which could be nitrated to form the nitro acetate **10** (Scheme 2.2).

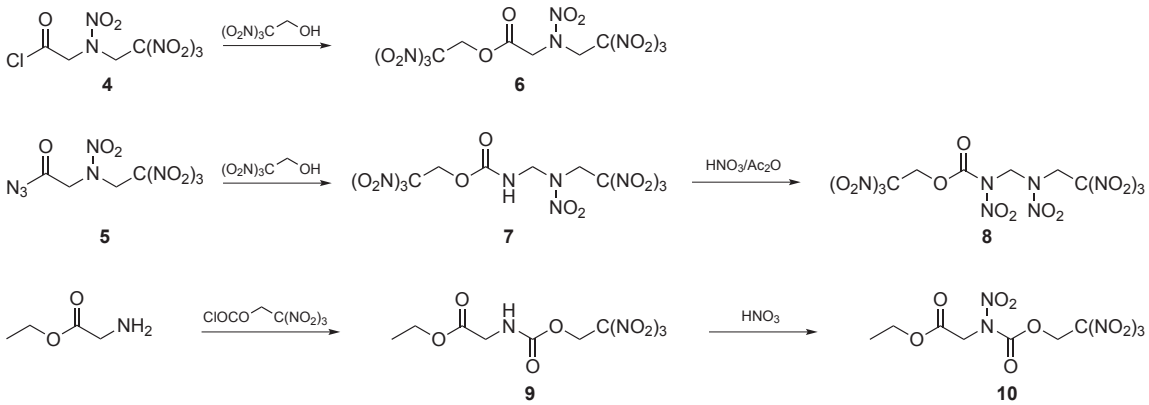

Scheme 2.2. Synthesis of compounds **6**–**10**.

Compounds **1**–**10** were soluble in various organic solvents, such as acetone, MeCN, $CHCl_3$, and MeOH, but were insoluble in water (except for compounds **3**, **4**, and **7**) and other solvents, such as *n*-hexane. The compounds were found to be sensitive towards both impact and friction.

NMR spectroscopy

The compounds reported herein were thoroughly characterized by ^{1}H, ^{13}C, and ^{14}N NMR spectroscopy. The multinuclear NMR spectra were recorded in CD_3CN (for compound **1**), $CDCl_3$ (for compounds **5**, **7**, and **10**), [D_6]DMSO (for compounds **2**–**4** and **6**), and [D_6]acetone (for compounds **8** and **9**). In the ^{1}H NMR spectra of compounds **2**–**10**, the $CH_2C(NO_2)_3$ groups appear as singlets within the range δ = 6.36–5.45 ppm. Resonances of the ethyl ester protecting groups in compounds **1**, **2, 9**, and **10** are observed as quartets within the range δ = 4.3–4.1 ppm for the OCH_2CH_3 protons and as triplets within the range δ = 1.32–1.21 ppm for the OCH_2CH_3 protons, with a coupling constant of 7.2 Hz. The resonances of the $COCH_2N$ protons in compounds **1**–**7** are observed as singlets within the range δ = 4.89–3.42 ppm. The amino hydrogen resonance in compound **1** is observed as a broad singlet at δ = 3.8 ppm in CD_3CN. In the ^{1}H NMR spectrum of compound **7**, the NH resonance is found as a broadened triplet at δ = 6.31 ppm, with ^{3}J(H,H) = 6.4 Hz. The corresponding methylene moiety appears as a doublet at δ = 5.20 ppm. A doublet at δ = 3.92 ppm, with a coupling constant of ^{3}J(H,H) = 6.3 Hz, is observed in the ^{1}H NMR spectrum of compound **9**, which corresponds to the methylene moiety that is connected to the NH atom of the vicinal carbamate group. In addition, the NH proton of the carbamate moiety in compound **9** is found as a broad resonance at δ = 7.38 ppm in [D_6]acetone. The resonances of the two methylene moieties of compound **5** ($OCCH_2N$ and $NCH_2C(NO_2)_3$) at δ = 6.01 and 5.97 ppm could not be assigned precisely.

The carbon atoms of the trinitromethyl moieties in the ^{13}C NMR spectra of compounds **2**–**8** always appeared as very broad resonances within the range δ = 124.9–122.2 ppm. In the spectra of compounds **1**, **5**, **9**, and **10**, these carbon resonances were not detected at all; however, in their ^{14}N NMR spectra, the corresponding resonances of the nitrogen atoms of the NO_2 moieties were positively identified between δ = –27 and –34 ppm in all cases. The ^{14}N NMR resonances of the azide moiety of compound **5** were observed at δ = –136 (γ), –149 (β), and –254 ppm (α) in $CDCl_3$. The nitramine NO_2 resonance was detected at δ = –50 ppm for compound **8**, but was not observed in the spectrum of compound **10**.[1a, 5]

Vibrational spectroscopy

The vibrational analyses of compounds **1**–**10** showed the characteristic asymmetric stretching vibrations of the NO_2 group, $\nu_{as}(NO_2)$, within the range 1608–1566 cm^{-1} and the symmetric stretching vibrations, $\nu_s(NO_2)$, within the range 1306–1288 cm^{-1} (Table 2.1 and Table 2.2). The trinitromethyl and nitramino moieties in compound **2**–**8** may be a reason for the observed shift of the $\nu_{as}(NO_2)$ vibrations. Typically, $\nu_{as}(NO_2)$ stretches for CNO_2 groups appear higher than those of NNO_2 moieties.[6] The C=O stretching vibrations for compounds **1**–**10** were found within the range 1807–1703 cm^{-1}. These stretching vibrations belonged to the corresponding ester, carbamate, and nitrocarbamate moieties. Compared with those for compound **9** (1753 and 1714 cm^{-1}), the C=O vibrations for compound **10** were shifted towards higher wavenumbers (1801 and 1740 cm^{-1}), owing to the introduced nitro group. Thus, it seems that the nitro moiety shifts both ν(C=O) vibrations to higher energies. We assumed that the carbamate was more influenced by the nitro moiety and, therefore, the signal at 1801 cm^{-1} was assigned to the ν(C=O) stretch of the nitrocarbamate moiety. The characteristic asymmetric stretching vibration of the azide moiety of compound **5** was observed at 2196 cm^{-1} as a moderately intense band in the IR spectrum and at 2188 (18) cm^{-1} in the Raman spectrum.[7] The C–N, C–O, and C–C vibrations of compounds **1**–**10** could be observed within the typical ranges for CHNO and CHClNO compounds, respectively.[6–8]

Table 2.1. IR and Raman bands of the carbonyl and nitro groups for **1**–**5**

	1		**2**		**3**		**4**		**5**	
	IR[a]	Raman[b]	IR[a]	Raman[b]	IR[a]	Raman[b]	IR[a]	Raman[b]	IR[a]	Raman[b]
ν CO	1724(s)	1732(16)	1743(s)	1754(23)	1729(s)	n o	1785(m)	1797(27)	1703(s)	1709(44)
ν_{as} NO_2	1600(s) 1576(vs)	1587(5)	1620(s) 1610(s) 1583(vs) 1566(s)	1610(24) 1586(7) 1567(10)	1609(vs) 1591(s) 1566(vs)	1617(46) 1584(3) 1568(10)	1625(m) 1594(vs) 1576(vs)	1621(15) 1606(22) 1592(6) 1573(13)	1604(s) 1583(s) 1563(s)	1608(5) 1588(4) 1566(8)
ν_s NO_2	1306(m)	1309(37)	1306(m) 1279(vs)	1306(8) 1283(64)	1276(s) 1267(s)	1300(19) 1275(49)	1297(s) 1272(vs)	1302(20) 1274(56)	1278(vs)	1299(20) 1280(52)

[a] IR intensities: vs = very strong, s = strong, m = medium, w = weak. [b] in cm^{-1}; Raman intensities at 300 mW in brackets; n.o. = not observed.

Table 2.2. IR and Raman bands of the carbonyl and nitro groups for **6**–**10**

	6		**7**		**8**		**9**		**10**	
	IR[a]	Raman[b]	IR[a]	Raman[b]	IR[a]	Raman[b]	IR[a]	Raman[b]	IR[a]	Raman[b]
ν CO	1772(m)	1786(15)	1745(m)	1750(12)	1759(m)	1759(13)	1753(m) 1714(s)	1579(16) 1719(27)	1807(m) 1740(s)	1807(17) 1747(17)
ν_{as} NO_2	1613(s) 1590(vs) 1576(vs)	1625(24) 1603(7) 1576(3) 1563(3)	1604(s) 1588(vs) 1572(vs)	1608(25) 1569(9)	1593(vs) 1573(s)	1621(23)	1605(s) 1593(s)	1617(35) 1596(5) 1571(2)	1582(vs)	1617(10) 1601(31)
ν_s NO_2	1294(s) 1276(s)	1302(15) 1277(28)	1288(vs)	1303(31) 1286(25)	1299(s) 1278(s) 1252(m)	1301(22) 1256(6)	1302(m) 1269(w)	1309(33) 1274(20)	1289(s)	1292(40)

[a] IR intensities: vs = very strong, s = strong, m = medium, w = weak. [b] in cm^{-1}; Raman intensities at 300 mW in brackets.

X-ray diffraction

Compounds **3**–**7**, **9**, and **10** were investigated by low-temperature single-crystal X-ray diffraction. The crystal and structure-refinement data from the structure determinations are listed in Table 2.3. Suitable single crystals for X-ray diffraction measurements were obtained by the slow evaporation of solutions of the compounds in organic solvents, such as 1,2-dichloroethane, EtOAc, tetrachloromethane, and $CHCl_3$.

The molecular structure of 2-(nitro-(2,2,2-trinitroethyl)amino)acetic acid (**3**) is shown in Figure 2.1. Compound **3** crystallized in the monoclinic space group $P2_1/c$, with four formula units per unit cell. The structure of compound **3** shows a density of 1.88 g cm^{-3} at 173 K. The bond lengths and angles are comparable to values reported in literature for CHNO compounds that contain a trinitromethyl moiety.[1a, 2b, 5, 9] The average N–O bond length of the trinitromethyl moiety (1.210(2) Å) is slightly shorter than that of the corresponding nitramine moiety (1.224(1) Å), owing to some shared π-electron density between the N–N bond and the N–O bonds of the nitramine group.[6] The dihedral angle C3–N1–N2–O4 within the nitramine group is –19.3(1)°, which is almost within the range of cyclic nitramines RDX and HMX.[10] Although a propeller-type orientation is typical of trinitromethyl moieties, the case of C1$(NO_2)_3$ is still surprising. It is known in the literature that the barrier to rotation about a single C–NO_2 bond is quite small. Therefore, disturbing effects, such as those provided by a neighboring nitramine group, normally sharply distort the preferred C_3 geometry.[6] Such compounds show an electrostatic attraction between the nitro group of the nitramine and the C$(NO_2)_3$ moiety (in compound **3**: N3•••O4 2.83 Å), which leads to an atypical conformation with one nitro group (N4O_2) that is oriented approximately planar to the corresponding C2–C1–N4–O7 plane and one nitro group that is oriented almost perpendicular to it (N3O_2). Comparing the C2–C1–N3–O6 (94.4(1)°) dihedral angle in compound **3** with the respective values of nitramine-affected C$(NO_2)_3$ orientations in the literature, such as in 1,1,1,3,6,8,8,8-octanitro-3,6-diazaoctane (ONDO),[6] it is evident that the C1$(NO_2)_3$ moiety interacts with the nitramine group.

An analysis of the intermolecular interactions in compound **3** showed various interactions, including weak improper hydrogen-bonding interactions and dipolar N•••O interactions. In addition, a strong classical intermolecular hydrogen bond with covalent character was formed at the carboxylic group, with the following distances and angles: O1–H5•••O2 1.836(1) Å, O1•••O2 2.688(1) Å, and O1–H5•••O2 176(2)°. This interaction led to a dimeric structure of compound **3** (see the Supporting Information).

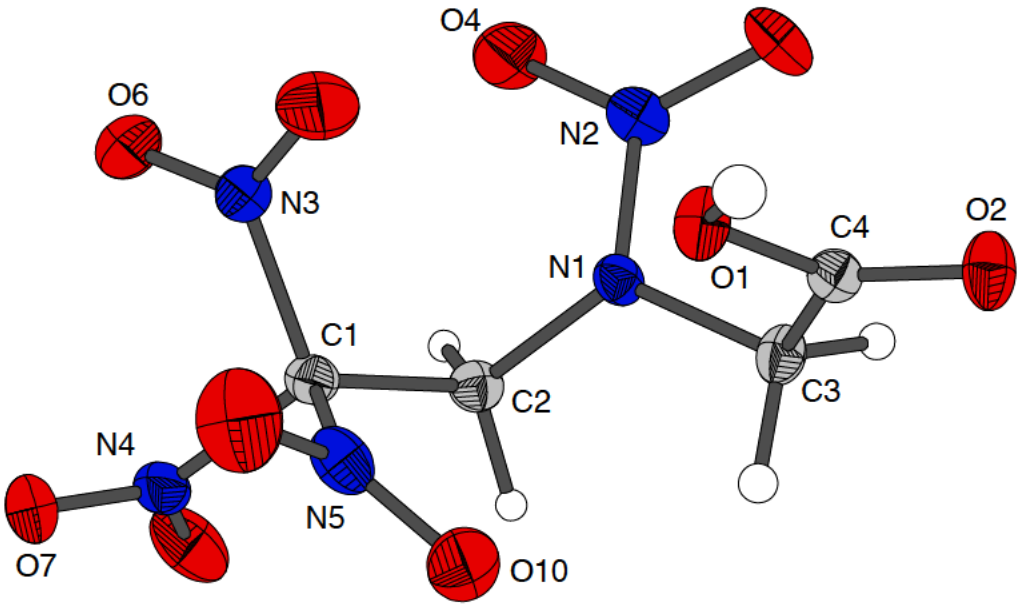

Figure 2.1. ORTEP of compound **3**. Selected distances [Å] and angles [°]: C3–C4 1.516(2), C1–$(NO_2)_{av}$ 1.525(2), C4–O1 1.301(2), C4–O2 1.216(1), N1–N2 1.371(2), O1–H5 0.85(2); C2–N1–C3 123.0(1), C2–N1–N2 115.7(1), C3–C4–O1 113.8(1), C3–C4–O2 120.8(1), O1–C4–O2 125.3(1); C2–C1–N3–O6 94.4(1), C2–C1–N4–O7 172.1(1), C2–C1–N5–O10 –22.4(1), C1–C2–N1–N2 –98.8(1), C2–N1–N2–O4 19.3(1), N2–N1–C3–C4 76.9(1), N1–C3–C4–O1 30.7(1).

The single-crystal structure of 2-(nitro-(2,2,2-trinitroethyl)amino)acetyl chloride (**4**) is displayed in Figure 2.2. Compound **4** crystallized in the triclinic space group $P\bar{1}$, with two formula units per unit cell and a density of 1.88 g cm^{-3} at 173 K. The bond lengths and angles in compound **4** are as expected for CHNO compounds that contain a trinitromethyl moiety.[1a, 2b, 5, 9] The average N–O bond length of the trinitromethyl moiety (1.209(2) Å) is slightly shorter than that of the corresponding nitramine moiety (1.220 Å), similar to compound **3**.[6] The C–Cl and C–O distances in the acid-chloride moiety are within the usual range for acid chlorides (1.761(2) and 1.177(2) Å, respectively).[11] The C3–N4–N5–O7 dihedral angle within the nitramine group is –18.7(2)°, which is close to the typical values in cyclic nitramines RDX and HMX.[10] The trinitroethyl moiety adopted a propeller-like structure, with C–C–N–O torsion angles of between 27.6(2)° and 74.0(2)°. Owing to the expected intramolecular interactions with the nitramine group at the N1 atom, the C3–C4–N5–O9 angle (74.0(2)°) was slightly outside of the usual range for trinitromethyl-containing compounds.[6] The length of the weak N•••O dipolar interaction between the nitramine and the trinitromethyl moiety is 2.950(2) Å, which approximately corresponds to the sum of the Van der Waals radii of oxygen and nitrogen

(about 2.9 Å).[6] An analysis of the intermolecular interactions of compound **4** showed various interactions, including weak improper hydrogen bonds and dipolar N•••O interactions.

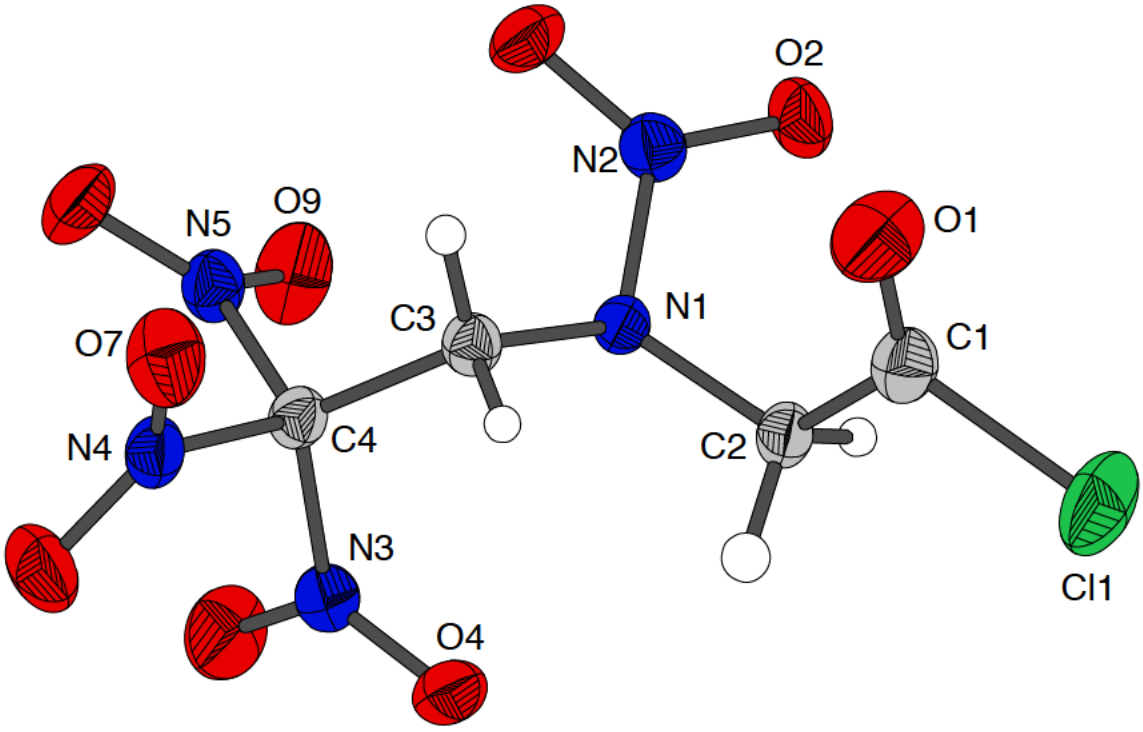

Figure 2.2. ORTEP of compound **4**. Selected distances [Å] and angles [°]: C1–C2 1.503(3), C1–O1 1.177(2), C1–Cl1 1.761(2), C4–$(NO_2)_{av}$ 1.523(2), N1–N2 1.398(2); C2–C1–O1 126.6(2), C2–C1–Cl1 111.9(1), C2–N1–N2 114.9(1), C3–C4–N3 113.1(1); C3–C4–N3–O4 28.2(2), C3–C4–N4–O7 27.6(2), C3–C4–N5–O9 74.0(2), C3–N1–N2–O2 163.1(2), N1–C2–C1–O1 –0.8(3).

Owing to the sensitivity of 2-(nitro-(2,2,2-trinitroethyl)amino)acetyl azide (**5**), single-crystal X-ray diffraction experiments turned out to be difficult. Suitable single crystals were obtained by recrystallization from $CHCl_3$. Compound **5** crystallized in the monoclinic space group $P2_1/n$, with four formula units in the unit cell and a theoretical maximum density of 1.84 g cm^{-3} at 173 K. The structure of compound **5** is shown in Figure 2.3. The bond lengths and angles in compound **5** are comparable to previously reported values for comparable CHNO compounds.[1a, 2b, 5, 9] The C3–N4–N5–O7 dihedral angle within the nitramine group is –18.3(3)°, which is approximately within the typical range of cyclic nitramines RDX and HMX.[10, 12] The average N-O bond length in the trinitromethyl moiety (1.206(3) Å) is shorter than that in the corresponding nitramine moiety (1.222(3) Å).[6] A similar behavior was observed in compounds **3**, **4**, and **6**. The

C4–N6 and C4–O1 distances of the carbonyl azide moiety are within the range for acid azides (1.380(3) and 1.206(3) Å, respectively).[13] Compared to compound **4**, the C4–O1 (1.206(3) Å) bond is slightly elongated, owing to the connected azide moiety. The N–N bond lengths (N6–N7 1.263(3), N7–N8 1.113(3) Å) in the azide moiety are typical of acid azides. The N6–N7–N8 angle (175.5(3) Å) indicates a slightly increased linearity compared to other substances that contain a carbonyl azide moiety.[13] The trinitromethyl moiety does not adopt a "real" propeller-like structure, with C2–C1–N–O torsion angles of between 11.4(3)° and 94.2(2)°. The expected intramolecular interaction with the N1 atom of the nitramine group leads to an atypical conformation, with an approximately planar-oriented nitro group ($N4O_2$), according to the corresponding C2–C1–N4–O6 (–11.4(3)°) plane, which is almost perpendicular (C2–C1–N3–O4 94.2(2)°) including the latter nitro group ($N3O_2$).[6] The length of the weak N•••O dipolar interaction between the nitramine and trinitromethyl moieties (2.879(3) Å) was shorter than the sum of the Van der Waals radii for oxygen and nitrogen (about 2.9 Å).[6] Analysis of the intermolecular interactions of compound **5** showed various interactions, including weak improper hydrogen bonds and dipolar N•••O interactions.

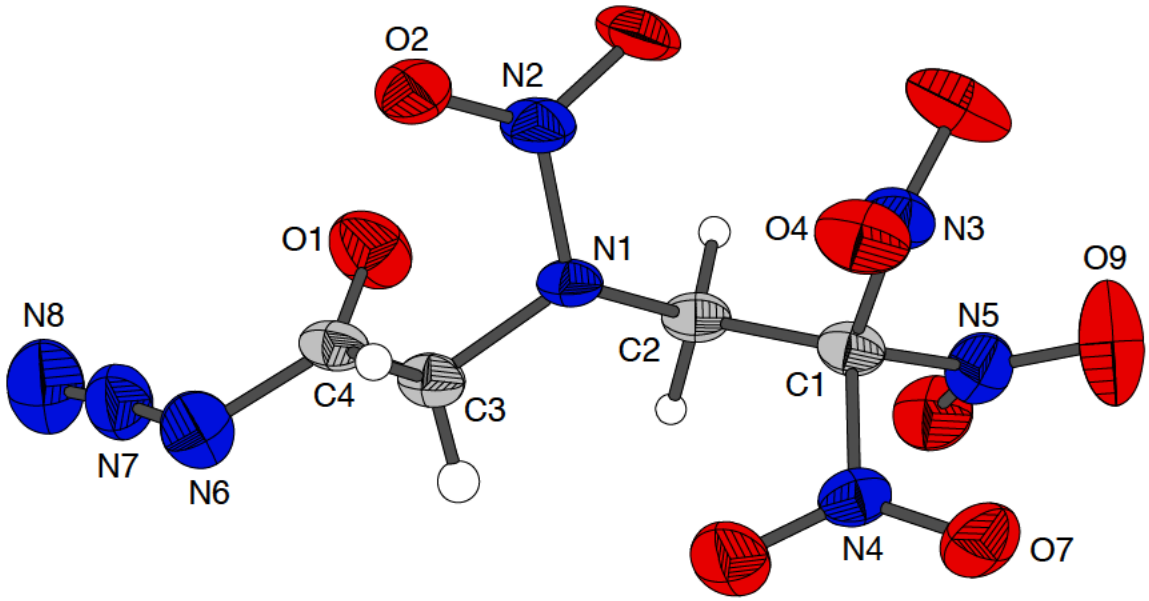

Figure 2.3. ORTEP of compound **5**. Selected distances [Å] and angles [°]: C3–C4 1.504(3), C4–O1 1.206(2), C1–$(NO_2)_{av}$ 1.529(3), C2–N1 1.453(3), C4–N6 1.380(3), N1–N2 1.388(3), N6–N7 1.263(3), N7–N8 1.113(3); C3–C4–N6 113.1(2), C3–C4–O1 122.9(2), C4–N6–N7 112.2(2), N6–N7–N8 175.5(3); C2–C1–N3–O4 94.2(2), C2–C1–N4–O7 169.0(2), C2–C1–N5–O9 155.8(2), C2–N1–N2–O2 164.3(2), O1–C4–N6–N7 4.3(3), C4–N6–N7–N8 157(3).

2,2,2-Trinitroethyl 2-(nitro-(2,2,2-trinitroethyl)amino)acetate (**6**) crystallized in the monoclinic space group $P2_1/c$, with four formula units in the unit cell (Figure 2.4). Suitable single crystals for X-ray diffraction measurements were obtained by recrystallization from EtOAc. The density at 173 K was calculated to be 1.92 g cm^{-3}. The bond lengths and angles in compound **6** were comparable with previously discussed values for CHNO compounds that contained a trinitromethyl moiety.[1a, 2b, 5, 9] As expected, the average N-O bond length in the trinitromethyl moieties (1.211(3) Å) was slightly shorter than that in the corresponding nitramine moiety (1.227(3) Å). The C3–O2 (1.192(3) Å), C3–O1 (1.355(3) Å), and C2–O1 (1.435(3) Å) bond lengths in the bridging ester moiety are within the typical range for organic compounds that contain an ester group.[14] The two trinitroethyl moieties display a molecular geometry, with a propeller-type orientation of the nitro groups that are connected to the C6 and C1 atoms. The twisted orientation is energetically favorable and leads to several N•••O dipolar interactions between the geminal NO_2 groups (2.59–2.61 Å), which are considerably shorter than the sum of the Van der Waals radii for oxygen and nitrogen (about 2.9 Å).[6] The shorter distances are caused by the fact that such twisting of the nitro groups decreases the intramolecular electrostatic repulsion between the oxygen atoms, whilst at the same time optimizing the attractive N•••O interactions between the geminal NO_2 groups. Therefore, disturbing effects, which are provided by a vicinal nitramine function, typically sharply distort the preferred C_3 geometry.[6] Such compounds show an electrostatic attraction between the nitro group of the nitramine and the $C(NO_2)_3$ moiety. In the case of compound **6**, this attraction can be observed in the N7•••O4 (2.825(3) Å) distance,[6] which leads to an atypical conformation with two nitro groups that are oriented approximately planar to the C5–C6 axis ($N6O_2$ and $N8O_2$) and one group that is almost perpendicular to it ($N7O_2$). The alignments of the nitro groups were characterized by the C5–C6–N6–O11 (–1.1(3)°), C5–C6–N8–O15 (7.3(3)°), and C5–C6–N7–O13 (88.7(2)°) torsion angles.[6] The trinitromethyl moiety that was connected to the C1 atom also showed a weak distortion compared to an idealized propeller configuration. Owing to the missing interaction with a nitramine group, the C2–C1–N–O dihedral angles in compound **5** are roughly within the typical range of propeller-type $XC(NO_2)_3$ compounds (23–67°).[6] The quite-high density for CHNO compounds is a result of various inter- and intramolecular dipolar interactions that affect the large number of nitro groups in compound **6**.

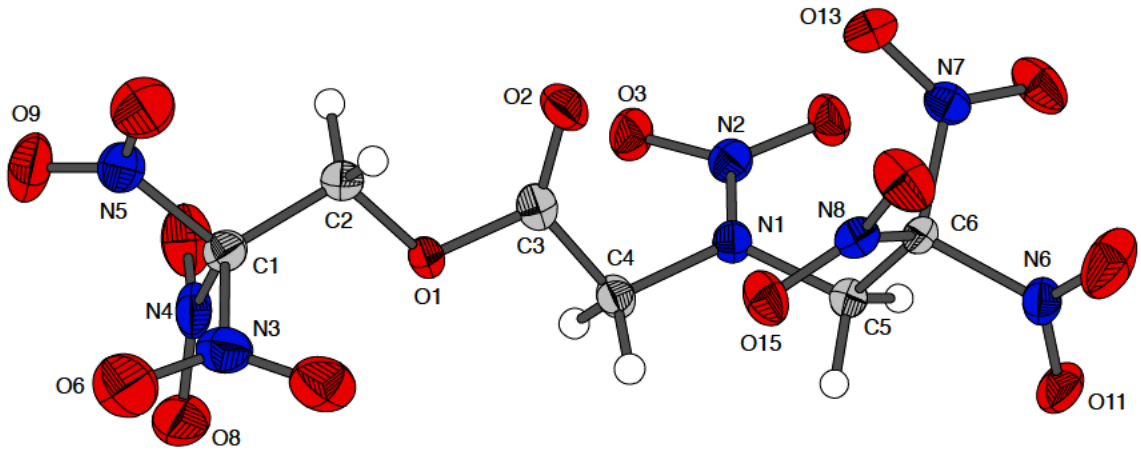

Figure 2.4. ORTEP of compound **6**. Selected distances [Å] and angles [°]: C3–C4 1.509(3), C3–O1 1.355(3), C3–O2 1.192(3), C1–$(NO_2)_{av}$ 1.518(3), C6–$(NO_2)_{av}$ 1.527(3), N1–N2 1.374(3); O1–C3–C4 108.9(2), C4–C3–O2 127.1(2), O1–C3–O2 124.0(2), C4–N1–N2 115.9(2); C2–C1–N3–O6 160.1(2), C2–C1–N4–O8 122.0(2), C2–C1–N5–O9 128.4(2), C2–O1–C3–O2 0.2(3), C4–N1–N2–O3 6.5(3), C5–C6–N6–O11 1.1(3), C5–C6–N7–O13 88.7(2), C5–C6–N8–O15 7.1(3).

2,2,2-Trinitroethyl (nitro-(2,2,2-trinitroethyl)amino)methyl carbamate (**7**) was crystallized from EtOAc/*n*-pentane by using diffusion techniques. Single-crystal X-ray diffraction experiments at 173 K showed that compound **7** crystallized in the monoclinic space group $P2_1/c$ with four molecular formula units per unit cell and a density of 1.81 g cm^{-3}. The molecular structure of compound **7** is shown in Figure 2.5. The bond lengths and angles in compound **7** are comparable to values reported in literature for CHNO compounds that contain a trinitromethyl moiety.[1a, 2b, 5, 9] The C3-N4-N5-O7 torsion angle is –17.20(19)°, which is comparable to the values in compounds **3**–**6**. The two trinitroethyl moieties displayed a molecular geometry with a propeller-type orientation of the nitro groups that were connected to the C6 and C1 atoms. As expected, a N•••O dipolar interaction was observed between a trinitromethyl group ($C1(NO_2)_3$) and the corresponding nitramine moiety (N3•••O8 2.961(2) Å),[6] which led to an atypical C2-C1-N3-O5 torsion angle of 72.2°. Octanitro-3,6-diazaoctane (ONDO)[6] and compounds **3**–**6** showed similar behavior. The N3•••O8 distance in compound **7** was rather elongated compared to those in ONDO (2.77 Å) and compound **3** (2.825 (3) Å). The trinitromethyl moiety that was connected to the C5 atom also showed weak distortion, owing to intramolecular attraction between the O10 and N8 atoms (2.667 (4) Å), although the C5–C6–N–O dihedral angles in compound **7** were within the typical range for propeller-type $XC(NO_2)_3$ compounds

(23–67°).[6] Analysis of the intermolecular interactions in compound **7** showed various interactions, including weak improper hydrogen bonds and dipolar N•••O interactions.

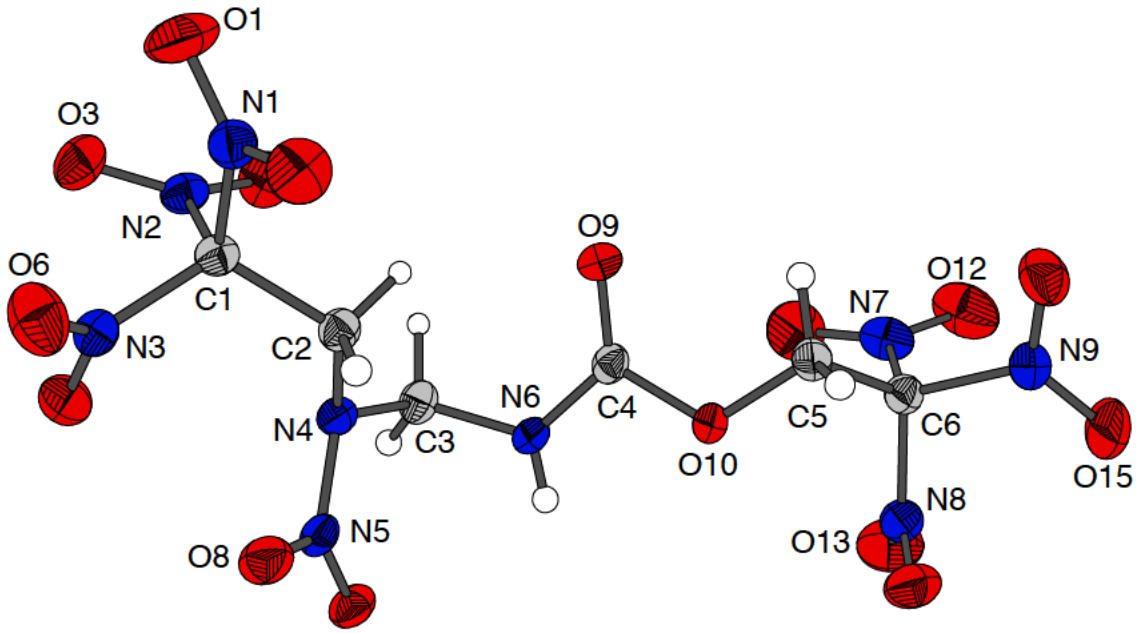

Figure 2.5. ORTEP of compound **7**. Selected distances [Å] and angles [°]: N4–N5 1.3976(18), C1–$(NO_2)_{av}$ 1.530(2), N6–H6 0.783(18), C6–$(NO_2)_{av}$ 1.522(2); N5–N4–C2 113.86(13), O9–C4–N6 126.78(15), O9–C4–O10 124.54(15), N6–C4–O10 108.67(13); C2–C1–N1–O1 142.6(1), C2–C1–N2–O3 1611.0(1), C2–C1–N3–O6 107.5(2), C5–C6–N7–O12 140.4(2), C5–C6–N8–O13 126.2(2), C5–C6–N9–O15 149.8(2), N6–C4–O9–O10 179.3(3), C2–N4–N5–O8 23.3 (2).

The single-crystal structure of compound **9** is shown in Figure 2.6. It crystallizes in the monoclinic space group $P2_1/c$, with four formula units per unit cell and a density of 1.60 g cm^{-3} at 173 K. The bond lengths and angles in compound **9** are comparable to literature values for CHNO compounds that contain a trinitromethyl moiety.[1a, 2b, 5, 9] The average N-O bond length of the trinitromethyl moiety (1.215(4) Å) is slightly longer than those in the previously discussed compounds **3**–**8**.[6] The carbamate moiety is characterized by the following bond lengths: C3–O8 (1.202(4) Å), C3–O7 (1.372(3) Å), and C3–N4 (1.337(4) Å). The carbamate moiety shows typical bond lengths and angles.[15] In addition, the N4–C3–O8–O7 torsion angle of 177.2(6)° indicates an almost-planar orientation of the carbamate moiety. The trinitromethyl moiety that is connected to the C1 atom also shows weak distortion compared to an idealized propeller configuration. Owing to the missing interaction with a nitramine group, the C2–C1–N–O dihedral angles (average: –46.0(3)°) in compound **8** are within the typical range for propeller-type

$XC(NO_2)_3$ compounds (23–67°).[6] The C5-O9 (1.212(4) Å) and C5–O10 bond lengths (1.316(3) Å) of the ester moiety are within the typical range for organic compounds that contain an ester group.[14]

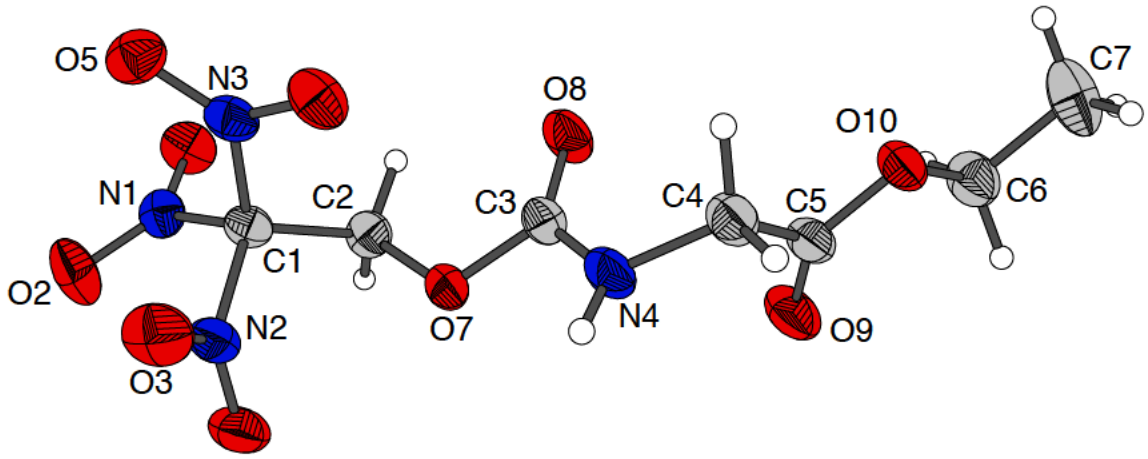

Figure 2.6. ORTEP of compound **9**. Selected distances [Å] and angles [°]: C1–$(NO_2)_{av}$ 1.513(4), C6–C7 1.478(4), N4–C3 1.337(4), O10–C5 1.316(3), O10–C6 1.462(3), O7–C3 1.372(3), O8–C3 1.202(4), O9–C5 1.212(4); C4–N4–C3 118.1(3), C5–O10–C6 116.5(2), O10–C5–O9 123.6(3), O7–C3–N4 109.8(3), O7–C3–O8 123.3(3), O8–C3–N4 126.8(3), O9–C5–C4 125.6(3); C2–C1–N1–O2 133.2(3), C2–C1–N2–O3 135.1(3), C2–N3–O5 135.8(3), C2–N4–C3–O8 –3.5(5), O7–C3–O8–N4 –177.2(6), C4–C5–O10–O9 179.2(5).

Ethyl 2-(nitro-((2,2,2-trinitroethoxy)carbonyl)amino)acetate (**10**) crystallized in the monoclinic space group $P2_1/c$, with four formula units per unit cell and a density of 1.63 g cm^{-3} at 173 K (Figure 2.7). The bond lengths and angles in compound **10** are comparable to literature values for CHNO compounds that contain a trinitromethyl moiety.[1a, 2b, 5, 9] The C4–N1–N2–O5 dihedral angle is –11.9(2)°, which is narrower than the typical range in cyclic nitramines RDX and HMX.[10] In addition, the N-nitro moiety is twisted away from the almost-planar carbamate moiety (N1–C5–O3–O4 177.0(3)°), with a C5–N1–N2–O6 torsion angle of –26.7(2)°. The average N-O bond length in the trinitromethyl moiety (1.208(4) Å) is slightly shorter than that in the corresponding N-nitrocarbamate moiety (1.216(2) Å), owing to some shared π-electron density between the N-N bond and the N-O bonds of the nitramine group.[6] The C3–O2 (1.201(2) Å), C3–O1 (1.321(3) Å), and C2–O1 bond lengths (1.460(2) Å) of the ester moiety are in agreement with the corresponding values in compound **9**. The $C7(NO_2)_3$ trinitromethyl moiety shows a rotational disorder of the nitro groups, with one non-disordered oxygen atom per

nitro group into a second structural domain. To yield the second disordered structure, the nitro moieties on the N3A, N4A, and N5A atoms are rotated around the O8 (35.3(3)°), O10 (44.8(3)°), and O12 atoms (40.7(3)°), respectively. The angles for each of the nitro groups to be turned through clockwise are shown in parentheses. The relative distributions of the A and B structures of the trinitromethyl moiety were assigned to be 50:50. The disorder of the trinitromethyl moiety is shown in the Supporting Information. Such disorders of the crystal structure are not uncommon for compounds that contain a trinitromethyl moiety. Even phase transformations at different temperatures have often been discovered with trinitromethyl CHNO compounds.[1a, 1b, 16] Nevertheless, both conformations A and B showed the typical propeller-type arrangement of the trinitromethyl moiety, with averaged C6–C7–N(A/B)-O(A/B) torsion angles of 38.1(4)° for conformation A and –38.3(4)° for conformation B.

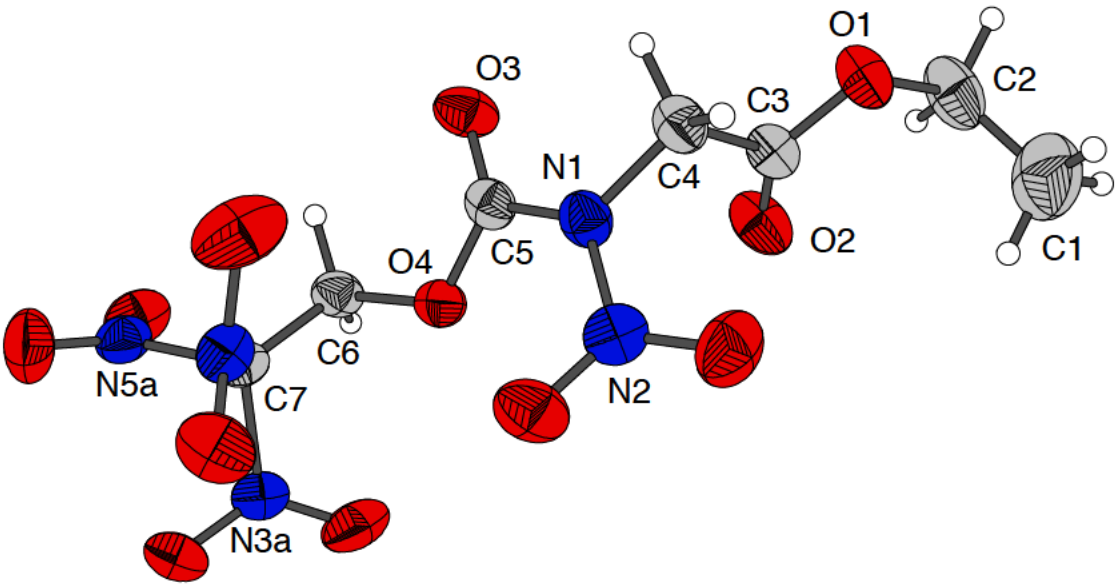

Figure 2.7. ORTEP of compound **10**, disorder not shown. Selected distances [Å] and angles [°]: C5–N1 1.402(2), N1–N2 1.415(2), N1–C4 1.457(2), O1–C2 1.460(2), O1–C3 1.321(2), O2–C3 1.201(2), O3–C5 1.195(2), O4–C5 1.338(2); O4–C5–O3 126.0(2), O4–C5–N1 112.2(1), O3–C5–N1 121.7(2), C5–N1–N2 123.7(1), C5–N1–C4 119.3(1), O1–C3–O2 126.3(2), O1–C3–C4 109.3(1), O2–C3–C4 124.3(2); O4–C5–O3–N1 –177.0(3), C5–N1–N2–O6 –26.7(2), C4–C3–O2–O1 178.3(3).

Table 2.3. Crystal and structure refinement data for **3**–**7**, **9**–**10**

	3	**4**	**5**	**6**	**7**	**9**	**10**
empirical formula	$C_4H_5N_5O_{10}$	$C_4H_4ClN_5O_9$	$C_4H_4N_8O_9$	$C_6H_6N_8O_{16}$	$C_6H_7N_9O_{16}$	$C_7H_{10}N_4O_{10}$	$C_7H_9N_5O_{12}$
formula mass /g mol^{-1}	283 1	301 6	308 1	446 2	461 2	310 2	355 2
temperature /K	173(2)	173(2)	173(2)	173(2)	173(2)	173(2)	173(2)
crystal size /mm	0 25 × 0 19 × 0 09	0 24 × 0 15 × 0 08	0 31 × 0 24 × 0 20	0 25 × 0 05 × 0 01	0 15 × 0 15 × 0 14	0 18 × 0 06 × 0 02	0 25 × 0 15 × 0 08
crystal description	colorless platelet	colorless platelet	colorless block	colorless needle	colorless block	colorless needle	colorless block
crystal system	monoclinic	triclinic	monoclinic	monoclinic	monoclinic	monoclinic	monoclinic
space group	$P2_1/c$	$P\bar{1}$	$P2_1/n$	$P2_1/c$	$P2_1/c$	$P2_1/c$	$P2_1/c$
a /Å	10 9200(4)	6 0538(5)	9 9618(7)	5 9751(1)	9 5960(8)	13 132(3)	12 8990(6)
b /Å	6 3120(2)	7 9260(5)	5 9327(4)	10 74990(29)	18 7730(13)	5 6826(17)	5 6642(3)
c /Å	14 9880(5)	11 9001(8)	19 1585(11)	24 01500(50)	9 5200(8)	18 028(6)	19 7870(9)
α /°	90	82 641(5)	90	90	90	90	90
β /°	103 984(4)	78 083(6)	100 053(6)	91 7041(14)	100 154(7)	106 28(3)	92 647(5)
γ /°	90	72 522(7)	90	90	90	90	90
V /Å^3	1002 46(6)	531 56(7)	1114 89(13)	1541 84	1688 1(2)	1291 4(6)	1444 15(12)
Z	4	2	4	4	4	4	4
ρ_{calc} /g cm^{-3}	1 87587(11)	1 8841(2)	1 8357(2)	1 92204(1)	1 8146(2)	1 5954(7)	1 63359(14)
μ /mm^{-1}	0 188	0 420	0 179	0 194	0 182	0 152	0 159
F(000)	576	304	624	904	936	640	728
θ range /°	4 28 – 28 00	4 26 – 26 00	4 25 – 26 00	3 17 – 25 35	4 28–25 75	4 23–25 24	4 15–25 75
index ranges	$-13 \le h \le 14$	$-7 \le h \le 7$	$-7 \le h \le 12$	$-7 \le h \le 7$	$-8 \le h \le 11$	$-13 \le h \le 15$	$-15 \le h \le 15$
	$-5 \le k \le 8$	$-9 \le k \le 9$	$-7 \le k \le 7$	$-12 \le k \le 12$	$-20 \le k \le 22$	$-6 \le k \le 5$	$-6 \le k \le 6$
	$-19 \le l \le 9$	$-14 \le l \le 14$	$-23 \le l \le 23$	$-28 \le l \le 28$	$-11 \le l \le 7$	$-21 \le l \le 21$	$-24 \le l \le 24$
reflections collected	5849	5399	5230	10049	8481	6035	13524
reflections observed	2403	2076	2174	2820	3210	2331	2742
reflections unique	1756	1509	1222	2026	2482	1485	2088
$R1$; $wR2$ (2σ data)	0 0316; 0 0705	0 0326; 0 0729	0 0368; 0 0735	0 0408; 0 0903	0 0330; 0 00699	0 0510; 0 1056	0 0391; 0 0906
$R1$; $wR2$ (all data)	0 0451; 0 0740	0 0484; 0 0769	0 0798; 0 0812	0 0691; 0 1013	0 0489; 0 0794	0 0903; 0 1267	0 0551; 0 1012
max ; min transmission	1 00000; 0 98965	0 99999; 0 93162	1 00000; 0 65045	1 00000; 0 03341	1 00000; 0 96187	1 00000; 0 50257	1 00000; 0 85790
data; restraints; parameters	2403; 0; 192	2076; 0; 188	2174; 0; 206	2820; 0; 271	3210; 0; 308	2331; 0; 194	2742; 0; 271
GOOF on F^2	0 925	0 936	0 830	1 090	1 022	1 008	1 032
diff peak; hole /e Å^{-3}	0 057; –0 319	0 284; –0 309	0 203; –0 177	0 414; –0 319	0 219; –0 200	0 296; –0 275	0 298; –0 237

Thermal and energetic properties

Compounds **2**, **3**, and **6**–**10** were stable when exposed to air and moisture. 2-(Nitro-(2,2,2-trinitroethyl)amino)acetyl azide (**5**) has to be handled very carefully, owing to its high sensitivity towards external stimuli. Reactions that were carried out with this explosive compound were performed under the rigorous exclusion of moisture. The thermal stabilities of compounds **1**–**10** were investigated by performing various DSC measurements (heating rate: 5 °C min^{-1}). The temperatures at which melting and decomposition occurred are shown in Table 2.4. A remarkably high melting point of 148 °C was observed for compound **3**, likely owing to its ability to form strong hydrogen bonds through the carboxylic acid moiety. Moreover, compounds **6** (133 °C) as **8** (132 °C) showed satisfying melting points for applications as high-energy dense oxidizers based on CHNO compounds.[1a, 1c, 5] The highest decomposition temperature was observed for compound **10** (190 °C), followed by compounds **6** and **9** (183 and 177 °C, respectively). The physical and chemical properties of these compounds are listed in Table 4.

The sensitivities of compounds **2**–**10** towards impact, friction, and electrostatic discharge were experimentally determined according to standards of the Federal Institute for Materials Research and Testing (BAM);[17] the results are displayed in Table 2.5. Compound **1** could not be measured properly, owing to its tendency to hydrolyze at ambient temperature, whereas compounds **3** and **4** showed moderate impact sensitivities of 15 and 30 J, respectively. Compounds **2** and **9** turned out to be insensitive towards impact stimuli, probably because of the ethyl-ester protecting group. Compounds **2**, **3**, **8**, and **10** showed moderate friction sensitivities. In addition, the flame test of compounds **1**–**10** showed smoke- and residue-less burning with a yellow flame in all cases.

Table 2.4. Physical and chemical properties of **1**–**10**

	1	**2**	**3**	**4**	**5**	**6**	**7**	**8**	**9**	**10**
formula	$C_6H_{10}N_4O_8$	$C_6H_9N_5O_{10}$	$C_4H_5N_5O_{10}$	$C_4H_4ClN_5O_9$	$C_4H_4N_8O_9$	$C_6H_6N_8O_{16}$	$C_6H_7N_9O_{16}$	$C_6H_6N_{10}O_{18}$	$C_7H_{10}N_4O_{10}$	$C_7H_9N_5O_{12}$
mol mass /g mol^{-1}	266 17	311 16	283 11	301 56	308 12	446 16	461 17	506 17	310 18	355 17
T_m /°C [a]	--	72	148	79	69	133	96	132	59	26
T_d /°C [b]	123	172	167	174	89	183	170	161	177	190
N /% [c]	21 05	22 51	24 74	23 22	36 37	25 12	27 33	27 67	18 06	19 72
N + O /% [d]	69 14	73 93	81 25	70 97	83 10	82 50	82 84	84 57	69 64	73 78
ΩCO /%[e]	–18 03	–2 57	19 78	18 57	15 58	25 10	22 55	28 45	–46 4	–29 3
ΩCO2 /% [f]	–54 10	–33 42	–2 83	–2 65	–5 19	3 59	1 73	9 48	–10 3	2 2
ρ /g cm^{-3} [g]	1 53	1 40	1 82	1 83	1 80	1 87	1 79	1 90	1 54	1 58
$-\Delta U°_f$ /kJ kg^{-1} [h]	1607 13	1163 04	1413 00	719 85	515 42	790 84	831 22	519 12	2711 11	2092 51
$-\Delta H°_f$ /kJ kg^{-1} [i]	1709 57	1258 63	1500 56	797 94	599 89	874 18	917 22	602 38	2806 90	2183 24

[a] Melting (T_m) and [b] decomposition temperatures (T_d) as determined by DSC measurement at a heating rate of 5 °C min^{-1}. [c] Nitrogen content. [d] Combined nitrogen and oxygen content. [e] Oxygen balance, assuming the formation of CO; the oxygen balance of ammonium perchlorate is 34.0 %. [f] Oxygen balance, assuming the formation of CO_2. [g] Experimentally determined density from pycnometer experiments. [h] Energy of formation. [i] Heat of formation.

Predictions of the detonation parameters by using the EXPLO5 code[18] have been performed based on the heats of formations that were obtained from ab initio calculations by using the Gaussian 09 program package[12, 19] at the CBS-4M level of theory. The energetic parameters were attributed to the density of the corresponding compound. The resulting heats of detonation (Q_v), detonation temperatures (T), pressures (p), and velocities (D) for compounds **1**–**10** are shown in Table 2.5, as well as the oxygen balances (Ω). The densities that were needed to estimate the detonation parameters with the EXPLO5 code[18] were derived from the single-crystal X-ray structures of compounds **3**–**10**. The densities of compounds **1** and **2** were determined experimentally by performing gas pycnometer measurements.

Table 2.5. Predicted detonation and combustion parameters (using the EXPLO5 code) and sensitivity data for **1–10**

	1	**2**	**3**	**4**	**5**	**6**	**7**	**8**	**9**	**10**
$-Q_v$ /kJ kg^{-1} [a]	4941	5478	5763	5508	6342	5922	5882	5479	4169	4882
T_{ex} /K [b]	3378	3960	4330	4575	4823	4566	4535	4345	3098	3642
V_0 /L kg^{-1} [c]	721	716	684	647	684	675	689	684	690	677
p /kbar [d]	200	184	323	302	342	345	319	340	181	214
D /m s^{-1} [e]	7259	7036	8351	8022	8591	8518	8340	8491	6890	7255
impact /J [f]	--	>40	15	30	<1	3	5	2	40	7
friction /N [f]	--	192	144	64	48	64	72	120	54	144
ESD /J [g]	--	0 035	0 036	0 17	0 03	0 25	0 035	0 035	0 2	0 2
grain size /µm [h]	--	<100	100–500	100–500	100–500	<100	<100	<100	<100	100–500
thermal shock [i]	burns	burns	burns	burns	burns violently	burns	burns	burns	burns	burns
I_s /sec [j]	210	242	241	234	250	240	241	237	192	227
I_s /sec [k]	--	--	250	239	--	258	256	262	--	--
Ω_{comp} /% [l]	--	--	–55 95	–55 82	--	–51 45	–52 75	–47 32	--	--
$I_{s(20\%Al)}$ /sec [m]	--	--	254	250	--	254	255	253	--	254
$\Omega_{(20\%Al)}$ /% [n]	--	--	–20 05	–19 91	--	–14 92	–16 00	–10 20	--	–41 27

[a] Heat of explosion. [b] Temperature of the explosion gases. [c] Volume of the explosion gases (assuming only gaseous products). [d] Detonation pressure. [e] Detonation velocity. [f] Impact and friction sensitivities, according to standard BAM methods.[17] [g] Sensitivity towards electrostatic discharge. [h] Grain size of the samples that were used for the sensitivity tests. [i] Response to fast heating in the "flame test". [j] Specific impulse for a pure compound by using the EXPLO5 code.[18] [k] Specific impulse for compositions with 70 % oxidizer, 16 % aluminum, 6 % polybutadiene acrylic acid, 6 % polybutadiene acrylonitrile, and 2 % bisphenol-A ether by using the EXPLO5 code (chamber pressure: 70.0 bar).[18] The specific impulse for a similar composition with ammonium perchlorate was also calculated (I_s(AP)=258 s, Ω_{comp}(AP)=–30.13 %). [l] Oxygen balance for the composition that was used in the combustion calculations; the oxygen balance for a comparable composition with ammonium perchlorate is –30.13 %. [m] Specific impulse for compositions with 80 % oxidizer and 20 % aluminum at by using the EXPLO5 code (chamber pressure: 70.0 kbar).[18] The specific impulse for a similar composition

with ammonium perchlorate was also calculated ($I_{s(20\ \%Al)}$(AP)=232 s, $\Omega_{(20\ \%Al)}$(AP)=9.44 %). [n] Oxygen balance for 80 % oxidizer and 20 % Al in the combustion calculations.

The specific impulses of compounds **3**, **4**, and **6**–**8** were calculated for compositions of 70 % oxidizer, 16 % aluminum, 6 % polybutadiene acrylic acid, 6 % polybutadiene acrylonitrile, and 2 % bisphenol-A ether, as modeled on rocket motor compositions for solid-state rocket boosters that are used in the NASA Space Shuttle Program.[20] These impulses were compared with the calculated impulse of ammonium perchlorate (AP) in an analogous composition. The chosen mixture with AP as an oxidizer provided a specific impulse of 258 s. The impulses for compounds **3**, **6**, and **7** (250–258 s) were within the range of AP. The specific impulse of a composition with compound **6** as an oxidizer (I_s=258 s) was comparable to that with AP. Compound **8** showed an increased specific impulse of 262 s. The lower oxygen balance of compounds **3**, **4, 6**, and **7** versus AP also led to a decreased oxygen balance for the calculated formulations, varying between –55.95 % and –51.47 %. The composition with compound **8** as an oxidizer led to an oxygen balance of –47.32 %. A similar composition with AP as an oxidizer had an oxygen balance of –30.13 %. In addition, the specific impulses were also calculated for compositions of 80 % oxidizer (**3**–**8** and **10**) with 20 % neat aluminum. The calculated impulses varied from 250–255 s and were significantly higher than that for a similar AP formulation (232 s). Moreover, the specific impulses were also calculated for the neat compounds. Calculations of the other compounds were omitted, owing to the insufficient resulting oxygen balance of the considered compositions or the missing stability data of the desired compound. The results of the calculations are shown in the Table 2.5.

2.4 CONCLUSION

Based on the previous work of Feuer et al.,[3a] new energetic glycine-based polynitro compounds with a positive oxygen balance were synthesized. All of the compounds were characterized by using multinuclear NMR spectroscopy, vibrational spectroscopy, elemental analysis, and mass spectrometry; in addition, most compounds were also characterized by single-crystal X-ray crystallography. The thermal stability of these compounds was investigated by performing DSC measurements. The sensitivities (according to BAM standards) of these compounds were determined and their energetic parameters were estimated from theoretical calculations. With respect to a possible application as high-energy dense oxidizers in solid rocket boosters, the specific impulses (I_s) of the most-promising compounds (**3**, **6**, **7**, and **8**) were calculated in formulations with fuel and additives. In particular, compounds **6** and **8** might be promising oxidizers with equal or even superior specific impulses (I_s(**6**)=258 s, I_s(**8**)=262 s) compared to similar formulations with ammonium perchlorate (AP, I_s(AP)=258 s) as an oxidizer. In addition, the sensitivities of compounds **6** and **8** were almost within the range of pentaerythritol tetranitrate (PETN), thereby fulfilling the minimum requirements of an oxidizer in terms of sensitivity.

2.5 EXPERIMENTAL SECTION

General Procedures

The syntheses and manipulation of air- and moisture-sensitive materials were performed under an inert atmosphere of dry argon (purity: 5.0, Air Liquide) by using flame-dried glassware and Schlenk techniques.[21] Glycine, thionyl chloride, aluminum(III) chloride, sodium hydroxide, acetic anhydride, sodium azide, magnesium sulfate, and all of the acids and solvents were purchased from Sigma-Aldrich and used as received. Ethyl 2-aminoacetate hydrochloride, 2,2,2-trinitroethanol, and 2,2,2-trinitroethyl chloroformate were prepared according to literature procedures.[1c, 3b, 4b]

Raman spectra were recorded on a Bruker FT-Raman-MultiRAM Spectrometer that was equipped with a Klaastech DENICAFC LC-3/40 laser source at 300 mW laser power; IR spectra were recorded on a Perkin-Elmer Spectrum BX-FTIR spectrometer that was equipped with a Smiths DuraSamplIR II ATR device. All of the spectra were recorded at ambient temperature as neat samples. Densities were determined at ambient temperature on a Quantachrome Ultrapyc1200e gas pycnometer that was equipped with helium gas (purity: 5.6, Air Liquide). NMR spectra were recorded on a JEOL Eclipse 400 spectrometer and the chemical shifts were determined with respect to external references Me_4Si (^1H: 399.8 MHz, ^{13}C: 100.5 MHz) or $MeNO_2$ (^{14}N: 28.9 MHz). Mass spectrometry data were recorded on a JEOL MStation JMS 700 spectrometer (DEI+/DCI+). Elemental analysis was performed on an Elementar Vario EL Analyzer. Melting points were measured on a Perkin-Elmer Pyris6 DSC at a heating rate of 5 °C min^{-1} and checked by using a Büchi Melting Point B-540 apparatus and are uncorrected. The sensitivity data were performed by using a BAM drop hammer and a BAM friction tester.[17]

Computational details

All of the quantum-chemical calculations were carried out by using the Gaussian 09 (Revision B.03)[12] program package and visualized by using Gaussview 5.08.[19] Structure optimizations and frequency analyses were performed by using Becke's B3 three-parameter hybrid functional with the LYP correlation functional (B3LYP). For the C, H, N, and O atoms, a correlation-consistent polarized double-zeta basis set was used (cc-pVDZ). The structures were optimized without symmetry constraints and the energies were corrected by using the zero-point vibrational energies.[22]

The enthalpies ($\Delta H°$) and free energies ($\Delta G°$) were calculated by using the complete basis set method (CBS-4M), based on ab initio optimized structures or on X-ray diffraction data to obtain accurate values.[22a] The CBS models use the known asymptotic convergence of a pair of natural orbital expressions to extrapolate from calculations by using a finite basis set to the estimated complete basis-set limit. CBS-4 starts with a HF/3-21G(d) structure optimization, which is the initial guess for the following SCF calculations as a base energy and final MP2/6-31+G calculations with a CBS extrapolation to correct the energy in second order. The re-parameterized CBS-4M method also implements MP4(SDQ)/6-31+(d,p) calculations to approximate higher-order contributions and includes some additional empirical corrections.[22b,c] The enthalpies of the gas-phase species were estimated according to the atomization energy method.[22a, 23]
All of the calculations that affected the detonation parameters were carried out by using the EXPLO5 V5.05 program package.[18, 24] The detonation parameters were calculated at the CJ point with the aid of the steady-state detonation model by using a modified Becker-Kistiakowski-Wilson equation of state for modeling the system. The CJ point was determined from the first derivative of the Hugoniot curve of the system.[24–25] The specific impulses were also calculated by using the EXPLO5 V5.05 program, assuming the isobaric combustion of a composition of 70 % oxidizer, 16 % aluminum as the fuel, 6 % polybutadiene acrylic acid, 6 % polybutadiene acrylonitrile as a binder, and 2 % bisphenol-A as the epoxy-curing agent.[20] A chamber pressure of 70.0 bar and an ambient pressure of 1.0 bar with frozen expansion conditions were estimated for the calculations.

X-ray crystallography

For the compounds measured, an Oxford Xcalibur3 diffractometer with a CCD area detector was employed for the data collection by using $Mo_{K\alpha}$ radiation (λ=0.71073 Å). The structures were solved by using direct methods (SIR97)[26] and refined by full-matrix least-squares on F^2 (SHELXL).[27] All non-hydrogen atoms were refined anisotropically. The hydrogen atoms were located in a difference Fourier map and placed with a C-H distance of 0.99 Å for CH_2 groups. ORTEP plots are shown with thermal ellipsoids at the 50 % probability level.
CCDC-916793 (**6**), CCDC-916794 (**9**), CCDC-916795 (**10**), CCDC-916796 (**5**), CCDC-916797 (**4**), CCDC-916798 (**3**), and CCDC-916799 (**7**) contain the supplementary crystallographic data for this paper. These data can be obtained free of charge from The Cambridge Crystallographic Data Centre via www.ccdc.cam.ac.uk/data_request/cif.

CAUTION! All compounds with high nitrogen and oxygen content are potentially explosive energetic materials, although no hazards were observed during our preparation and handling of these compounds. Nevertheless, this property necessitates the meticulous use of additional safety precautions (earthed equipment, Kevlar gloves, Kevlar sleeves, face shield, leather coat, and ear plugs). In addition, 2,2,2-trinitroethanol has shown significant levels of toxicity,[28] including in own recent results.[29] Therefore, particular care should be exercised in the handling of those materials and their derivatives.

*Ethyl 2-(2,2,2-trinitroethylamino)acetate (**1**)*

Compound **1** was prepared according to a literature procedure.[3a, 30] Owing to its low stability, compound **1** was converted into compound **2** immediately after drying.

^{1}HNMR (CD_3CN): δ = 4.14 (q, ^{3}J(H,H)=7.0 Hz, 2 H; OCH_2CH_3), 3.80 (br s, 1 H; NH), 3.77 (s, 2 H; $NCH_2C(NO_2)_3$), 3.43 (s, 2 H; $COCH_2N$), 1.23 ppm (t, 3 H; CH_3); $^{13}C\{^{1}H\}$ NMR (CD_3CN): δ = 171.1 (COO), 73.5 ($OCCH_2N$), 61.8 (OCH_2), 54.0 ($NCH_2C(NO_2)_3$), 14.4 ppm (CH_3); ^{14}N NMR (CD_3CN): δ = –29 ppm (br; $C(NO_2)_3$); IR: ν = 3433 (w), 2989 (vw), 1724 (s), 1600 (s), 1576 (vs), 1482 (vw), 1467 (vw), 1447 (vw), 1413 (vw), 1392 (vw), 1373 (vw), 1347 (vw), 1330 (vw), 1306 (m), 1204 (m), 1134 (vw), 1097 (vw), 1015 (w), 961 (w), 872 (vw), 855 (vw), 803 (w), 777 (vw), 734 (vw), 697 cm^{-1} (vw); Raman: ν = 2988 (9), 2962 (71), 2948 (2), 2898 (3), 2859 (3), 1732 (16), 1616 (2), 1602 (18), 1587 (5), 1484 (17), 1455 (18), 1438 (4), 1418 (8), 1388 (13), 1357 (22), 1309 (37), 1182 (3), 1129 (3), 1098 (11), 1016 (6), 976 (3), 898 (28), 857 (100), 807 (8), 775 (5), 703 (4), 665 (6), 553 (12), 503 (3), 465 (2), 418 (20), 401 (7), 369 (37), 273 (28), 248 (2), 208 cm^{-1} (10); MS (DEI^{+}): *m*/*z* (%): 267 (3) $[M+H]^{+}$, 220 (38) $[M-NO_2]^{+}$, 193 (100) $[M-COOC_2H_5]^{+}$, 147 (68) $[M-COOC_2H_5-NO_2]^{+}$, 116 (7) $[M-C(NO_2)_3]^{+}$.

*Ethyl 2-(nitro-(2,2,2-trinitroethyl)amino)acetate (**2**)*

Compound **2** was prepared by the nitration of compound **1**.[3a]

^{1}H NMR ([D_6]DMSO): δ = 6.01 (s, 2 H; $NCH_2C(NO_2)_3$), 4.73 (s, 2 H; $COCH_2N$), 4.17 (q, ^{3}J(H,H)=7.1 Hz, 2 H; OCH_2CH_3), 1.21 ppm (t, 3 H; CH_3); $^{13}C\{^{1}H\}$ NMR ([D_6]DMSO): δ = 166.6 (COO), 123.7 (br; $C(NO_2)_3$), 61.6 (OCH_2CH_3), 55.0/53.7 ($OCCH_2N/NCH_2C(NO_2)_3$), 13.9 ppm (CH_3); ^{14}N NMR ([D_6]DMSO): δ = –32 (br; NO_2), –34 ppm (br; NO_2); ^{1}H NMR (CD_3CN): δ = 5.64 (s, 2 H; $NCH_2C(NO_2)_3$), 4.60 (s, 2 H; $COCH_2N$), 4.21 (q, ^{3}J(H,H)=7.2 Hz, 2 H; OCH_2CH_3), 1.24 ppm (t, 3 H; CH_3); $^{13}C\{^{1}H\}$ NMR (CD_3CN): δ = 62.9 (OCH_2CH_3), 55.5/54.7 ($OCCH_2N/NCH_2C(NO_2)_3$), 14.0 ppm

(CH_3); ^{14}N NMR (CD_3CN): δ = –32 (NO_2), –34 ppm (NO_2); IR: ν = 3007 (m), 2969 (w), 2911 (w), 1743 (s), 1620 (s), 1610 (s), 1583 (vs), 1566 (s), 1475 (vw), 1434 (w), 1399 (m), 1378 (m), 1354 (w), 1333 (vw), 1306 (m), 1279 (vs), 1221 (vs), 1138 (vw), 1100 (vw), 1021 (m), 945 (w), 890 (vw), 868 (w), 853 (w), 804 (m), 787 (w), 766 (w), 719 (vw), 640 (vw), 610 cm^{-1} (vw); Raman: ν = 3024 (8), 3007 (24), 2984 (91), 2979 (14), 2946 (17), 2932 (3), 2881 (7), 2785 (4), 2738 (2), 1754 (23), 1632 (5), 1610 (24), 1586 (7), 1567 (10), 1455 (16), 1434 (9), 1400 (11), 1348 (38), 1306 (8), 1283 (64), 1138 (4), 1102 (10), 1014 (4), 991 (10), 945 (7), 933 (2), 891 (54), 871 (8), 858 (100), 806 (4), 789 (5), 769 (3), 723 (7), 670 (3), 641 (15), 611 (8), 555 (10), 445 (4), 432 (23), 388 (30), 364 (54), 345 (8), 283 cm^{-1} (24); MS (DEI$^+$): *m*/*z* (%): 312 (<1) $[M+H]^+$, 266 (2) $[M–OC_2H_5]^+$, 238 (14) $[M–COOC_2H_5]^+$, 219 (13) $[M–2\ NO_2]^+$, 173 (11) $[M–3\ NO_2]^+$, 147 (23) $[H_5C_2OOCCH_2NNO_2]^+$, 145 (16) $[M–3\ NO_2–C_2H_4]^+$, 119 (8) $[HOOCCH_2NNO_2]^+$, 46 (90) $[NO_2]^+$, 29 (100) $[C_2H_5]^+$; sensitivities: impact: >40 J, friction: 192 N, grain size: <100 µm.

*2-(Nitro-(2,2,2-trinitroethyl)amino)acetic acid (**3**)*

Compound **3** was prepared according to a literature procedure.[3a]

^{1}H NMR (CD_3CN): δ = 5.64 (s, 2 H; $NCH_2C(NO_2)_3$), 4.61 ppm (s, 2 H; $COCH_2N$); ^{13}C{^{1}H} NMR (CD_3CN): δ = 168.1 (COO), 55.4/54.9 ppm (CH_2); ^{14}N NMR (CD_3CN): δ = –32 (br; NNO_2), –34 ppm ($C(NO_2)_3$); ^{1}H NMR ([D$_6$]DMSO): δ = 5.99 (s, 2 H; $NCH_2C(NO_2)_3$), 4.64 ppm (s, 2 H; $COCH_2N$); ^{13}C{^{1}H} NMR ([D$_6$]DMSO): δ = 168.1 (COO), 123.8 (br; $C(NO_2)_3$), 55.1/53.7 ppm (CH_2); ^{14}N NMR ([D$_6$]DMSO): δ = –33 ppm (br; NO_2); IR: ν = 3011 (w), 2970 (w), 2866 (w), 2650 (vw), 2584 (vw), 2362 (vw), 2336 (vw), 1729 (s), 1609 (vs), 1591 (s), 1566 (vs), 1447 (m), 1428 (m), 1391 (m), 1345 (vw), 1276 (s), 1267 (s), 1198 (vw), 1138 (vw), 1098 (vw), 1016 (vw), 945 (w), 897 (w), 878 (vw), 866 (w), 854 (w), 804 (w), 787 (vw), 770 (w), 714 cm^{-1} (vw); Raman: ν = 3030 (11), 3013 (27), 2990 (63), 2973 (28), 2859 (4), 1662 (3), 1617 (46), 1584 (3), 1568 (10), 1452 (6), 1429 (18), 1393 (25), 1385 (6), 1346 (55), 1319 (9), 1300 (19), 1275 (49), 1138 (7), 1098 (4), 1016 (3), 998 (8), 945 (11), 894 (41), 880 (23), 855 (100), 806 (4), 789 (6), 771 (5), 724 (6), 669 (3), 627 (16), 607 (9), 558 (11), 466 (3), 451 (8), 436 (27), 389 (63), 365 (23), 348 (10), 288 (29), 247 (18), 235 cm^{-1} (9); MS (DCI$^+$): *m*/*z* (%): 284 (1) $[M+H]^+$, 220 (1) $[M–OH–NO_2]^+$, 178 (2) $[M–CH_2COOH–NO_2]^+$, 146 (8) $[M–COOH–2\ NO_2]^+$, 99 (61) $[M–4\ NO_2]^+$; MS (DEI$^+$): *m*/*z* (%): 238 (8) $[M–COOH]^+$, 193 (18) $[M–CO_2–NO_2]^+$, 147 (10) $[M–CO_2–2\ NO_2]^+$, 118 (10) $[CH_2C(NO_2)_3]^+$, 101 (4) $[M–CO_2–$

3 $NO_2]^+$, 46 (46) $[NO_2]^+$, 30 (100) $[NO]^+$; sensitivities: impact: 15 J, friction: 144 N, grain size: 100–500 μm.

*2-(Nitro-(2,2,2-trinitroethyl)amino)acetyl chloride (**4**)*

In contrast to the procedure reported in ref. [3a], compound **3** (2.73 g, 9.64 mmol) was dissolved in thionyl chloride (40 mL, 66 g, 550 mmol) and the mixture was heated at reflux (80–85 °C) for 4.5 h. The volatile materials were removed under reduced pressure and the residue was dissolved in refluxing CCl_4 (10 mL), filtered whilst hot, and allowed to crystallize at 4 °C to obtain compound **4** as colorless crystals (2.34 g, 80 % yield).

^{1}H NMR (CD_3CN): δ = 5.66 (s, 2 H; $NCH_2C(NO_2)_3$), 5.09 ppm (s, 2 H; $COCH_2N$); $^{13}C\{^1H\}$ NMR (CD_3CN): δ = 170.4 (CO), 63.6 ($OCCH_2N$), 54.4 ppm ($NCH_2C(NO_2)_3$); ^{14}N NMR (CD_3CN): δ = –32 (br; NNO_2), –34 ppm ($C(NO_2)_3$); ^{1}H NMR ([D_6]DMSO): δ = 6.01 (s, 2 H; $NCH_2C(NO_2)_3$), 4.65 ppm (s, 2 H; $COCH_2N$); $^{13}C\{^1H\}$ NMR ([D_6]DMSO): δ = 168.0 (CO), 123.8 (br; $C(NO_2)_3$), 55.1 (CH_2), 53.7 ppm (CH_2); ^{14}N NMR ([D_6]DMSO): δ = –34 ppm (br; NO_2); IR: ν = 3008 (vw), 2964 (vw), 1785 (m), 1729 (vw), 1625 (m), 1594 (vs), 1576 (vs), 1427 (w), 1383 (w), 1350 (vw), 1297 (s), 1272 (vs), 1204 (w), 1135 (vw), 1100 (w), 967 (m), 952 (m), 926 (m), 878 (vw), 860 (m), 854 (m), 807 (s), 788 (s), 776 (s), 754 (m), 719 (vw), 670 cm^{-1} (vw); Raman: ν = 3009 (30), 2974 (55), 1797 (27), 1621 (15), 1606 (22), 1592 (6), 1573 (13), 1516 (3), 1428 (8), 1392 (20), 1351 (44), 1324 (15), 1302 (20), 1274 (56), 1207 (4), 1135 (4), 1102 (5), 999 (7), 969 (3), 927 (5), 879 (32), 855 (100), 808 (7), 793 (36), 759 (22), 721 (4), 673 (3), 633 (11), 613 (6), 552 (11), 461 (95), 447 (6), 425 (18), 409 (29), 388 (37), 373 (24), 289 (13), 266 (32), 246 (14), 222 cm^{-1} (12); MS (DCI^+): *m*/*z* (%): 302 (11) $[M+H]^+$, 266 (91) $[M–Cl]^+$, 238 (55) $[M–Cl–CO]^+$, 208 (6) $[M–Cl–CO–NO]^+$, 193 (22) $[M–Cl–CO–NO_2+H]^+$, 117 (16) $[M–4\ NO_2]^+$, 99 (15) $[HOOCCH_2NCH_2C]^+$; sensitivities: impact: 30 J, friction: 64 N, ESD: 0.17 J, grain size: 100–500 μm.

*2-(Nitro-(2,2,2-trinitroethyl)amino)acetyl azide (**5**)*

Compound **5** was prepared according to a literature procedure.[3a] Compound **5** must be handled with extreme caution and further conversion is recommended, owing to its high tendency for decomposition.

^{1}H NMR ([D_6]DMSO): δ = 6.00 (s, 2 H; $NCH_2C(NO_2)_3$), 4.85 ppm (s, 2 H; $COCH_2N$); $^{13}C\{^1H\}$ NMR ([D_6]DMSO): δ = 174.2 (CO), 123.6 (br; $C(NO_2)_3$), 56.8 ($COCH_2N$), 53.6 ppm ($NCH_2C(NO_2)_3$); ^{1}H NMR ($CDCl_3$): δ = 5.46 (s, 2 H; $NCH_2C(NO_2)_3$), 4.61 ppm (s,

2 H; $COCH_2N$); $^{13}C\{^1H\}$ NMR ($CDCl_3$): δ = 173.4 (CO), 122.0 (br; $C(NO_2)_3$), 55.3 (CH_2), 53.9 ppm (CH_2); ^{14}N NMR ($CDCl_3$): δ = –36 (br; $C(NO_2)_3$) –136 (br; OCNNN), –149 (br; OCNNN), –254 ppm (br; OCNNN); IR: ν = 3015 (vw), 2972 (vw), 2862 (vw), 2248 (w), 2196/2129 (m, ν N_3), 1734 (vw), 1703 (s), 1604 (s), 1583 (s), 1563 (s), 1436 (w), 1397 (m), 1359 (w), 1330 (w), 1278 (vs), 1229 (vw), 1183 (vs), 1096 (w), 1075 (vw), 1009 (vw), 940 (m), 876 (vw), 861 (m), 854 (m), 806 (s), 786 (w), 774 (s), 750 (vw), 722 (w), 675 cm^{-1} (vw); Raman: ν = 3017 (34), 2984 (71), 2973 (3), 2873 (4), 2245 (4), 2188 (18), 2127 (7), 1709 (44), 1623 (18), 1608 (5), 1588 (4), 1566 (8), 1434 (19), 1397 (13), 1345 (41), 1299 (20), 1280 (52), 1135 (7), 1099 (5), 941 (4), 926 (61), 878 (10), 855 (100), 806 (3), 787 (7), 749 (25), 725 (5), 676 (5), 643 (9), 604 (3), 548 (14), 504 (13), 451 (3), 430 cm^{-1} (40); MS (DEI^+): *m*/*z* (%): 309 (<1) $[M+H]^+$, 262 (<1) $[M-NO_2]^+$, 238 (30) $[CH_2N(NO_2)C(NO_2)_3]^+$, 216 (12) $[M-2\ NO_2]^+$, 118 (28) $[CH_2C(NO_2)_2]^+$, 70 (20) $[OCNCH_2N]^+$, 56 (32) $[OCNCH_2]^+$, 46 (100) $[NO_2]^+$, 30 (100) $[NO]^+$, 28 (50) $[N_2]^+$; sensitivities: impact: <1 J, friction: 48 N, ESD: 0.03 J, grain size: 100–500 µm.

*2,2,2-Trinitroethyl 2-(nitro-(2,2,2-trinitroethyl)amino)acetate (**6**)*

2,2,2-Trinitroethanol (0.75 g, 4.1 mmol) and compound **4** (1.00 g, 3.32 mmol) were dissolved in boiling CCl_4 (10 mL). Dry aluminum(III) chloride (0.5 g, 3.7 mmol) was added slowly to prevent extensive gas evolution and the reaction mixture was heated at reflux for 1 h. Then, the mixture was filtered, washed with cold hydrochloric acid (2 M, 50 mL) and water (50 mL), and dried *in vacuo* to afford compound **6** as a colorless solid (0.72 g, 49 % yield).

^1H NMR ([D_6]DMSO): δ = 6.06 (s, 2 H; $CH_2C(NO_2)_3$), 5.97 (s, 2 H; $CH_2C(NO_2)_3$), 4.89 ppm (s, 2 H; $COCH_2N$); $^{13}C\{^1H\}$ NMR ([D_6]DMSO): δ = 164.9 (CO), 124.3 (br; $C(NO_2)_3$), 61.3 ($OCH_2C(NO_2)_3$), 55.0 (CH_2), 53.8 ppm (CH_2); ^{14}N NMR ([D_6]DMSO): δ = –31 (br; NO_2), –34 ppm (br; NO_2); IR: ν = 3020 (vw), 2978 (vw), 2890 (vw), 1772 (m), 1613 (s), 1590 (vs), 1576 (vs), 1435 (w), 1392 (m), 1366 (vw), 1326 (vw), 1294 (s), 1276 (vs), 1195 (s), 1139 (vw), 1099 (vw), 1035 (vw), 1011 (vw), 939 (w), 915 (vw), 878 (vw), 863 (m), 854 (w), 805 (s), 780 (m), 768 (w), 727 (vw), 711 (vw), 664 cm^{-1} (vw); Raman: ν = 3009 (27), 2964 (51), 2864 (3), 1786 (15), 1625 (24), 1603 (7), 1576 (3), 1563 (3), 1525 (2), 1440 (12), 1396 (20), 1374 (13), 1347 (35), 1302 (15), 1277 (28), 1217 (2), 1186 (5), 1131 (3), 1095 (10), 1054 (14), 1020 (3), 997 (6), 954 (7), 923 (14), 881 (26), 857 (100), 807 (7), 780 (4), 755 (4), 722 (4), 671 (4), 649 (2), 600 (5), 546 (11), 457 (4), 433 (22), 378 (53), 360 (13), 329 (6), 304 (6), 282 (27), 240 (13), 220 cm^{-1} (2);

MS (EI^+): *m/z* (%): 399 (<1) $[M–NO_2–H]^+$, 354 (1) $[M–2\ NO_2]^+$, 308 (<1) $[M–3\ NO_2]^+$, 238 (7) $[CH_2N(NO_2)C(NO_2)_3]^+$, 118 (29) $[CH_2C(NO_2)_2]^+$, 46 (100) $[NO_2]^+$; elemental analysis calcd (%) for $C_6H_6N_8O_{16}$: C 16.2, H 1.4, N 25.1; found: C 16.5, H 1.1, N 24.4; sensitivities: impact: 3 J, friction: 64 N, ESD: 0.25 J, grain size: <100 μm.

2,2,2-Trinitroethyl (nitro-(2,2,2-trinitroethyl)amino)methyl carbamate (7)

2,2,2-Trinitroethanol (0.47 g, 2.6 mmol) and compound **5** (0.50 g, 1.6 mmol) were dissolved in dry $CHCl_3$ (5 mL) and a catalytic amount of anhydrous aluminum(III) chloride was added. The reaction mixture was heated at reflux under an inert atmosphere for 5 h. CH_2Cl_2 (10 mL) was added and the reaction mixture was washed with HCl (2 M, 5×100 mL) and water (5×100 mL). The organic layer was dried with magnesium sulfate and concentrated under reduced pressure to give a mixture of a colorless solid and a yellow oil. Complete solidification was achieved by ultrasound treatment of the mixture in water. Carbamate **7** was obtained after recrystallization from CCl_4 as colorless crystals (0.45 g, 61 % yield).

^1H NMR ([D_6]acetone): δ = 8.49 (br t, 1 H; NH), 6.01 (s, 2 H; $OCH_2C(NO_2)_3$), 5.81 (s, 2 H; $NCH_2C(NO_2)_3$), 5.38 ppm (d, ^3J(H,H)=6.4 Hz, 2 H; $NHCH_2N$); $^{13}C\{^1H\}$ NMR ([D_6]acetone): δ = 155.1 (CO), 124.9 (br; $C(NO_2)_3$), 124.4 (br; $C(NO_2)_3$), 62.0 ($OCH_2C(NO_2)_3$), 59.6 (NCH_2N), 54.0 ppm ($CH_2C(NO_2)_3$); ^{14}N NMR ([D_6]acetone): δ = –34 ppm (br; NO_2); ^1H NMR ($CDCl_3$): δ = 6.31 (t, ^3J(H,H)=6.4 Hz, 1 H; NH), 5.67 (s, 2 H; $OCH_2C(NO_2)_3$), 5.46 (s, 2 H; $NCH_2C(NO_2)_3$), 5.20 ppm (d, 2 H; $NHCH_2N$); $^{13}C\{^1H\}$ NMR ($CDCl_3$): δ = 154.4 (CO), 122.6 (br; $C(NO_2)_3$), 62.4 ($OCH_2C(NO_2)_3$), 58.3 (NCH_2N), 52.9 ppm ($CH_2C(NO_2)_3$); ^{14}N NMR ($CDCl_3$): δ = –35 (br; NO_2), –36 ppm (br; NO_2); IR: ν = 3381 (w), 3002 (vw), 2963 (vw), 2886 (vw), 1745 (m), 1623 (m), 1604 (s), 1588 (vs), 1572 (vs), 1531 (s), 1444 (m), 1410 (w), 1397 (w), 1346 (vw), 1288 (vs), 1227 (vs), 1195 (s), 1171 (m), 1124 (w), 1047 (m), 1004 (m), 954 (m), 907 (w), 875 (m), 851 (s), 803 (m), 784 (s), 775 (s), 738 (w), 720 (w), 679 cm^{-1} (w); Raman: ν = 3379 (2), 3059 (10), 3013 (34), 3003 (21), 2965 (37), 2887 (4), 1750 (12), 1629 (17), 1608 (25), 1569 (9), 1447 (21), 1412 (11), 1399 (15), 1378 (21), 1342 (40), 1303 (31), 1286 (25), 1232 (7), 1161 (5), 1125 (8), 1103 (5), 1041 (13), 1003 (9), 953 (7), 908 (10), 871 (16), 857 (100), 803 (10), 787 (7), 722 (7), 642 (8), 604 (9), 570 (11), 539 (16), 453 (12), 416 (44), 397 (41), 376 (61), 289 (32), 272 cm^{-1} (25); MS (DCI^+): *m/z* (%): 462 (<1) $[M+H]^+$, 266 (32) $[CH_2NCH_2NHCO_2CH_2C(NO_2)_3]^+$, 237 (34) $[CH_2NHCO_2CH_2C(NO_2)_3]^+$, 57 (100) $[CH_2NCO+H]^+$, 43 (15) $[NCO+H]^+$; elemental analysis calcd (%) for $C_6H_7N_9O_{16}$: C

15.63, H 1.53, N 27.33; found: C 15.79, H 1.46, N 27.15; sensitivities: impact: 5 J, friction: 72 N, ESD: 0.035 J, grain size: <100 µm.

*2,2,2-Trinitroethyl (nitro-(2,2,2-trinitroethyl)amino)methyl nitrocarbamate (**8**)*

Carbamate **7** (0.30 g, 0.64 mmol) was slowly added at 0 °C into a mixture of acetic anhydride (8.0 mL) and fuming nitric acid (8.0 mL, 100 %). The reaction mixture was stirred at 0 °C for 15 min then at ambient temperature for 3 h, before being poured onto a large excess of ice. The colorless precipitate was filtered, washed with water, and dried in vacuo to obtain compound **8** (0.24 g, 73 % yield) as a colorless powder.

^{1}H NMR ([D$_6$]acetone): δ = 6.36 (s, 2 H; $OCH_2C(NO_2)_3$), 6.22 (s, 2 H; $NCH_2C(NO_2)_3$), 6.12 ppm (s, 2 H; NCH_2N); $^{13}C\{^{1}H\}$ NMR ([D$_6$]acetone): δ = 64.2 ($OCH_2C(NO_2)_3$), 64.0 (NCH_2N), 54.1 ppm ($NCH_2C(NO_2)_3$); ^{14}N NMR ([D$_6$]acetone): δ = –34 (br; $OCH_2C(NO_2)_3$), –35 (br; $NCH_2C(NO_2)_3$), –50 ppm (br; NNO_2); IR: ν = 3017 (vw), 2967 (vw), 2893 (vw), 1759 (m), 1593 (vs), 1573 (s), 1518 (w), 1437 (w), 1409 (w), 1396 (w), 1363 (vw), 1341 (vw), 1299 (s), 1278 (vs), 1252 (m), 1228 (m), 1171 (w), 1160 (w), 1125 (w), 1064 (w), 999 (w), 983 (w), 924 (w), 878 (w), 868 (w), 855 (m), 851 (m), 801 (s), 784 (m), 761 (w), 735 (w), 719 (vw), 662 cm^{-1} (vw); Raman: ν = 3062 (4), 3020 (18), 2971 (29), 1759 (13), 1621 (23), 1440 (8), 1397 (11), 1344 (37), 1301 (22), 1256 (6), 1127 (4), 1093 (3), 1032 (6), 927 (9), 870 (12), 856 (101), 803 (7), 787 (3), 637 (7), 609 (3), 547 (16), 487 (9), 413 (14), 401 (9), 377 (59), 331 (15), 291 (7), 260 cm^{-1} (11); MS (DEI$^+$): *m*/*z* (%): 507 (<1) $[M+H]^+$, 283 (3) $[M–N(NO_2)CH_2C(NO_2)_3]^+$, 268.2 (2) $[M–CH_2N(NO_2)CH_2C(NO_2)_3]^+$; elemental analysis calcd (%) for $C_6H_6N_{10}O_{18}$: C 14.24, H 1.19, N 27.67; found: C 14.86, H 1.29, N 27.00; sensitivities: impact: 2 J, friction: 120 N, ESD: 0.035 J, grain size: <100 µm.

*Ethyl 2-((2,2,2-trinitroethoxy)carbamato)acetate (**9**)*

Ethyl 2-aminoacetate hydrochloride (0.89 g, 6.37 mmol) and 2,2,2-trinitroethyl chloroformate (2.0 g, 8.21 mmol) were dissolved in MeCN (25 mL) and heated at reflux for 40 min at 85 °C. The reaction mixture was poured onto a large excess of ice water and stirred vigorously. The then formed colorless precipitate was filtered, washed with water (500 mL), and dried in vacuo to obtain acetate **9** as a colorless solid (1.08 g, 55 % yield).

^{1}H NMR ([D$_6$]acetone): δ = 5.77 (s, 2 H; $OCH_2C(NO_2)_3$), 4.16 (q, ^{3}J(H,H)=7.1 Hz, 2 H; OCH_2CH_3), 3.92 (s, 2 H; $OCOCH_2N$), 1.22 ppm (t, 2 H; OCH_2CH_3); $^{13}C\{^{1}H\}$ NMR ([D$_6$]acetone): δ = 169.3 (CH_2COOCH_2), 154.0 ($NHCOOCH_2$), 61.5 ($OCH_2C(NO_2)_3$),

60.9 ($NHCH_2COO$), 42.6 (OCH_2CH_3), 13.7 ppm (OCH_2CH_3); ^{14}N NMR ([D_6]acetone): δ = –33 ppm ($C(NO_2)_3$); IR: ν = 3327 (w), 3040 (vw), 2998 (vw), 2958 (vw), 2905 (vw), 1753 (m), 1714 (s), 1605 (s), 1593 (vs), 1529 (m), 1476 (vw), 1445 (vw), 1420 (w), 1404 (vw), 1382 (w), 1354 (vw), 1302 (m), 1269 (w), 1216 (m), 1156 (m), 1100 (vw), 1058 (m), 1017 (m), 937 (vw), 906 (w), 868 (w), 856 (w), 804 (m), 783 (m), 730 (w), 694 (vw), 663 cm^{-1} (vw); Raman: ν = 3323 (4), 2999 (18), 2960 (100), 2877 (5), 2834 (2), 2735 (3), 1759 (16), 1719 (27), 1617 (35), 1596 (5), 1571 (2), 1449 (17), 1422 (15), 1384 (22), 1355 (37), 1309 (33), 1274 (20), 1227 (5), 1148 (5), 1113 (10), 1060 (3), 1037 (24), 1011 (3), 938 (4), 908 (19), 868 (11), 858 (85), 805 (10), 787 (7), 734 (4), 649 (7), 575 (5), 536 (12), 410 (53), 372 (72), 299 (19), 282 (3), 229 cm^{-1} (6); MS (DEI^+): *m*/*z* (%): 310 (1) $[M]^+$, 281 (1) $[M–CH_2CH_3]^+$, 266 (1) $[M–OCH_2CH_3]^+$, 265 (7) $[M–CH_3CH_2O]^+$, 237 (100) $[M–COOCH_2CH_3]^+$, 147 (1) $[M–CH_2C(NO_2)_3+H]^+$, 118 (<1) $[CH_2C(NO_2)_2]^+$; elemental analysis calcd (%) for $C_7H_{10}N_4O_{10}$: C 27.11, H 3.25, N 18.06; found: C 26.98, H 3.16, N 17.89; sensitivities: impact: 40 J, friction: 54 N, grain size: <100 µm.

*Ethyl 2-(nitro-((2,2,2-trinitroethoxy)carbamato)acetate (**10**)*

Acetate **9** (1.08 g, 3.49 mmol) was dissolved in fuming nitric acid (1.5 mL, 100 %) at 0 °C and stirred for 30 min at 0 °C and then for 2 h at ambient temperature. The mixture was poured onto a large excess of ice (600 g) and the as-obtained colorless precipitate was filtered and dried to obtain compound **10** as a colorless solid (0.61 g, 49 % yield).

^1H NMR ($CDCl_3$): δ = 5.56 (s, 2 H; $OCH_2C(NO_2)_3$), 4.71 (s, 2 H; $OCOCH_2N$), 4.28 (q, ^3J(H,H)=7.1 Hz, 2 H; OCH_2CH_3), 1.32 ppm (t, 2 H; OCH_2CH_3); $^{13}C\{^1H\}$ NMR ($CDCl_3$): δ = 165.7 (CH_2COOCH_2), 148.0 ($NHCOOCH_2$), 63.2 ($OCH_2C(NO_2)_3$), 62.9 (NCH_2COO), 49.6 (OCH_2CH_3), 14.0 ppm (OCH_2CH_3); ^{14}N NMR ($CDCl_3$): δ = –36 (br; $C(NO_2)_3$), –51 ppm (br; NNO_2); IR: ν = 3021 (vw), 2986 (vw), 2902 (vw), 1796 (m), 1740 (s), 1592 (vs), 1466 (vw), 1439 (w), 1414 (w), 1380 (m), 1357 (vw), 1290 (s), 1220 (s), 1145 (vs), 1094 (s), 1071 (m), 1015 (m), 927 (w), 884 (m), 872 (w), 851 (m), 801 (m), 782 (m), 736 (m), 663 cm^{-1} (w); Raman: ν = 3012 (17), 2971 (100) 2948 (24), 2934 (6), 2875 (5), 1807 (17), 1747 (17), 1617 (10), 1601 (31), 1475 (2), 1444 (17), 1421 (9), 1382 (27), 1362 (14), 1351 (7), 1322 (11), 1292 (40), 1228 (9), 1157 (5), 1135 (3), 1112 (17), 1017 (14), 993 (8), 941 (6), 893 (47), 871 (21), 857 (83), 803 (8), 785 (4), 761 (5), 716 (5), 660 (8), 626 (4), 568 (3), 547 (20), 485 (13), 413 (23), 372 (57), 316 (7), 273 (28), 232 cm^{-1} (16); MS (DEI^+): *m*/*z* (%): 356 (<1) $[M+H]^+$, 310 (19) $[M–OCH_2CH_3]^+$, 282 (8) $[M–COOCH_2CH_3]^+$, 264 (2) $[M–2\,NO_2+H]^+$, 237 (100) $[M–COOCH_2CH_3–$

NO_2 $]^+$, 191 (100) $[M–CH_2C(NO_2)_3]^+$, 119 (38) $[CH_2C(NO_2)_2+H]^+$, 102 (14) $[CH_3CH_2OCOCH_2N+H]^+$, 74 (21) $[CH_3CH_2OCO+H]^+$; elemental analysis calcd (%0 for $C_7H_9N_5O_{12}$: C 23.67, H 2.65, N 19.72; found: C 23.71, H 2.65, N 19.37; sensitivities: impact: 7 J, friction: 144 N, grain size: 100–500 μm.

2.6 ACKNOWLEDGEMENT

Financial support of this work by the Ludwig-Maximilian University of Munich (LMU), the U.S. Army Research Laboratory (ARL) under grant no. W911NF-09-2-0018, the Armament Research, Development and Engineering Center (ARDEC) under grant no. W911NF-12-1-0467, and the Office of Naval Research (ONR) under grant nos. ONR.N00014-10-1-0535 and ONR.N00014-12-1-0538 is gratefully acknowledged. The authors acknowledge collaborations with Dr. Mila Krupka (OZM Research, Czech Republic) in the development of new testing and evaluation methods for energetic materials and with Dr. Muhamed Suceska (Brodarski Institute, Croatia) in the development of new computational codes to predict the detonation and propulsion parameters of novel explosives. We are indebted to and thank Drs. Betsy M. Rice and Brad Forch (ARL, Aberdeen, Proving Ground, MD) for many inspired discussions.

2.7 REFERENCES

[1] a) T. M. Klapötke, B. Krumm, R. Moll, S. F. Rest, *Z. Anorg. Allg. Chem.* **2011**, *637*, 2103–2110; b) T. M. Klapötke, S. F. Rest, *New Trends Res. Energ. Mater. Proc. Semin. 13th* **2010**, *Pt. 2*, 642–651; c) M. Göbel, T. M. Klapötke, *Adv. Funct. Mater.* **2009**, *19*, 347–365; d) M. E. Hill, US 3306939, **1967**.

[2] a) T. M. Klapötke, *Chemistry of High-Energy Materials*, 2nd ed., de Gruyter, Berlin, **2012**; b) M. Göbel, T. M. Klapötke, *Z. Anorg. Allg. Chem.* **2007**, *633*, 1006–1017.

[3] a) H. Feuer, G. B. Bachman, C. R. Koller, W. A. Swarts, *Tetrahedron* **1963**, *19*, 165–176; b) H. Feuer, T. Kucera, *J. Org. Chem.* **1960**, *25*, 2069–2070.

[4] a) W. H. Gilligan, S. L. Stafford, United States Department of the Navy, US, **1981**, p. 21, p. Avail, NTIS order no. PAT-APPL-224 776; b) W. H. Gilligan, S. L. Stafford, *Synthesis* **1979**, 600–602.

[5] M. Göbel, T. M. Klapötke, *Acta Crystallogr.* **2007**, *63C*, o562–o564.

[6] Y. Oyumi, T. B. Brill, A. L. Rheingold, *J. Phys. Chem.* **1985**, *89*, 4824–4828.

[7] G. Socrates, *Infrared and Raman Characteristic Group Frequencies: Tables and Charts*, 3rd ed., John Wiley & Sons, Chichester, **2004**.

[8] A. B. Sheremetev, I. L. Yudin, *Mendeleev Commun.* **2005**, *15*, 204–205.

[9] a) M. Göbel, B. H. Tchitchanov, J. S. Murray, P. Politzer, T. M. Klapötke, *Nat. Chem.* **2009**, *1*, 229–235; b) M. Göbel, T. M. Klapötke, P. Mayer, *Z. Anorg. Allg. Chem.* **2006**, *632*, 1043–1050; c) S. K. Bhattacharjee, H. L. Ammon, *Acta Crystallogr.* **1982**, *38B*, 2503–2505.

[10] a) R. E. Cobbledick, R. W. H. Small, *Acta Crystallogr.* **1974**, *30B*, 1918–1922; b) C. S. Choi, *Acta Crystallogr.* **1972**, *28B*, 2857–2862; c) C. S. Choi, H. P. Boutin, *Acta Crystallogr.* **1970**, *26B*, 1235–1240; d) H. H. Cady, A. C. Larson, D. T. Cromer, *Acta Crystallogr.* **1963**, *16B*, 617–623.

[11] a) C. Jones, M. Waugh, *J. Organomet. Chem.* **2007**, *692*, 5086–5090; b) M. C. Grossel, M. B. Hursthouse, J. B. Orton, *CrystEngComm* **2005**, *7*, 279–283.

[12] Gaussian 03, Revision B.03, M. J. Frisch, G. W. Trucks, H. B. Schlegel, G. E. Scuseria, M. A. Robb, J. R. Cheeseman, J. A. Montgomery Jr., T. Vreven, K. N. Kudin, J. C. Burant, J. M. Millam, S. S. Iyengar, J. Tomasi, V. Barone, B. Mennucci, M. Cossi, G. Scalmani, N. Rega, G. A. Petersson, H. Nakatsuji, M.

Hada, M. Ehara, K. Toyota, R. Fukuda, J. Hasegawa, M. Ishida, T. Nakajima, Y. Honda, O. Kitao, H. Nakai, M. Klene, X. Li, J. E. Knox, H. P. Hratchian, J. B. Cross, V. Bakken, C. Adamo, J. Jaramillo, R. Gomperts, R. E. Stratmann, O. Yazyev, A. J. Austin, R. Cammi, C. Pomelli, J. W. Ochterski, P. Y. Ayala, K. Morokuma, G. A. Voth, P. Salvador, J. J. Dannenberg, V. G. Zakrzewski, S. Dapprich, A. D. Daniels, M. C. Strain, O. Farkas, D. K. Malick, A. D. Rabuck, K. Raghavachari, J. B. Foresman, J. V. Ortiz, Q. Cui, A. G. Baboul, S. Clifford, J. Cioslowski, B. B. Stefanov, G. Liu, A. Liashenko, P. Piskorz, I. Komaromi, R. L. Martin, D. J. Fox, T. Keith, M. A. Al-Laham, C. Y. Peng, A. Nanayakkara, M. Challacombe, P. M. W. Gill, B. Johnson, W. Chen, M. W. Wong, C. Gonzalez, J. A. Pople, Gaussian, Inc., Wallingford CT, **2003**.

[13] a) D. Siebler, C. Forster, T. Gasi, K. Heinze, *Organometallics* **2011**, *30*, 313–327; b) J. Lapic, A. Pezerovic, M. Cetina, S. Djakovic, V. Rapic, *J. Mol. Struct.* **2011**, *990*, 209–216; c) G. Laus, V. Kahlenberg, K. Wurst, S. Nerdinger, H. Schottenberger, *Z. Naturforsch.* **2011**, *66B*, 479–486; d) M. Cetina, S. Djakovic, M. C. Semencic, V. Rapic, *J. Mol. Struct.* **2009**, *920*, 134–141; e) L. Párkányi, G. Besenyei, *J. Mol. Struct.* **2004**, *691*, 97–106; f) F. M. Menger, J. Bian, V. A. Azov, *Angew. Chem.* **2002**, *114*, 2693–2696; *Angew. Chem. Int. Ed.* **2002**, *41*, 2581–2584; g) Y. Jiao, E. Valente, S. T. Garner, X. Wang, H. Yu, *Tetrahedron Lett.* **2002**, *43*, 5879–5881; h) S. Ryng, Z. Machon, T. Glowiak, *J. Chem. Crystallogr.* **1994**, *24*, 483–488.

[14] a) A. F. Yepes, A. Palma, A. Marchal, J. Cobo, C. Glidewell, *Acta Crystallogr.* **2012**, *68C*, o199–203; b) I. N. Hassan, B. M. Yamin, M. B. Kassim, *Acta Crystallogr.* **2010**, *66E*, o2784.

[15] T. Ishida, Y. In, C. Tanaka, M. Inoue, *Acta Crystallogr.* **1991**, *47B*, 806–813.

[16] R. W. Crowe, C. P. Smyth, *J. Am. Chem. Soc.* **1950**, *72*, 4009–4015.

[17] Laying down test methods in accordance with EC regulation no. 1907/2006 of the European Parliament and of the Council on the Evaluation, Authorisation and Restriction of Chemicals (REACH), ABl. L 142, **2008**.

[18] M. Sućeska, *EXPLO5 V5.05*, Brodarski Institute, Zagreb, Croatia, **2010**.

[19] R. Dennington, T. Keith, J. Millam, *GaussView*, *Version 5*, Semichem Inc., Shawnee Mission KS, **2009**.

[20] a) NASA, *Space Shuttle News Reference*, 2–20–22–21, http://de.scribd.com/doc/17005716/NASA-Space-Shuttle-News-Reference-1981;

b) NASA, *Press release: STS-122 The Voyage of Columbus*, **2008**, 82–84, http://www.nasa.gov/pdf/203212main_sts122_presskit2.pdf.

[21] D. F. Shriver, M. A. Drezdzon, *The Manipulation of Air-Sensitive Compounds*, 2nd ed., John Wiley & Sons, New York, **1986**.

[22] a) T. M. Klapötke, J. Stierstorfer, *Phys. Chem. Chem. Phys.* **2008**, *10*, 4340–4346; b) J. J. A. Montgomery, M. J. Frisch, J. W. Ochterski, G. A. Petersson, *J. Chem. Phys.* **2000**, *112*, 6532–6542; c) J. W. Ochterski, G. A. Petersson, J. J. A. Montgomery, *J. Chem. Phys.* **1996**, *104*, 2598–2619.

[23] a) E. F. C. Byrd, B. M. Rice, *J. Phys. Chem. A* **2005**, *109*, 1005–1013; b) B. M. Rice, S. V. Pai, J. Hare, *Combust. Flame* **1999**, *118*, 445–458; c) L. A. Curtiss, K. Raghavachari, P. C. Redfern, J. A. Pople, *J. Chem. Phys.* **1997**, *106*, 1063–1079.

[24] M. Sućeska, *Propellants Explos. Pyrotech.* **1991**, *16*, 197–202.

[25] T. M. Klapötke, B. Krumm, F. X. Steemann, K. D. Umland, *Z. Anorg. Allg. Chem.* **2010**, *636*, 2343–2346.

[26] a) A. Altomare, M. C. Burla, M. Camalli, G. L. Cascarano, C. Giacovazzo, A. Guagliardi, A. G. G. Moliterni, G. Polidori, R. Spagna, *J. Appl. Crystallogr.* **1999**, *32*, 115–119; b) A. Altomare, G. Cascarano, C. Giacovazzo, A. Guagliardi, A. G. G. Moliterni, M. C. Burla, G. Polidori, M. Camalli, R. Spagna, *SIR97*, **1997**.

[27] a) A. L. Spek, *Acta Crystallogr. Sect. D* **2009**, *65*, 148–155; b) G. M. Sheldrick, *Acta Crystallogr. Sect. A* **2008**, *64*, 112–122; c) L. J. Farrugia, *J. Appl. Cryst.* **1999**, *32*, 837–838; d) G. M. Sheldrick, *SHELX-97*, University of Göttingen, Göttingen (Germany), **1997**.

[28] a) A. L. Fridman, O. B. Kremleva, V. S. Zalesov, Z. V. Platonova, F. A. Gabitov, L. A. Rubinshtein, A. N. Plaksina, *Pharm. Chem. J.* **1977**, *11*, 64–67; b) M. B. Frankel, G. L. Bauerle, L. R. Grant, R. L. Kistner, J. V. Lecce, E. R. Wilson, D. O. I. Woolery, *Process studies on nitroform and related compounds: Final report for period 30 January 1984 to 31 March 1987*, UCRL-15908, Rockwell International Corp., Rocketdyne Division, Canoga Park, CA, March **1987**, pp. 1–66.

[29] R. Scharf, T. M. Klapötke, *Private communication*, LMU Munich, **2012**.

[30] C. Harries, M. Weiss, *Justus Liebigs Ann. Chem.* **1903**, *327*, 355–384.

3. THE ENERGETIC NITROCARBAMATE $O_2NN(H)CO[OCH_2C(NO_2)_3]$ DERIVED FROM PHOSGENE

Quirin J. Axthammer, Thomas M. Klapötke, Burkhard Krumm, Richard Moll and Sebastian F. Rest

As published in: Zeitschrift für anorganische und allgemeine Chemie **2014,** *640*, 76–83.

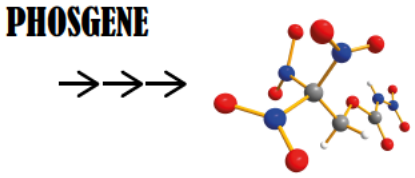

3.1 ABSTRACT

A new simple synthesis route for 2,2,2-trinitroethyl chloroformate (**1**), from easily available starting materials 2,2,2-trinitroethanol and phosgene is presented. 2,2,2-Trinitroethyl carbamate (**2**) was obtained by the reaction of **1** with aqueous ammonia. The nitration of **2** with anhydrous nitric acid and sulfuric acid yields 2,2,2-trinitroethyl nitrocarbamate (**3**), which has potential as a perchlorate free high energetic dense oxidizer with a high oxygen balance of $\Omega(CO_2)$ = +14.87 %. The thermal stability was studied using differential scanning calorimetry and the energies of formation were calculated on the CBS-4M level of theory, as well as several denotation parameters and propulsion properties were determined. In addition to full spectroscopic characterization, X-ray diffraction studies were performed for **2** and **3**.

3.2 INTRODUCTION

The 1,1,1-trinitroethyl moiety is a widely-used building block in the chemistry of high energetic explosives, especially if performing as a high energy dense oxidizer (HEDO).[1] Such compounds can be used as high performance, halogen-free propellants. These might overcome the environmental problems of hydrogen chloride formation during the use of ammonium perchlorate as oxidizer in rocket propellant formulations.[2] Furthermore, the perchlorate anion has negative health effects, scientific research indicates that perchlorate contaminated water can disrupt the thyroid's ability to produce hormones needed for normal growth and development.[3]

There are three synthesis routes for the chemical transfer of a 1,1,1-trinitroethyl functionality known. The most common way is the nucleophilic substitution of halogen atoms in reactive organic compounds like haloalkanes, acid halides and esters of the formic acid with the easy available alcohol 2,2,2-trinitroethanol.[4] An alternative to this is the widespread Mannich reaction, which is a multi component condensation between a nitroalkane, an aldehyde and a primary or secondary amine. The mechanism of the reaction starts with the formation of an iminium ion from the amine and formaldehyde. This cationic intermediate can be attacked from the trinitromethanide anion to form the 2,2,2-trinitroethylamine unit.[1b, 5] The third and less applied route, is the transfer of the 1,1,1-trinitroethyl moiety by a chloroformate.[6]

3.3 RESULTS AND DISSCUSSION

SYNTHESIS

The standard synthesis of chloroformates is the reaction between alcohols and an excess of phosgene with a base as acid acceptor.[7] Pure 2,2,2-trinitroethyl chloroformate (**1**) was first prepared in 1979 in a three step synthesis via *S*-ethyl chloroformate as starting material and claimed that a direct chloroformylation of *β*-nitro alcohols such as 2,2,2-trinitroethanol does not work properly.[6] This was explained by the very fast reaction to the by-product *bis*(2,2,2-trinitroethyl) carbonate and a reverse HENRY reaction with a decomposition of the alcohol to the corresponding aldehyde and nitroalkane introduced by the required base.[4c, 6] Therefore, for the synthesis of **1** was used the phosgene analogue *S*-ethyl chlorothioformate with a subsequent replacement of the ethylthio group by chlorine with sulfuryl chloride.[6]

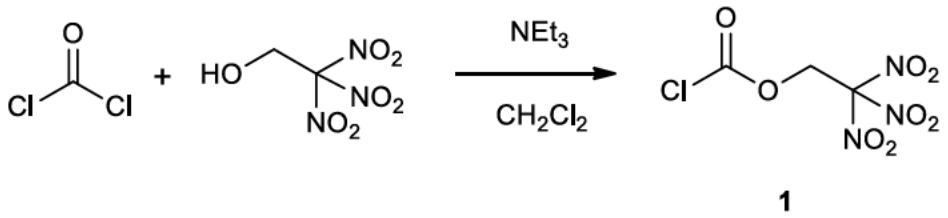

1

Scheme 3.1. Synthesis of 2,2,2-trinitroethyl chloroformate (**1**).

In contrast to the literature prediction, the direct chloroformylation with phosgene and 2,2,2-trinitroethanol was successful (Scheme 3.1). The reaction works best with an excess of phosgene and the aid of one equivalent of non-nucleophilic bases, such as triethylamine. The product can easily be removed from the reaction mixture and was obtained as a colorless liquid in very good yields around 86 %. The described one-pot reaction procedure has several advantages such as a reduced consumption of chemicals and reduced reaction time.

In the 1990ies it was briefly mentioned, that 2,2,2-trinitroethyl carbamate (**2**) could be synthesized by the reaction of 2,2,2-trinitroethanol and carbamoyl chloride.[8] However, the synthesis of **2** via the chloroformate **1** and aqueous ammonia in methylene chloride is the more preferred route of choice (Scheme 3.2). The nitration of the carbamate **2** with a mixture of sulphuric (95 %) and nitric acid (100 %) (1:1) leads to the formation of 2,2,2-trinitroethyl nitrocarbamate (**3**). Recrystallization from tetrachloromethane yielded almost quantitatively pure colorless product **3** as fine needles.

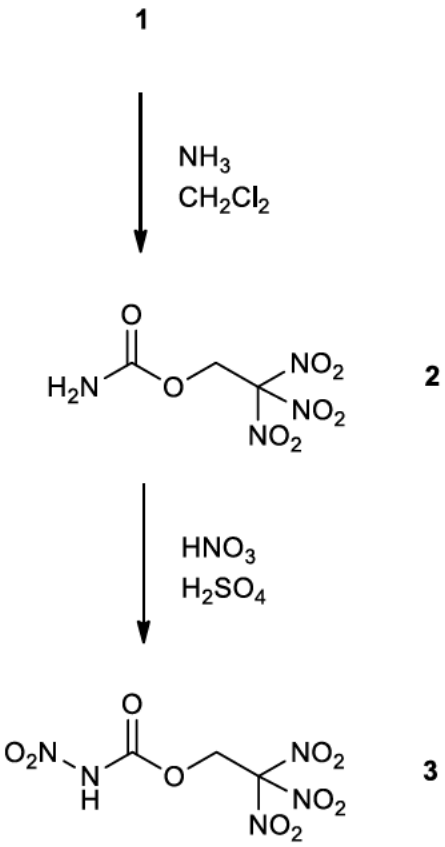

Scheme 3.2. Synthesis of 2,2,2-trinitroethyl carbamate (**2**) and 2,2,2-trinitroethyl nitrocarbamate (**3**).

NMR SPECTROSCOPY

All compounds were characterized by ^{1}H, ^{13}C and ^{14}N NMR spectroscopy (Table 3.1). In the ^{1}H NMR spectra of **1**–**3** the CH_2 group is observed at 5.68–5.51 ppm. The ^{1}H NMR spectrum of the carbamate **2** shows an interesting temperature dependent dynamic behavior of the NH_2 resonance of the amide group, which splits at 25 °C into two different signals. This is due to a restricted rotation along the C–NH_2 bond of the amide **2**. Temperature-dependent ^{1}H NMR spectra were recorded in DMSO-D_6 in the range of +25 to +60 °C (Figure 1). From these measurements, a coalescence temperature T_c of 42.5 °C and the corresponding chemical shift difference $\Delta\nu$ (= 42.5 °C) 75.2 Hz, are determined. With these data, the free enthalpy of activation $\Delta G^{\ddagger}$ (15.3 kcal mol^{-1}) is calculated by applying the Eyring equation.[9] This activation barrier of rotation is within the range of other values obtained for amides.[10] Furthermore, a diamagnetic shift of the amine resonance with increasing temperature is observed. This temperature dependence is the result of weakening the hydrogen bond and therefore lessening the electron

withdrawing effect of the hydrogen bond acceptor on the proton. As a result the proton becomes more shielded and its resonance is shifted upfield.[11]

Table 3.1. Multinuclear NMR resonances of **1**–**3** (ppm) in acetone-D_6

	1	**2**	**3**
^{1}H	5.51 (CH_2)	6.77 (s, NH)	10.07 (s, NH)
		6.49 (s, NH)	5.53 (CH_2)
		5.68 (CH_2)	
^{13}C	149.5 (CO$_2$Cl)	154.5 (CO$_2$N)	145.2 (CO$_2$N)
	121.4 [C(NO$_2$)$_3$]	125.7 [C(NO$_2$)$_3$]	122.2 [C(NO$_2$)$_3$]
	63.3 (CH$_2$)	61.8 (CH$_2$)	62.1 (CH$_2$)
^{14}N	–36 (NO$_2$)	–33 (NO$_2$)	–36 (NO$_2$)
		−310 (NH$_2$)	−55 (NNO$_2$)
			−292 (NNO$_2$)

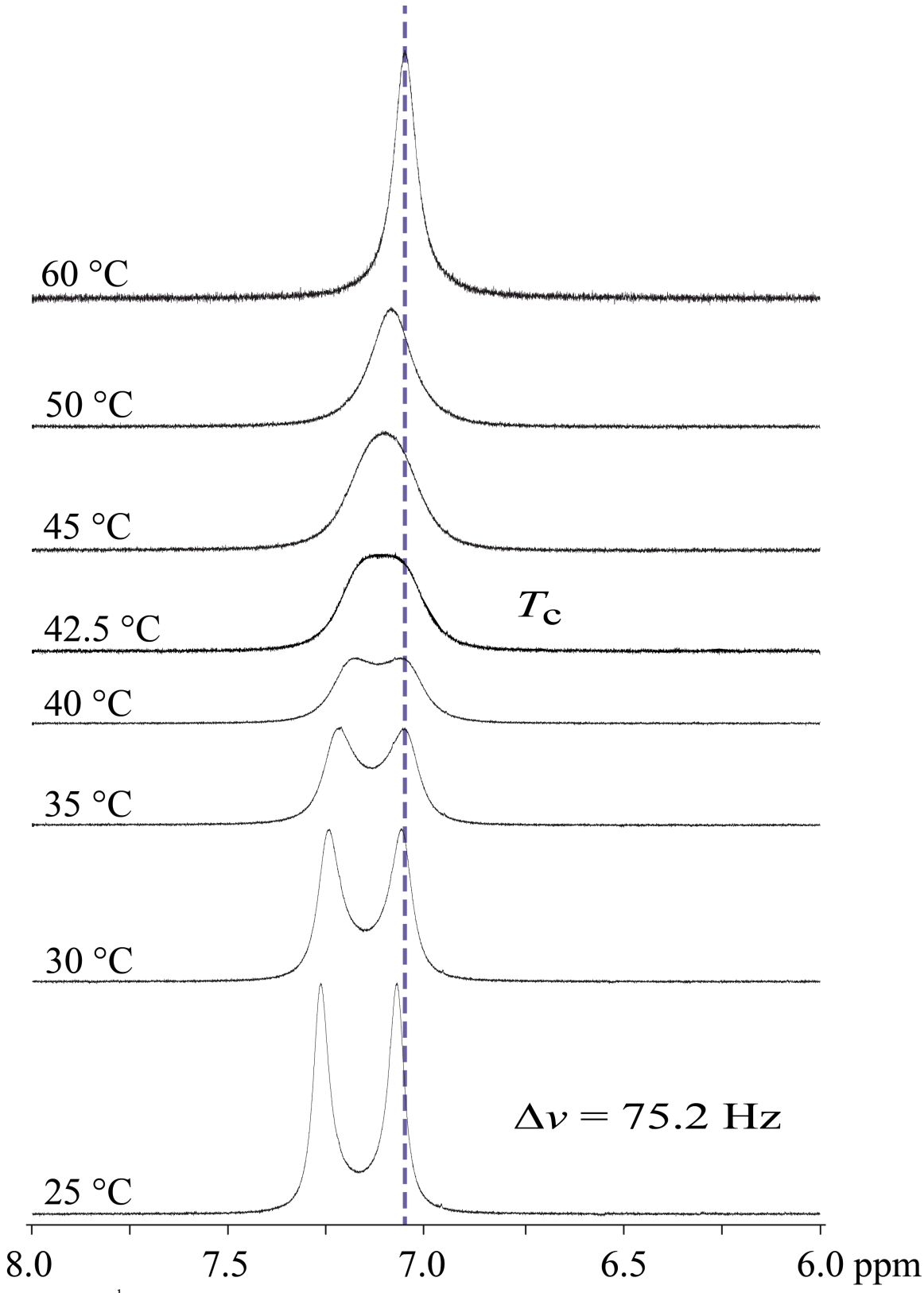

Figure 3.1. ^{1}H NMR resonance of the NH_2 group of **2** at variable temperatures in [D_6]DMSO.

The NH resonance of the nitrocarbamate **3** compared to the NH_2 of **2** is shifted downfield to 10.70 ppm. In the $^{13}C\{^{1}H\}$ NMR spectra the resonances of the carbon atoms of the

methylene groups were observed at 63.3–61.8 ppm, those of the trinitromethyl groups broadened at 125.7–121.4 ppm and the carbonyl groups at 149.5 (**1**), 154.5 (**2**) and 145.2 ppm (**3**). The nitro resonances in the ^{14}N NMR of the trinitromethane moiety were found for **1**–**3** between –33 and –36 ppm and in addition, that of the nitrocarbamate of **3** was observed at −55 ppm. For compounds **2** and **3** a very broad resonance for the amide nitrogen atom was detected at −310 (**2**) and −292 ppm (**3**).

VIBRATIONAL SPECTROSCOPY

The vibrational analysis of **1**–**3** showed the characteristic asymmetric NO_2 stretching vibrations in the range of 1615 to 1588 cm^{-1} and the symmetric stretching vibrations at 1304 to 1271 cm^{-1} (Table 3.2). All vibrations of the nitro groups for **1**–**3** are in a close range, explained by the similarity of the functional groups. The carbonyl stretching vibration was observed in the typical range between 1785 and 1721 cm^{-1}. The N−H stretching vibrations for **2** and **3** were found in the range of 3447–3062 cm^{-1}.

Table 3.2. Characteristic IR and Raman vibrations [a] /cm^{-1} of **1**–**3**

	1		**2**		**3**	
	Raman	IR	Raman	IR	Raman	IR
ν NH			3300 (4)	3447 w	3170 (9)	3168 w
				3352 m		3062 w
				3302 w		
ν CO	1785 (14)	1777 m	1721 (17)	1729 m	1768 (49)	1772 m
ν_{as} NO_2	1615 (26)	1598 s	1622 (31)	1590 s	1609 (46)	1588 s
ν_s NO_2	1301 (32)	1293 m	1304 (31)	1300 m	1303 (55)	1271 w

a) Raman intensities in brackets. IR intensities: s = strong, m = medium, w = weak.

SINGLE CRYSTAL STRUCTURAL ANALYSIS

Single crystals of **2** and **3** were obtained from tetrachloromethane at ambient temperature (Table 3.3). Both compounds crystallize in the monoclinic space group $P2_1/c$ with four formula units per unit cell. The asymmetric unit with selected bond lengths and angles are shown in Figure 3.2 (**2**) and Figure 3.3 (**3**).

Table 3.3. X-ray data and parameters of **2** and **3**

	2	**3**
Formula	$C_3H_4N_4O_8$	$C_3H_3N_5O_{10}$
FW /g mol^{-1}	224.09	269.08
Temperature /K	173(2)	243(2)
Crystal size /mm	0.28 × 0.10 × 0.05	0.25 × 0.02 × 0.02
Crystal system	monoclinic	monoclinic
Crystal description	colorless needle	colorless needle
Space group	$P2_1/c$	$P2_1/c$
a /Å	12.838(1)	10.784(2)
b /Å	6.572(1)	11.527(2)
c /Å	9.869(1)	8.752(2)
β /°	103.57(1)	108.20(2)
V /Å^3	809.34(1)	1033.5(7)
Z	4	4
$\rho_{calc.}$ /g cm^{-3}	1.839(3)	1.730(2)
μ /mm^{-1}	0.186	0.178
F(000)	456	544
θ range /°	4.28–25.99	4.30–26.00
Index ranges	$-7 \le h \le 15$	$-13 \le h \le 13$
	$-8 \le k \le 7$	$-13 \le k \le 14$
	$-12 \le l \le 12$	$-7 \le l \le 10$
Reflections collected	3596	5001
Reflection observed	1572	1945
Independent reflections	1082	681
Rint	0.0234	0.0526
R_1, wR$_2$ (2σ data)	0.0292, 0.0574	0.0612, 0.1277
R_1, wR$_2$ (all data)	0.0485, 0.0610	0.1759, 0.1633
GOOF on F^2	0.883	0.806
Resd. dens. /e Å^3	−0.165/0.188	−0.198/0.362

The molecular structure of the carbamate **2** shows a large part with nearly planar arrangement. This planar range comprised the carbamate, the C2 carbon of the methylene group and C3 of the trinitromethyl moiety. The conformation of the substituents at C2 and C3 is nearly staggered [N2−C3−C2−H3A 43.3(1)°, N3−C3−C2−H3B 42.6(1)°, N4−C3−C2−O2 42.7(1)°]. The C−N bond lengths of the trinitromethyl moiety are in the range of 1.52 Å, which is significantly longer than a regular C−N bond (1.47 Å).[12] This is typical for molecules with the trinitromethyl moiety and is due to steric repulsion effects.[1b, 4a] The three nitro groups arrange in a propeller like constitution, which optimize the non-bonded intramolecular attractions [partial charge distribution of nitrogen (δ^+) and oxygen (δ^-) atom in the nitro group] and electrostatic repulsion of two neighboring nitro groups. The N···O attractions (N2···O6, N3···O8, N4···O3) can be found in **2** with distances in the range of 2.55–2.67 Å, which are much shorter than the sum of the van der Waals radii for nitrogen and oxygen (3.07 Å).[13] In addition, another strong attractive intramolecular N···O interaction with 2.60 Å, is observed between the nitrogen atom N4 of the trinitro functionality and the oxygen O2. The carbamate group with a short C−NH_2 bond (1.333 Å) and shortened N−H bonds (0.87 and 0.91 Å) shows typical values for carbamates.[14]

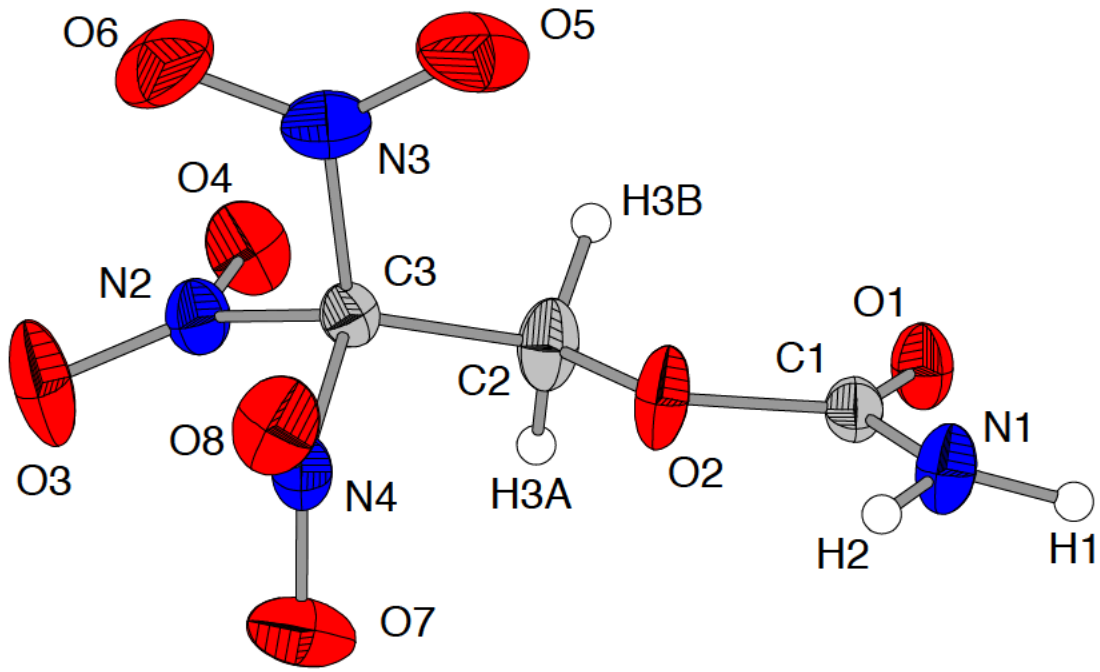

Figure 3.2. Molecular structure of 2,2,2-trinitroethyl carbamate (**2**), with thermal ellipsoids at the 50% probability level. Bond lengths /Å and angles /°: O1−C1 1.210(2), O3−N2 1.212(2), O7−N4 1.206(2), O2−C2 1.425(2), O2−C1 1.362(2), O6−N3 1.207(2), O8−N4 1.211(2), N2−O4 1.206(2), N2−C3 1.519(2), C2−H3A 0.991(1), C2−H3B 0.990(1), C2−C3 1.509(2), N4−C3 1.521(2), N3−O5 1.212(2), N3−C3 1.528(2), N1−C1 1.333(2), N1−H1 0.91(2), N1−H2 0.87(2), C1−O2−C2 114.8(1), C2−C3−N2 111.8(1), N2−C3−N4 108.0(1), C2−C3−N3 113.8(1), N2−C3−N3 106.4(1), C1−N1−H1 118.1(11), C1−N1−H2 119.2(12), H1−N1−H2 119.1(16), O1−C1−N1 127.8(2), O1−C1−O2 122.1(1), N1−C1−O2 110.1(1), N1−C1−O2−C2 176.8(1), O1−C1−O2−C2 −4.7(2), C1−O2−C2−C3 −172.4(1), H1−N1−C1−O1 −170.1(14), H2−N1−C1−O1 169.5(14).

The molecules of **2** are cross-linked *via* hydrogen bonds. The intermolecular hydrogen-bond lengths and angles are shown in Table 3.4. In the structure can been found three classical NH···O hydrogen bondings with the carbonyl and the nitro group as acceptors. The two hydrogen interactions with the carbonyl (O1), can be classified as strong, while the interaction with the nitro group (O5) is moderate on the basis of the distance and angle of the hydrogen bond.[15] Also an unusual hydrogen bond with carbon as donor (CH···O) can be observed in **2**, between the methylene (C2−H3A) and one nitro group (O7), which is only weak.[16]

Table 3.4. Hydrogen-bond distances /Å and angles /° of **2**

D–H···*A*	*D*–H	H···*A*	*D*···*A*	∢(*D*–H···*A*)
N1–H1···O1^{i}	0.91	2.160	3.012	156.0
N1–H2···O5^{ii}	0.87	2.709	3.189	116.3
N1–H2···O1^{iii}	0.87	2.310	3.152	163.9
C2–H3A···O7^{iv}	0.99 [a)]	2.634	3.379	132.1

a) Normalized C–H length 0.99 Å. Symmetry codes of acceptor molecules: (*i*) −*x*, 1−*y*, −*z*; (*ii*) −*x*, −½+*y*, ½−*z*; (*iii*) *x*, 1½−*y*, ½+*z*; (*iv*) *x*, 1½−*y*, −½+*z*.

The data collection of **3** had to be performed at higher temperature, because the compound showed a phase transition at about −62 °C. This phase transition leads to microfracture of the single crystal, which made a measurement impossible. Thus, the data collection was carried out at −30 °C, causing much greater thermal vibrations of the atoms, especially of the trinitromethyl group.

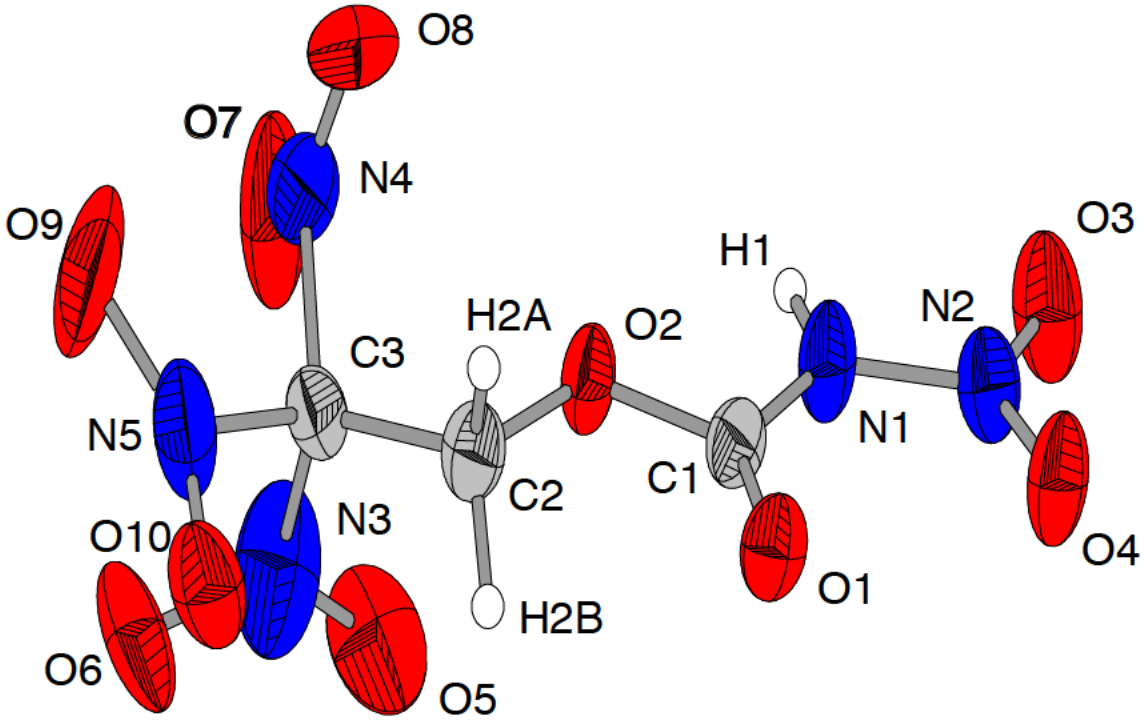

Figure 3.3. Molecular structure of 2,2,2-trinitroethyl nitrocarbamate (**3**), with thermal ellipsoids at the 30% probability level. Bond lengths /Å and angles /°: O1–C1 1.182(5), O2–C1 1.333(4), O2–C2 1.437(6), O3–N2 1.201(6), O4–N2 1.213(5), O5–N3 1.15(1), O6–N3 1.31(1), O7–N4 1.40(1), O8–N4 1.16(1), O9–N5 1.267(7), O10–N5 1.238(8), N1–N2 1.373(5), N1–C1 1.358(6), N1–H1 0.82(5), N3–C3 1.49(1), N4–C3 1.473(8), N5–C3 1.529(8), C2–C3 1.472(6), O3–N2–N1 126.4(4), N1–N2–O4 114.7(4), O4–N2–O3 118.9(4), N2–N1–H1 112(3), H1–N1–C1 123(3), C1–N1–N2 124.6(4), O4–N2–N1–C1 −2.0(6), O4–N2–N1–H1 −177(3), O3–N2–N1–C1 −177.9(4), N2–N1–C1–O2 177.8(4), N2–N1–C1–O1 −1.4(7), N1–C1–O2–C2 −179.8(3), C1–O2–C2–C3 −166.7(3).

In the literature only one single crystal X-ray structure of a nitrocarbamate, alkylated at the carbamate nitrogen, is known.[17] The nitrocarbamate moiety of compound **3** shows a perfect planarity as shown by the sum of the angles around the C1 and the two nitrogen atoms N1/N2, where the angle sum is 360.0° each. The N1–N2 bond of the nitramine moiety is 1.373 Å, which indicates a substantial of a double bond character, achieved by delocalization of the nitrogen lone pair. This is also evidenced by a shortened N–H bond (0.82 Å) compared with the carbamate structure of **2**. The carbonyl group, *cis* orientated to the nitro group, shows also a slight shortening (1.182 Å). The trinitroethyl moiety has the same propeller like configuration compared to **2**, which is stabilized with short strong attractive interactions of N···O atoms (N3···O7, N4···O9, N4···O2, N5···O6). The nitrocarbamate **3** shows two classical hydrogen bonds, which links the hydrogen attached

to N1 to two oxygen atoms (O1^{i}, O4^{i}), of symmetry related nitrocarbamate functionality. Here, the interaction between the carbonyl (O1) and the NH group is significantly the strongest. Also an improper hydrogen bond with carbon as donor (CH···O) can be observed, between the methylene (C2−H2A/B) and neighboring nitro groups (Table 3.5).[16] This extensive hydrogen-bonding may help to explain the good thermal stability.[17]

Table 3.5. Hydrogen-bond distances /Å and angles /° of **3**

D–H···*A*	*D*–H	H···*A*	*D*···*A*	∢(*D*–H···*A*)
N1–H1···O1^{i}	0.82	2.015	2.797	159.8
N1–H1···O4^{i}	0.82	2.634	3.117	119.3
C2–H2B···O3^{ii}	0.99	2.711	3.635	154.1
C2–H2B···O4^{ii}	0.99	2.516	3.424	157.2
C2–H2A···O10^{iii}	0.99	2.607	3.448	143.9

a) Normalized C−H length 0.99 Å. Symmetry codes of acceptors molecules: (*i*) *x*, ½−*y*, −½+*z*; (*ii*) 1−*x*, −½+*y*, 1½−*z*; (*iii*) −*x*, −*y*, 1−*z*.

THERMAL AND ENERGETIC PROPERTIES

2,2,2-trinitroethyl carbamate (**2**) melts at 91 °C (onset) and is thermally stable up to a temperature of 169 °C (onset) (Table 3.6). It burns residue-free with a smokeless flame due to a balanced amount of oxygen and shows no sensitivity towards impact, but it is very sensitive to friction.

Table 3.6. Physical and chemical properties of **2** and **3**

	2	**3**
Formula	$C_3H_4N_4O_8$	$C_3H_3N_5O_{10}$
FW /g mol^{-1}	224.09	269.08
T_m /°C (onset) [a]	91	109
T_{dec} /°C (onset) [b]	169	153
N /% [c]	25.00	26.03
$N + O$ /% [d]	82.12	85.49
Ω_{CO} /% [e]	+21.4	+32.7
Ω_{CO2} /% [f]	+0.0	+14.9
ρ /g cm^{-3} [g]	1.84 (173 K)	1.73 (243 K)
$\Delta U°_f$ /kJ mol^{-1} [h]	−459	−366
$\Delta H°_f$ /kJ kg^{-1} [i]	−1960	−1278

a) Melting (T_m) and b) decomposition (T_d) point from DSC measurement carried out at a heating rate of 5 °C min^{-1}. c) Nitrogen content. d) Combined nitrogen and oxygen content. e) Oxygen balance assuming the formation of CO. f) Oxygen balance assuming the formation of CO_2. g) Calculated density from X-ray measurement. h) Energy of formation and i) Heat of formation calculated with CBS-4M method.

By a low temperature DSC measurement of 2,2,2-trinitroethyl nitrocarbamate (**3**) an endothermic solid phase transformation can be observed at −62 °C (onset). Upon further heating, the compound showed a melting point at 109 °C (onset) and decomposition starts at 153 °C (onset). The sensitivities of **3** are in the range of RDX, and therefore it is sensitive to friction, impact and electrostatic discharge.

For the calculation of the performance parameters using the EXPLO5 program, the cell parameters of **2** and **3** were determined at 25 °C in order to obtain the density of the substances at standard conditions (Table 3.7). The performance data of **2** and **3** are summarized in Table 3.8.

Table 3.7. Cell parameters of **2** and **3** at 25 °C

	2	**3**
Temperature /K	298(1)	298(1)
Crystal system	monoclinic	monoclinic
Space Group	$P2_1/c$	$P2_1/c$
a /Å	12.91(4)	10.79(4)
b /Å	6.59(2)	11.540(3)
c /Å	9.88(4)	8.76(4)
β /°	103.5(3)	108.2(4)
V /Å^3	817(3)	1037(4)
Z	4	4
$\rho_{calc.}$ /g cm^{-3}	1.821	1.722

Table 3.8. Predicted detonation, combustion parameters (using EXPLO5 V5.05) and sensitivity data for **2** and **3**

	2	**3**
Q_v /kJ kg^{-1} a)	−5261	−4420
T_{ex} /K b)	4081	3832
V_0 /L kg^{-1} c)	696	687
P_{CJ} /kbar d)	309	242
V_{Det} /m s^{-1} e)	8224	7541
IS /J f)	>40	10
FS /N g)	64	96
ESD /J h)	0.15	0.10
grain size /μm i)	<500	500-1000

a) Heat of combustion. b) Temperature of the combustion gases. c) Volume of the explosion gases. d) Detonation pressure. e) Detonation velocity. f) Impact and g) Friction sensitivities. h) Sensitivity towards electrostatic discharge. i) Grain size of the samples used for sensitivity tests.

$$I_s^* = \frac{I_s}{g}\sqrt{\frac{2\,\gamma\,R\,T_c}{(\gamma-1)M}} \qquad \gamma = \frac{C_p}{C_v} \tag{1}$$

The determining parameter for high energy dense oxidizers (HEDO) is the specific impulse I_s. It is used to evaluate the performance of solid rocket propellants and the used high energy dense oxidizers. An expression for I_s is given in Equation (1), were γ is the ratio of specific heats for the combustion gases, R the ideal gas constant, T_c the burning temperature in the combustion chamber and M the molecular weight of the gaseous combustions products at the nozzle.[1a] I_s is therefore dependent on the burning temperature proportional and the molecular weight of the combustions products reciprocal. The heat of combustion can be increased by adding a high performing fuel, which has an increased heat of combustion ΔH_c.

$$1½O_{2\,(g)} + 2Al_{\,(s)} \rightarrow Al_2O_{3\,(s)} \qquad \Delta H_c = -1590\ \text{kJ} \tag{2}$$

$$3CO_{2\,(g)} + 2Al_{\,(s)} \rightarrow 3CO_{\,(g)} + Al_2O_{3\,(s)} \qquad \Delta H_c = -741\ \text{kJ} \tag{3}$$

$$3H_2O_{\,(g)} + 2Al_{\,(s)} \rightarrow 3H_{2\,(g)} + Al_2O_{3\,(s)} \qquad \Delta H_c = -866\ \text{kJ} \tag{4}$$

$$3CO_{\,(g)} + 2Al_{\,(s)} \rightarrow 3C_{\,(s)} + Al_2O_{3\,(s)} \qquad \Delta H_c = -1251\ \text{kJ} \tag{5}$$

Aluminum has a very high heat of combustion ΔH_c and the combustion products (Al_2O_3) are not harmful to the environment. The oxidation of aluminum with oxygen is highly exothermic and produces a lot of heat [Equation (2)[18]], which increases T_c. In the case of an oxygen deficit, the aluminum reacts further with the gaseous products water and carbon dioxide, to form hydrogen and carbon monoxide. Also, these two reactions in an oxygen-deficient composition produce a great amount of heat [Equation (3) and Equation (4)[18]] and no change in the volume of produced gas. However, there is a limit to the amount of aluminum that can be added, because aluminum can also react with carbon monoxide to form carbon and alumina. This reaction also causes an increase of heat but the gas volume decreases radically from 3 to 0 moles for this reaction [Equation (5)[18]]. An increase of the value for I_s by 20 s leads empirically to a doubling of the usual payload.[1a] Therefore, the development of new energetic oxidizers based on CHNO compounds decomposing into small aerialy molecules is a promising way to increase the specific impulse of solid rocket boosters.

The specific impulse of **2** in a mixture of 20 % of aluminum as fuel is 249 s. The specific impulse of **3** achieved with an admixture of 25 % aluminum, is a specific impulse of 247 s and is therefore in the range of the standard mixture of ammonium perchlorate (Table 3.9).

Table 3.9. Predicted specific impulse I_s of mixtures with aluminum (using EXPLO5 V5.05) and sensitivity data for **2** and **3**

	2	**3**	**AP**
I_s /s [a)]	234	223	153
I_s /s (30 % Al) [b)]	- [d)]	244	243
I_s /s (25 % Al) [b)]	249	247	242
I_s /s (20 % Al) [b)]	249	247	232
I_s /s (15 % Al) [b)]	248	247	234
I_s /s (10 % Al) [b)]	245	239	181
I_s /s (5 % Al) [b)]	240	233	178
I_s /s (15 % Al, 14 % binder) [c)]	- [d)]	257	257
I_s /s (10 % Al, 14 % binder) [c)]	- [d)]	251	253
I_s /s (5 % Al, 14 % binder) [c)]	- [d)]	244	247

a) Specific impulse. b) Specific impulse for mixtures with the compound **2**, **3** and ammonium perchlorate (AP) as oxidizer with different values of aluminum. c) Specific impulse for mixtures with different values of aluminum and binder (6 % polybutadiene acrylic acid, 6 % polybutadiene acrylonitrile and 2 % bisphenol-A ether) at 70.0 kbar chamber pressure and isobaric combustion condition (1 bar) d) too low oxygen balance of the composition to calculate.

3.4 CONCLUSION

The facile synthesis route of choice for 2,2,2-trinitroethyl chloroformate (**1**) is a direct chloroformulation of 2,2,2-trinitroethanol with phosgene. This route has compared to the known route several advantages. The reaction with aqueous ammonia gives 2,2,2-trinitroethyl carbamate (**2**) and nitration furnishes 2,2,2-trinitroethyl nitrocarbamate (**3**). By a low temperature DSC measurement an endothermic solid phase transformation of **3** was observed at −62 °C. On further heating melting occurs at 109 °C and decomposing at 153 °C. The nitrocarbamate **3** has a very high positive oxygen balance (CO_2) Ω of +14.9 %. Thus, the molecule consists of 59.5 % of oxygen and 26.0 % of nitrogen. These examples demonstrate that the 2,2,2-trinitroethylformate group is a very promising energetic moiety, which combines very high oxygen content and relative high stability. The specific impulse I_s of compositions with **3** is comparable with compositions using ammonium perchlorate as oxidizer. Advantageously, the burning of **3** with aluminum produces no toxic substances such as hydrogen chloride.

3.5 EXPERIMENTAL SECTION

General Procedures

Raman spectra were recorded on a Bruker Multi-RAM Raman Sample Compartment D418 equipped with a Nd-YAG-Laser (1064 nm) and a Ge diode detector. Infrared spectra were measured with a Perkin–Elmer Spectrum BX-FTIR spectrometer equipped with a Smiths DuraSampl*IR* II ATR device. All spectra were recorded at ambient temperature. NMR spectra were recorded with a JEOL Eclipse 400 instrument and chemical shifts were determined with respect to external Me_4Si (^1H, 399.8 MHz; ^{13}C, 100.5 MHz) and $MeNO_2$ (^{14}N, 28.9 MHz). Mass spectrometric data were obtained with a JEOL MStation JMS 700 spectrometer (DCI+, DEI+). Elemental analyses of C/H/N were performed with an Elementar Vario EL analyzer. Melting points were measured with a Linseis DSC-PT10 instrument, using a heating rate of 5 °C min^{-1} and checked by a Büchi Melting Point B-540 apparatus and are not corrected. The sensitivity data (impact, friction, and electrostatic discharge) were performed with a drophammer, friction tester, and electrostatic discharge device conform to the directive of the Federal Institute for Materials Research and Testing (BAM).[1b]

Computational Details

All *ab initio* calculations were carried out using the program package Gaussian 03 (Revision B.03)[19] and visualized by GaussView 5.0.8.[20] Structure optimizations and frequency analyses were performed with Becke's B3 three parameter hybrid functional using the LYP correlation functional (B3LYP). For C, H, N and O a correlation consistent polarized double-zeta basis set was used (cc-pVDZ). The structures were optimized without symmetry constraints and the energy is corrected with the zero point vibrational energy.[21]

The enthalpies (*H*) and free energies (*G*) were calculated using the complete basis set (CBS) method in order to obtain accurate values.[21a] The CBS models use the known asymptotic convergence of pair natural orbital expressions to extrapolate from calculations using a finite basis set to the estimated complete basis set limit. CBS-4 starts with a HF/3-21G(d) geometry optimization, which is the initial guess for the following SCF calculation as a base energy and a final MP2/6-31+G calculation with a CBS extrapolation to correct the energy in second order. The used reparametrized CBS-4M method additionally implements a MP4(SDQ)/6-31+(d,p) calculation to approximate

higher order contributions and also includes some additional empirical corrections.[22] The enthalpies of the gas-phase species were estimated according to the atomization energy method.[23]

All calculations affecting the detonation parameters were carried out using the program package EXPLO5 V5.05.[24] The detonation parameters were calculated at the CJ point with the aid of the steady-state detonation model using a modified Becker-Kistiakowski-Wilson equation of state for modeling the system. The CJ point is found from the Hugoniot curve of the system by its first derivative. The specific impulses were also calculated with the EXPLO5 V5.05 program, assuming an isobaric combustion of a composition of **2** and **3** as oxidizer, aluminum as fuel, 6 % polybutadiene acrylic acid, 6 % polybutadiene acrylonitrile as binder and 2 % bisphenol-A as epoxy curing agent. A chamber pressure of 70.0 bar and an ambient pressure of 1.0 bar with frozen expansion conditions were estimated for the calculations.

X-ray Crystallography

For all compounds, an Oxford Xcalibur3 diffractometer with a CCD area detector was employed for data collection using Mo-K_α radiation (λ = 0.71073 Å). The structures were solved by direct methods (SIR97)[25] and refined by full-matrix least-squares on F^2 (SHELXL-97).[26] All non-hydrogen atoms were refined anisotropically. The hydrogen atom positions were calculated, except for the N-terminal hydrogen which were located in a difference Fourier map and then refined freely. Crystallographic data (excluding structure factors) for the structures reported in this paper have been deposited with the Cambridge Crystallographic Data Centre, CCDC, 12 Union Road, Cambridge CB21EZ, UK. Copies of the data can be obtained free of charge on quoting the depository numbers CCDC-923988 (**2**) and CCDC-923989 (**3**) (fax.: + 44 1223/336-033; e-mail: deposit@ccdc.cam.ac.uk).

Synthesis

CAUTION! *All of the described compounds are energetic with sensitivities towards heat, impact and friction. Although no hazards occurred during preparation and manipulation, additional proper protective precautions (face shield, leather coat, earthened equipment and shoes, Kevlar® gloves and ear plugs) should be used when undertaking work with these compounds.*

CAUTION! *Phosgene is a highly toxic, irritating and corrosive gas. Inhalation can cause fatal respiratory damage. Phosgene reacts violently and decomposes to toxic compounds on contact with moisture, including chlorine and carbon monoxide.*

*2,2,2-Trinitroethyl chloroformate (**1**)*

In a four-necked, 250 mL round-bottomed flask cooled in a dry-ice/ethanol bath and equipped with a magnetic stirrer, gas inlet, septum, dry-ice/ethanol cooled reflux condenser with gas outlet, and a thermometer, phosgene (14.0 g, 13.9 mmol) was condensed at −70 °C. A solution of 2,2,2-trinitroethanol (5.0 g, 27.6 mmol) in dichloromethane (100 mL) was added, while the temperature was maintained below −50 °C. A solution of triethylamine (2.9 g, 4.0 mL, 29.0 mmol) diluted in dichloromethane (50 mL) was added dropwise within 1 h, still maintaining the temperature below –50 °C. Afterwards, the mixture and the reflux condenser were allowed to warm up and were stirred for 12 h at ambient temperature. The organic solvent was removed and the light yellow residue was extracted with diethyl ether (3 × 50 mL). The insoluble triethylammonium chloride was filtered off and the combined organic phase was washed with ice-cold water (200 mL) and dried with magnesium sulfate. All volatiles were removed *in vacuo* and the residue was distilled (oil bath 65 °C, 0.03 mbar) yielding 8.9 g of **1** (86 %) as a colorless liquid.

IR: ν = 3024 (w), 2974 (w), 2893 (w), 1777 (m), 1598 (s), 1438 (w), 1384 (w), 1347 (w), 1293 (m), 1124 (s), 1088 (s), 979 (w), 853 (w), 826 (w), 796 (s), 778 (m), 721 (w), 676 (m) cm^{-1}. **Raman** (200 mW): ν = 3020 (16), 2972 (56), 1785 (14), 1615 (26), 1439 (14), 1384 (25), 1349 (42), 1301 (32), 1170 (6), 1091 (8), 1034 (24), 892 (21), 856 (100), 827 (10), 800 (16), 777 (9), 723 (7), 641 (8), 549 (14), 531 (14), 501 (55), 462 (14), 398 (45), 374 (75), 338 (17), 285 (46), 234 (31) cm^{-1}. **^{1}H NMR** ([D$_6$]acetone) δ = 5.51 (s, CH_2) ppm. **^{13}C{^{1}H} NMR** ([D$_6$]acetone) δ = 149.5 (CO$_2$Cl), 121.4 (C(NO$_2$)$_3$), 63.3 (CH$_2$) ppm. **^{14}N NMR** ([D$_6$]acetone) δ = −36 (C(NO$_2$)$_3$) ppm. **EA** ($C_3H_2N_3O_8Cl$, 243.52) calcd.: C 14.80, H 0.83, N 17.26, Cl 14.56 %; found: C 15.01, H 0.73, N 17.01, Cl 14.16 %.

*2,2,2-Trinitroethyl carbamate (**2**)*

Into a stirring solution of **1** (0.50 g, 2.1 mmol) in dichloromethane (5 mL), chilled to −30 °C, concentrated ammonia (30 %, 0.5 mL, 8.0 mmol) was added dropwise. The

mixture was stirred for 1 h at −30 °C. The precipitate formed was filtered off and recrystallized from hot water, to obtain 0.38 g (83 %) colorless needles of the carbamate **2**.

DSC (5 K min^{-1}): 91 °C (onset mp.) (Ref.[8] 92–93 °C)), 169 °C (onset dec.); **IR**: ν = 3447 (w), 3352 (w), 3302 (w), 2962 (m), 1729 (m), 1590 (s), 1441 (w), 1399 (m), 1367 (w), 1325 (m), 1300 (m), 1248 (w), 1167 (w), 1138 (w), 1105 (m), 1027 (w), 910 (w), 873 (w), 858 (w), 804 (m), 784 (m), 772 (m), 741 (w), 673 (w), 646 (w), 606 (w), 546 (m), 527 (m) cm^{-1}. **Raman** (200 mW): ν = 3300 (4), 3004 (23), 2964 (51), 2828 (3), 1721 (17), 1622 (31), 1608 (28), 1587 (18), 1445 (17), 1404 (8), 1369 (54), 1304 (31), 1250 (15), 1171 (10), 1145 (10), 1112 (9), 1091 (9), 1027 (17), 910 (19), 878 (10), 859 (100), 802 (14), 786 (12), 745 (10), 674 (10), 647 (12), 549 (18), 524 (9), 426 (55), 397 (46), 377 (72), 305 (53), 265 (17), 212 (30) cm^{-1}. **^{1}H NMR** ([D$_6$]acetone) δ = 6.77 (s, 1H, NH_2), 6.49 (s, 1H, NH_2), 5.68 (s, 2H, CH_2) ppm. **^{13}C{^{1}H} NMR** ([D$_6$]acetone) δ = 154.5 (CO_2N), 125.7 ($C(NO_2)_3$), 61.8 (CH_2) ppm. **^{14}N NMR** ([D$_6$]acetone) δ = −33 ($C(NO_2)_3$), −310 (NH_2) ppm. **MS** (DEI+) *m/z* (%): 225 (15) [$(M + H)^+$], 59 (13) [$CHNO_2^+$], 46 (59) [NO_2^+], 44 (100) [$(M - OCH_2(NO_2)_3)^+$, $CONH_2^+$], 43 (31) [$CHNO^+$], 30 (71) [NO^+]. **EA** ($C_3H_4N_4O_8$, 224.10) calc.: C 16.08, H 1.80; N 25.00 %; found: C 15.89; H 1.78; N 24.50 %. **BAM drophammer:** >40 J; **friction tester:** 64 N; **ESD:** 0.15 J (grain size <500 µm).

*2,2,2-Trinitroethyl nitrocarbamate (**3**)*

Into concentrated sulfuric acid (1 mL) was dropped red fuming nitric acid (>99.5 %, 1 mL) at 0 °C. To this chilled nitration mixture, 2,2,2-trinitroethyl carbamate (**2**) (0.25 g, 1.1 mmol) was added in small portions. The solution was stirred for 2 h at 0 °C and for 2 h at ambient temperature. The mixture was poured onto ice-water (200 mL), extracted with ethyl acetate (3 x 50 mL) and the combined organic phase was dried with magnesium sulfate. The solvent was removed under reduced pressure and the crude solid product was recrystallized from carbon tetrachloride to obtain 0.30 g (99 %) colorless needles of **3**.

DSC (5 K min^{-1}): 109 °C (onset mp.), 153 °C (onset dec.); **IR**: (cm^{-1}): ν = 3168 (w), 3062 (w), 3013 (w), 2900 (w), 1772 (m), 1588 (s), 1466 (m), 1444 (w), 1390 (w), 1351 (w), 1326 (m), 1398 (s), 1271 (w), 1170 (s), 990 (m), 972 (s), 882 (w), 856 (w), 826 (m),

792 (m), 777 (m), 760 (m), 745 (m), 710 (w) 668 (w) cm^{-1}. **Raman** (200 mW): ν = 3170 (9), 3013 (33), 2966 (48), 2868 (9), 1768 (49), 1609 (46), 1468 (23), 1442 (23), 1393 (32), 1353 (46), 1324 (75), 1303 (55), 1272 (26), 1183 (19), 1095 (16), 1050 (51), 998 (62), 883 (21), 859 (100), 794 (17), 781 (18), 761 (19), 657 (18), 542 (25), 461 (58), 377 (72), 407 (85), 376 (92), 271 (69) cm^{-1}. **^{1}H NMR** ([D_6]acetone) δ = 10.70 (s, 1H, N*H*), 5.53 (s, 2H, CH_2) ppm. **^{13}C{^{1}H} NMR** ([D_6]acetone) δ = 145.2 (*C*O_2N), 122.2 (*C*$(NO_2)_3$), 62.1 (*C*H_2) ppm. **^{14}N NMR** ([D_6]acetone) δ = −36 (C(*N*$O_2)_3$), −55 (N*N*O_2), −292 (*N*NO_2) ppm. **MS** (DCI+) *m*/*z* (%): 270 (1) [$(M + H)^+$], 225 (2) [$(M-NO_2)^+$]. **EA** ($C_3H_3N_4O_{10}$, 269.08) calc.: C 13.39; H 1.12; N 26.03 %; found: C 13.54; H 1.09; N 25.70 %. **BAM drophammer:** 10 J; **friction tester:** 96 N; **ESD**: 0.10 J (grain size 500–1000 µm).

3.6 ACKNOWLEDGEMENT

The Hanns Seidel Foundation (HSF) is gratefully acknowledged for the award of a Ph.D. scholarship (Q. J. A.). Financial support of this work by the Ludwig-Maximilian University of Munich (LMU), the U.S. Army Research Laboratory (ARL) under grant no. W911NF-09-2-0018, the Armament Research, Development and Engineering Center (ARDEC) under grant no. W911NF-12-1-0467, and the Office of Naval Research (ONR) under grant nos. ONR.N00014-10-1-0535 and ONR.N00014-12-1-0538 is gratefully acknowledged. The authors acknowledge collaborations with Dr. Mila Krupka (OZM Research, Czech Republic) in the development of new testing and evaluation methods for energetic materials and with Dr. Muhamed Sućesca (Brodarski Institute, Croatia) in the development of new computational codes to predict the detonation and propulsion parameters of novel explosives. We are indebted to and thank Drs. Betsy M. Rice and Brad Forch (ARL, Aberdeen, Proving Ground, MD) for many inspired discussions.

3.7 REFERENCES

[1] a) T. M. Klapötke, *Chemistry of High-Energy Materials*, 2nd ed., de Gruyter, Berlin, **2012**; b) M. Göbel, T. M. Klapötke, *Adv. Funct. Mater.* **2009**, *19*, 347–365.

[2] M. Göbel, T. M. Klapötke, *Z. Anorg. Allg. Chem.* **2007**, *633*, 1006–1017.

[3] C. Hogue, *Chem. Eng. News* **2011**, *89*, 6.

[4] a) T. M. Klapötke, B. Krumm, R. Moll, S. F. Rest, *Z. Anorg. Allg. Chem.* **2011**, *637*, 2103–

2110; b) T. M. Klapötke, B. Krumm, R. Moll, *Chem. Eur. J.* **2013**, *19*, 12113–12123; c) H. Feuer, T. Kucera, *J. Org. Chem.* **1960**, *25*, 2069–2070; d) M. Göbel, T. M. Klapötke, *Acta Crystallogr., Sect. C* **2007**, *63*, o562–o564.

[5] S. V. Lieberman, E. C. Wagner, *J. Org. Chem.* **1949**, *14*, 1001–1012.

[6] W. H. Gilligan, S. L. Stafford, *Synthesis* **1979**, 600–602.

[7] L. Cotarca, H. Eckert, in *Phosgenations - A Handbook*, Wiley-VCH, Weinheim, **2005**.

[8] O. A. Luk'yanov, G. V. Pokhvisneva, *Russ. Chem. Bull.* **1992**, *41*, 1286–1288.

[9] a) M. Oki, *Applications of dynamic NMR spectroscopy to organic chemistry*, VCH Publishers, Deerfield Beach, FL, **1985**; b) T. M. Klapötke, B. Krumm, P. Mayer, K. Polborn, O. P. Ruscitti, *Inorg. Chem.* **2001**, *40*, 5169–5176.

[10] K. B. Wiberg, P. R. Rablen, *J. Am. Chem. Soc.* **1995**, *117*, 2201–2209.

[11] D. S. Raiford, C. L. Fisk, E. D. Becker, *Anal. Chem.* **1979**, *51*, 2050–2051.

[12] A. F. Holleman, E. Wiberg, N. Wiberg, *Lehrbuch der anorganischen Chemie*, 102nd ed., de Gruyter, Berlin, **2008**.

[13] A. Bondi, *J. Phys. Chem.* **1964**, *68*, 441–451.

[14] B. Sepehrnia, J. R. Ruble, G. A. Jeffrey, *Acta Crystallogr, Sect. C* **1987**, *43*, 249–251.

[15] T. Steiner, *Angew. Chem.* **2002**, *114*, 50–80.

[16] Y. Gu, T. Kar, S. Scheiner, *J. Am. Chem. Soc.* **1999**, *121*, 9411–9422.

[17] R. Butcher, R. Gilardi, C. George, J. Flippen-Anderson, *J. Chem. Crystallogr.* **1996**, *26*, 381–388.

[18] J. Akhavan, *The Chemistry of Explosives* 2nd ed., The Royal Society of Chemistry, Cambridge, **2004**.

[19] M. J. Frisch, G. W. Trucks, H. B. Schlegel, G. E. Scuseria, M. A. Rob, J. R. Cheeseman, J. A. Montgomery Jr., T. Vreven, K. N. Kudin, J. C. Burant, J. M. Millam, S. S. Iyengar, J. Tomasi, V. Barone, B. Mennucci, M. Cossi, G. Scalmani, N. Rega, G. A. Petersson, H. Nakatsuji, M. Hada, M. Ehara, K. Toyota, R. Fukuda, J. Hasegawa, M. Ishida, T. Nakajima, Y. Honda, O. Kitao, H. Nakai, M. Klene, X. Li, J. E. Knox, H. P. Hratchian, J. B. Cross, V. Bakken, C. Adamo, J. Jaramillo, R. Gomperts, R. E. Stratmann, O. Yazyev, A. J. Austin, R. Cammi, C. Pomelli, J. W. Ochterski, P. Y. Ayala, K. Morokuma, G. A. Voth, P. Salvador, J. J. Dannenberg, V. G. Zakrzewski, S. Dapprich, A. D. Daniels, M. C. Strain, O. Farkas, D. K. Malick, A. D. Rabuck, K. Raghavachari, J. B. Foresman, J. V. Ortiz, Q. Cui, A. G. Baboul, S. Clifford, J. Cioslowski, B. B. Stefanov, G. Liu, A. Liashenko, P. Piskorz, I. Komaromi, R. L. Martin, D. J. Fox, T. Keith, M. A. Al-Laham, C. Y. Peng, A. Nanayakkara, M. Challacombe, P. M. W. Gill, B. Johnson, W. Chen, M. W. Wong, C. Gonzalez, J. A. Pople, *Gaussian 03,* Rev. B.03, Gaussian, Inc., Wallingford CT (USA), **2003**.

[20] R. D. Dennington II, T. A. Keith, J. M. Millam, *GaussView*, Version 5.0.8, Semichem Inc., Shawnee Mission KS (USA), **2009**.

[21] a) T. M. Klapötke, J. Stierstorfer, *Phys. Chem. Chem. Phys.* **2008**, *10*, 4340–4346; b) J. A. Montgomery Jr., M. J. Frisch, J. W. Ochterski, G. A. Petersson, *J. Chem. Phys.* **2000**, *112*, 6532–6542.

[22] J. W. Ochterski, G. A. Petersson, J. A. Montgomery Jr., *J. Chem. Phys.* **1996**, *104*, 2598–2619.

[23] a) E. F. C. Byrd, B. M. Rice, *J. Phys. Chem.* **2005**, *110*, 1005-1013; b) L. A. Curtiss, K. Raghavachari, P. C. Redfern, J. A. Pople, *J. Chem. Phys.* **1997**, *106*, 1063–1079.

[24] M. Sućeska, *EXPLO5 V5.05*, Brodarski Institut, Zagreb (Croatia), **2011**.

[25] a) A. Altomare, M. C. Burla, M. Camalli, G. L. Cascarano, C. Giacovazzo, A. Guagliardi, A. G. G. Moliterni, G. Polidori, R. Spagna, *J. Appl. Crystallogr.* **1999**, *32*, 115–119; b) A. Altomare, G. Cascarano, C. Giacovazzo, A. Guagliardi, A. G. G. Moliterni, M. C. Burla, G. Polidori, M. Camalli, R. Spagna, *SIR97*, **1997**.

[26] G. M. Sheldrick, *SHELX-97*, University of Göttingen, Göttingen (Germany), **1997**.

4. ASYMMETRIC FLUORODINITROMETHYL DERIVATIVES OF 2,2,2-TRINITROETHYL N-(2,2,2-TRINITROETHYL)CARBAMATE

Thomas M. Klapötke, Burkhard Krumm, Richard Moll, Sebastian F. Rest, Wolfgang Schnick, Markus Seibald

As published in: Journal of Fluorine Chemistry ***2013***, *156*, 253–261.

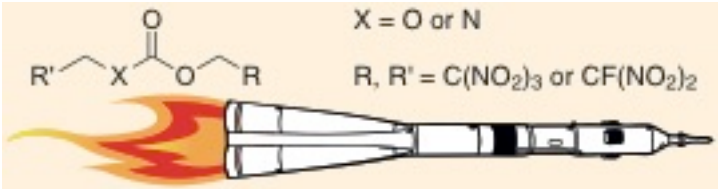

4.1 ABSTRACT

The energetic polynitro compounds 2,2,2-trinitroethyl 2,2,2-trinitroethylcarbamate, 2-fluoro-2,2-dinitroethyl 2,2,2-trinitroethylcarbamate, 2,2,2-tinitroethyl 2-fluoro-2,2-dinitroethylcarbamate and 2-fluoro-2,2-dinitroethyl 2,2,2-trinitroethylcarbonate were synthesized and investigated as potential high energy dense oxidizers. Due to their structural similarity, the compounds have been compared with each other by using various analytical methods, like single-crystal X-ray diffraction, vibrational spectroscopy (IR and Raman), multinuclear NMR spectroscopy, elemental analysis, mass spectrometry and multi-temperature DSC measurements. The suitability of the compounds as potential oxidizers in energetic formulations has been investigated. In addition, the heats of formation of the products were calculated with the program package Gaussian 09. Several detonation parameters such as the detonation pressure, velocity, energy and temperature were computed using the EXPLO5 code. Furthermore, the sensitivity toward impact, friction and electrical discharge was tested using a BAM drop hammer, a friction tester as well as a small-scale electrical discharge device.

4.2 INTRODUCTION

The widely used oxidizer in solid-rocket propellants is ammonium perchlorate (AP). This cheap and oxygen rich substance comes along with several problems for the environment. Especially the large amount of hydrogen chloride produced is an undesirable side effect. A solid-rocket motor consists of about >70% oxidizer besides fuel and additives.[1,2] Therefore, it is important to drive research towards environmental friendly chlorine free compounds with a great excess of oxygen.

The relative amount of oxygen excess is calculated as oxygen balance. For high energy dense oxidizers, this value should be positive and preferable greater than AP with 34%. For calculating the oxygen balance of a CHFNO compound, it is assumed that the compounds are converted into H_2O, N_2, CO_2 and HF during the combustion. Alternatively, due to the high temperature of combustion, CO can be assumed to be formed instead of CO_2. The oxygen balance is defined according to Eqs. (1) and (2) for a general formula $C_aH_bF_cN_dO_e$ while M is the molecular mass of the compound.[3]

$$\Omega_{CO_2} = \frac{e - 2a - ((b-c)/2)}{M} \times 1600$$

Eq (1): Oxygen balance for a CHFNO compound assuming CO_2 as product of combustion in %.

$$\Omega_{CO} = \frac{e - a - ((b-c)/2)}{M} \times 1600$$

Eq (2): Oxygen balance for a CHFNO compound assuming CO as product of combustion in %.

Based on previous investigations, compounds derived from 2,2,2-trinitroethanol as well as 2-fluoro-2,2-dinitroethanol (though containing the halogen fluorine) might be useful as starting materials for preparing chlorine free possible high energy dense oxidizers.[1,4-6] In order to improve the thermal stability of polynitrated CH(F)NO-compounds, we focused on molecules containing the carbamate and the carbonate moiety.

The specific impulse I_s is one of the main parameters specifying the performance of solid-rocket boosters. It is proportional to the reciprocal of the molecular weight of the decomposition products and the temperature inside the combustion chamber during combustion of the composite.[3,7,8] An increase of the value for I_s by 20 s leads empirically to a doubling of the usual payload.[3,7] Therefore, the development of new energetic oxidizers based on CH(F)NO compounds decomposing into small volatile molecules and

achieving an increase of the temperature of combustion is a promising way to increase the specific impulse of solid-rocket boosters.

A detailed study of the synthesis and characterization of some fluorine containing energetic materials is presented in this work. Potential high energy dense oxidizers with comparable sensitivities toward PETN were prepared and additional analytical data were given for those compounds, which were only poorly described.[9-11]

4.3 RESULTS AND DISSCUSSION

SYNTHESIS

The important precursor S-ethyl N-(2,2,2-trinitroethyl)thiocarbamate (**1**) was synthesized via the reported reaction pathway from S-ethyl thiocarbamate and 2,2,2-trinitroethanol using a Mannich like reaction in a buffered aqueous solution (Scheme 4.1).[9]

Compound **1** was further reacted with chlorine gas in a one-pot reaction together with 2,2,2-trinitroethanol or 2-fluoro-2,2-dinitroethanol (without isolation of the isocyanate intermediate), yielding 2,2,2-trinitroethyl 2,2,2-trinitroethylcarbamate (**2**) or 2-fluoro-2,2-dinitroethyl 2,2,2-trinitroethylcarbamate (**3**), previously prepared by Sitzmann and Gilligan[9] (Scheme 4.1).

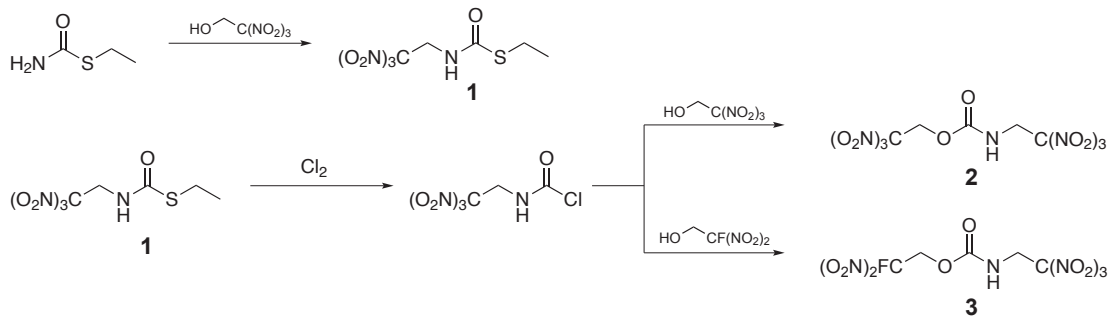

Scheme 4.1. Synthesis of the compounds **2**–**3** via **1**.

2,2,2-Trinitroethyl 2-fluoro-2,2-dinitroethylcarbamate (**4**) and 2-fluoro-2,2-dinitroethyl 2,2,2-trinitroethylcarbonate (**5**) were synthesized from 2,2,2-trinitroethyl chloroformate and the corresponding starting materials 2-fluoro-2,2-dinitroethyl amine or 2-fluoro-2,2-dinitroethanol, respectively (Scheme 2). The reaction has to take place under inert gas conditions. Due to the tendency to spontaneous and violent decomposition at ambient temperature, 2-fluoro-2,2-dinitroethyl amine should only be handled highly diluted in chloroform or dichloromethane. The existence of **5** was previously only noted in a patent, but no further details given.[10]

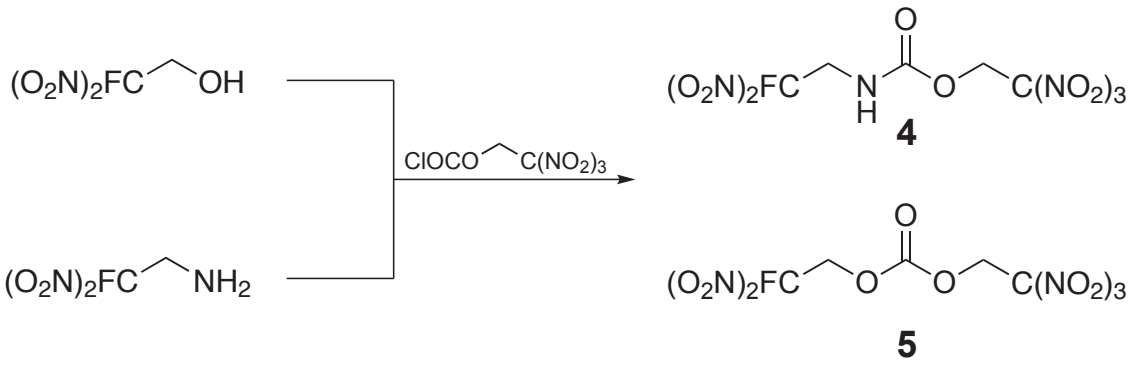

Scheme 4.2. Synthesis of the compounds **4**–**5**.

NMR SPECTROSCOPY

The compounds were thoroughly characterized by ^{1}H, ^{13}C, ^{14}N and ^{19}F NMR spectroscopy. The multinuclear NMR spectra were recorded in $CDCl_3$ (**1**, **3**, **4**), or acetone-D_6 (**2**, **5**) as solvent. In the ^{1}H NMR spectra of **2, 4** and **5** the singlets for the $CH_2C(NO_2)_3$ groups can be observed at 6.07–5.43 ppm. The corresponding resonances for **1, 2** and **3** were observed as doublets at 4.93 ppm (^{3}J(H,H) = 6.8 Hz), 5.25 ppm (^{3}J(H,H) = 6.8 Hz) and 4.84 ppm (^{3}J(H,H) = 6.6 Hz) due to the coupling with the adjacent NH moiety, respectively. The N*H* resonances for the compounds **1**–**4** were observed in the range of 8.21–5.52 ppm as a broad resonance, appearing as triplets. The compounds **3**–**5** have a $CH_2CF(NO_2)_2$ moiety in common, which shows up in the ^{1}H NMR spectra as a doublet due to a ^{3}J(H,F) coupling (15.2–14.4 Hz) in the range of 5.76–4.55 ppm. The corresponding resonance of **4** shows an additional ^{3}J(H,H) = 6.7 Hz coupling with a connected NH group and therefore, a doublet of doublets was observed. Resonances of the ethyl ester group of **1** were determined as quartet at 2.96 ppm for OCH_2CH_3 and as triplet at 1.29 ppm with a coupling constant of 7.4 Hz. The carbon atoms of the trinitromethyl moieties in the ^{13}C NMR spectra were always identified as very broad resonances in the range 126.4–124.4 ppm for **1**, **2** and **4**. In the case of **3** and **5** these carbon resonances were not detected at all. But in the ^{14}N NMR spectra, between –33 and –35 ppm the corresponding resonances of the nitrogen atoms of the NO_2 moieties were positively identified in all cases. The carbamate moieties of **2**–**4** were observed as weak resonances in the ^{13}C NMR spectra in the range of 155.8–152.8 ppm. The resonances of the thiocarbamate **1** and the carbonate group of **5** were identified at 169.5 and 152.4 ppm, respectively. The carbon resonance of the fluorodinitromethyl moiety of **4** was observed as a doublet at 120.9 ppm (^{1}J(C,F) = 289.4 Hz). Additionally, the resonances of the

C$H_2CF(NO_2)_2$ moieties of **3–5** were also observed as doublets in the range of 65.6–643.2 ppm with a ^2J(C,F) coupling constant of 20.1–19.2 Hz. The ^{14}N NMR spectra also show resonances of the fluorodinitromethyl moieties of **3–5** between –22 and –26 ppm. The ^{19}F NMR spectra showed the resonances of the fluorodinitromethyl moieties of **3–5** as broadened triplets between –110 and –112 ppm, because of the quadrupolar influence of the ^{14}N nucleus of the nitro groups.

VIBRATIONAL SPECTROSCOPY

The vibrational analyses of **1–5** showed the characteristic asymmetric stretching vibrations $\nu_{as}(NO_2)$ in the range of 1620–1583 cm^{-1} and the symmetric stretching vibrations $\nu_s(NO_2)$ at 1310–1295 cm^{-1} (Table 4.1). C=O stretching vibrations for **2–5** were found in the range of 1776–1738 cm^{-1}. These stretching vibrations belong to the corresponding carbamate and carbonate moieties. The thiocarbamate moiety of compound **1** causes a decrease of the C=O stretching vibration towards lower energies (1662 cm^{-1}). For compound **1–4** the N–H stretching vibration of the carbamate, respectively thiocarbamate, moieties were observed in the range of 3434–3286 cm^{-1}. The C–N, C–O, C–F and C–C vibrations of **1–5** could be observed in the typical ranges for CHNO and CHFNO compounds, respectively.[12-14]

Table 4.1. IR and Raman bands of carbonyl and nitro groups for **1–5**

	1		**2**		**3**		**4**		**5**	
	IR[a]	Raman[b]	IR[a]	Raman[b]	IR[a]	Raman[b]	IR[a]	Raman[b]	IR[a]	Raman[b]
ν NH	3286 (w)	3290 (7)	3434 (w)	n o	3399 (w)	3399 (6)	3337 (w)	3349 (4)		
ν CO	1662 (m)	1661 (35)	1764 (m)	1765 (12)	1770 (s)	1770 (29)	1738 (m)	1740 (20)	1772 (s)	1776 (12)
ν_{as} NO_2	1583 (vs)	1609 (27)	1587 (vs)	1607 (28)	1590 (vs)	1612 (45)	1588 (vs)	1620 (21)	1590 (vs)	1614 (26)
						1594 (29)		1606 (26)		1598 (27)
ν_s NO_2	1295 (s)	1306 (25)	1306 (m)	1310 (24)	1309 (m)	1310 (42)	1304 (m)	1307 (30)	1302 (s)	1310 (29)

[a] in cm^{-1}; IR intensities: vs = very strong, s = strong, m = medium, w = weak. [b] in cm^{-1}; Raman intensities at 300 mW in brackets; n.o. = not observed.

X-RAY DIFFRACTION

The compounds **1–5** were investigated by low-temperature, single crystal X-ray diffraction. Crystallographic data for all compounds are summed up in Table 4.2. Suitable single crystals for X-ray diffraction were obtained by slow evaporation of chloroform. Additional data on intermolecular interactions of **1–5** are given as supplementary information.

The molecular structure of S-ethyl N-(2,2,2-trinitroethyl)thiocarbamate (**1**) is shown in Fig. 4.1. Compound **1** crystallizes in the monoclinic space group $P2_1/c$ with eight formula units per unit cell and a density of 1.59 g cm^{-3} at 173 K. The bond lengths and angles of **1** are comparable with values reported in literature for CHNO compounds containing a trinitromethyl moiety.[8,15-19] The average N–O bond lengths of the trinitromethyl moieties are 1.21(3) Å for the two molecules in the asymmetric unit. For the top molecule, a typical propeller-type orientation of the trinitromethyl moiety with C–C–N–O torsion angles between –41.3(3) ° and –49.4(3) ° was observed. Amazingly, the trinitromethyl group of the bottom molecule shows an atypical conformation with an approximately planar oriented nitro group ($N7O_2$) according to the corresponding C6–C7 bond and one perpendicular to it ($N5O_2$). Comparing the dihedral angle C6–C7–N7–O13 (–7.4(3) °) and C6–C7–N5–O9 (89.2(3) °) confirm this observation. Though a propeller-type orientation is typical for trinitromethyl moieties, the case of $C7(NO_2)_3$ is surprising. It is known to literature that the barrier of rotation about a single $C–NO_2$ bond is quite small. Therefore, disturbing effects, caused by interactions with nearby moieties, normally sharply distort the preferred C_3 symmetry.[14] This leads to this atypical conformation of the $C7(NO_2)_3$ moiety. The weak improper H-bond between C2H2B and O10 (O10···H2B = 2.418(2) Å) might be one interaction, for example. Besides the described interactions, there are various intermolecular attractions in terms of further weak improper hydrogen bonds and N···O dipolar interactions.

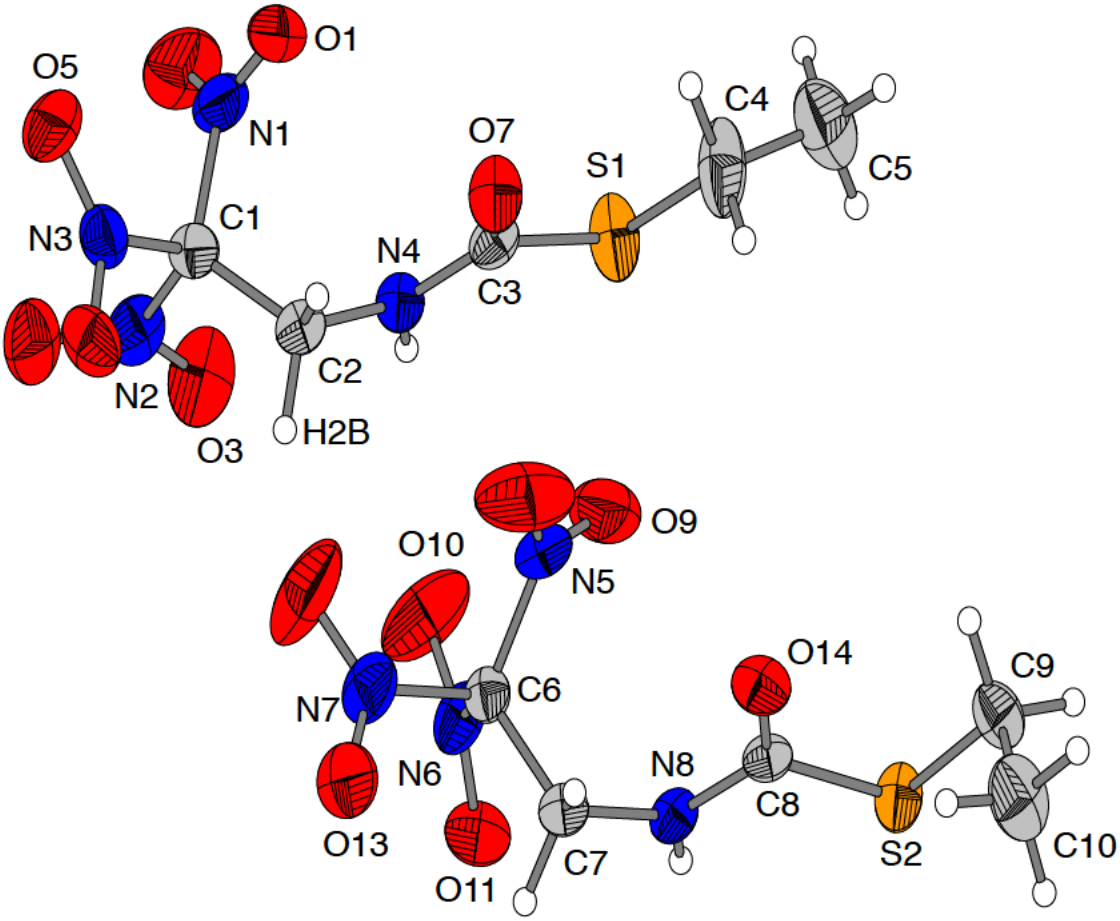

Fig. 4.1. Molecular structure of **1** with two independent molecules. Selected distances [Å] and angles [°]: C1–C2 1.521(3), C1–$(NO_2)_{av}$ 1.521(3), C2–N4 1.440(3), C3–N4 1.357(3), C3–O7 1.218(3), C3–S1 1.770(2), C4–S1 1.802(3), C6–C7 1.522(3), C6–$(NO_2)_{av}$ 1.530(3), C7–N8 1.441(3), C8–N8 1.358(3), C8–O14 1.221(2), C8–S2 1.773(2), C9–S2 1.810(3), N4–C3–O7 123.9(2), O7–C3–S1 122.8(2), C2–N4–C3 118.8(2), C3–S1–C4 100.7(1), O14–C8–S2 123.8(2), C7–N8–C8 120.2(2), C8–S2–C9 99.5(1), N8–C8–O14 122.8(2), C2–C1–N1–O1 –49.4(3), C2–C1–N2–O3 –43.3(3), C2–C1–N3–O6 –41.3(3), S1–C3–O7–N4 179.4(4), C7–C6–N5–O9 89.2(3), C7–C6–N6–O11 16.2(3), C7–C6–N7–O13 –7.4(3), N8–C8–O14–S2 179.4(4).

The crystal structure of 2,2,2-trinitroethyl 2,2,2-trinitroethylcarbamate (**2**) is displayed in Fig. 4.2. It crystallizes in the orthorhombic space group *Pnn*2 with two formula units per unit cell and a density of 1.90 g cm^{-3} at 173 K. The bond lengths and angles of **2** are as expected for CHNO compounds containing a trinitromethyl moiety.[8,15-19] The average N–O bond length of the trinitromethyl moiety for $C1(NO_2)_3$ is 1.216(3) Å, comparable to **1**.[14] The trinitromethyl group shows a typical propeller-type orientation of the nitro groups owned by the trinitromethyl moieties. The related torsion C2–C1–N–O angles varying between 38.0(2) and 47.3(2) ° and are therefore in the usual range for

trinitromethyl containing compounds. The structure shows an interesting disorder of the single molecules in the unit cell. Statistically every second molecule is turned through 180 ° along C3=O14. As a result, a pseudo C_2 axis along C3=O14 occurs and therefore at N13/O13 a mixed occupation of oxygen and nitrogen (1:1) has to be assumed. The C–O and C–N distances and angles are in the usual range for compounds containing a trinitromethyl moiety. The quite high crystal density of the compound is a result of various intermolecular H···O and N···O dipolar interactions.

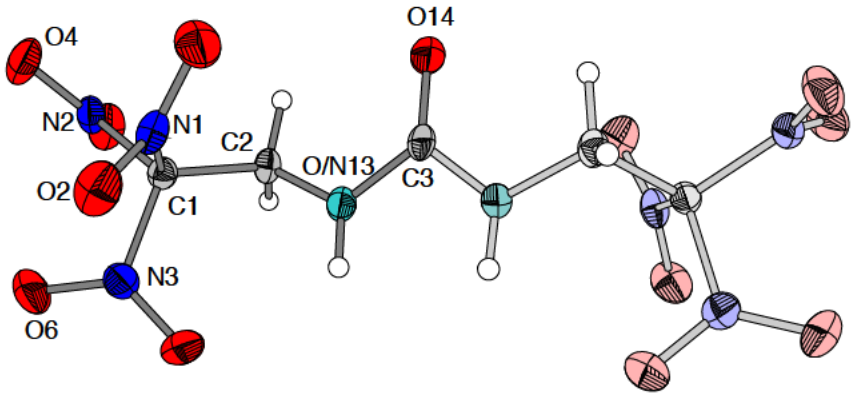

Fig. 4.2. Molecular structure of **2** (showing disorder). Selected distances [Å] and angles [°]: C1–C2 1.531(2), C1–$(NO_2)_{av}$ 1.524(3), C2–N/O13 1.425(2), C3–N/O13 1.373(2), C3–O14 1.2196(3), N/O13–C3–O14 126.3(2), N/O13–C3–N/O13(i) 107.3(2), C2–C1–N1–O2 47.3(2), C2–C1–N2–O3 44.3(2), C2–C1–N3–O5 38.0(2), N/O13–C3–O14–N/O13(i) 180.0(4). i = 1–x, 1–y, z.

2-Fluoro-2,2-dinitroethyl 2,2,2-trinitroethylcarbamate (**3**) crystallizes in the monoclinic space group $P2_1/c$ with four formula units per unit cell (Fig. 4.3). The density at 173 K was calculated with 1.83 g cm^{-3}. The bond lengths and angles of **3** are comparable with previously discussed values for CHNO compounds containing a trinitromethyl moiety.[8,15-19] The average N–O bond length of the trinitromethyl moiety is 1.217(4) Å. The C3–O8 (1.374(2) Å), C3–O7 (1.204(3) Å) and C3–N4 (1.351(4) Å) bonds of the carbamate moiety are in the typical range for organic compounds containing a carbamate group. The O8–C3–O7–N4 (–179.2(4) °) torsion angle shows the planarity of this moiety, as expected. The trinitroethyl moiety displays a molecular geometry with a propeller-type orientation of the nitro groups connected to C1. The twisted orientation is energetically favorable and leads to several N···O-dipolar interactions between the geminal NO_2 groups (range of 2.56–2.59 Å), which are considerably shorter than the sum of the van der Waals radii for oxygen and nitrogen (about 2.9 Å).[14] The shorter distances are caused by the

fact that such twisting of the nitro groups reduces the intramolecular electrostatic repulsion between the oxygen atoms, while at the same time optimizing the attractive N···O interactions between the geminal NO_2 groups. The average N–O bond length of the fluorodinitromethyl moiety $C5F1(NO_2)_2$ (1.213(3) Å) is comparable with the trinitromethyl group. The C4–C5–N–O torsion angles (32.3(3) °/ 53.7(4) °) are also in the typical range (23–67 °) of a propeller-type orientation of the nitro groups attached. The C–F distance with 1.335(3) Å is comparable with a C–F single bond and typical for a fluorodinitromethyl moiety.[20-22]

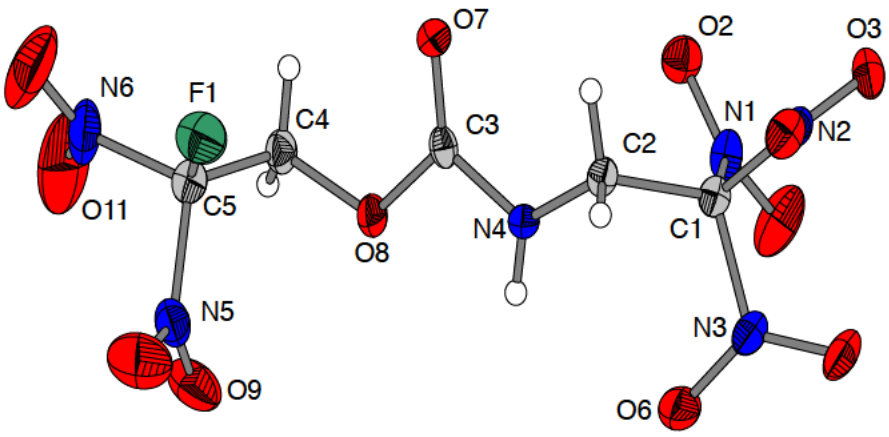

Fig. 4.3. Molecular structure of **3**. Selected distances [Å] and angles [°]: C1–C2 1.523(4), C1–$(NO_2)_{av}$ 1.528(3), C2–N4 1.442(3), C3–N4 1.351(3), C3–O7 1.204(3), C3–O8 1.374(2), C4–O8 1.426(3), C4–C5 1.511(4), C5–F1 1.335(3), C5–$(NO_2)_{av}$ 1.533(4), N4–C3–O7 127.1(2), O7–C3–O8 124.3(2), C2–N4–C3 120.1(2), C3–O8–C4 116.4(2), C4–C5–F1 113.7(2), C2–C1–N1–O2 41.1(3), C2–C1–N2–O4 43.3(3), C2–C1–N3–O6 36.7(3), C4–C5–N5–O9 –32.3(3), C4–C5–N6–O11 53.7(4), N4–C3–O7–O8 179.4(4).

Single crystal X-ray diffraction experiments at 100 K showed that **4** crystallizes in the monoclinic space group $P2_1/c$ with four molecular formula units per unit cell and a density of 1.86 g cm^{-3}. The molecular structure of **4** is shown in Fig. 4.4. The bond lengths and angles of **4** are comparable with values reported in literature for CHNO compounds containing a trinitromethyl moiety.[8,15-19] The trinitromethyl moiety displays a molecular form with a propeller-type orientation of the nitro groups connected to C1. The C2-C1-N-O dihedral angles of compound **4** are in the typical range of propeller-type $XC(NO_2)_3$ compounds (23–67 °), similar to **3**.[14] The average N–O bond length of the trinitromethyl moiety is with 1.215(3) Å similar compared to compound **3**. The C3–O7 (1.369(2) Å), C3–O8 (1.210(2) Å) and C3–N4 (1.343(2) Å) bonds are typical for a

carbamate moiety. The O7–C3–O8–N4 (179.5(3) °) dihedral angle displays the planarity of the carbamate moiety. The fluorodinitromethyl moiety reveals a similar averaged N–O distance (1.213(3) Å) as the trinitromethyl moiety. The C5–F1 distance with 1.336(4) Å is also typical for a fluorodinitromethyl moiety.[20-22] The nitro groups of the fluorodinitromethyl moiety are not oriented in a typical propeller-type matter. The C4–C5–N5–O10 (10.5(2) °) and the C4–C5–N6–O12 (93.3(2) °) torsion angle show an almost planar and a perpendicular orientation of the nitro groups according to the C4–C5 bond. Analysis of intermolecular interactions of **4** shows various interactions in terms of weak improper hydrogen bonds as well as dipolar N···O interactions.

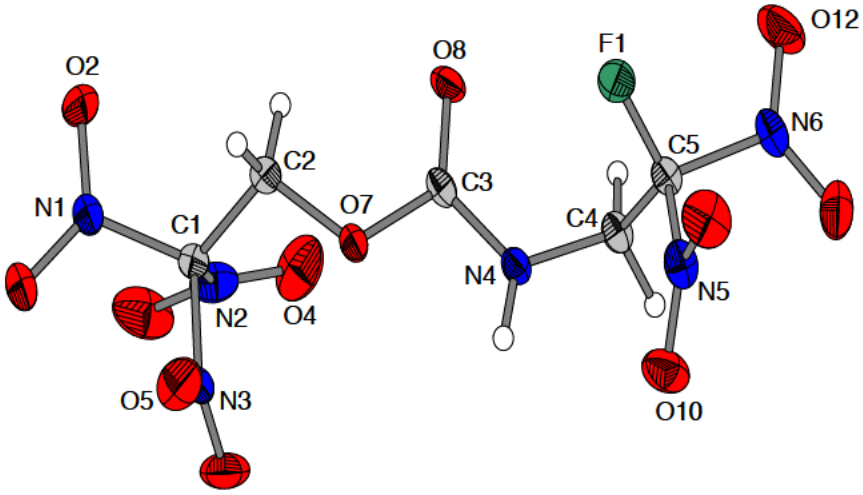

Fig. 4.4. Molecular structure of **4**. Selected distances [Å] and angles [°]: C1–C2 1.518(2), C1–$(NO_2)_{av}$ 1.520(3), C2–O7 1.421(2), C3–O7 1.369(2), C3–O8 1.210(2), C3–N4 1.343(2), C4–N4 1.440(2), C4–C5 1.517(2), C5–F1 1.335(2), C5–$(NO_2)_{av}$ 1.532(3), N4–C3–O7 108.5(1), N4–C3–O8 127.5(1), O7–C3–O8 124.0(1), C3–N4–C4 120.0(1), C2–O7–C3 116.2(1), C4–C5–F1 112.7(1), C2–C1–N1–O2 39.9(2), C2–C1–N2–O4 26.1(2), C2–C1–N3–O5 58.6(2), C4–C5–N5–O10 10.5(2), C4–C5–N6–O12 93.3(2), O7–C3–O8–N4 179.5(3).

Compound **5** crystallizes in the monoclinic space group *Pn* with two formula units per unit cell and a density of 1.87 g cm^{-3}. The molecular structure of **5** is shown in Fig. 4.5. The bond lengths and angles of **5** are comparable to literature known CHNO compounds containing a trinitromethyl moiety.[8,15-19] The trinitromethyl moiety displays a molecular geometry with a propeller-type orientation of the nitro groups connected to C1 with an average N–O bond length of 1.212(3) Å. Similar to **1**–**4**, the C2–C1–N–O dihedral angles of compound **4** are in the usual range of propeller-type $XC(NO_2)_3$ compounds

(23–67 °).[14] The C3–O7 (1.350(4) Å), C3–O8 (1.189(4) Å) and C3–O9 (1.339(4) Å) bonds are comparable with a common carbonate moiety. As expected, the C3–O8 bond of the carbonate is slightly shorter compared with the previously discussed carbamates, whereas the C–O distances of the bridging oxygen atoms are almost similar compared with the compounds **1**–**4**. The carbonate moiety is with an O7–C3–O8–O9 dihedral angle of 178.2(6) ° almost planar. The fluorodinitromethyl moiety reveals a similar averaged N–O distance (1.212(3) Å) as the trinitromethyl moiety. The C–F distance with 1.331(4) Å is shorter compared with compound **4**. Analysis of intermolecular interactions of **4** shows various interactions in terms of weak improper hydrogen bonds as well as dipolar N···O interactions.

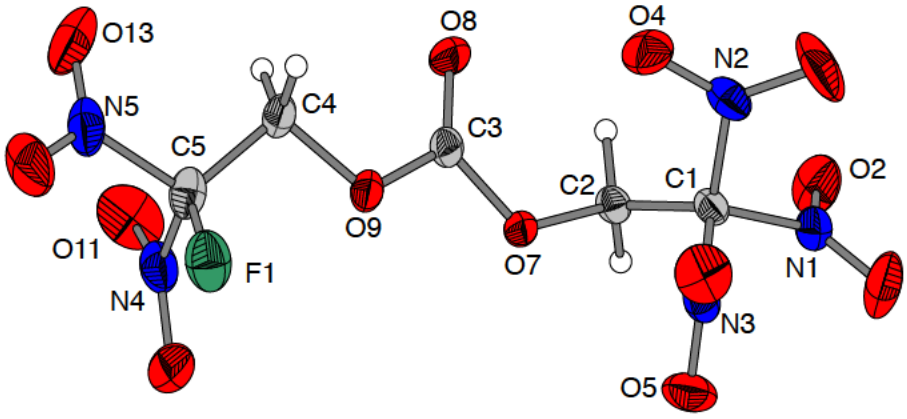

Fig. 4.5. Molecular structure of **5**. Selected distances [Å] and angles [°]: C1–C2 1.519(4), C1–$(NO_2)_{av}$ 1.522(3), C2–O7 1.439(3), C3–O7 1.350(4), C3–O8 1.189(4), C3–O9 1.339(4), C4–O9 1.441(4), C4–C5 1.509(4), C5–F1 1.331(4), C5–$(NO_2)_{av}$ 1.537(3), O7–C3–O8 127.5(3), O8–C3–O9 127.0(3), C2–O7–C3 116.5(2), C3–O9–C4 114.9(2), C4–C5–F1 113.7(3), C2–C1–N1–O2 37.2(3), C2–C1–N2–O4 36.8(4), C2–C1–N3–O5 57.1(3), C4–C5–N4–O11 –60.5(4), C4–C5–N5–O13 35.6(4), O7–C3–O8–O9 178.2(6).

Table 4.2. Crystal and structure refinement data for **1**–**5**

	1	**2**	**3**	**4**	**5**
Empirical formula	$C_5H_8N_4O_7S$	$C_5H_5N_7O_{14}$	$C_5H_5FN_6O_{12}$	$C_5H_5FN_6O_{12}$	$C_5H_4FN_5O_{13}$
Formula mass /g mol^{-1}	268.21	387.13	360.13	360.13	361.11
Temperature /K	173(2)	173(2)	173(2)	100(2)	173(2)
Crystal size /mm^3	0.22 × 0.05 × 0.03	0.14 × 0.12 × 0.09	0.28 × 0.03 × 0.02	0.15 × 0.10 × 0.02	0.30 × 0.02 × 0.01
Crystal description	Colorless needle	Colorless block	Colorless needle	Colorless needle	Colorless needle
Crystal system	Monoclinic	Orthorhombic	Monoclinic	Monoclinic	Monoclinic
Space group	$P2_1/c$ (no. 14)	$Pnn2$ (no. 34)	$P2_1/c$ (no. 14)	$P2_1/c$ (no. 14)	Pn (no. 7)
a /Å	13.0367(5)	11.1356(5)	11.414(8)	20.1316(11)	5.9437(6)
b /Å	18.1953(7)	10.3757(5)	11.021(5)	6.7612(4)	10.9783(9)
c /Å	9.4523(3)	5.8534(4)	11.645(9)	9.6063(5)	9.8638(9)
β /	93.746(3)	90	117.099(9)	100.823(5)	95.752(8)
V /Å^3	2237.36(14)	676.30(6)	1304.1(2)	1284.29(12)	640.4(1)
Z	8	2	4	4	2
ρ_{calc} /g cm^{-3}	1.59249(10)	1.90110(17)	1.8342(14)	1.86254(17)	1.8727(3)
μ /mm^{-1}	0.322	0.193	0.190	0.193	0.197
F(000)	1104	392	728	728	364
θ range /	4.24–26.00	4.14–32.47	4.24–25.40	4.25–25.99	4.15–26.50
Index ranges	$-16 \le h \le 16$	$-16 \le h \le 16$	$-7 \le h \le 13$	$-24 \le h \le 24$	$-7 \le h \le 7$
	$-22 \le k \le 22$	$-15 \le k \le 15$	$-11 \le k \le 13$	$-8 \le k \le 7$	$-13 \le k \le 13$
	$-11 \le l \le 11$	$-8 \le l \le 8$	$-14 \le l \le 13$	$-11 \le l \le 11$	$-12 \le l \le 12$
Reflections collected	22191	9909	4429	5787	6512
Reflections observed	4380	1545	2370	2516	2656
Reflections unique	3458	1414	1998	2116	2127
$R1$, $wR2$ (2σ data)	0.0488, 0.1537	0.0284, 0.0517	0.0442, 0.1040	0.0342, 0.0816	0.0416, 0.0875
$R1$, $wR2$ (all data)	0.0637, 0.1679	0.0344, 0.0544	0.0543, 0.1120	0.0427, 0.0875	0.0578, 0.0982
Max. / min. transmission	1.00000/0.93150	1.00000/0.93407	1.00000/0.97703	1.00000/0.95536	1.00000/0.61978
Data/restraints/parameters	3458/0/311	1545/1/119	2370/0/237	2516/0/218	22656/2/217
GOOF on F^2	1.225	1.066	1.088	1.046	1.001
Larg. diff. peak/hole /e Å^{-3}	0.815/–0.407	0.218/–0.157	0.646/–0.256	0.298/–0.218	0.195/–0.168
CCDC entry	937512	937513	937514	937515	937516

THERMAL AND ENERGETIC PROPERTIES

The compounds **1**–**5** are stable when exposed to air and moisture. The thermal stabilities for **1**–**5** were investigated with various DSC measurements (heating rate: 5 °C min^{-1}). The results are shown in the Table 4.3. Relatively high and satisfying melting points of 164 °C and 161 °C were observed for compound **2**, respectively **4**.[5,8,17] Above 180 °C, decomposition for **2**–**5** becomes significant. The highest decomposition temperature showed **3** and **4** with 191 °C. The physical and chemical properties of the compounds described are shown in the Table 4.3.[11]

The sensitivities toward impact, friction and electrostatic discharge for **1**–**5** were determined experimentally according to standards of the Federal Institute for Materials Research and Testing (BAM),[23] and the results displayed in Table 4.4. The compounds **3**–**5** showed the same sensitivity values due to their chemical similarity. The impact sensitivity was determined with 3 J. With 360 N, **3**–**5** were found to be insensitive towards friction and an energy of 0.4 J of an electrostatic discharge was needed to initiate decomposition. Compound **2** is more sensitive toward friction (96 N), but has comparable impact sensitivity (4 J). The precursor **1** showed improved impact sensitivity due to the S-ethyl thiocarbamate moiety. In summary, all compounds are more sensitive towards impact than AP. Additionally, the flame test of **1**–**5** showed a smoke- and residue-less burning with a yellow flame.

Predictions of the detonation parameters using the EXPLO5 code[24] have been performed based on heats of formations calculated *ab initio* using the Gaussian 09 program package[25,26] at the CBS-4M level of theory. Energetic parameters are attributed to the density of the corresponding compound. The resulting heats of detonation (Q_v), detonation temperatures (T), pressures (p) and velocities (D) for **1**–**5** are shown in the Table 5, as well as the oxygen balances (Ω). The ambient temperature densities needed for the estimation of the detonation parameters with the EXPLO5 code[24] were derived from experimental determinations via pycnometer measurements for **2**–**5**.

The specific impulses of the compounds **2**–**5** were calculated for compositions of 70% oxidizer, 16% aluminum, 6% polybutadiene acrylic acid, 6% polybutadiene acrylonitrile and 2% bisphenol-A ether modeled on rocket-motor compositions for solid-rockets boosters used by the NASA Space Shuttle program.[27,28] These impulses were compared with the calculated impulse of AP in an analogous composition. The chosen mixture with AP as oxidizer provides a specific impulse of 258 sec. The impulses for **2**–**5** (248–257 s) are slightly below a comparable mixture with AP as oxidizer. Compound **2** shows a high

impulse with 257 s. The lesser oxygen balance of the compounds **2–5** according to AP, also leads to a decreased oxygen balance for the calculated formulations varying between –54.0% and –49.3%. A similar composition with AP as oxidizer has an oxygen balance of –30.1%. Due to the sulfur content of **1** the energetic properties could not be estimated with the program EXPLO5. The results of the calculations are shown in Table 4.4.

Table 4.3. Physical and chemical properties of **1–5**

	1	**2**	**3**	**4**	**5**
Formula	$C_5H_8N_4O_7S$	$C_5H_5N_7O_{14}$	$C_5H_5FN_6O_{12}$	$C_5H_5FN_6O_{12}$	$C_5H_4FN_5O_{13}$
Mol mass /g mol^{-1}	268.20	387.13	360.13	360.13	361.11
T_m /°C [a]	62	164	113	161	59
T_d /°C [b]	167	186	191	191	189
N /% [c]	20.89	25.33	23.34	23.34	19.39
$N + O$ /% [d]	62.65	83.19	76.65	76.65	76.99
Ω_{CO} /% [e]	–23.9	+26.9	+22.2	+22.2	+28.8
Ω_{CO2} /% [f]	–53.7	+6.2	0.0	0.0	+6.6
ρ /g cm^{-3} [g]	1.60	1.87	1.80	1.81	1.83
$-\Delta U°_f$ /kJ kg^{-1} [h]	---	1108.2	1793.2	1772.8	2114.5
$-\Delta H°_f$ /kJ mol^{-1} [i]	---	461.1	675.5	668.7	792.1

a, b) Melting (T_m) and decomposition (T_d) point from DSC measurement carried out at a heating rate of 5 °C min^{-1}. c) Nitrogen content. d) Combined nitrogen and oxygen content. e) Oxygen balance assuming the formation of CO. The oxygen balance of ammonium perchlorate is 34.0% f) Oxygen balance assuming the formation of CO_2. g) Experimental density from pycnometer measurement. h) Calculated energy of formation. i) Calculated heat of formation.

Table 4.4. Predicted detonation and combustion parameters (using the EXPLO5 code) and sensitivity data for **1–5**

	1	**2**	**3**	**4**	**5**
$-Q_v$ /kJ kg^{-1}	---	5338	5170	5177	4763
T_{ex} /K [a]	---	3954	4001	3999	3817
V_0 /L kg^{-1} [b]	---	740	730	729	719
p /kbar [c]	---	331	345	350	329
D /m s^{-1} [d]	---	8661	8517	8553	8369
Impact /J [e]	10	4	3	3	3
Friction /N [e]	160	96	360	360	360
ESD /J [f]	0.18	0.4	0.4	0.4	0.4
Grain size /µm [g]	100–500	100–500	<100	<100	<100
Thermal shock [h]	burns	burns	burns	burns	burns
I_s /s [i]	---	257	248	249	251
Ω_{comp} /% [j]	---	–49.62	–53.96	–53.96	–49.3

a) Temperature of the explosion gases. b) Volume of the explosion gases (assuming only gaseous products). c) Detonation pressure. d) Detonation velocity. e) Impact and friction sensitivities according to standard BAM methods.[23] f) Sensitivity towards electrostatic discharge. g) Grain size of the samples used for sensitivity tests. h) Response to fast heating in the "flame test". i) Specific impulse for compositions with 70% oxidizer, 16% aluminum, 6% polybutadiene acrylic acid, 6% polybutadiene acrylonitrile and 2% bisphenol-A ether at 70.0 bar chamber pressure using the EXPLO5 code.[24] j) Oxygen balance for the composition used for combustion calculations.

4.4 CONCLUSION

Based on the previous work of Adolph, Gilligan & Sitzmann, the new energetic polynitro compound **4** containing a fluorodinitromethyl moiety with a positive oxygen balance was synthesized. For compounds **1**–**3** and **5**, which were previously synthesized in the 1980ies, additional analytical data and calculations of the energetic parameters are now provided. The compounds were characterized using multinuclear NMR, vibrational spectroscopy, elemental analysis and mass spectrometry and X-ray methods. The crystal structures revealed a typical propeller-type orientation of the trinitromethyl moiety for all compounds. Relatively high crystal densities for **2**–**5** in the range of 1.83–1.90 g cm^{-3} were determined. The thermal stability was investigated by DSC measurements. The sensitivities according to BAM standards were determined and the energetic parameters calculated. The sensitivities of **2**–**5** are comparable with pentaerythritol tetranitrate (**PETN**).[2] The structural similarities of **3**–**5** imply the same values for the sensitivities against impact (3 J), friction (360 N) and electrostatic discharge (0.4 J). The surprising insensitivity toward friction (> 360 N classified as insensitive) are positive parameters in the case of a possible application in (chlorine-free) solid-rocket compositions. Unfortunately, the impact sensitivity of the neat compounds might be too sensitive for the desired application. The precursor **1** even shows an improved impact sensitivity of 10 J. With respect to a possible application as high energy dense oxidizer in solid-rocket boosters, the specific impulses (I_s) of **2**–**5** were calculated in formulations with fuel, oxidizer & additives. Especially **2** turned out to be a promising oxidizer with an almost equal specific impulse (I_s(**2**) = 257 sec, I_s(**5**) = 251 sec) compared to similar formulations with ammonium perchlorate (**AP**) (I_s(**AP**) = 258 sec) as oxidizer.

4.5 EXPERIMENTAL SECTION

General Procedures

The syntheses and manipulations of air- and moisture-sensitive materials were performed in an inert atmosphere of dry argon (purity 5.0 Air Liquide) using flame-dried glass vessels and Schlenk techniques.[29] Commercially available chemicals (all Sigma Aldrich) were used as received. S-Ethyl thiocarbamate, 2-fluoro-2,2-dinitroethylamine, 2-fluoro-2,2-dinitroethanol, 2,2,2-trinitroethanol and 2,2,2-trinitroethyl chloroformate were prepared according to literature known procedures.[5,6,9,10,17,30–35]

Raman spectra were recorded with a Bruker FT-Raman-MultiRAM Spectrometer equipped with a Klaastech DENICAFC LC-3/40 laser source at 300 mW laser power; infrared spectra were measured with a Perkin–Elmer Spectrum BX-FTIR spectrometer equipped with a Smiths DuraSamplIR II ATR device. All spectra were recorded at ambient temperature as neat samples. Densities were determined at ambient temperature using a Quantachrome Ultrapyc1200e gas pycnometer equipped with helium (purity 5.6 Air Liquide). NMR spectra were recorded with a JEOL Eclipse 400 instrument and chemical shifts were determined with respect to external Me_4Si (^{1}H, 399.8 MHz; ^{13}C, 100.5 MHz), $MeNO_2$ (^{14}N, 28.9 MHz) and CCl_3F (^{19}F, 376.5 Hz). Mass spectrometric data were obtained with a JEOL MStation JMS 700 spectrometer (DEI+/DCI+). Analyses of C/H/N were performed with an Elementar Vario EL Analyzer. Melting points were measured with a Perkin-Elmer Pyris6 DSC, using a heating rate of 5 °C min^{-1} and checked by a Büchi Melting Point B-540 apparatus and are not corrected. The sensitivity data were performed using a BAM drophammer and a BAM friction tester.[23]

Computational Details

All ab initio calculations were carried out using the program package Gaussian 09 (Revision B.03)[26] and visualized by GaussView 5.08.[25] Structure optimizations and frequency analyses were performed with Becke's B3 three parameter hybrid functional using the LYP correlation functional (B3LYP). For C, H, F, N and O a correlation consistent polarized double-zeta basis set was used (cc-pVDZ). The structures were optimized without symmetry constraints and the energy is corrected with the zero point vibrational energy.[36-38]

The enthalpies ($H°$) and free energies ($G°$) were calculated using the complete basis set method (CBS-4M) based on ab initio optimized structures or X-ray diffraction data, in

order to obtain accurate values.[36] The CBS models use the known asymptotic convergence of pair natural orbital expressions to extrapolate from calculations using a finite basis set to the estimated complete basis set limit. CBS-4 starts with a HF/3-21G(d) structure optimization, which is the initial guess for the following SCF calculation as a base energy and a final MP2/6-31+G calculation with a CBS extrapolation to correct the energy in second order. The used reparametrized CBS-4M method additionally implements a MP4(SDQ)/6-31+(d,p) calculation to approximate higher order contributions and also includes some additional empirical corrections.[37,38] The enthalpies of the gas-phase species were estimated according to the atomization energy method.[36,39-41]

All calculations affecting the detonation parameters were carried out using the program package EXPLO5 V6.01.[24,42] The detonation parameters were calculated at the CJ point with the aid of the steady-state detonation model using a modified Becker-Kistiakowski-Wilson equation of state for modeling the system. The CJ point is found from the Hugoniot curve of the system by its first derivative.[42,43] The specific impulses were also calculated with the EXPLO5 V5.05 program, assuming an isobaric combustion of a composition of 70% oxidizer, 16% aluminum as fuel, 6% polybutadiene acrylic acid, 6% polybutadiene acrylonitrile as binder and 2% bisphenol-A ether as epoxy curing agent.[27,28] A chamber pressure of 70.0 bar and an ambient pressure of 1.0 bar with frozen expansion conditions were estimated for the calculations.

Crystal structure determination

For all compounds, an Oxford Xcalibur3 diffractometer with a CCD area detector was employed for data collection using Mo-K_α radiation (λ = 0.71073 Å). The structures were solved by direct methods (SIR97)[44,45] and refined by full-matrix least-squares on F^2 (SHELXL).[46–49] All non-hydrogen atoms were refined anisotropically. The hydrogen atoms were located in a difference Fourier map and placed with a C–H distance of 0.99 Å for CH_2 groups and a N–H distance of 0.88 Å for NH groups. ORTEP plots are shown with thermal ellipsoids at the 50% probability level. Crystallographic data for the structures reported in this paper have been deposited with the Cambridge Crystallographic Data Centre as supplementary publication no. CCDC-937512 – CCDC-937516. These data can be obtained free of charge from The Cambridge Crystallographic Data Centre via www.ccdc.cam.ac.uk/data_request/cif.

CAUTION! All high nitrogen and oxygen containing compounds are potentially explosive energetic materials, although no hazards were observed during preparation and handling these compounds. Nevertheless, this necessitates additional meticulous safety precautions (earthed equipment, Kevlar® gloves, Kevlar® sleeves, face shield, leather coat, and ear plugs). In addition, especially 2,2,2-trinitroethanol show significant degrees of toxicity,[50,51] including own recent results.[52] Particular care should be exercised in handling of those materials and derivatives.

S-Ethyl N-(2,2,2-trinitroethyl)thiocarbamate (**1**)

Prepared according to Refs. [9,33].

DSC: T_m = 62 °C, T_{dec} = 167 °C. NMR ^{1}H NMR ($CDCl_3$): δ 6.01 (s, br, 1 H, N*H*), 4.93 (d, ^3J(H,H) = 6.8 Hz, 2 H, $CH_2C(NO_2)_3$), 2.96 (q, ^3J(H,H) = 7.4 Hz, 2 H, SCH_2CH_3), 1.29 (t, 2H, SCH_2CH_3). $^{13}C\{^1H\}$ NMR ($CDCl_3$): δ 169.5 (NH*C*OS), 124.6 ($C(NO_2)_3$), 43.5 ($CH_2C(NO_2)_3$), 25.0 (SCH_2CH_3), 15.2 (SCH_2CH_3). ^{14}N NMR ($CDCl_3$): δ –33 (NO_2). IR: 3286 (w), 2937 (vw), 1662 (m), 1583 (vs), 1512 (s), 1448 (w), 1412 (w), 1375 (w), 1295 (s), 1185 (vs), 1125 (w), 1104 (w), 1051 (m), 1040 (m), 968 (w), 903 (w), 853 (w), 802 (m), 769 (w), 713 (w) cm^{-1}. Raman (300 mW): 3290 (7), 2976 (7), 2940 (81), 2880 (10), 2738 (6), 1661 (35), 1609 (27), 1458 (14), 1419 (20), 1377 (21), 1344 (35), 1306 (25), 1271 (3), 1251 (3), 1189 (4), 1107 (11), 1064 (9), 1044 (3), 972 (7), 910 (24), 855 (100), 823 (13), 804 (4), 773 (4), 716 (3), 670 (40), 540 (10), 495 (17), 478 (3), 404 (9), 372 (47), 275 (16), 225 (6) cm^{-1}. MS (DEI$^+$) *m/z* (rel. Int.): 268 (11) [M^+], 119 (1) [$M^+ - C(NO_2)_3$], 118 (6) [$CH_2C(NO_2)_3^+$], 62 (100) [$HSCH_2CH_3^+$], 61 (15) [$SCH_2CH_3^+$]. Anal. calcd. for $C_5H_8N_4O_7S$: C, 22.39; H, 3.01; N, 20.89. Found: C, 22.42; H, 3.01; N, 20.88. BAM drophammer: 10 J. Friction tester: 160 N. ESD: 0.18 J. Grain size: 100–500 µm.

2,2,2-Trinitroethyl 2,2,2-trinitroethylcarbamate (**2**)

In contrast to reference [9], compound **1** (0.58 g, 2.16 mmol) was dissolved in tetrachloromethane (20 mL) and the solution was treated with a weak stream of chlorine gas for 15 min. After removing the volatiles *in vacuo*, the oily residue was diluted with 1,2-dichloroethane (15 mL), 2,2,2-trinitroethanol (0.469 g, 2.59 mmol) and iron(III) acetylacetonate (5 mg) were added and the reaction mixture was stirred for 3 h at 80 °C. The volatiles were removed *in vacuo* and the red residue was washed with water.

Recrystallization from chloroform (20 mL) gave 0.64 g (76%, 1.64 mmol) colorless crystals of **2**.

DSC: T_m = 164 °C, T_{dec} = 186 °C. NMR ^{1}H NMR (acetone-D$_6$): δ 8.21 (t, br, ^3J(H,H) = 6.8 Hz, 1 H, N*H*), 5.85 (s, 2 H, OC*H*$_2$C(NO$_2$)$_3$), 5.25 (d, 2 H, NC*H*$_2$C(NO$_2$)$_3$). ^{13}C{^{1}H} NMR (acetone-D$_6$): δ 154.8 (*C*O), 126.4 (br, *C*(NO$_2$)$_3$), 125.2 (br, *C*(NO$_2$)$_3$), 62.7 (O*C*H$_2$C(NO$_2$)$_3$), 45.9 (N*C*H$_2$C(NO$_2$)$_3$). ^{14}N NMR (acetone-D$_6$): δ –32 (*N*O$_2$), –33 (*N*O$_2$). IR: 3434 (w), 3012 (vw), 2961 (vw), 2898 (vw), 1764 (m), 1587 (vs), 1510 (s), 1438 (w), 1422 (w), 1383 (w), 1345 (w), 1306 (m), 1280 (m), 1213 (s), 1170 (m), 1120 (w), 1096 (w), 1061 (w), 1002 (vw), 940 (vw), 888 (vw), 856 (m), 806 (s), 801 (s), 781 (m), 760 (m), 735 (w), 676 (vw), 659 (vw) cm^{-1}. Raman (300 mW): 3012 (11), 2961 (31), 2879 (2), 2832 (2), 1765 (12), 1618 (2), 1607 (28), 1424 (6), 1379 (36), 1345 (15), 1310 (24), 1280 (7), 1216 (4), 1151 (3), 1135 (5), 1064 (7), 1016 (8), 941 (17), 891 (4), 859 (101), 804 (4), 784 (3), 738 (3), 644 (9), 543 (18), 411 (55), 377 (98), 318 (4), 281 (18), 231 (4), 216 (20) cm^{-1}. MS (DEI$^+$) *m/z* (rel. Int.): 387 (12) [M$^+$], 295 (2) [M$^+$ – 2 NO$_2$], 249 (2) [M$^+$ – 3 NO$_2$], 203 (2) [M$^+$ – 4 NO$_2$], 224 (<1) [M$^+$ – CH$_2$C(NO$_2$)$_3$ + H]. Anal. calcd. for C$_5$H$_5$N$_7$O$_{14}$: C; 15.51; H, 1.30; N, 25.33. Found: C, 16.05; H, 1.29; N, 25.73. BAM drophammer: 4 J. Friction tester: 96 N. ESD: 0.4 J. Grain size: 500–1000 µm.

2-Fluoro-2,2-dinitroethyl 2,2,2-trinitroethylcarbamate (**3**)

In contrast to reference [9], 2,2,2-trinitroethylcarbamoyl chloride (0.523 g, 2.16 mmol) was dissolved in CCl_4 (15 mL) and stirred at 75 °C for 2 h. The solvent was removed in vacuo and the residual yellow oil was dissolved in 1,2-dichloroethane (15 mL). 2-Fluoro-2,2-dinitroethanol (0.40 g, 2.60 mmol) and catalytic amounts of Fe(acac)$_3$ were added. The mixture was stirred at 80 °C for 3 h. The solvent was removed, the residue was washed with water (50 mL) and the cream-colored solid was filtered off. After recrystallization from chloroform (20 mL), 0.64 g (76%) colorless crystals of **3** were obtained.

DSC: T_m = 112 °C, T_{dec} = 191 °C. ^{1}H NMR ($CDCl_3$): δ 5.70 (t, br, 1 H, N*H*), 5.24 (d, ^3J(H,F) = 15.4 Hz, 2 H, OC*H*$_2$CF(NO$_2$)$_2$), 4.84 (d, ^3J(H,H) = 6.6 Hz, 2 H, NC*H*$_2$C(NO$_2$)$_3$). ^{13}C {^{1}H} NMR ($CDCl_3$): δ 152.8 (*C*O), 61.9 (d, ^2J(C,F) = 20.1 Hz, O*C*H$_2$CF(NO$_2$)$_2$), 44.8 (N*C*H$_2$C(NO$_2$)$_3$). ^{14}N NMR ($CDCl_3$): δ –34 (OCH$_2$C(*N*O$_2$)$_3$), –26 (OCH$_2$CF(*N*O$_2$)$_2$) ppm. ^{19}F NMR ($CDCl_3$): δ –110.4 (t, br, OCH$_2$C*F*(NO$_2$)$_2$). IR: 3399 (w), 2999 (vw), 2961 (vw), 2903 (vw), 1770 (s), 1590 (vs), 1518 (s), 1448 (w),

1429 (w), 1386 (w), 1348 (w), 1309 (m), 1288 (m), 1251 (w), 1227 (s), 1167 (m), 1127 (w), 1094 (m), 1053 (w), 1018 (w), 1002 (vw), 922 (vw), 866 (w), 858 (w), 851 (w), 803 (s), 780 (w), 763 (w), 725 (vw), 667 (w) cm^{-1}. Raman (300 mW): 3407 (6), 3399 (6), 3060 (5), 3029 (15), 3002 (39), 2962 (97), 1770 (29), 1677 (4), 1612 (45), 1594 (29), 1430 (27), 1382 (51), 1350 (47), 1310 (42), 1281 (13), 1255 (8), 1229 (13), 1171 (4), 1138 (7), 1096 (10), 1056 (10), 1017 (29), 977 (6), 937 (16), 924 (16), 859 (100), 853 (57), 809 (8), 781 (8), 732 (5), 669 (5), 640 (8), 600 (5), 591 (5), 542 (21), 413 (68), 400 (35), 376 (62), 341 (12), 314 (24), 275 (9), 254 (9), 226 (14), 212 (15) cm^{-1}. MS (DEI^+) *m/z*: 361 (<1) [M^++H], 313 (92) [$M^+ - NO_2$], 268 (18) [$M^+ - 2\ NO_2$], 210 (8) [($M^+ - C(NO_2)_3 + H$], 207 (11) [$M - OCH_2CF(NO_2)_2$], 46 (65) [NO_2], 30 (100) [NO]. Anal. calcd. for $C_5H_5N_7O_{14}$: C, 16.68; H, 1.40; N, 23.34. Found: C, 16.78; H, 1.36; N, 23.23. BAM drophammer: 3 J. Friction tester: 360 N. ESD: 0.4 J. Grain size: < 100 µm.

2,2,2-Trinitroethyl 2-fluoro-2,2-dinitroethylcarbamate (**4**)

2,2,2-Trinitroethyl chloroformate (0.44 g, 1.80 mmol) was slowly added to a solution of 2-fluoro-2,2-dinitroethylamine[35] (0.25 g, 1.63 mmol) dissolved in dichloromethane (15 mL) at 0 °C. The yellow solution was allowed to warm up and the reaction mixture was stirred for 12 h at ambient temperature. The volatiles were removed *in vacuo*, the solid residue washed with water, filtrated, dried and recrystallized in chloroform to obtain 0.38 g colorless crystals of **4** (65%).

DSC: T_m = 94 °C, T_{dec} = 188 °C. NMR ^{1}H NMR ($CDCl_3$): δ 5.52 (t, br, 1 H, N*H*), 5.43 (s, 2 H, $CH_2C(NO_2)_3$), 4.55 (dd, ^3J(H,H) = 6.7 Hz, ^3J(H,F) = 14.2 Hz, 2 H, $NHCH_2CF(NO_2)_2$). $^{13}C\{^1H\}$ NMR ($CDCl_3$): δ 152.8 (NH*C*OO), 118.0 ($CF(NO_2)_2$), 62.1 ($CH_2C(NO_2)_3$), 43.2 (d, ^2J (C,F) = 20.8 Hz, $CH_2CF(NO_2)_2$). ^{14}N NMR ($CDCl_3$): δ –35 ($C(NO_2)_3$), –24 ($CF(NO_2)_2$). ^{1}H NMR (acetone-D_6): δ 5.79 (s, 2 H, $CH_2C(NO_2)_3$), 4.79 (d, ^3J(H,F) = 16.2 Hz, 2H, $NHCH_2CF(NO_2)_2$). $^{13}C\{^1H\}$ NMR (acetone-D_6): δ = 154.0 (NH*C*OO), 124.4 (br, $C(NO_2)_3$), 120.9 (d, ^1J(C,F) = 289.4 Hz, $CF(NO_2)_2$), 61.8 ($CH_2C(NO_2)_3$), 43.2 (d, ^2J (C,F) = 20.1 Hz, $CH_2CF(NO_2)_2$). ^{14}N NMR (acetone-D_6): δ –34 ($C(NO_2)_3$), –22 ($CF(NO_2)_2$). ^{19}F NMR (acetone-D_6): δ –110.1 (t, br, ^3J(H,F) = 15.7 Hz, $CF(NO_2)_2$). IR: 3337 (w), 3053 (vw), 3015 (vw), 2966 (vw), 2895 (vw), 1764 (w), 1738 (m), 1588 (vs), 1537 (s), 1439 (w), 1417 (m), 1390 (w), 1304 (m), 1260 (m), 1237 (s), 1176 (m), 1120 (m), 1099 (w), 1063 (w), 1000 (w), 961 (vw), 898 (vw), 868 (vw), 850 (w), 802 (s), 784 (m), 764 (m), 735 (w) cm^{-1}. Raman (300 mW): 3349 (4), 3016 (20),

2970 (41), 1740 (20), 1620 (21), 1606 (26), 1441 (11), 1416 (18), 1384 (27), 1354 (37), 1307 (30), 1266 (15), 1161 (5), 1120 (6), 1064 (7), 1028 (16), 963 (7), 900 (17), 857 (100), 807 (11), 786 (6), 628 (7), 551 (9), 499 (8), 421 (48), 398 (33), 377 (58), 356 (17), 318 (17), 277 (11), 256 (11), 223 (10) cm^{-1}. MS (DEI^+) *m/z*: 361 (<1) [M^++H], 313 (9) [$M^+ - NO_2$], 268 (2) [$M^+ - 2\ NO_2$], 191 (1) [$M^+ - F - C(NO_2)_3$], 180 (1) [$OCNHCH_2CF(NO_2)_2^+$], 164 (2) [$CNHCH_2CF(NO_2)_2^+$], 133 (2) [$NHCH_2C(NO_2)_2^+$], 118 (6) [$CH_2C(NO_2)_2^+$], 104 (1) [$C(NO_2)_2^+$], 87 (9) [$CH_2OCNHCH_2^+$], 59 (5) [$OCONH^+$], 58 (3) [CNO_2^+], 46 (43) [NO_2], 30 (100) [NO]. Anal. calcd. for $C_5H_5FN_6O_{12}$: C, 16.68; H, 1.40; N, 23.34. Found: C, 16.78; H, 1.37; N, 23.11. BAM drophammer: 3 J. Friction tester: 360 N. ESD: 0.4 J. Grain size: < 100 µm.

2-Fluoro-2,2-dinitroethyl 2,2,2-trinitroethyl carbonate (**5**)

2,2,2-Trinitroethyl chloroformate (0.35 g, 1.43 mmol) was dissolved in CH_2Cl_2 (5 mL) and 2-fluoro-2,2-dinitroethanol (0.25 g, 1.62 mmol) with catalytic amounts of $SbCl_5$ were added. The reaction mixture was stirred at 85 °C for 24h.[35] The solvent was removed *in vacuo* and the residual yellow oil was diluted with hydrochloric acid (1 m, 15 mL) at 0 °C in an ultrasonic bath. The colorless precipitate was filtered, washed with water and dried *in vacuo*. After recrystallization from $CHCl_3$ (20 mL), 0.12 g (23%) colorless crystals of **5** were obtained.

DSC: T_m = 59 °C, T_{dec} = 189 °C; ^{1}H NMR (acetone-D_6): δ 6.07 (s, 2 H, $OCH_2C(NO_2)_3$), 5.76 (d, ^3J(H,F) = 15.4 Hz, 2 H, $OCH_2CF(NO_2)_2$). ^{13}C {^{1}H} NMR (acetone-D_6): δ 152.4 (*C*O), 65.6 (d, ^3J(C,F) = 19.2 Hz, $OCH_2CF(NO_2)_2$), 65.4 ($OCH_2C(NO_2)_3$). ^{14}N NMR (acetone-D_6): δ –35 ($C(NO_2)_3$), –25 ($CF(NO_2)_2$). ^{19}F NMR (acetone-D_6): δ –111.9 (t, br, $OCH_2CF(NO_2)_2$). IR: 3024 (w), 2982 (w), 2902 (w), 1772 (s), 1590 (vs), 1446 (m), 1405 (m), 1302 (s), 1267 (s), 1237 (s), 1154 (w), 1125 (w), 1098 (w), 1039 (w), 996 (m), 971 (w), 918 (w), 881 (w), 856 (w), 812 (m), 797 (m), 782 (m), 772 (m), 703 (w) cm^{-1}. Raman (300 mW): 3025 (25), 2981 (33), 2966 (37), 2881 (4), 1776 (12), 1614 (26), 1598 (27), 1446 (17), 1392 (19), 1356 (42), 1310 (29), 1172 (3), 1151 (3), 1126 (7), 1099 (7), 1044 (29), 973 (9), 917 (8), 882 (8), 859 (100), 801 (7), 783 (4), 767 (3), 646 (6), 544 (14), 501 (6), 416 (42), 374 (64), 313 (17), 290 (13), 241 (13), 221 (6) cm^{-1}. MS (DCI+) m/z: 362 (2) [M^+ + H], 328 (6) [$M^+ + H - O_2$], 299 (6) [$M^+ - NO_2 - O$], 146 (1) [$M^+ - OCOCH_2CF(NO_2)_2$], 117 (25) [$CH_3NO_2^+$], 88 (62) [$CH_2OCOCH_2^+$], 57 (100) [$CHNO_2^+$], 30 (2) [NO^+]. Anal. calcd. for $C_5H_4FN_5O_{13}$: C, 16.63; H, 1.12; N, 19.39.

Found: C, 16.74; H, 1.06; N, 19.40. BAM drophammer: 3 J. Friction tester: 360 N. ESD: 0.4 J. Grain size: < 100 µm.

4.6 ACKNOWLEDGEMENT

Financial support of this work by the Ludwig Maximilian University of Munich (LMU), the U.S. Army Research Laboratory (ARL) under grant no. W911NF-09-2-0018, the Armament Research, Development and Engineering Center (ARDEC) under grant no. W911NF-12-1-0467, and the Office of Naval Research (ONR) under grant nos. ONR.N00014-10-1-0535 and ONR.N00014-12-1-0538 is gratefully acknowledged. The authors acknowledge collaborations with Dr. Mila Krupka (OZM Research, Czech Republic) in the development of new testing and evaluation methods for energetic materials and with Dr. Muhamed Suceska (Brodarski Institute, Croatia) in the development of new computational codes to predict the detonation and propulsion parameters of novel explosives. Camilla Evangelisti is also thanked for the support with the quantum chemical calculations. We are indebted to and thank Drs. Betsy M. Rice and Brad Forch (ARL, Aberdeen, Proving Ground, MD) for many inspired discussions.

4.7 REFERENCES

[1] T. M. Klapötke, S. F. Rest, New Trends Res. Energ. Mater., Proc. Semin., 13th Pt. 2 (2010) 642–651.

[2] J. P. Agrawal, High Energy Materials Propellants, Explosives and Pyrotechnics, 1st Ed., Wiley-VCH, Weinheim, 2010.

[3] T. M. Klapötke, Chemistry of High-Energy Materials, 2nd Ed., de Gruyter, Berlin, 2012.

[4] M. E. Hill, US3306939 (1967).

[5] M. Göbel, T. M. Klapötke, Adv. Funct. Mater. 19 (2009) 347–365.

[6] T. M. Klapötke, B. Krumm, R. Moll, *Chem. Eur. J.* **2013**, *19*, 12113–12123.

[7] T. M. Klapötke, Chemie der hochenergetischen Materialien, 1 Ed., de Gruyter, Berlin, 2009.

[8] T. M. Klapötke, B. Krumm, R. Moll, S. F. Rest, Z. Anorg. Allg. Chem. 637 (2011) 2103–2110.

[9] M. E. Sitzmann, W. H. Gilligan, J. Org. Chem. 50 (1985) 5879–5881.

[10] W. H. Gilligan, S. L. Stafford, US4332744 (1982).

[11] Q. J. Axthammer, M. A. Kettner, T. M. Klapötke, R. Moll, S. F. Rest, New Trends Res. Energ. Mater., Proc. Semin., 16th Pt. 1 (2013) 29–39.

[12] A. B. Sheremetev, I. L. Yudin, Mendeleev Commun. 15 (2005) 204–205.

[13] G. Socrates, Infrared and Raman Characteristic Group Frequencies: Tables and Charts, 3rd Ed., John Wiley & Sons, Chichester, 2004.

[14] Y. Oyumi, T. B. Brill, A. L. Rheingold, J. Phys. Chem. 89 (1985) 4824–4828.

[15] M. Göbel, B. H. Tchitchanov, J. S. Murray, P. Politzer, T. M. Klapötke, Nature Chem. 1 (2009) 229–235.

[16] M. Göbel, T. M. Klapötke, Z. Anorg. Allg. Chem. 633 (2007) 1006–1017.

[17] M. Göbel, T. M. Klapötke, Acta Crystallogr. 63C (2007) o562–o564.

[18] M. Göbel, T. M. Klapötke, P. Mayer, Z. Anorg. Allg. Chem. 632 (2006) 1043–1050.

[19] S. K. Bhattacharjee, H. L. Ammon, Acta Crystallogr. 38B (1982) 2503–2505.

[20] H. L. Ammon, S. K. Bhattacharjee, Acta Crystallogr. 38B (1982) 2718–2721.

[21] H. L. Ammon, S. K. Bhattacharjee, S. R. Hall, B. Skelton, Acta Crystallogr. 39C (1983) 1565–1568.

[22] H. L. Ammon, S. K. Bhattacharjee, Acta Crystallogr. 40C (1984) 487–490.

[23] Laying down test methods pursuant to Regulation (EC) No 1907/2006 of the European Parliament and of the Council on the Evaluation, Authorisation and Restriction of Chemicals (REACH), ABl. L 142, 2008.

[24] M. Sućeska, EXPLO5 V6.01, Brodarski Institute, Zagreb, Croatia, 2012.

[25] R. Dennington, T. Keith, J. Millam, *GaussView, Version 5*, Semichem Inc., Shawnee Mission KS, **2009**.

[26] M. J. Frisch, G. W. Trucks, H. B. Schlegel, G. E. Scuseria, M. A. Robb, J. R. Cheeseman, J. A. Montgomery Jr., T. Vreven, K. N. Kudin, J. C. Burant, J. M. Millam, S. S. Iyengar, J. Tomasi, V. Barone, B. Mennucci, M. Cossi, G. Scalmani, N. Rega, G. A. Petersson, H. Nakatsuji, M. Hada, M. Ehara, K. Toyota, R. Fukuda, J. Hasegawa, M. Ishida, T. Nakajima, Y. Honda, O. Kitao, H. Nakai, M. Klene, X. Li, J. E. Knox, H. P. Hratchian, J. B. Cross, V. Bakken, C. Adamo, J. Jaramillo, R. Gomperts, R. E. Stratmann, O. Yazyev, A. J. Austin, R. Cammi, C. Pomelli, J. W. Ochterski, P. Y. Ayala, K. Morokuma, G. A. Voth, P. Salvador, J. J. Dannenberg, V. G. Zakrzewski, S. Dapprich, A. D. Daniels, M. C. Strain, O. Farkas, D. K. Malick, A. D. Rabuck, K. Raghavachari, J. B. Foresman, J. V. Ortiz, Q. Cui, A. G. Baboul, S. Clifford, J. Cioslowski, B. B. Stefanov, G. Liu, A. Liashenko, P. Piskorz, I. Komaromi, R. L. Martin, D. J. Fox, T. Keith, M. A. Al-Laham, C. Y. Peng, A. Nanayakkara, M. Challacombe, P. M. W. Gill, B. Johnson, W. Chen, M. W. Wong, C. Gonzalez, J. A. Pople, *Gaussian 03, Rev. B.03*, Gaussian, Inc., Wallingford CT, **2003**.

[27] NASA, *Space Shuttle News Reference*, 2–20–22–21, http://ntrs.nasa.gov/archive/nasa/casi.ntrs.nasa.gov/19810022734_1981022734.pdf.

[28] NASA, *press release: STS-122 The Voyage of Columbus*, **2008**, 82–84, http://www.nasa.gov/pdf/203212main_sts122_presskit2.pdf.

[29] D. F. Shriver, M. A. Drezdzon, The Manipulation of Air-Sensitive Compounds, 2nd Ed., John Wiley & Sons, New York, 1986.

[30] W. H. Gilligan, S. L. Stafford, Synthesis 08 (1979) 600–602.

[31] H. Feuer, T. Kucera, J. Org. Chem. 25 (1960) 2069–2070.

[32] V. Grakauskas, A. M. Guest, J. Org. Chem. 43 (1978) 3485–3488.

[33] M. E. Sitzmann, W. H. Gilligan, US4849540 (1989).

[34] H. Adolph, J. Org. Chem. 37 (1972) 747–751.

[35] H. G. Adolph, M. J. Kamlet, J. Org. Chem. 34 (1969) 45–50.

[36] T. M. Klapötke, J. Stierstorfer, Phys. Chem. Chem. Phys. 10 (2008) 4340–4346.

[37] J. A. Montgomery Jr., M. J. Frisch, J. W. Ochterski, G. A. Petersson, J. Chem. Phys. 112 (2000) 6532–6542.

[38] J. W. Ochterski, G. A. Petersson, J. A. Montgomery Jr., J. Chem. Phys. 104 (1996) 2598–2619.

[39] E. F. C. Byrd, B. M. Rice, J. Phys. Chem. A 110 (2005) 1005–1013.

[40] B. M. Rice, S. V. Pai, J. Hare, Combust. Flame 118 (1999) 445–458.

[41] L. A. Curtiss, K. Raghavachari, P. C. Redfern, J. A. Pople, J. Chem. Phys. 106 (1997) 1063–1079.

[42] M. Sućeska, Propellants, Explos., Pyrotech. 16 (1991) 197–202.

[43] T. M. Klapötke, B. Krumm, F. X. Steemann, K. D. Umland, Z. Anorg. Allg. Chem. 636 (2010) 2343–2346.

[44] A. Altomare, M. C. Burla, M. Camalli, G. L. Cascarano, C. Giacovazzo, A. Guagliardi, A. G. G. Moliterni, G. Polidori, R. Spagna, J. Appl. Crystallogr. 32 (1999) 115–119.

[45] A. Altomare, G. Cascarano, C. Giacovazzo, A. Guagliardi, A. G. G. Moliterni, M. C. Burla, G. Polidori, M. Camalli, R. Spagna, *SIR97,* **1997**.

[46] A. L. Spek, Acta Crystallogr. 65D (2009) 148–155.

[47] G. M. Sheldrick, Acta Crystallogr. 64A (2008) 112–122.

[48] L. J. Farrugia, J. Appl. Crystallogr. 32 (1999) 837–838.

[49] G. M. Sheldrick, *SHELX-97,* University of Göttingen, Göttingen (Germany), **1997**.

[50] A. L. Fridman, O. B. Kremleva, V. S. Zalesov, Z. V. Platonova, F. A. Gabitov, L. A. Rubinshtein, A. N. Plaksina, Pharm. Chem. J. 11 (1977) 64–67.

[51] M. B. Frankel, G. L.; Grant, L. R.; Kistner, R. L.; Lecce, J. V.; Wilson, E. R.; Woolery, D. O. I., Process studies on nitroform and related compounds: Final report for period January 30 1984 – March 31 1987, UCRL-15908, Rockwell International Corp., Rocketdyne Division, Canoga Park, CA (USA), **1987**, 1–66.

[52] R. Scharf, T. M. Klapötke, Private communication, LMU Munich September **2012**.

5. POLYNITRO CONTAINING ENERGETIC MATERIALS BASED ON CARBONYLDIISOCYANATE AND 2,2-DINITROPROPANE-1,3-DIOL

Thomas M. Klapötke, Burkhard Krumm, Sebastian F. Rest and Muhamed Sućeska*

Dedicated to Prof. Ingo-Peter Lorenz 70th Birthday

As published in: Zeitschrift für anorganische und Allgemeine Chemie **2014**, *640*(*1*), 84–92.

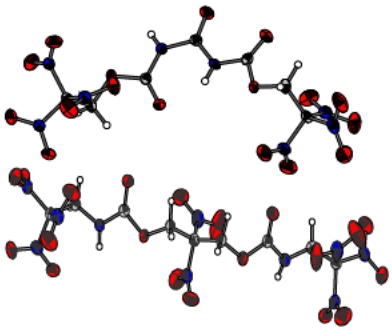

5.1 ABSTRACT

New polynitro compounds containing a carbonyl biscarbamate moiety derived from the precursor carbonyldiisocyanate were synthesized. In addition, 2,2-dinitropropane-1,3-diyl bis(2,2,2-trinitroethylcarbamate) and 2,2-dinitropropane-1,3-diyl bis(2,2,2-trinitroethyl) dicarbonate, were synthesized using 2,2-dinitropropane-1,3-diol as starting material. The compounds have been characterized by using the analytical methods, single crystal X-ray diffraction, vibrational spectroscopy (IR and Raman), multinuclear NMR spectroscopy, elemental analysis and mass spectrometry. The thermal behavior was investigated with DSC measurements. The suitability of the compounds as potential oxidizers in energetic formulations has been determined. The heats of formation of the compounds were calculated with GAUSSIAN 09. The detonation parameters such as the detonation pressure, velocity, energy and temperature were computed using the EXPLO5 code. For a secure handling of the materials, the sensitivity towards impact, friction and electrical discharge

was tested using the BAM drop hammer, BAM friction tester as well as a small-scale electrical discharge device, respectively.

5.2 INTRODUCTION

The readily available cheap compound ammonium perchlorate (**AP**) is widely used as oxidizer in solid rocket compositions. Solid rocket boosters equipped with **AP** produce a very large amount hydrogen chloride during combustion. This fact causes severe problems for the environment.[1] Therefore, environmental friendly alternative materials are desired for modern propellant composites and research is driven towards environmental friendly chlorine free compounds, which provide a great excess of oxygen for the combustion of the used fuel aluminum. The relative amount of oxygen excess is calculated as oxygen balance. This value should be at least greater than zero to deliver free oxygen for the oxidation of the fuel during its own decomposition. The most difficult challenge in the course of the development of new potential high energy dense oxidizers is to overcome the oxygen balance of **AP** with 34.0%. For calculating the oxygen balance of a CHFNO compound, it is assumed that the compounds are converted into H_2O, N_2, CO_2 and HF during the combustion in the combustion chamber. Alternatively, due to the high temperatures of combustion, CO can be assumed to be formed instead of CO_2. The oxygen balance is defined according to equation 1 and 2 for a general formula $C_aH_bF_cN_dO_e$ while *M* is the molecular mass of the compound.[2]

$$\Omega_{CO_2} = \frac{e - 2a - \frac{b-c}{2}}{M} \bullet 1600$$

Equation (1): Oxygen balance for a CHFNO compound assuming CO_2 as product of combustion in %.

$$\Omega_{CO} = \frac{e - a - \frac{b-c}{2}}{M} \bullet 1600$$

Equation (2): Oxygen balance for a CHFNO compound assuming CO as product of combustion in %.

Apart from the oxygen balance, the specific impulse is one of the most important parameters for the performance of solid-rocket boosters. It is proportional to the reciprocal of the molecular weight of the decomposition products *M* and the temperature inside the combustion chamber T_c during combustion of the composite.[2,3] An increase of

the value for I_s by 20 s leads empirically to a doubling of the usual payload.[2] Therefore, the development of new oxidizers is based on compounds decomposing into small volatile molecules as well as an increase of the temperatures of combustion. Highly nitrated CH(F)NO compounds were found to be interesting as potential oxidizers because of their high oxygen content.[1a,4]

During the course of our investigations the interesting precursor carbonyldiisocyanate was examined, which is highly reactive towards nucleophiles.[5] Based on our previous work, compounds derived from 2,2,2-trinitroethanol and 2-fluoro-2,2-dinitroethanol might be useful as starting materials for preparing new chlorine free potential high energy dense oxidizers, which decompose more environmental friendly, though they contain the halogen fluorine.[1a,4,6] The reaction of carbonyldiisocyanate with the fore-mentioned alcohols lead to interesting polynitrated molecules with improved thermal stabilities and a positive oxygen balance. Furthermore, two polynitro compounds derived from 2,2-dinitropropane-1,3-diol as the starting material were examined and studied in detail.

5.3 RESULTS AND DISCUSSION

SYNTHESIS

The important precursor carbonyldiisocyanate was synthesized by reaction of isocyanuric acid with phosgene gas at elevated temperatures.[5] Due to the use of phosgene gas as well as the production of chlorine gas and hydrogen chloride, proper safety equipment should be used for the reaction. It turned out to be helpful to set up a closed apparatus, which can manage the reaction to the crude product as well as the purification *via* distillation under inert gas conditions. Due to the high tendency of hydrolysis, reaction and storage must be kept free of moisture.

Bis-(2,2,2-trinitroethyl)carbonyl N,N-dicarbamate (**1**), as well as bis-(2-fluoro-2,2-dinitroethyl)carbonyl N,N-dicarbamate (**2**) were synthesized *via* the reaction of carbonyldiisocyanate with 2,2,2-trinitroethanol or 2-fluoro-2,2-dinitroethanol under anhydrous conditions (Scheme 5.1).

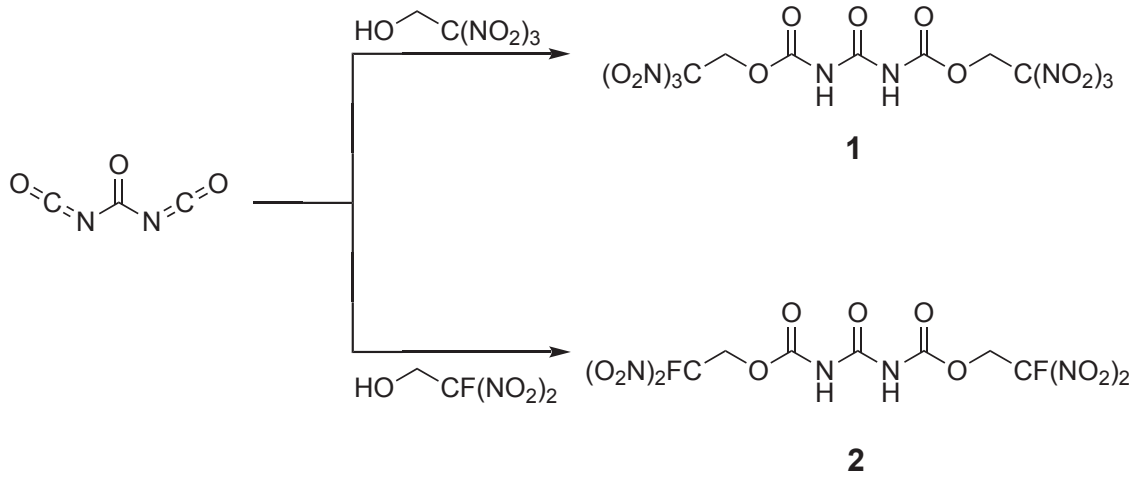

Scheme 5.1. Polynitro containing compounds based on carbonyldiisocyanate.

The starting material 2,2-dinitropropane-1,3-diol was reacted with 2,2,2-trinitroethylisocyanate, freshly prepared according to reference,[7] yielding satisfying amounts of 2,2-dinitropropane-1,3-diyl bis(2,2,2-trinitroethylcarbamate) (**3**). With 2,2,2-trinitroethyl chloroformate in the presence of catalytic amounts of triethylamine the 2,2-dinitropropane-1,3-diyl bis(2,2,2-trinitroethyl) dicarbonate (**4**) was prepared (Scheme 5.2).[8] Because of the moisture sensitivity of both reagents, as above it is also strongly advisable to work under anhydrous conditions.

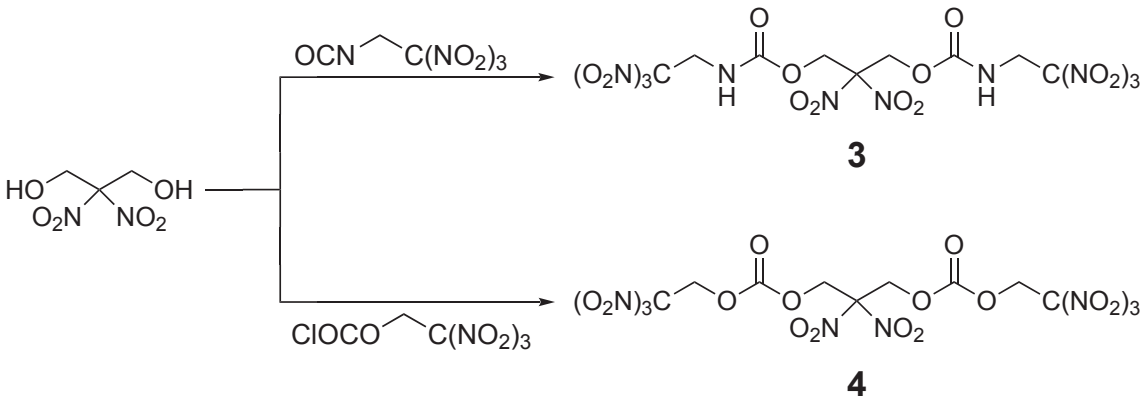

Scheme 5.2. Polynitro containing materials based on 2,2-dinitropropane-1,3-diol.

NMR SPECTROSCOPY

In the ^{1}H NMR spectrum of **1** the resonances of the amino hydrogen and methylene hydrogen atoms were detected as singlets at $\delta = 10.29$ ppm (N*H*) and 5.96 ppm, respectively. In the $^{13}C\{^{1}H\}$ NMR spectrum at $\delta = 150.7$ ppm the resonance of the carbamoyl carbon atoms was found, and at $\delta = 147.3$ ppm that of the NH*C*ONH moiety. A broadened resonance at $\delta = 124.8$ ppm is assigned for the trinitromethyl carbon atoms, the methylene carbon atoms were assigned to the resonances at $\delta = 62.6$ ppm [O*C*H$_2$C(NO$_2$)$_2$], respectively. In the ^{15}N NMR spectrum the nitro groups of the trinitromethyl moieties appear as triplets at $\delta = -33.8$ ppm with a $^{3}J_{N,H}$ coupling constant of 2.0 Hz and the amino nitrogens at $\delta = -260.7$ ppm as a doublet ($^{1}J_{N,H} = 91.9$ Hz). For compound **2**, the resonance of the amino hydrogens appeared at $\delta = 10.19$ ppm (N*H*) and the methylene hydrogen atoms were determined as doublets at $\delta = 5.63$ ppm [C*H*$_2$CF(NO$_2$)$_2$, $^{3}J_{H,F} = 15.8$ Hz] in the ^{1}H NMR spectrum. A resonance at $\delta = -111.7$ ppm, appearing as triplet, was observed for the fluorodinitromethyl fluorine atom in the ^{19}F NMR spectrum. At $\delta = 150.6$ ppm in the $^{13}C\{^{1}H\}$ NMR spectrum the resonance of the carbamoyl carbons and at $\delta = 146.7$ ppm the NH*C*ONH group was detected. A broadened doublet signal at $\delta = 119.8$ ppm ($^{1}J_{C,F} = 291.3$ Hz) was found for the fluorodinitromethyl carbon. Another doublet signal at $\delta = 62.0$ ppm with a $^{3}J_{C,F}$ coupling of 19.6 Hz was assigned to the methylene carbons. In the ^{15}N NMR spectrum a doublet of multiplet signal was observed at $\delta = -24.4$ ppm [CF(NO$_2$)$_2$, $^{2}J_{N,F} = 15.2$ Hz] for the nitro groups. The amine nitrogen was detected as doublet at $\delta = -261.0$ ppm (NH, $^{1}J_{N,H} = 92.1$ Hz). In the ^{1}H NMR spectrum of **3** the resonances of the methylene

hydrogens were detected as a doublet signal at $\delta = 5.18$ ppm (CH_2NH) with a $^3J_{H,F}$ coupling of 6.9 Hz and as a singlet signal at $\delta = 5.12$ ppm [$OCH_2C(NO_2)_2$]. The amine hydrogens appeared as a broadened triplet at $\delta = 7.98$ ppm. At $\delta = 154.7$ ppm the carbamate carbons were detected in the $^{13}C\{^1H\}$ NMR spectrum. A broadened resonance at $\delta = 125.7$ ppm was found for the trinitromethyl carbon atoms. The two different methylene carbon atoms were assigned to the resonances at $\delta = 62.1$ ppm [$OCH_2C(NO_2)_2$] and $\delta = 45.1$ ppm [$NHCH_2C(NO_2)_3$], respectively. The nitro groups were determined as broadened resonances at –18 ppm for the dinitromethylene moiety and at $\delta = -32$ ppm for the trinitromethyl functionality. For compound **4** the methylene hydrogens appeared at $\delta = 6.01$ ppm [$CH_2C(NO_2)_3$] and $\delta = 5.44$ ppm [$CH_2C(NO_2)_2$] in the ^1H NMR spectrum, respectively. At $\delta = 151.6$ ppm in the $^{13}C\{^1H\}$ NMR spectrum the carbonate carbons were detected. A broadened resonance at $\delta = 120.4$ ppm was found for the trinitromethyl carbon. In the ^{14}N NMR spectrum the two different nitro groups were found as broadened resonances at $\delta = -20$ ppm for the dinitromethylene moiety and at $\delta = -35$ ppm for the trinitromethyl functionality.

VIBRATIONAL SPECTROSCOPY

The vibrational spectra of **1**–**3** showed the NH stretching vibrations between 3418 cm^{-1} and 3260 cm^{-1}. In the range of 1824–1732 cm^{-1} the C=O stretching vibrations were observed. The multiple appearance of these vibration bands could be explained by the diversity of the neighbored functionalities (O or NH). In the range of 1603–1583 cm^{-1} and at 1316–1284 cm^{-1} the characteristic asymmetric stretching vibrations $\nu_{as}(NO_2)$ and the symmetric stretching vibrations $\nu_s(NO_2)$ were determined, respectively (Table 5.1). The C–N, C–O, C–F (for **2** only) and C–C vibrations could be observed in the typical ranges for CHFNO compounds, respectively.[9]

Table 5.1. IR and Raman bands of carbonyl and nitro groups for **1**–**4**

	1		**2**		**3**		**4**	
	IR[a)]	Raman[b)]	IR[a)]	Raman[b)]	IR[a)]	Raman[b)]	IR[a)]	Raman[b)]
ν (NH)	3296 (w)	3296 (2)	3275 (w)	3260 (4)	3418 (m)	n.o.		
			3166 (w)	3149 (4)				
ν (CO)	1824 (s)	1823 (27)	1819 (s)	1808 (44)	1758 (s)	1761 (20)	1785 (s)	1782 (11)
	1809 (m)	1803 (13)	1756 (s)	1757 (33)				
	1732 (s)	1740 (12)						
ν_{as} (NO_2)	1603 (vs)	1601 (22)	1600 (vs)	1590 (30)	1583 (vs)	1601 (30)	1589 (vs)	1613 (24)
	1589 (vs)		1588 (s)					
ν_s (NO_2)	1306 (s)	1307 (32)	1311 (s)	1316 (22)	1310 (s)	1309 (20)	1284 (s)	1304 (26)
	1289 (s)	1293 (29)	1294 (s)		1290 (s)			

a) In cm^{-1}; IR intensities: vs = very strong, s = strong, m = medium, w = weak. b) In cm^{-1}; Raman intensities at 300 mW in brackets.

X-RAY DIFFRACTION

Suitable single crystals for X-ray diffraction experiments of the compounds **1**–**3**, were obtained by crystallization from chloroform at ambient temperature. The crystal and structure refinement data of the structure determinations are given in Table 5.2. Additional data on intermolecular interactions of **1** and **2** are given in the Supporting Information.

Bis-(2,2,2-trinitroethyl)carbonyl *N*,*N*-dicarbamate (**1**) crystallizes in the triclinic space group $P\bar{1}$ with eight formula units per unit cell and a calculated density of 1.8991(2) g cm^{-1} at 173(2) K. The asymmetric unit consists of four molecules with different orientations. For clear view reasons, only one molecule of the asymmetric unit of **1** with selected bond lengths and angles is shown in Figure 5.1 exemplarily. A figure with all four molecules of the asymmetric unit is presented in the Supporting Information. The bond lengths and angles of **1** are in the typical range for CHNO-compounds containing a trinitromethyl moiety.[3,6,10] The molecular structure of **1** shows a large planar arrangement area. This planar range consists of two carbamoyl moieties around C3 and C5, as well as a carbonyl functionality at C4. This planarity is proven by the dihedral angles O7–C3–O8–N4 178.7(6), N4–C4–O9–N5 177.6(6) and N5–C5–O10–O11 178.8(6) of almost 180 °.[11] The average C–N bond of all trinitromethyl units in the asymmetric unit is 1.518(4) Å and is significantly longer than a normal C–N bond (1.47 Å).[12] Due to steric reasons, this is typically for molecules containing a trinitromethyl moiety.[3,4b,9b] A propeller-type orientation of three nitro groups connected to one carbon atom is a second typical attribute for trinitromethyl moieties. The C–C–N–O torsion angles of all trinitromethyl units are between 20 and 62 °, which implements a real propeller-type orientation.[9b] The average N–O bond length of the nitro moieties is

1.210(4) Å. Amazingly, each molecule of the asymmetric unit forms intramolecular hydrogen bonds leading to a six membered ring within the planar area of the molecule. The hydrogen bond along N5–H21···O8 (2.03(5) Å) is one example for this purpose. In addition, several weak improper hydrogen bonds and various attractive intermolecular N···O interactions lead to the quite high crystal density of compound **1**.

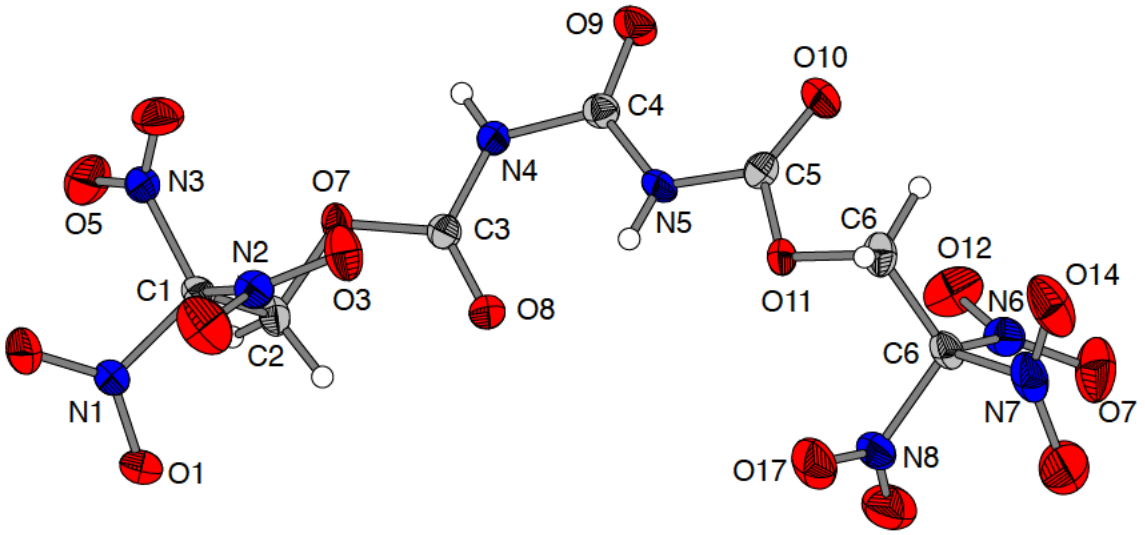

Figure 5.1. Molecular structure of **1**. Selected distances /Å and angles /°: C1–C2 1.527(4), C2–O7 1.424(4), O7–C3 1.352(3), C3–O8 1.210(3), C3–N4 1.352(4), N4–C4 1.401(4), C4–O9 1.202(4), C4–N5 1.367(4), N5–C5 1.371(4), C5–O10 1.181(4), C5–O11 1.377(3), O11–C6 1.426(4), C6–C7 1.508 (4), C1–$(NO_2)_{av}$ 1.518(4), C7–$(NO_2)_{av}$ 1.523(4), C1–C2–O7 109.4(2), C2–O7–C3 116.3(2), O7–C3–O8 123.7(3), O8–C3–N4 126.4(3), C3–N4–C4 127.4(3), N4–C4–O9 120.3(3), O9–C4–N5 125.0(3), N5–C5–O10 128.9(3), O10–C5–O11 125.2(3), C5–O11–C6 116.8(2), O11–C6–C7 108.6(2), C2–C1–N1–O1 34.2(4), C2–C1–N2–O3 36.1(4), C2–C1–N3–O5 60.8(4), C6–C7–N6–O12 –39.5(4), C6–C7–N7–O14 –20.8(4), C6–C7–N8–O17 –46.5(4), O7–C3–O8–N4 178.7(6), N4–C4–O9–N5 177.6(6), N5–C5–O10–O11 178.8(6).

Bis-(2-fluoro-2,2-dinitroethyl)carbonyl *N*,*N*-dicarbamate (**2**) crystallizes in the triclinic space group $P\bar{1}$ with two formula units per unit cell and a calculated density of 1.8839(5) g cm^{-1} at 173(2) K. The asymmetric unit with selected bond lengths and angles are shown in Figure 5.2. The bond lengths and angles of **2** are comparable with values reported in literature for CHNO-compounds containing a fluorodinitromethyl or a trinitromethyl moiety.[3,6,10] The molecular structure of **2** shows a large planar arrangement area. This planar range comprises two carbamoyl moieties around C3 and C5, as well as a carbonyl functionality at C4 and is shown by the dihedral angles of almost 180 ° [O9–C5–O8–N4 180.0(5), N4–C4–O7–N3 179.2(5), N3–C3–O6–O5 –

179.7(6)].[11] The C–N bond lengths of the fluorodinitromethyl units are all in the range of 1.53 Å, which is significantly longer than a normal C–N bond (1.47 Å).[3,4b,12] The nitro groups of both fluorodinitromethyl groups are twisted into a propeller type conformation.[9b] In addition six membered ring is formed along O8–C5–N4–C4–N3–H1 via the intramolecular hydrogen bond N3–H1···O8 [2.03(4) Å)] and several attractive intermolecular N···O interactions as well as weak hydrogen bonds were observed.

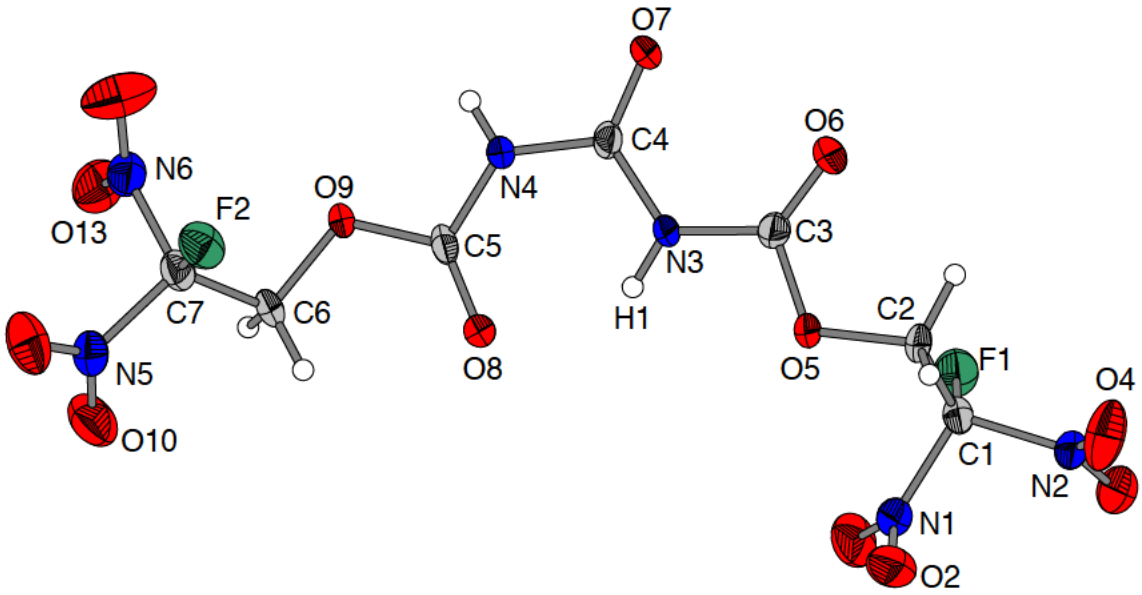

Figure 5.2. Molecular structure of **2**. Selected distances /Å and angles /°: C1–F1 1.331(3), C1–C2 1.505(4), C2–O5 1.442(4), C3–O6 1.190(3), C3–N3 1.377(4), C3–O5 1.350(4), N3–C4 1.377(4), C4–O7 1.215(3), C4–N4 1.376(4), N4–C5 1.371(3), C5–O8 1.193(4), C5–O9 1.350(4), O9–C6 1.441(3), C6–C7 1.498(5), C7–F2 1.316(3), C1–$(NO_2)_{av}$ 1.528(4), C7–$(NO_2)_{av}$ 1.531(4), F1–C1–C2 113.6(2), C2–O5–C3 115.2(2), C4–N3–C3 122.7(3), C4–N4–C5 128.1(3), C5–O9–C6 115.9(2), F2–C7–C6 113.3(2), C2–C1–N1–O2 –56.5(3), C2–C1–N2–O4 14.6(4), C6–C7–N5–O10 –19.7(4), C6–C7–N6–O13 55.9(3), O9–C5–O8–N4 180.0(5), N4–C4–O7–N3 179.2(5), N3–C3–O6–O5 –179.7(6).

The molecular structure of 2,2-dinitropropane-1,3-diyl bis(2,2,2-trinitroethylcarbamate) (**3**) is shown in Figure 5.3. Compound **3** crystallizes in the triclinic space group $P\bar{1}$ with two formula units per unit cell and a density of 1.82 g cm^{-1} at 173 K. The bond lengths and angles of **2** are comparable with values reported in literature for CHNO-compounds containing a trinitromethyl moiety.[3,6,10] The average N–O bond lengths of the trinitromethyl moieties are 1.211(3) Å for C1$(NO_2)_3$ and 1.201(3) Å for C9$(NO_2)_3$. The C9$(NO_2)_3$ group has shortened N–O bond lengths compared to the C1$(NO_2)_3$ group. The

two nitro groups of the dinitromethyl functionality at C5 have an averaged N–O bond length of 1.208(3) Å. For the top molecule, a typical propeller-type orientation of the trinitromethyl moieties with C–C–N–O torsion angles between 34.0(3) ° and 60.7(3) ° was observed.[9b] Additionally, the $C5(NO_2)_2$ group also shows the propeller type orientation in a comparable range. Both carbamate moieties appeared almost planar with the dihedral angles 178.6(5) ° (N4–C3–O7–O8) and –178.1(5) ° (N7–C7–O14–O13), respectively.[11] Several weak intermolecular improper hydrogen bonds may are a reason for the quite high density of **3**.

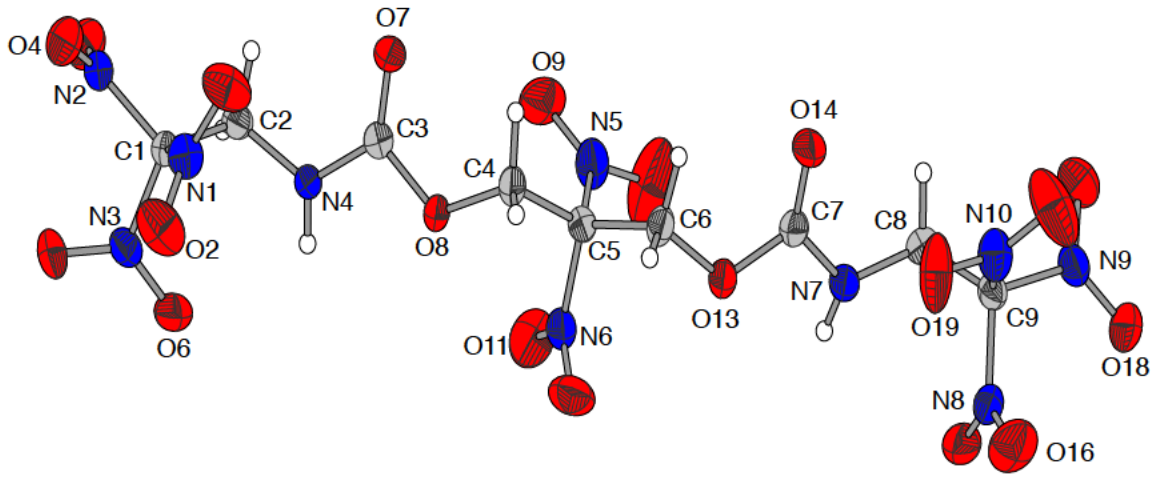

Figure 5.3. Molecular structure of **3**. Selected distances /Å and angles /°: C1–C2 1.511(4), C2–N4 1.439(4), N4–C3 1.1347(4), C3–O7 1.204(3), C3–O8 1.367(3), O8–C4 1.426(3), C4–C5 1.518 (4), C5–C6 1.526(4), C6–O13 1.421(4), O13–C7 1.266(3), C7–O14 1.201(3), C7–N7 1.347(4), N7–C8 1.429(4), C8–C9 1.526(4), C1–$(NO_2)_{av}$ 1.520(4), C5–(NO_2)av. 1.517(3), C9–(NO_2)av. 1.518(3), C2–N4–C3 121.0(2), O8–C3–O7 124.6(2), C4–O8–C3 116.6(2), C6–O13–C7 115.9(2), O13–C7–O14 126.0(2), C7–N7–C8 120.8(2), C2–C1–N1–O1 46.1(3), C2–C1–N2–O3 44.4(3), C2–C1–N3–O6 37.5(3), N4–C3–O7–O8 178.6(5), C6–C5–N5–O10 50.0(3), C6–C5–N6–O12 40.4(3), N7–C7–O14–O13 –178.1(5), C8–C9–N8–O15 34.0(3), C8–C9–N9–O17 38.4(3), C8–C9–N10–O19 60.7(3).

Table 5.2. Crystal and structure refinement data for **1**–**3**

	1	**2**	**3**
Empirical formula	$C_7H_6N_8O_{17}$	$C_7H_6F_2N_6O_{13}$	$C_9H_{10}N_{10}O_{20}$
Formula mass /g mol^{-1}	474.168	420.152	578,23
Temperature /K	173(2)	173(2)	173(2)
Crystal size /mm	0.28 × 0.16 × 0.04	0.23 × 0.11 × 0.08	0.23 × 0.16 × 0.03
Crystal description	triclinic	triclinic	triclinic
Crystal system	colorless block	colorless block	colorless platelet
Space group	*P*–1	*P*–1	*P*–1
a /Å	14.6462(9)	5.4261(8)	5.9824(2)
b /Å	14.7794(9)	10.0136(14)	11.0183(5)
c /Å	17.7372(11)	14.166(2)	16.7482(9)
α /°	70.738(6)	103.369(12)	73.844(2)
β /°	72.133(6)	97.361(12)	86.558(3)
γ /°	69.630(6)	92.313(12)	86.136(3)
V /Å^3	3316.9(4)	740.70(18)	1056.98(8)
Z	8	2	2
ρ_{calc} /g cm^{-3}	1.8991(2)	1.8839(5)	1.81685(14)
μ /mm^{-1}	0.191	0.196	0.18
F(000)	1920	424	588
θ range /°	4.19–25.50	4.19–25.50	3.42–25.38
Index ranges	$-17 \leq h \leq 15$	$-6 \leq h \leq 5$	$-6 \leq h \leq 7$
	$-17 \leq k \leq 17$	$-12 \leq k \leq 11$	$-13 \leq k \leq 13$
	$-21 \leq l \leq 13$	$-17 \leq l \leq 16$	$-20 \leq l \leq 10$
Reflections collected	16694	4510	6936
Reflections observed	11856	2725	3824
Reflections unique	8503	1910	2623
*R*1, *wR*2 (2σ data)	0.0627, 0.1401	0.0571, 0.1292	0.0452, 0.0987
*R*1, *wR*2 (all data)	0.0899, 0.1612	0.0841, 0.1491	0.0809, 0.1144
Max. / min. transmission	1.00000/0.71722	1.00000/0.70421	1.00000/0.9995
Data/restraints/parameters	11856/0/1185	2725/0/261	3824/0/360
GOOF on F^2	1.014	1.016	1.039
Larg. diff. peak/hole /e Å^{-3}	0.618/–0.419	0.570/–0.315	0.348/–0.309

THERMAL AND ENERGETIC PROPERTIES

The compounds **1**–**4** are air-stable, despite the fact that they must be synthesized under inert gas conditions. The exclusion of moisture is necessary to avoid side reactions and decomposition of the starting materials. For **1**–**4** the thermal stability was determined using DSC experiments (heating rate: 5 °C min^{-1}). Compound **1** starts to melt at 129 °C and decomposition occurs at 169 °C (onset). In contrast, the melting point of compound **2** was found at 159 °C and noticeable decomposition started above 211 °C. The melting point of compound **3** was found at 169 °C with subsequent decomposition of the substance. For compound **4** a melting point at 153 °C was detected and noticeable decomposition occurred above 176 °C. The investigated physical and chemical properties are shown in Table 5.3.

The sensitivities toward external stimuli for **1**–**4** were determined according to standards of the Federal Institute for Materials Research and Testing (BAM) [13] and the results are displayed in Table 5.4. The compounds **1** and **2** are moderate sensitive towards impact

with 7 J for **1** and 10 J for **2**, respectively. Both compounds are less sensitive than pentaerythritol tetranitrate (**PETN**) (4 J), which is a minimum requirement for new possible high energy dense oxidizers. Compounds **3** and **4** turned out to be sensitive towards impact with 3 J for **3** and 5 J for **4**, respectively. Values of 288 N (**1**) and 240N (**2**) show that both compounds are moderate sensitive towards friction. In contrast, the compounds **3** and **4** are sensitive towards friction with values of 160 N (**3**) and 144 N (**4**). Predictions of the detonation parameters using the EXPLO5 code[14] were performed based on heats of formations calculated ab initio using Gaussian 09 revision C.01[15] at the CBS-4M level of theory. Energetic parameters are attributed to the density of the corresponding compound at ambient temperature. The resulting heats of detonation (Q_v), detonation temperatures (T), pressures (p) and velocities (D) for **1** and **2** are shown in the Table 5.4, as well as the oxygen balances (Ω) in Table 5.3. The densities needed for the estimation of the detonation parameters with the EXPLO5 code[14] were derived from pycnometer measurements for compound **1**–**4**. The calculated detonation velocities of **1** (8363 m s^{-1}) and **2** (7620 m s^{-1}) are comparable with literature known values for **PETN** (8400 m s^{-1}) and nitroglycerine (**NG**) with 7700 m s^{-1}, respectively.[16] However, the velocities of **3** (8050 m s^{-1}) and **4** (8083 m s^{-1}) are comparable with literature known values for erythritol tetranitrate (ETN, 8100 m s^{-1}).[16]

The specific impulses of the compounds **1**–**4** were calculated for the combustion of the neat compounds as well as for compositions of 70 % oxidizer, 16 % aluminum, 6 % polybutadiene acrylic acid, 6 % polybutadiene acrylonitrile and 2 % bisphenol-A ether modeled on rocket-motor compositions for solid-rocket boosters used by the NASA Space Shuttle program[17] and have been compared with the calculated impulse of **AP** in an analogous composition. The chosen mixture with **AP** as oxidizer has a specific impulse of 258 sec. The impulses for **1**–**4** in the modeled compositions were estimated with 249 s for **1**, 230 s for **2** and 223 s for **3** as well as for **4**, respectively. All values are below the predicted value for an **AP** composition and even decrease from compound **1** to **4**. A reason might be the lack of oxygen within the mixture of **1** to **4**, in comparison with **AP** ($\Omega_{comp,\ \mathbf{AP}}$ = –30.13 %). The specific impulses for the neat compounds **1** (233 s) and **2** (221 s) show a similar tendency compared with the calculated compositions. Surprisingly, the impulses for the neat compounds **1** (234 s) and **2** (227 s) are greater compared with the chosen mixtures. Unfortunately, owing the estimated specific impulses, the compounds **1**–**4** are rather unlikely for use as oxidizers in solid rocket propellants. But,

due to the moderate sensitivities, the compounds **1** and **2** might be useful for other applications.

Table 5.3. Physical and chemical properties of **1**–**4**

	1	**2**	**3**	**4**
formula	$C_7H_6N_8O_{17}$	$C_7H_6F_2N_6O_{13}$	$C_9H_{10}N_{10}O_{20}$	$C_9H_8N_8O_{22}$
mol mass /g mol^{-1}	474.17	420.15	578.23	580.20
T_m /°C [a]	129	159	169	153
T_d /°C [b]	169	211	169	176
N /% [c]	23.63	20.00	24.22	19.31
$N + O$ /% [d]	80.99	69.50	79.56	79.98
Ω_{CO} /% [e]	+23.6	+15.2	+16.6	+24.8
Ω_{CO2} /% [f]	0	–11.4	–8.3	0
ρ /g cm^{-3} [g]	1.86	1.76	1.79	1.81
$-\Delta U°_f$ /kJ kg^{-1} [h]	970.07	3304.26	1439.25	1886.16
$-\Delta H°_f$ /kJ mol^{-1} [i]	1964.83	1421.75	881.80	1144.45

a, b) Melting (T_m) and decomposition (T_d) point from DSC measurement carried out at a heating rate of 5 °C min^{-1}. c) Nitrogen content. d) Combined nitrogen and oxygen content. e) Oxygen balance assuming the formation of CO. The Oxygen balance of ammonium perchlorate is 34.0 % f) Oxygen balance assuming the formation of CO_2. g) Experimentally determined density from pycnometer experiments. h) Calculated Energy of formation. i) Heat of formation.

Table 5.4. Predicted detonation and combustion parameters and sensitivity data for **1**–**4**

	1	**2**	**3**	**4**
$-Q_v$ /kJ kg^{-1} [a]	4580	3833	4414	4427
T_{ex} /K [b]	3521	3112	3332	3415
V_0 /L kg^{-1} [c]	740	683	728	715
p /kbar [d]	298	245	276	274
D /m s^{-1} [e]	8363	7620	8050	8083
impact /J [f]	7	10	3	5
friction /N [f]	288	240	160	144
ESD /J [f]	0.1	0.18	--	--
grain size /µm [g]	<100	<100	100–500	<100
thermal shock [h]	burns	burns	burns	burns
I_s /sec [i]	233	221	234	227
$I_{s(comp)}$ /sec [j]	249	230	223	223
Ω_{comp} /% [k]	–49.1	–62.0	–55.7	–49.5

a) Heat of detonation. b) Temperature of the explosion gases. c) Volume of the explosion gases (assuming only gaseous products). d) Detonation pressure. e) Detonation velocity. f) Impact and friction sensitivities according to standard BAM methods[13] and sensitivities against electrostatic discharge (ESD). g) Grain size of the samples used for sensitivity tests. h) Response to fast heating in the "flame test". i) Specific impulse of the neat compound using the EXPLO5 code[14]. j) Specific impulse for compositions using the EXPLO5 code[14]. The specific impulse for similar composition with ammonium perchlorate ($I_{s\,AP}$ = 258 s, $\Omega_{comp,\,AP}$ = –30.13 %) has been calculated. k) Oxygen balance for the composition used for combustion calculations.

5.4 CONCLUSION

The herein presented reactions of carbonyldiisocyanate with two polynitro substituted ethanoles lead to new energetic materials containing a carbonyl biscarbamate moiety (compounds **1** and **2**). Furthermore, starting from 2,2-dinitropropane-1,3-diol, the synthesis of the dicarbamate **3** and the dicarbonate **4** was accomplished. Single crystal X-ray diffraction experiments of compounds **1**–**3** showed a total planarity of the carbonyl biscarbamate moiety as well as a propeller-type orientation of the polynitromethyl moieties. The compounds **3** and **4** turned out to be more sensitive towards impact, but all compounds **1**–**4** achieve the minimum requirement of new possible high energy dense oxidizers, with an impact sensitivity not worse than **PETN**. In the case of thermal stabilities and sensitivities, the compounds **1** and **2** might be interesting for certain energetic applications. In addition, the use of carbonyldiisocyanate as starting material might be interesting for the development of new energetic molecules or even polymers. Metal free combustion purposes for the compounds **3** and **4** might be worth to consider, owing the increased specific impulse as neat compound compared to the calculated compositions.

5.4 EXPERIMENTAL SECTION

General Procedures

The syntheses and manipulation of air- and moisture-sensitive materials were performed in an inert atmosphere of dry argon (purity 5.0 Air Liquide) using flame-dried glass vessels and Schlenk techniques.[18] Commercially available chemicals (all Sigma Aldrich) were used as received. Carbonyldiisocyanate, 2-fluoro-2,2-dinitroethanol, 2,2,2-trinitroethylchloroformate, 2,2,2-trinitroethylisocyanate, 2,2-dinitropropane-1,3-diol and 2,2,2-trinitroethanol were prepared according to literature known procedures.[5a,7,19]

Raman spectra were recorded with a Bruker FT-Raman-MultiRAM Spectrometer equipped with a Klaastech DENICAFC LC-3/40 laser source at 300 mW laser power; infrared spectra were measured with a Perkin–Elmer Spectrum BX-FTIR spectrometer equipped with a Smiths DuraSamplIR II ATR device. All spectra were recorded at ambient temperature as neat samples. Densities were determined at ambient temperature using a Quantachrome Ultrapyc1200e gas pycnometer equipped with helium (purity 5.6 Air Liquide). NMR spectra were recorded with a JEOL Eclipse 400 instrument and chemical shifts were determined with respect to external Me_4Si (^{1}H, 399.8 MHz; ^{13}C, 100.5 MHz), $MeNO_2$ (^{14}N, 28.9 MHz; ^{15}N, 40.6 MHz) and CCl_3F (376.5 MHz). Mass spectrometric data were obtained with a JEOL MStation JMS 700 spectrometer (DEI+/DCI+). Analyses of C/H/N were performed with an Elementar Vario EL Analyzer. Melting points were measured with a Perkin-Elmer Pyris6 DSC, using a heating rate of 5 °C min^{-1} and checked by a Büchi Melting Point B-540 apparatus and are not corrected. The sensitivity data were performed using a BAM drophammer and a BAM friction tester.[13]

Computational Details

All ab initio calculations were carried out using the program package Gaussian 09 (Revision C.01)[15] and visualized by GaussView 5.08.[20] Structure optimizations and frequency analyses were performed with Becke's B3 three parameter hybrid functional using the LYP correlation functional (B3LYP). For C, H, N and O a correlation consistent polarized double-zeta basis set was used (cc-pVDZ). The structures were optimized without symmetry constraints and the energy is corrected with the zero point vibrational energy.[21]

The enthalpies (H°) and free energies (G°) were calculated using the complete basis set method (CBS-4M) based on ab initio optimized structures or X-ray diffraction data, in order to obtain accurate values.[21a] The CBS models use the known asymptotic convergence of pair natural orbital expressions to extrapolate from calculations using a finite basis set to the estimated complete basis set limit. CBS-4 starts with a HF/3-21G(d) structure optimization, which is the initial guess for the following SCF calculation as a base energy and a final MP2/6-31+G calculation with a CBS extrapolation to correct the energy in second order. The used reparametrized CBS-4M method additionally implements a MP4(SDQ)/6-31+(d,p) calculation to approximate higher order contributions and also includes some additional empirical corrections.[21b,21c] The enthalpies of the gas-phase species were estimated according to the atomization energy method.[21a,22]

All calculations affecting the detonation parameters were carried out using the program package EXPLO5 V6.01.[14,23] The detonation parameters were calculated at the CJ point with the aid of the steady-state detonation model using a modified Becker-Kistiakowski-Wilson equation of state for modeling the system. The CJ point is found from the Hugoniot curve of the system by its first derivative.[23-24] The specific impulses were also calculated with the EXPLO5 V6.01 program, assuming an isobaric combustion of a composition of 70% oxidizer, 16% aluminum as fuel, 6% polybutadiene acrylic acid, 6% polybutadiene acrylonitrile as binder and 2% bisphenol-A ether as epoxy curing agent.[17] A chamber pressure of 70.0 bar and an ambient pressure of 1.0 bar with equilibrium expansion conditions were estimated for the calculations.

Crystal structure determination

For all compounds, an Oxford Xcalibur3 diffractometer with a CCD area detector was employed for data collection using Mo-K_α radiation (λ = 0.71073 Å). The structures were solved by direct methods (SIR97)[25] and refined by full-matrix least-squares on F^2 (SHELXL).[26] All non-hydrogen atoms were refined anisotropically. The hydrogen atoms were located in a difference Fourier map and placed with a C–H distance of 0.99 Å for CH_2 groups. ORTEP plots are shown with thermal ellipsoids at the 50% probability level. Crystallographic data for the structures reported in this paper have been deposited with the Cambridge Crystallographic Data Centre as supplementary publication no. CCDC-956223 (**1**), CCDC-956224 (**2**) and CCDC-951974 (**3**). These data can be obtained free of

charge from The Cambridge Crystallographic Data Centre via www.ccdc.cam.ac.uk/data_request/cif.

Synthesis

CAUTION! *All high nitrogen and oxygen containing compounds are potentially explosive energetic materials, although no hazards were observed during preparation and handling these compounds. Nevertheless, this necessitates additional meticulous safety precautions (earthed equipment, Kevlar® gloves, Kevlar® sleeves, face shield, leather coat, and ear plugs). In addition, especially 2,2,2-trinitroethanol and 2-fluoro-2,2-dinitroethanol show significant degrees of toxicity,[27] including own recent results.[28] Particular care should be exercised in handling of those materials and derivatives.*

*Bis(2,2,2-trinitroethyl) carbonyl-N,N-dicarbamate (**1**)*

The reaction has to take place under inert gas conditions. Carbonyldiisocyanate (0.21 g, 1.8 mmol) was slowly added to a solution of 2,2,2-trinitroethanol (0.73 g, 4.1 mmol) in dry diethyl ether (15 mL) and stirred at ambient temperature for 12 h. The solvent was removed in vacuo and the residue was washed with water with the aid of ultra sonic yielding a colorless solid. After recrystallization from chloroform, 0.59 g (68 %) of **1** were obtained as colorless platelets.

DSC: T_m = 129 °C, T_{dec} = 169 °C. ^{1}H NMR ([D$_6$]acetone): δ = 10.29 (s, H, N*H*), 5.96 [s, 2H, OC*H*$_2$C(NO$_2$)$_3$], ppm. ^{13}C{^{1}H} NMR ([D$_6$]acetone): δ = 150.7 (O*C*ONH), 147.3 (NH*C*ONH), 124.8 [br, *C*(NO$_2$)$_3$), 62.6 (*C*H$_2$C(NO$_2$)$_3$] ppm. ^{15}N NMR ([D$_6$]acetone): δ = –33.8 [t, C(*N*O$_2$)$_3$, $^3J_{N–H}$ = 2.0 Hz], –260.7 (d, *N*H, $^1J_{N–H}$ = 91.9 Hz) ppm. IR: ν = 3296 (w), 3250 (w), 3012 (vw), 2969 (vw), 2885 (vw), 1824 (s), 1809 (m), 1732 (s), 1717 (m), 1603 (vs), 1589 (vs), 1532 (s), 1523 (s), 1478 (s), 1437 (m), 1384 (w), 1352 (w), 1306 (s), 1289 (s), 1272 (m), 1208 (vs), 1168 (vs), 1129 (s), 1111 (m), 1096 (w), 1071 (s), 951 (w), 882 (w), 855 (w), 828 (w), 805 (m), 783 (s), 765 (vs), 719 (w), 680 (w) cm^{-1}. Raman (300 mW): ν = 3296 (2), 3017 (6), 2973 (16), 1823 (27), 1803 (13), 1752 (8), 1740 (12), 1618 (21), 1601 (22), 1534 (3), 1481 (5), 1437 (12), 1387 (14), 1353 (43), 1307 (32), 1293 (29), 1205 (6), 1157 (2), 1133 (2), 1096 (3), 1073 (6), 1026 (14), 993 (15), 961 (19), 886 (10), 857 (100), 809 (3), 790 (5), 744 (3), 717 (2), 638 (6), 548 (9), 498 (6), 416 (46), 398 (38), 375 (74), 349 (13), 268 (17), 227 (6) cm^{-1}. EA (C$_7$H$_6$N$_8$O$_{17}$, 474.17 g mol^{-1}) calcd: C 17.73 H 1.28 N 23.63, found: C 17.59 H 1.33 N 23.00. MS (DEI$^+$) m/z (rel. Int.):

475 (2) $[M+H]^+$, 339 (11) $[M - HOCH_2C(NO_2)_2]^+$, 294 (15) $[M - OCH_2C(NO_2)_3]^+$, 251 (9) $[M - NHCOOCH_2C(NO_2)_3]^+$, 204 (9) $[CONCOOCH_2C(NO_2)_3]^+$, 135 (12) $[HOCH_2C(NO_2)_2]^+$, 113 (10) $[HOCONHCONH]^+$, 70 (70) $[NHCONHC]^+$, 46 (23) $[NO_2]^+$, 30 (100) $[NO]^+$. Impact sensitivity: 7 J. Friction sensitivity: 288 N. ESD: 0.1 J. Grain size: < 100 µm.

*Bis(2-fluoro-2,2-diinitroethyl) carbonyl-N,N-dicarbamate (**2**)*

The reaction has to take place under inert gas conditions. Carbonyldiisocyanate (0.34 g, 3.0 mmol) was slowly added to a solution of 2-fluoro-2,2-dinitroethanol (1.0 g, 6.6 mmol) in freshly distilled diethyl ether (20 mL) and stirred at ambient temperature for 6 h. The solvent was removed in vacuo and the residue was washed with water with the aid of ultra sonic yielding a colorless solid. After recrystallization from chloroform, 0.82 g (65 %) of **2** were obtained as colorless platelets.

DSC: T_m = 159 °C, T_{dec} = 221 °C. ^{1}H NMR ([D$_6$]acetone): δ = 10.19 (s, H, N*H*), 5.63 [d, 2H, OC*H*$_2$CF(NO$_2$)$_2$, $^3J_{H-F}$ = 15.8 Hz] ppm. ^{13}C{^{1}H} NMR ([D$_6$]acetone): δ = 150.5 (O*C*ONH), 146.7 (NH*C*ONH), 119.8 [br, d, *C*F(NO$_2$)$_2$, $^1J_{C-F}$ = 291.3 Hz], 62.0 [d, *C*H$_2$CF(NO$_2$)$_2$, $^3J_{C-F}$ = 19.6 Hz] ppm. ^{15}N NMR ([D$_6$]acetone): δ = –24.4 [dm, CF(*N*O$_2$)$_2$, $^1J_{N-F}$ = 15.2 Hz], –261 (d, *N*H, $^1J_{N-H}$ = 92.1 Hz) ppm. ^{19}F NMR ([D$_6$]acetone): δ = –111.7 [t, C*F*(NO$_2$)$_2$] ppm. IR: ν = 3275 (w), 3166 (w), 3031 (w), 2985 (w), 1819 (s), 1756 (s), 1710 (m), 1614 (s), 1600 (vs), 1588 (s), 1503 (vs), 1444 (m), 1387 (w), 1329 (m), 1311 (s), 1294 (s), 1246 (m), 1224 (m), 1161 (s), 1133 (m), 1109 (m), 1069 (s), 1032 (w), 998 (w), 961 (w), 923 (w), 851 (w), 815 (m), 776 (s), 759 (vs), 735 (w), 677 (w) cm^{-1}. Raman (300 mW): ν = 3260 (4), 3149 (4), 3138 (4), 3122 (4), 3034 (16), 2987 (45), 1808 (44), 1757 (33), 1713 (10), 1590 (30), 1525 (6), 1483 (13), 1446 (22), 1387 (26), 1361 (49), 1316 (22), 1248 (22), 1230 (12), 1067 (12), 1033 (44), 999 (9), 963 (29), 922 (20), 853 (100), 777 (6), 748 (4), 641 (4), 578 (8), 518 (17), 458 (10), 436 (20), 421 (24), 403 (26), 373 (10), 338 (40), 286 (7), 267 (4), 211 (29) cm^{-1}. EA ($C_7H_6F_2N_6O_{13}$, 420.17 g mol^{-1}) calcd: C 20.01 H 1.44 N 20.00, found: C 19.89 H 1.43 N 20.18. MS (DEI$^+$) m/z (rel. Int.): 421 (3) $[M+H]^+$, 374.1 (7) $[M - NO_2]^+$, 328 (2) $[M - 2\ NO_2]^+$, 267.1 (38) $[M - OCH_2CF(NO_2)_2]^+$, 224 (15) $[M - NHCOOCH_2CF(NO_2)_2]^+$, 70 (100) $[NHCONHC]^+$, 46 (23) $[NO_2]^+$, 30 (86) $[NO]^+$. Impact sensitivity: 10 J. Friction sensitivity: 240 N. ESD: 0.18 J. Grain size: < 100 µm.

*2,2-Dinitropropane-1,3-diyl bis(2,2,2-trinitroethylcarbamate) (**3**)*

2,2-Dinitropropane-1,3-diol (100 mg, 0.6 mmol) was diluted in dry dichloromethane (25 mL) under argon atmosphere and 2,2,2-trinitroethylisocyanate (273 mg, 1.3 mmol) was added. The reaction mixture was refluxed for 4 h. The volatile materials were removed *in vacuo*, the resulting brownish solid was washed with water with the aid of ultrasonic and dried. Recrystallization from chloroform gave 155 mg (45 %) colorless crystals of **3**.

DSC: T_m = 169 °C (dec.). ^{1}H NMR ([D$_6$]acetone): δ = 7.98 (t, br, 1H, NH), 5.18 (d, 2H, CH_2NH, $^3J_{H–H}$ = 6.9 Hz), 5.12 [2H, $CH_2C(NO_2)_3$] ppm $^{13}C\{^1H\}$ NMR ([D$_6$]acetone): δ = 154.7 (OCONH), 125.7 [$C(NO_2)_3$], 114.5 [$(CH_2)_2C(NO_2)_2$], 62.1 (CH_2), 45.1 [$CH_2C(NO_2)_3$] ppm. ^{14}N NMR ([D$_6$]acetone): δ = –18 (br, NO_2), –32 [br, $C(NO_2)_3$] ppm. IR: ν = 3418 (m), 3018 (w), 2972 (w), 2896 (w), 1758 (s), 1622 (w), 1583 (vs), 1517 (s), 1449 (m), 1416 (w), 1386 (w), 1349 (w), 1334 (w), 1310 (s), 1290 (s), 1226 (s), 1168 (m), 1133 (m), 1099 (m), 1034 (m), 997 (w), 955 (w), 874 (w), 855 (s), 805 (s), 780 (m), 763 (m), 686 (w), 664 (w) cm^{-1}. Raman: ν = 3017 (17), 2974 (41), 2859 (5), 1761 (20), 1618 (14), 1601 (30), 1452 (3), 1417 (10), 1388 (16), 1349 (32), 1309 (20), 1265 (7), 1234 (5), 1132 (8), 1064 (4), 1008 (9), 955 (17), 858 (100), 807 (6), 666 (6), 638 (5), 541 (13), 412 (41), 378 (39), 335 (9), 273 (8), 227 (6) cm^{-1}. MS (DCI+) m/z (%): 579 (11) [M + H]$^+$, 532 (2) [M – NO_2 + H]$^+$, 484 (32) [M – 2 HNO_2]$^+$, 428 (25) [M – $C(NO_2)_3$]$^+$, 355 (5) [M – $OCONHCH_2C(NO_2)_3$]$^+$, 310 (3) [$C_6H_8N_5O_{10}$]$^+$, 220 (9) [$OCOCH_2C(NO_2)_2CH_2OCO$]$^+$, 191 (13) [$CNHCH_2C(NO_2)_3$]$^+$, 134 (10), [$CH(NO_2)_2CH_2NH$]$^+$, 46 (1) [NO_2]$^+$, 30 (57) [NO]$^+$. EA ($C_9H_{10}N_{10}O_{20}$, 578,23) calcd.: C 18.69, H 1.74, N 24.22 found: C 18.71, H 1.68, N 24.00. impact sensitivity: 3 J; friction sensitivity: 160 N; grain size: 100–500 µm.

*2,2-Dinitropropane-1,3-diyl bis(2,2,2-trinitroethyl) dicarbonate (**4**)*

Prepared according to reference [7].

DSC: T_m = 153 °C, T_{dec} = 176 °C. ^{1}H NMR (acetone–D$_6$): δ = 6.01 (CH_2), 5.44 [$CH_2C(NO_2)_3$] ppm $^{13}C\{^1H\}$ NMR (acetone–D$_6$): δ = 151.6 (OCOO), 123.7 [$C(NO_2)_3$], 113.2 [$(CH_2)_2C(NO_2)_2$], 65.2 (CH_2), 64.5 [$CH_2C(NO_2)_3$] ppm. ^{14}N NMR (acetone–D$_6$): δ = –20 (br, NO_2), –35 [br, $C(NO_2)_3$] ppm. IR: ν = 3021 (w), 2972 (w), 2898 (w), 1785 (s), 1589 (vs), 1459 (w), 1441 (w), 1391 (m), 1284 (s), 1230 (vs), 1152 (w), 1095 (w), 1033 (m), 992 (m), 881 (w), 859 (w), 856 (m), 803 (s), 784 (s), 772 (s), 735 (w), 681

(w) cm^{-1}. Raman: ν = 3022 (20), 2974 (47), 2899 (4), 2859 (5), 1782 (11), 1613 (24), 1457 (10), 1446 (13), 1392 (15), 1378 (10), 1351 (33), 1304 (26), 1137 (6), 1093 (4), 1071 (7), 1044 (16), 1001 (10), 972 (6), 942 (9), 881 (10), 858 (100), 787 (6), 748 (5), 650 (5), 545 (9), 418 (24), 375 (46), 320 (10), 292 (14), 254 (12), 230 (6) cm^{-1}. MS (DCI+) m/z (%): 581 (86) $[M + H]^+$, 534 (1) $[M - NO_2]^+$, 356 (1) $[C_7H_6N_4O_{13}]^+$, 280 (3) $[M - 2\ C(NO_2)_3]^+$, 222 (11) $[C_5H_6N_2O_8]^+$, 193 (20) $[CHOCH_2C(NO_2)_3]^+$, 164 (4) $[CH_2C(NO_2)_3]^+$, 46 (2) $[NO_2]^+$, 30 (2) $[NO]^+$. EA ($C_9H_8N_8O_{22}$, 580.20) calcd.: C 18.63, H 1.39, N 19.31 found: C 18.74, H 1.38, N 19.05. impact sensitivity: 5 J; friction sensitivity: 144 N; grain size: < 100 µm.

5. ACKNOWLEDGEMENT

Financial support of this work by the Ludwig Maximilian University of Munich (LMU), the U.S. Army Research Laboratory (ARL) under grant no. W911NF-09-2-0018, the Armament Research, Development and Engineering Center (ARDEC) under grant nos. W911NF-12-1-0467/-0468, and the Office of Naval Research (ONR) under grant nos. ONR.N00014-10-1-0535 and ONR.N00014-12-1-0538 is gratefully acknowledged. The authors acknowledge collaboration with *Dr. Mila Krupka* (OZM Research, Czech Republic) in the development of new testing and evaluation methods for energetic materials. *Mrs. Camilla Evangelisti* is also thanked for the support with the quantum chemical calculations. We are indebted to and thank *Drs. Betsy M. Rice* and *Brad Forch* (ARL, Aberdeen, Proving Ground, MD) for many inspired discussions.

5.7 REFERENCES

[1] a) T. M. Klapötke, S. F. Rest, *New Trends Res. Energ. Mater., Proc. Semin., 13th* **2010**, *Pt. 2*, 642–651; b) J. P. Agrawal, *High Energy Materials Propellants, Explosives and Pyrotechnics*, 1st Ed., Wiley-VCH, Weinheim, **2010**.

[2] T. M. Klapötke, *Chemistry of High-Energy Materials*, 2nd Ed., de Gruyter, Berlin, **2012**.

[3] T. M. Klapötke, B. Krumm, R. Moll, S. F. Rest, *Z. Anorg. Allg. Chem.* **2011**, *637*, 2103–2110.

[4] a) M. E. Hill, US3306939, **1967**; b) M. Göbel, T. M. Klapötke, *Adv. Funct. Mater.* **2009**, *19*, 347–365.

[5] a) E. Nachbaur, *Monatsh. Chem.* **1966**, *97*, 361–367; b) B. Akteries, J. C. Jochims, *Chem. Ber.* **1986**, *119*, 83-95.

[6] T. M. Klapötke, B. Krumm, R. Moll, *Chem. Eur. J.* **2013**, *19*, 12113–12123.

[7] M. E. Sitzmann, W. H. Gilligan, *Journal of Organic Chemistry* **1985**, *50*, 5879–5881.

[8] W. H. Gilligan, S. L. Stafford, US4332744, **1982**.

[9] a) G. Socrates, *Infrared and Raman Characteristic Group Frequencies: Tables and Charts*, 3rd Ed., John Wiley & Sons, Chichester, **2004**; b) Y. Oyumi, T. B. Brill, A. L. Rheingold, *J. Phys. Chem.* **1985**, *89*, 4824–4828.

[10] a) T. M. Klapötke, B. Krumm, R. Moll, S. F. Rest, W. Schnick, M. Seibald, *J. Fluorine Chem.* **2013**, *156,* 253–261; b) T. M. Klapoetke, B. Krumm, S. F. Rest, M. Reynders, R. Scharf, *Eur. J. Inorg. Chem.* **2013**, 5871–5878; c) A. Baumann, A. Erbacher, C. Evangelisti, T. M. Klapoetke, B. Krumm, S. F. Rest, M. Reynders, V. Sproll, *Chem. Eur. J.* **2013**, *19*, 15627–15638; d) Q. J. Axthammer, T. M. Klapoetke, B. Krumm, R. Moll, S. F. Rest, *Z. Anorg. Allg.* **2013**, DOI: 10.1002/zaac.201300426; e) Q. J. Axthammer, M. A. Kettner, T. M. Klapötke, R. Moll, S. F. Rest, *New Trends Res. Energ. Mater., Proc. Semin., 16th* **2013**, *Pt. 1*, 29–39; f) Q. J. Axthammer, C. Evangelisti, T. M. Klapoetke, *New Trends Res. Energ. Mater., Proc. Semin., 16th* **2013**, *Pt. 2*, 511–521.

[11] B. Sepehrnia, J. R. Ruble, G. A. Jeffrey, *Acta Crystallogr., Sect. C* **1987**, *43*, 249–251.

[12] A. F. Holleman, *Lehrbuch der anorganischen Chemie*, 102 Ed., de Gruyter, Berlin, **2007**.

[13] *Laying down test methods pursuant to Regulation (EC) No 1907/2006 of the European Parliament and of the Council on the Evaluation, Authorisation and Restriction of Chemicals (REACH), ABl. L 142*, **2008**.

[14] M. Sućeska, *EXPLO5 V6.01*, Brodarski Institute, Zagreb, Croatia, **2012**.

[15] M. J. Frisch, G. W. Trucks, H. B. Schlegel, G. E. Scuseria, M. A. Robb, J. R. Cheeseman, V. B. G. Scalmani, B. Mennucci, G. A. Petersson, H. Nakatsuji, M. Caricato, X. Li, H. P. Hratchian, A. F. Izmaylov, J. Bloino, G. Zheng, J. L. Sonnenberg, M. Hada, M. Ehara, K. Toyota, R. Fukuda, J. Hasegawa, M. Ishida, T. Nakajima, Y. Honda, O. Kitao, H. Nakai, T. Vreven, J. J. A. Montgomery, J. E. Peralta, F. Ogliaro, M. Bearpark, J. J. Heyd, E. Brothers, K. N. Kudin, V. N. Staroverov, R. Kobayashi, J. Normand, K. Raghavachari, A. Rendell, J. C. Burant, S. S. Iyengar, J. Tomasi, M. Cossi, N. Rega, J. M. Millam, M. Klene, J. E. Knox, J. B. Cross, V. Bakken, C. Adamo, J. Jaramillo, R. Gomperts, R. E. Stratmann, O. Yazyev, A. J. Austin, R. Cammi, C. Pomelli, J. W. Ochterski, R. L. Martin, K. Morokuma, V. G. Zakrzewski, G. A. Voth, P. Salvador, J. J. Dannenberg, S. Dapprich, A. D. Daniels, Ö. Farkas, J. B. Foresman, J. V. Ortiz, J. Cioslowski, D. J. Fox, *Gaussian 09, Rev. C.01*, Gaussian, Inc., Wallingford CT, **2009**.

[16] P. W. Cooper, *Explosives Engineering*, 1 Ed., Wiley VCH, New York, **1996**.

[17] a) NASA, *Space Shuttle News Reference*, 2–20–22–21, http://de.scribd.com/doc/17005716/NASA-Space-Shuttle-News-Reference-1981; b) NASA, *press release: STS-122 The Voyage of Columbus*, **2008**, 82–84, http://www.nasa.gov/pdf/203212main_sts122_presskit2.pdf.

[18] D. F. Shriver, M. A. Drezdzon, *The Manipulation of Air-Sensitive Compounds*, 2nd Ed., John Wiley & Sons, New York (USA), **1986**.

[19] a) M. Göbel, T. M. Klapötke, *Acta Crystallogr., Sect C* **2007**, *63*, o562–o564; b) V. Grakauskas, A. M. Guest, *J. Org. Chem.* **1978**, *43*, 3485–3488; c) H. Feuer, G. B. Bachman, J. P. Kispersky, *J. Am. Chem. Soc.* **1951**, *73*, 1360.

[20] R. Dennington, T. Keith, J. Millam, *GaussView,* Version 5, Semichem Inc., Shawnee Mission KS (USA), **2009**.

[21] a) T. M. Klapötke, J. Stierstorfer, *Phys. Chem. Chem. Phys.* **2008**, *10*, 4340–4346; b) J. J. A. Montgomery, M. J. Frisch, J. W. Ochterski, G. A. Petersson, *J. Phys.*

Chem. **2000**, *112*, 6532–6542; c) J. W. Ochterski, G. A. Petersson, J. J. A. Montgomery, *J. Phys. Chem.* **1996**, *104*, 2598–2619.

[22] a) E. F. C. Byrd, B. M. Rice, *The Journal of Physical Chemistry A* **2005**, *110*, 1005–1013; b) B. M. Rice, S. V. Pai, J. Hare, *Combust. Flame* **1999**, *118*, 445–458; c) L. A. Curtiss, K. Raghavachari, P. C. Redfern, J. A. Pople, *J. Phys. Chem.* **1997**, *106*, 1063–1079.

[23] M. Sućeska, *Propellants, Explos., Pyrotech.* **1991**, *16*, 197–202.

[24] T. M. Klapötke, B. Krumm, F. X. Steemann, K. D. Umland, *Z. Anorg. Allg. Chem.* **2010**, *636*, 2343–2346.

[25] a) A. Altomare, M. C. Burla, M. Camalli, G. L. Cascarano, C. Giacovazzo, A. Guagliardi, A. G. G. Moliterni, G. Polidori, R. Spagna, *J. Appl. Crystallogr.* **1999**, *32*, 115–119; b) A. Altomare, G. Cascarano, C. Giacovazzo, A. Guagliardi, A. G. G. Moliterni, M. C. Burla, G. Polidori, M. Camalli, R. Spagna, *SIR97,* **1997**.

[26] a) A. L. Spek, *Acta Crystallogr., Sect. D* **2009**, *65*, 148–155; b) G. M. Sheldrick, *Acta Crystallogr., Sect. A* **2008**, *64*, 112–122; c) L. J. Farrugia, *J. Appl. Crystallogr.* **1999**, *32*, 837–838; d) G. M. Sheldrick, *SHELX-97,* University of Göttingen, Göttingen (Germany), **1997**.

[27] a) A. L. Fridman, O. B. Kremleva, V. S. Zalesov, Z. V. Platonova, F. A. Gabitov, L. A. Rubinshtein, A. N. Plaksina, *Pharm Chem J* **1977**, *11*, 64–67; b) M. B. Frankel, G. L. Bauerle, L. R. Grant, R. L. Kistner, J. V. Lecce, E. R. Wilson, D. O. I. Woolery, Process studies on nitroform and related compounds: Final report for period January 30 1984 – March 31 1987, UCRL-15908, Rockwell International Corp., Rocketdyne Division, Canoga Park, CA (USA), **1987**, 1–66.

[28] R. Scharf, T. M. Klapötke, Private communication, LMU Munich, September **2012**.

6. FLUORODINITROETHYL ORTHOCARBONATE AND FORMATE AS POTENTIAL HIGH ENERGY DENSE OXIDIZERS

Thomas M. Klapötke, Burkhard Krumm, Richard Moll, Sebastian F. Rest and Muhamed Sućeska*

As published in: Zeitschrift für Naturforschung **2014**, *69(b)*, 8–16.

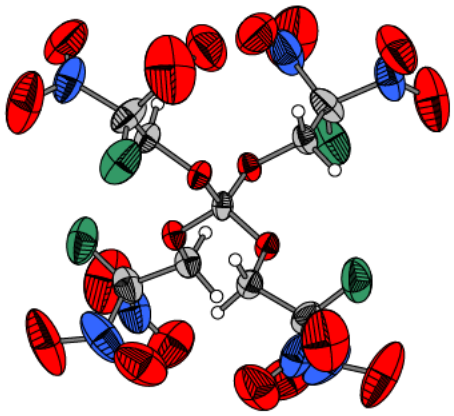

6.1 ABSTRACT

Tetrakis(2-fluoro-2,2-dinitroethyl) ortho-carbonate (**1**) and tris(2-fluoro-2,2-dinitroethyl) ortho- formate (**2**) were synthesized by the reaction of carbon tetrachloride, respectively chloroform, with 2-fluoro-2,2-dinitroethanol and catalytic amounts of anhydrous iron(III) chloride. The compounds were characterized by single-crystal X-ray diffraction, vibrational spectroscopy (IR and Raman), multinuclear NMR spectroscopy, elemental analysis, and multi-temperature DSC measurements. The suitability of the compounds as potential oxidizers in energetic formulations has been investigated and discussed. The heats of formation of the products were determined experimentally using bomb calorimetric methods. With this value and the experimental (X-ray) density, several detonation parameters such as the detonation pressure, velocity, energy, and temperature were computed using the EXPLO5 code. The sensitivity towards impact, friction and electrostatic discharge was tested using the BAM drop hammer, a friction tester and a small-scale electrostatic discharge device.

6.2 INTRODUCTION

In our current investigations we have focused our research towards highly nitrated CHNO compounds derived from 2,2,2-trinitroethanol as new potential chlorine free high energy dense oxidizers.[1-7] Especially the interesting compound tetrakis(2,2,2- trinitroethyl) ortho-carbonate seemed to be a promising candidate in replacing ammonium perchlorate (AP) as the widely used oxidizer in solid rocket propellants. AP comes along with known problems for the environment, like the large amount of hydrogen chlo- ride produced during combustion. Additionally, scientific research indicates that perchlorate-contaminated water can disrupt the thyroid's ability to produce hormones needed for normal growth and development.[8-9] Unfortunately, tetrakis(2,2,2-trinitroethyl) ortho-carbonate is very sensitive towards mechanical stimuli, which makes a future application rather un- likely.

A very important parameter for the development of new potential high energy dense oxidizers is the oxygen balance (Ω). It represents the relative amount of oxygen excess (or deficit) of a molecule, which can be used for further oxidation of an added fuel. For high energy dense oxidizers, this value should be positive and preferable greater than that of AP (34%). For calculating the oxygen balance of a CHFNO compound, it is assumed that the compounds are converted into H_2O, N_2 , CO_2 and HF during the combustion. Alter- natively, due to the high temperatures of combustion, CO can be assumed to be formed instead of CO_2. The oxygen balance can be calculated according to Eqs. 1 and 2 for a general formula $C_aH_bF_cN_dO_e$, were M is the molecular mass of the compound.[9]

$$\Omega_{CO_2} = \frac{e - 2a - \frac{b-c}{2}}{M} \bullet 1600 \qquad \text{(Equation 1)}$$

$$\Omega_{CO} = \frac{e - a - \frac{b-c}{2}}{M} \bullet 1600 \qquad \text{(Equation 2)}$$

The specific impulse (I_s) is a key parameter for assessing the performance of a solid rocket propellant. It is proportional to the temperature inside the combustion chamber T_c and the reciprocal of the molecular weight of the decomposition products M (Eq. 3).[9]

$$I_s \propto \sqrt{\frac{T_c}{M}} \qquad \text{(Equation 3)}$$

An increase of the value for Is by 20 s leads empirically to a doubling of the usual payload.[9] Obviously, it is of advantage, if the used oxidizer decomposes into small volatile molecules to increase the specific impulse of solid rocket boosters. Therefore, two interesting CHFNO derivatives, which where mentioned first in the 1960's with only very few analytical data,[10-12] prior to our initial results,[13] were investigated and are presented in this contribution.

6.3 RESULTS AND DISCUSSION

Synthesis

The reaction of 2,2,2-trinitroethanol with carbon tetrachloride, respectively chloroform, with catalytic amounts of a Lewis acid is the literature known synthesis for 2,2,2-trinitroethyl ortho-carbonate and the corresponding ortho-formate, which has also been investigated in our group.[1,14] By using 2-fluoro- 2,2-dinitroethanol instead of 2,2,2-trinitroethanol for this type of reaction, tetrakis(2-fluoro-2,2-dinitroethyl) ortho-carbonate (**1**) and tris(2-fluoro-2,2-dinitroethyl) ortho-formate (**2**) were synthesized with anhydrous iron(III) chloride as Lewis acid (Scheme 6.1).

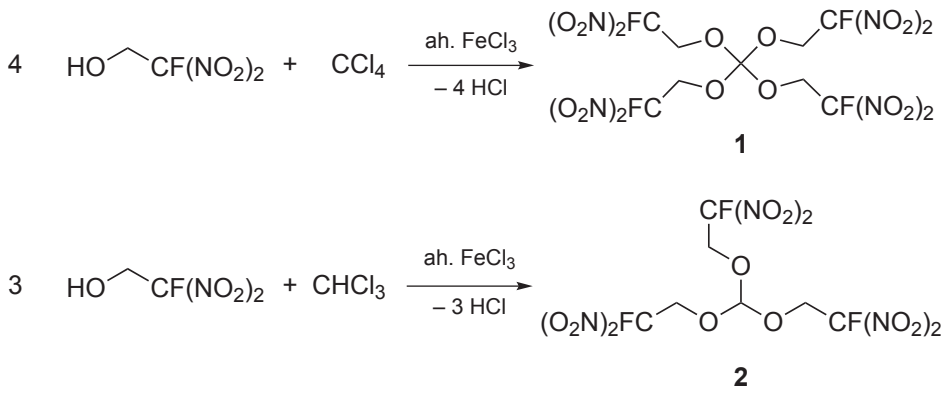

Scheme 6.1. Synthesis of ortho-carbonate **1** and -formate **2**.

NMR Spectroscopy

In the ^{1}H NMR spectra of **1** and **2** the resonances for the methylene hydrogen atoms were found as doublets at 5.24 and 5.15 ppm with $^{3}J_{H-F}$ coupling constants of 16.2 and 16.7 Hz, respectively; the ortho-formate hydrogen atom was found at 6.11 ppm. The ^{19}F NMR resonances were detected as broadened multiplets at −112.1 (**1**) and −112.2 (**2**) ppm, due to overlapping effects of the quadrupolar influence of the ^{14}N nucleus and coupling with nitrogen and hydrogen. The ^{13}C NMR resonances for the ortho-carbonate and -formate carbon atoms were detected at 119.1 (1) and 112.2 (2) ppm. The fluorodinitromethyl carbon atoms were found as doublets at 119.7 (1) and 120.4 (2) ppm, both with $^{1}J_{C-F}$ couplings of 293.3 Hz, and broadened by the quadrupolar influence of the ^{14}N nucleus. The methylene carbon atoms appeared as doublets both at 62.9 ppm ($^{2}J_{C-F}$ = 20.1 (**1**), 18.8 (**2**) Hz). The ^{14}N NMR resonances of the nitro groups were found at −25 (**1**) and −24 (**2**) ppm..

Vibrational spectroscopy

In the vibrational spectra of **1** and **2** the characteristic asymmetric NO_2 stretching vibrations were assigned in the range of 1611 – 1592 cm^{-1}, and the symmetric stretching vibrations at 1324 – 1311 cm^{-1} (Table 6.1). The C–H stretching vibrations for **1** and **2** were found in the range of 3016 – 2859 cm^{-1}. C–N, C–O, C–F and C–C vibrations of **1** and **2** were observed in the expected ranges.[15-16]

Table 6.1. IR and Raman bands of **1** and **2**, characteristic vibrations and their assignments[a]

	1		**2**	
	Raman	IR	Raman	IR
ν CH	3010 (25)	3012 (w)	2960 (42)	3016 (w)
	2969 (71)	2969 (w)	2890 (8)	2957 (w)
	2888(10)	2897 (w)	2859 (9)	2893 (w)
ν_{as} NO_2	1593 (40)	1592 (vs)	1611 (14)	1606 (vs)
			1590 (24)	
ν_s NO_2	1317 (30)	1311 (s)	1324 (14)	1311 (vs)
δ CNO_2 /ν chain	8592(100)	851 (m)	854 (100)	850 (m)

a) in cm^{-1}; Raman intensities in brackets; IR intensities: vs = very strong, s = strong, m = medium, w = weak.

Single Crystal Structural Analysis

Because of an observed phase transition of **1** (***α*-1** ⇆ ***β*-1**, for more details see below), only single crystals of ***β*-1** could be obtained by crystallization from chloroform. The modification ***β*-1** crystallizes in the tetragonal space group $P\bar{4}2_1c$ with two formula units per unit cell and a calculated maximum density of 1.84 g cm^{-3} at 258(2) K. The density is slightly higher compared to tetrakis(2,2,2-trinitroethyl) ortho-carbonate (1.81 g cm^{-3} at 258(2) K)[1], which also crystallizes in a tetragonal space group. All bond lengths and angles were found in the typical range for polynitro CH(F)NO compounds.[17-18] The structure of ***β*-1** is shown in Fig. 6.1. The displacement vectors of ***β*-1** are shown only at the 30 % probability level owing to the measurement temperature of 258 K. Below 247 K (−26 °C), *α*-**1** is the preferred conformation of **1**, which unfortunately could not be obtained as single crystals. The crystal structure and refinement data for ***β*-1** are given in Table 6.2.

The average N–O bond length of the fluorodinitromethyl moieties 1.20(3) Å. C1 is surrounded by four symmetry-equivalent oxygens (O1) in a tetrahedral coordination. In contrast to tetrakis(2,2,2- trinitroethyl) ortho-carbonate[1], the structure of ***β*-1** does not show attractive intramolecular interactions between the nitro groups. This structure motif is also found in the starting material 2-fluoro-2,2-dinitroethanol and further derivatives.[6] The C–F distance with 1.38(3) Å is comparable with a C–F single bond and in the usual range for a fluorodinitromethyl moiety.[6,7,13]

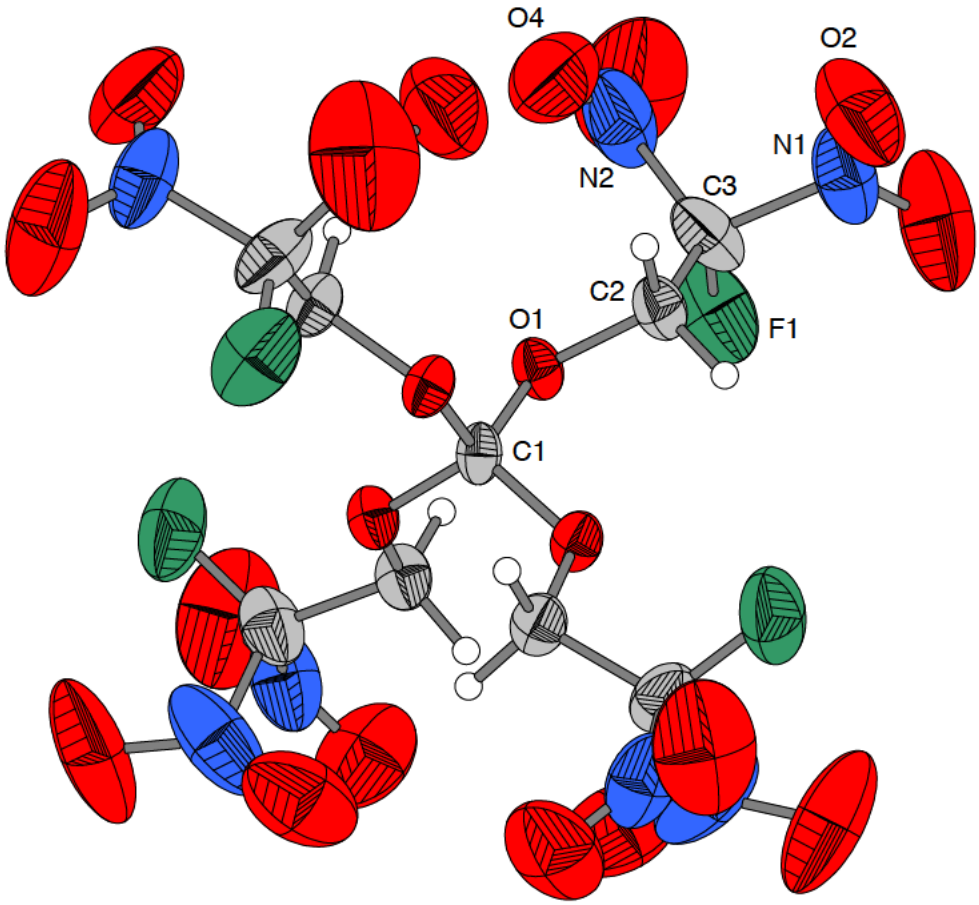

Figure 6.1. Molecular structure of ***β*-1**. Thermal ellipsoids are shown at the 30 % probability level. Selected distances [Å] and angles [deg]: C2–C3 1.48(1), C2–O1 1.422(7), O1–C1 1.386(3), C3–F1 1.38(1), C3–(NO_2)av. 1.51, C3–C2–O1 104.4(5), C2–O1–C1 115.7(3), C2–C3–N1–O2 – O2(2), C2–C3–N2–O4 51(1).

Table 6.2. Crystal and structure refinement data for **β-1**

	β-1
empirical formula	$C_9H_8F_4N_8O_{20}$
formula mass /g mol^{-1}	624.20
temperature /K	258(2)
crystal size /mm	0.10 × 0.05 × 0.04
crystal description	colorless block
crystal system	tetragonal
space group	*P*–421*c*
a /Å	11.027(3)
b /Å	11.027(3)
c /Å	9.254(6)
β /°	90.0
V /Å^3	1125.3(9)
Z	2
ρ_{calc} /g cm^{-3}	1.842
μ /mm^{-1}	0.199
F(000)	628
θ range /°	4.13–25.21
index ranges	$-13 \le h \le 9$
	$-13 \le k \le 13$
	$-11 \le l \le 11$
reflections collected	5203
reflections observed	1005
reflections unique	645
*R*1, *wR*2 (2σ data)	0.0897, 0.1257
*R*1, *wR*2 (all data)	0.2538, 0.2950
max. / min. transmission	0.9921/0.9803
data/restraints/parameters	1005/0/93
GOOF on F^2	1.037
larg. diff. peak/hole /e Å^{-3}	0.398/–0.247

Thermal and Energetic Properties

The investigated physical and chemical properties of compound **1** and **2** are shown in Table 6.3. Even though compound **1** has to be prepared under inert gas conditions, the pure compound is stable towards moisture and air. DSC measurements of compound **1** have shown that the product melts at 133 °C. The compound starts to boil at 193 °C (onset), an exothermic decomposition was not detected at higher temperatures. Additional measurements at low temperatures revealed a phase transition (exothermic peak) between the α- and β-configuration of **1** starting at −26 °C (onset) during cooling the compound to −80 °C. Upon reheating the sample an endothermic signal appeared at −22 °C (onset), which indicates the phase transition reversibility. The rate of heating was ±5 °C. Therefore, the α-configuration of **1** is metastable above −22 °C. Between −26 and −22 °C both phases of **1** are coexistent (Fig. 6.2). 2,2-Dinitroethene-1,1-diamine (FOX-7) and tetrakis(2,2,2-trinitroethyl) ortho-carbonate show a comparable behavior between two different phases at a temperature of 116 °C for the former and with hysteresis between −16 and 33 °C for the latter one.[1,19]

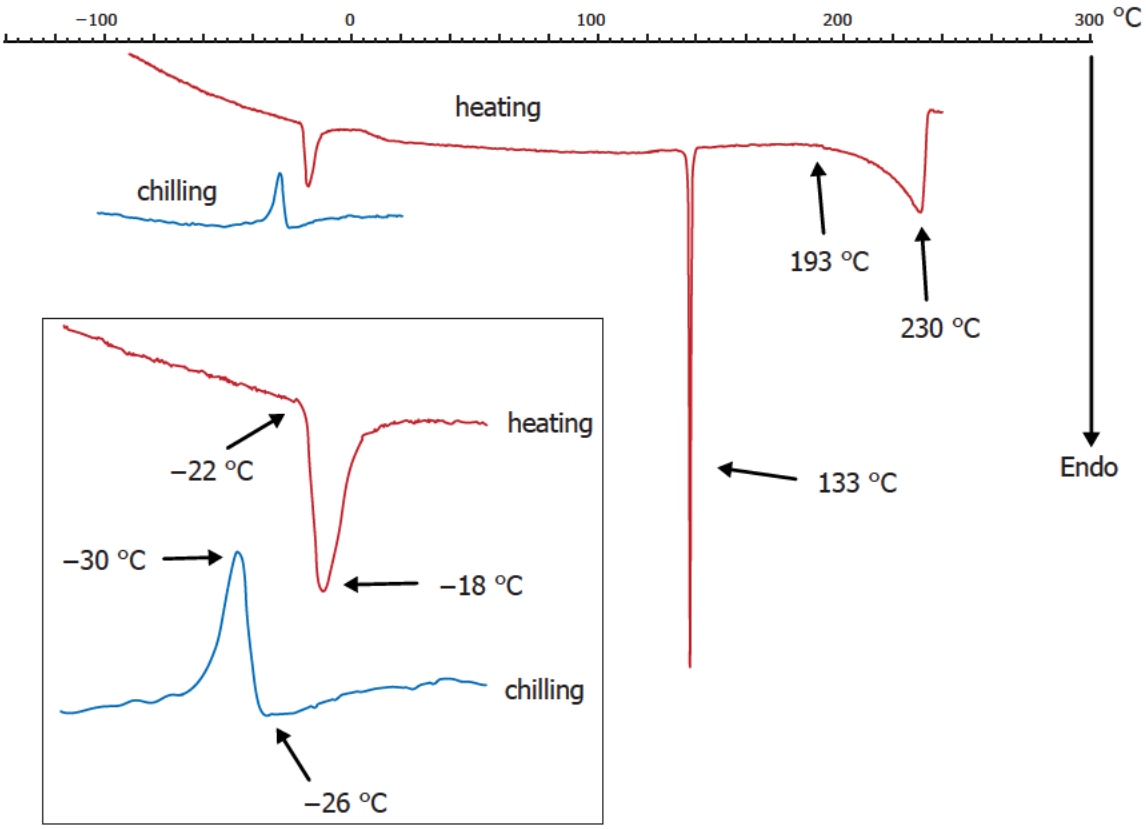

Figure 6.2. DSC measurement for **1** from –100 to 240 °C with a chilling/heating rate of ±5 °C min^{-1}.

The ortho-formate **2** was prepared under similar conditions as **1**. It is stable towards air and moisture and decomposes notably at 211 °C after melting at 110 °C. However, here no phase transition was observed.

The results of the performed sensitivity tests against friction, impact and electrostatic discharge (ESD) are given in Table 6.4. Compound **1** showed moderate sensitivities with 9 J (impact), 192 N (friction) and 0.25 J (ESD). With 25 J towards impact and 0.45 J (ESD), compound **2** is even much less sensitive. Additionally, **2** is insensitive towards friction.

Predictions of the detonation parameters using the EXPLO5 code have been performed based on heats of formation calculated *ab initio* using the GAUSSIAN 09 program package [20-21] (Table 6.4). The densities at ambient temperature needed for the estimation of the detonation parameters with the EXPLO 5 code[22] ere derived from the single-crystal X-ray structure for **1** and experimentally by gas pycnometer measurements for **2**. The resulting heats of detonation (Q_v), detonation temperatures (T_{ex}), pressures (p) and velocities (D) for **1** and **2** are shown in Table 6.4, as well as the oxygen balances (Ω). The

detonation velocity of **1** (8440 m s^{-1}) is comparable with that of pentaerythritol tetranitrate (PETN, 8400 m s^{-1}) and tetrakis(2,2,2-trinitroethyl) ortho-carbonate (8419 m s^{-1}).[1,23] The predicted velocity of **2** (8404 m s^{-1}) is only slightly below that of compound **1**.

Table 6.3. Physical and chemical properties of **1** and **2**

	1	**2**
formula	$C_9H_8F_4N_8O_{20}$	$C_7H_7F_3N_6O_{15}$
mol mass /g mol^{-1}	624.20	472.16
T_m /°C [a)]	133	110
T_d /°C [b)]	193 (boiling)	211
N /% [c)]	17.95	17.80
$N + O$ /% [d)]	69.21	68.63
Ω_{CO} /% [e)]	23.1	20.3
Ω_{CO2} /% [f)]	0	–3.4
ρ /g cm^{-3} [g)]	1.84	1.80
$-\Delta U°_f$ /kJ kg^{-1} [h)]	2548.7	2512.3
$-\Delta H°_f$ /kJ kg^{-1} [i)]	1640.5	1224.6

a, b) Melting (T_m) and decomposition (T_d) point from DSC measurement carried out at a heating rate of 5 °C min^{-1}. c) Nitrogen content. d) Combined nitrogen and oxygen content. e) Oxygen balance assuming the formation of CO. The Oxygen balance of ammonium perchlorate is 34.0 %. f) Oxygen balance assuming the formation of CO_2. g) Experimentally determined density from X-ray diffraction experiments at ambient temperature (**1**) or pycnometer measurements (**2**). h) Energy of formation at 298 K. i) Heat of formation at 298 K.

Table 6.4. Predicted detonation and combustion parameters and sensitivity data for **1** and **2**

	1	**2**
$-Q_v$ /kJ kg^{-1}	4539	4826
T_{ex} /K [a]	3800	3906
V_0 /L kg^{-1} [b]	700	702
p /kbar [c]	372	362
D /m s^{-1} [d]	8440	8405
impact /J [e]	9	25
friction /N [e]	192	360
ESD /J [f]	0.25	0.45
grain size /µm [g]	100–250	100–250
thermal shock [h]	burns	burns
I_s /sec [i]	249	252
$I_{s(comp)}$ /sec [j]	246	246
Ω_{comp} /% [k]	–53.96	–56.33

a) Temperature of the explosion gases. b) Volume of the explosion gases (assuming only gaseous products). c) Detonation pressure. d) Detonation velocity. e) Impact and friction sensitivities according to standard BAM methods.[24] f) Sensitivity towards electrostatic discharge. g) Grain size of the samples used for sensitivity tests. h) Response to fast heating in the "flame test". i) Specific impulse of the neat compound using the EXPLO5 code[22]. j) Specific impulse for compositions. The specific impulse for similar composition with ammonium perchlorate ($I_{s\ AP}$ = 258 s, $\Omega_{comp,\ AP}$ = –30.13 %) has been calculated. k) Oxygen balance for the composition used for combustion calculations.

The specific impulses of the compounds **1** and **2** were calculated for compositions of 70 % oxidizer (compound **1** or **2**), 16 % aluminum, 6 % polybutadiene acrylic acid, 6 % polybutadiene acrylonitrile and 2 % bisphenol A ether modeled on rocket motor compositions for solid rockets boosters used by the NASA Space Shuttle program.[25-26] These impulses were compared with the calculated impulse of ammonium perchlorate (AP) in an analogous composition. The chosen mixture with AP as oxidizer provides a specific impulse of 258 s. The impulses for **1** and **2** in the modeled compositions were calculated with a value of 246 s for both, which is below the predicted value for an AP composition. A reason might be the decreased oxygen balance within the mixture of −53.96 % for 1 and −56.33 % for **2**, respectively (Ω_{comp}(AP) = −30.13 %). Interestingly, the impulses for the neat compounds **1** (249 s) and even 252 s for **2** are greater compared with the chosen mixtures and are therefore in the range of a typical composition using AP as oxidizer.

6.4 CONCLUSION

Tetrakis(2-fluoro-2,2-dinitroethyl) ortho-carbonate (**1**) and tris(2-fluoro-2,2-dinitroethyl) ortho-formate (**2**) were synthesized and fully characterized using multinuclear NMR, IR and Raman spectroscopy, as well as mass spectrometry and elemental analysis. These compounds were also examined in terms of sensitivity, compared with tetrakis(2,2,2-trinitroethyl) ortho-carbonate, and found to be less sensitive. Both materials might be of potential interest for application in metal-free propulsion systems.

6.5 EXPERIMENTAL SECTION

General Procedures

The synthesis and manipulation of air- and moisture- sensitive materials were performed under an inert atmosphere of dry nitrogen in flame-dried glass vessels by SCHLENK techniques.[27] The solvents carbon tetrachloride and chloroform (both Sigma Aldrich) were dried by standard methods and freshly distilled prior to use. Anhydrous iron(III) chloride and 2-fluoro-2,2-dinitroethanol were prepared according to literature known procedures.[6,28-29] Raman spectra were recorded with a BRUKER MultiRAM FT- Raman instrument equipped with a KLASTECH DENICAFC LC-3/40 Nd:YAG laser source (λ = 1064 nm, 300 mW) and a liquid nitrogen-cooled germanium detector. Infrared (IR) spectra were measured with a PERKIN-ELMER Spectrum BX- FTIR spectrometer equipped with a SMITHS DuraSamplIR II ATR device. All spectra were recorded at ambient temperature, the samples were neat solids. Densities were determined at ambient temperature using a QUANTACHROME Ultrapyc1200e gas pycnometer equipped with helium gas (AIR LIQUIDE, purity 5.6). NMR spectra were recorded at 25 °C with a JEOL ECLIPSE 400 instrument, and chemical shifts were determined with respect to external Me_4Si (^1H, 399.8 MHz; ^{13}C, 100.5 MHz), $MeNO_2$ (^{14}N, 28.9 MHz) and CCl_3F (^{19}F, 376.5 MHz). Mass spectrometric data were obtained with a JEOL MStation JMS 700 spectrometer (DEI+). Elemental analyses (C/H/N) were performed with an ELEMENTAR VARIO EL analyzer. Melting points were measured with a PERKIN-ELMER Pyris6 DSC instrument, with a heating rate of 5 °C min^{-1} and checked by a BÜCHI Melting Point B-540 apparatus. Sensitivity data (impact, friction and electrostatic discharge) were performed with a drophammer, friction tester and electrostatic discharge device conform to the directive of the Federal Institute for Materials Research and Testing (BAM).[24]

Computational Details

All quantum-chemical calculations were carried out using the program package GAUSSIAN 09 (revision C.01)[21], visualized with GAUSSVIEW 5 (version 5.0.8).[20] The initial geometries of the structures were taken from the experimentally determined crystal structure (**1**) or from the previously calculated ab initio-optimized structure (**2**). The enthalpies (*H*) and free energies (*G*) were calculated by the complete basis set (CBS) method in order to obtain very accurate values.[30-32] The CBS model uses the known

asymptotic convergence of pair natural orbital expressions to extrapolate from calculations using a finite basis set to the estimated complete basis set limit. CBS-4 starts with a HF/3-21G(d) structure optimization, which is the initial guess for the following SCF calculation as a base energy and a final MP2/6-31+G calculation with a CBS extrapolation to correct the energy in second order. The used re-parametrized CBS-4M method additionally implements a MP4(SDQ)/6-31+(d,p) calculation to approximate higher-order contributions and also includes some additional empirical corrections.[37-38]

The solid-state enthalpies and energies of formation were calculated from the corresponding enthalpy derived from these quantum chemical CBS-4M calculations (H_{CBS-4M}). Therefore, the enthalpies of formation of the gas-phase species were computed according to the atomization energy method.[30,33-35] All calculations affecting the detonation parameters were carried out using the program package EXPLO5 V6.01.[22,36] The detonation parameters were calculated at the CJ point with the aid of the steady-state detonation model using a modified Becker-Kistiakowski-Wilson equation of state for modeling the system. The CJ point is found from the Hugoniot curve of the system by its first derivative.[36-37] The specific impulses were also calculated with the EXPLO5 V6.01 program, assuming an isobaric combustion of a composition of 70 % oxidizer, 16 % aluminum (as fuel), 6 % polybutadiene acrylic acid, 6 % polybutadiene acrylonitrile (both as binder) and 2 % bisphenol A ether (as epoxy curing agent).[25-26] A chamber pressure of 70.0 bar and an ambient pressure of 1.0 bar with equilibrium expansion conditions were estimated for the calculations.

X-ray structure determination

For compound **1**, an Oxford Xcalibur3 diffractometer with a CCD area detector was employed for data collection using MoK_α radiation(λ=0.71073A°). The structures were solved by Direct Methods (SIR97)[41-42] and refined by full-matrix least-squares on F^2 (SHELXL-97).[43-46] All non-hydrogen atoms were refined anisotropically. The hydrogen atoms were located in difference Fourier maps and placed with a C–H distance of 0.99 Å for CH_2 groups. Table 6.2 summarizes the most important crystal structure data.

CCDC 951973 contains the supplementary crystallographic data for this paper. These data can be obtained free of charge from The Cambridge Crystallographic Data Centre via www.ccdc.cam.ac.uk/data request/cif.

Synthesis

CAUTION! All nitrogen- and oxygen-rich compounds are potentially explosive energetic materials, although no hazards were observed during preparation and handling these compounds. Nevertheless, this necessitates additional meticulous safety precautions (earthed equipment, Kevlar® gloves, Kevlar® sleeves, face shield, leather coat, and ear plugs). In addition, especially 2-fluoro-2,2-trinitroethanol shows significant degrees of toxicity,[38-39] including own recent results.[40] Particular care should be exercised in handling of those materials and derivatives.

*Tetrakis(2-fluoro-2,2-dinitroethyl) orthocarbonate (**1**)*

2-Fluoro-2,2-dinitroethanol (1.54 g, 10.0 mmol) and anhydrous iron(III) chloride (0.15 g, 0.92 mmol) were diluted in carbon tetrachloride (4.2 mL) under careful exclusion of moisture. The mixture was heated up in an oil bath (85 °C) and refluxed for 24 h. The solvent was removed *in vacuo*. To remove the remaining iron(III) chloride, the residue was washed with iced dilute hydrochloric acid (25 mL, 1 M) and the product was filtered off. After crystallization of the crude product from chloroform, 0.89 g of **1** (57 %) was obtained.

DSC: T_m = 133 °C, T_{dec} = 193 °C. – Raman: ν = 3010 (25), 2969 (71), 2888 (10), 2794 (5), 1593 (40), 1455 (37), 1395 (18), 1359 (79), 1317 (30), 1255 (16), 1171 (6), 1116 (15), 1068 (21), 1025 (16), 930 (21), 859 (89), 852 (100), 815 (5), 806 (6), 775 (5), 747 (6), 579 (8), 518 (13), 468 (9), 421 (49), 377 (54), 351 (29), 306 (14), 266 (6), 213 (23) cm^{-1}. – IR: ν = 3012 (w), 2969 (w), 2897 (w), 1740 (w), 1592 (vs), 1449 (w), 1402 (w), 1358 (w), 1311 (s), 1252 (w), 1159 (s), 1133 (s), 1109 (vs), 1067 (s), 1009 (m), 919 (w), 851 (m), 803 (s), 776 (w), 764 (w), 745 (w), 678 (w) cm^{-1}. – ^{1}H NMR (acetone–D_6): δ = 5.24 (d, CH_2, $^3J_{H-F}$ = 16.2 Hz). – $^{13}C\{^1H\}$ NMR (acetone–D_6): δ = 119.7 (d,

*C*F(NO$_2$)$_2$, $^1J_{C–F}$ = 293.3 Hz), 119.1 (*C*(OCH$_2$)$_4$), 62.9 (d, O*C*H$_2$, $^2J_{C–F}$ = 20.1 Hz). – ^{19}F NMR (acetone-D_6): δ = –112.1 (m, br, C*F*(NO$_2$)$_2$). – ^{14}N NMR (acetone–D_6): δ = –25 (br, *N*O$_2$). – MS (DEI+): *m*/*z* (%) = 471 (5) [M – OCH$_2$CF(NO$_2$)$_2$]$^+$, 395 (2) [M – CH$_2$CF(NO$_2$)$_2$ – 2 NO$_2$]$^+$, 319 (4) [M – 2 OCH$_2$CF(NO$_2$)$_2$ + H]$^+$, 137 (18) [CH$_2$CF(NO$_2$)$_2$]$^+$, 46 (35) [NO$_2$]$^+$, 30 (100) [NO]$^+$. – EA for C$_9$H$_8$F$_4$N$_8$O$_{20}$ (624.20) calcd. C 17.32, H 1.29, N 17.95; found C 17.39, H 1.24, N 17.72 %. – Sensitivities (grain size: 100–500 µm): impact: 9 J; friction: 192 N; electrostatic: 0.25 J.

*Tris(2-fluoro-2,2-dinitroethyl) formate (**2**)*

2-Fluoro-2,2-dinitroethanol (2.5 g, 16.2 mmol) and anhydrous iron(III) chloride (0.2 g, 1.23 mmol) were dissolved in dry chloroform (5 mL) under careful exclusion of moisture. The mixture was heated up in an oil bath (85 °C) and refluxed for 120 h. Upon cooling, the reaction mixture was poured into diethyl ether (60 mL). The ether phase was washed with water (3 × 60 mL) and dried over sodium sulfate. Removing the solvent left a cream colored crude product, which was re-crystallized from dichloromethane/pentane (50:50). 1.9 g (74 %) of **2** as colorless crystals was obtained.

DSC: T_m = 110 °C, T_{dec} = 211 °C. – Raman: ν = 2960 (42), 2890 (8), 2859 (9), 2427 (3), 1611 (14), 1590 (24), 1456 (18), 1397 (11), 1375 (20), 1358 (35), 1324 (14), 1246 (9), 1118 (10), 1079 (8), 1025 (11), 969 (5), 924 (8), 854 (100), 760 (4), 725 (3), 625 (4), 542 (10), 421 (28), 380 (37), 361 (23), 300 (5), 221 (5) cm^{-1}. – IR: ν = 3016 (w), 2957 (w), 2893 (w), 1606 (vs), 1452 (w), 1399 (w), 1311 (vs), 1250 (w), 1172 (w), 1134 (s), 1114 (s), 1074 (s), 1026 (m), 1010 (m), 928 (w), 850 (m), 817 (w), 801 (vs), 761 (w) cm^{-1}. – ^{1}H NMR (acetone–D_6): δ = 6.11 (C*H*), 5.15 (d, CH_2, $^3J_{H–F}$ = 16.7 Hz). – ^{13}C{^{1}H} NMR (acetone–D_6): δ = 120.4 (d, *C*F(NO$_2$)$_2$, $^1J_{C–F}$ = 293.3 Hz), 112.2 (*C*H(OCH$_2$)$_3$), 62.9 (d, O*C*H$_2$, $^2J_{C–F}$ = 18.8 Hz). – ^{19}F NMR (acetone-D_6): δ = –112.2 (m, br, C*F*(NO$_2$)$_2$). – ^{14}N NMR (acetone–D_6): δ = –24 (br, *N*O$_2$). – MS (DEI+): *m*/*z* (%) = 471 (1) [M – H]$^+$, 319

(10) $[M - OCH_2CF(NO_2)_2]^+$, 137 (16) $[CH_2CF(NO_2)_2]^+$, 91 (4) $[CH_2CFNO_2]^+$, 46 (23) $[NO_2]^+$, 30 (100) $[NO]^+$. – EA for $C_7H_7F_3N_6O_{15}$ (472.16) calcd. C 17.81, H 1.49, N 17.80; found C 17.88, H 1.47, N 17.60 %. – Sensitivities (grain size: 100–250 µm): impact: 25 J; friction: 360 N; electrostatic: 0.45 J.

6.6 ACKNOWLEDGEMENT

Financial support of this work by the Ludwig-Maximilian University of Munich (LMU), the U.S. Army Research Laboratory (ARL), the Armament Research, Development and Engineering Center (ARDEC), the Strategic Environmental Research and Development Program (SERDP), and the Office of Naval Research (ONR Global, title: "Synthesis and Characterization of New High Energy Dense Oxidizers (HEDO) - NICOP Effort") under contract nos. W911NF-09-2-0018 (ARL), W911NF-09-1-0120 (ARDEC), W011NF-09-1-0056 (ARDEC), and 10WP-SEED01-002/WP-1765 (SERDP) is gratefully acknowledged. The authors acknowledge collaborations with Dr. Mila Krupka (OZM Research, Czech Republic) in the development of new testing and evaluation methods for energetic materials and with Dr. Muhamed Sućeska (Brodarski Institute, Croatia) in the development of new computational codes to predict the detonation and propulsion parameters of novel explosives. We are indebted to and thank Drs. Betsy M. Rice and Brad Forch (ARL, Aberdeen, Proving Ground, MD) and Mr. Gary Chen (ARDEC, Picatinny Arsenal, NJ) for many helpful and inspired discussions and support of our work. Stefan Huber is also thanked for assistance during sensitivity measurements. Special thanks are provided to Gerhard Sax for several DSC measurements. We thank Dr. Cliff Bedford for suggesting this study to us.

6.7 REFERENCES

[1] T. M. Klapötke, B. Krumm, R. Moll, S. F. Rest, *Z. Anorg. Allg. Chem.* **2011**, *637*, 2103–2110.

[2] T. M. Klapötke, S. F. Rest, *New Trends Res. Energ. Mater., Proc. Semin., 13th* **2010**, *Pt. 2*, 642–651.

[3] Q. J. Axthammer, T. M. Klapötke, B. Krumm, R. Moll, S. F. Rest, *Z. Anorg. Allg. Chem.* **2014**, *in press*.

[4] A. Baumann, A. Erbacher, C. Evangelisti, T. M. Klapötke, B. Krumm, S. F. Rest, M. Reynders, V. Sproll, *Chem. Eur. J.* **2013**, *19,* 15627–15638.

[5] T. M. Klapötke, B. Krumm, S. F. Rest, M. Reynders, R. Scharf, *Eur. J. Inorg. Chem.* **2013**, 5871–5878.

[6] T. M. Klapötke, B. Krumm, R. Moll, *Chem. Eur. J.* **2013**, *19*, 12113–12123.

[7] T. M. Klapötke, B. Krumm, R. Moll, S. F. Rest, W. Schnick, M. Seibald, *J. Fluorine Chem.* **2013**, *153*, 253–261.

[8] H. H. Cady, A. C. Larson, *Acta Crystallogr.* **1965**, *18*, 485–496.

[9] T. M. Klapötke, *Chemistry of High-Energy Materials*, 2nd Ed., de Gruyter, Berlin, **2012**.

[10] M. J. Kamlet, K. G. Shipp, M. E. Hill, US3388147, **1968**.

[11] A. B. Sheremetev, I. L. Yudin, *Mendeleev Communications* **2005**, *15*, 204–205.

[12] K. F. Mueller, R. H. Renner, W. H. Gilligan, H. G. Adolph, M. J. Kamlet, *Combust. Flame* **1983**, *50*, 341–349.

[13] Q. J. Axthammer, M. A. Kettner, T. M. Klapötke, R. Moll, S. F. Rest, *New Trends Res. Energ. Mater., Proc. Semin., 16th* **2013**, *Pt. 1*, 29–39.

[14] M. E. Hill, US3306939, **1967**.

[15] Y. Oyumi, T. B. Brill, A. L. Rheingold, *J. Phys. Chem.* **1985**, *89*, 4824–4828.

[16] G. Socrates, *Infrared and Raman Characteristic Group Frequencies: Tables and Charts*, 3rd ed., John Wiley & Sons, Chichester, **2004**.

[17] M. Göbel, T. M. Klapötke, *Adv. Funct. Mater.* **2009**, *19*, 347–365.

[18] T. N. Hall, *Tetrahedron* **1963**, *19*, 115–120.

[19] J. Evers, T. M. Klapötke, P. Mayer, G. Oehlinger, J. Welch, *Inorg. Chem.* **2006**, *45*, 4996–5007.

[20] R. Dennington, T. Keith, J. Millam, *GaussView, Version 5*, Semichem Inc., Shawnee Mission KS, **2009**.

[21] M. J. Frisch, G. W. Trucks, H. B. Schlegel, G. E. Scuseria, M. A. Robb, J. R. Cheeseman, V. B. G. Scalmani, B. Mennucci, G. A. Petersson, H. Nakatsuji, M. Caricato, X. Li, H. P. Hratchian, A. F. Izmaylov, J. Bloino, G. Zheng, J. L. Sonnenberg, M. Hada, M. Ehara, K. Toyota, R. Fukuda, J. Hasegawa, M. Ishida, T. Nakajima, Y. Honda, O. Kitao, H. Nakai, T. Vreven, J. A. Montgomery, Jr., J. E. Peralta, F. Ogliaro, M. Bearpark, J. J. Heyd, E. Brothers, K. N. Kudin, V. N. Staroverov, R. Kobayashi, J. Normand, K. Raghavachari, A. Rendell, J. C. Burant, S. S. Iyengar, J. Tomasi, M. Cossi, N. Rega, J. M. Millam, M. Klene, J. E. Knox, J. B. Cross, V. Bakken, C. Adamo, J. Jaramillo, R. Gomperts, R. E. Stratmann, O. Yazyev, A. J. Austin, R. Cammi, C. Pomelli, J. W. Ochterski, R. L. Martin, K. Morokuma, V. G. Zakrzewski, G. A. Voth, P. Salvador, J. J. Dannenberg, S. Dapprich, A. D. Daniels, Ö. Farkas, J. B. Foresman, J. V. Ortiz, J. Cioslowski, D. J. Fox, *Gaussian 09, Rev. C.01*, Gaussian, Inc., Wallingford CT, **2009**.

[22] M. Sućeska, *EXPLO5 V6.01*, Brodarski Institute, Zagreb, Croatia, **2012**.

[23] P. W. Cooper, *Explosives Engineering*, 1st ed., Wiley VCH, New York, **1996**.

[24] Test procedure *A.14 Explosive Properties* according to Council Regulation (EC) No 440/2008 of 30 May 2008 laying down test methods pursuant to Regulation (EC) No 1907/2006 of the European Parliament and of the Council on the Registration, Evaluation, Authorisation and Restriction of Chemicals (REACH), **OJ L 142**, 93–103, **2008**.

[25] NASA, *Space Shuttle News Reference*, 2-20-22-21, http://de.scribd.com/doc/17005716/NASA-Space-Shuttle-News-Reference-1981.

[26] NASA, *press release: STS-122 The Voyage of Columbus*, **2008**, 82–84, http://www.nasa.gov/pdf/203212main_sts122_presskit2.pdf.

[27] D. F. Shriver, M. A. Drezdzon, *The Manipulation of Air-Sensitive Compounds*, 2nd ed., John Wiley & Sons, New York, **1986**.

[28] A. F. Holleman, E. Wiberg, N. Wiberg, *Lehrbuch der Anorganischen Chemie*, 102nd ed., de Gruyter, Berlin, **2008**.

[29] E. Nachbaur, *Monatsh. Chem.* **1966**, *97*, 361–367.

[30] T. M. Klapötke, J. Stierstorfer, *Phys. Chem. Chem. Phys.* **2008**, *10*, 4340–4346.

[31] J. A. Montgomery, Jr., M. J. Frisch, J. W. Ochterski, G. A. Petersson, *J. Phys. Chem.* **2000**, *112*, 6532–6542.

[32] J. W. Ochterski, G. A. Petersson, J. A. Montgomery, Jr., *J. Phys. Chem.* **1996**, *104*, 2598–2619.

[33] E. F. C. Byrd, B. M. Rice, *J. Phys. Chem. A* **2006**, *110*, 1005–1013.

[34] B. M. Rice, S. V. Pai, J. Hare, *Combust. Flame* **1999**, *118*, 445–458.

[35] L. A. Curtiss, K. Raghavachari, P. C. Redfern, J. A. Pople, *J. Phys. Chem.* **1997**, *106*, 1063–1079.

[36] M. Sućeska, *Propellants, Explos., Pyrotech.* **1991**, *16*, 197–202.

[37] T. M. Klapötke, B. Krumm, F. X. Steemann, K. D. Umland, *Z. Anorg. Allg. Chem.* **2010**, *636*, 2343–2346.

[38] A. L. Fridman, O. B. Kremleva, V. S. Zalesov, Z. V. Platonova, F. A. Gabitov, L. A. Rubinshtein, A. N. Plaksina, *Pharm. Chem. J.* **1977**, *11*, 64–67.

[39] M. B. Frankel, G. L. Bauerle, L. R. Grant, R. L. Kistner, J. V. Lecce, E. R. Wilson, D. O. I. Woolery, *Process studies on nitroform and related compounds: Final report for period 30 January 1984 to 31 March 1987*, UCRL-15908, Rockwell International Corp., Rocketdyne Division, Canoga Park, CA (USA), **1987**, 1–66.

[40] R. Scharf, T. M. Klapötke, *Private communication*, LMU Munich, September **2012**.

[41] A. Altomare, M. C. Burla, M. Camalli, G. L. Cascarano, C. Giacovazzo, A. Guagliardi, A. G. G. Moliterni, G. Polidori, R. Spagna, *Journal of Applied Crystallography* **1999**, *32*, 115–119.

[42] G. M. Sheldrick, *Acta Crystallogr.* **2008**, *A64*, 112–122.

[43] A. L. Spek, *Acta Crystallogr.* **2009**, *D65*, 148–155.

[44] L. J. Farrugia, *Journal of Applied Crystallography* **1999**, *32*, 837–838.

7. (2-FLUORO-2,2-DINITROETHYL)-2,2,2-TRINITROETHYLNITRAMINE, A POSSIBLE HIGH ENERGY DENSE OXIDIZER

Thomas M. Klapötke, Burkhard Krumm, Sebastian F. Rest, Martin Reynders, Regina Scharf

As published in: European Journal of Inorganic Chemistry **2013**, *34*, *5871–5878.*

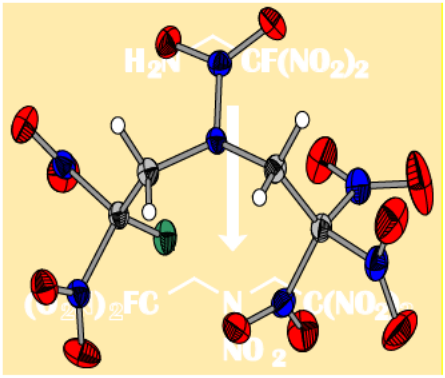

7.1 ABSTRACT

The fluorine-containing polynitro energetic molecule (2-fluoro-2,2-dinitroethyl)-2,2,2-trinitroethylnitramine and the corresponding precursors were synthesized and investigated as potential high-energy dense oxidizers. The compounds have been characterized by using various analytical methods, single crystal X-ray diffraction, vibrational spectroscopy (IR and Raman), multinuclear NMR spectroscopy, elemental analysis, mass spectrometry and differential scanning calorimetry (DSC) measurements. The suitability of the compounds as potential oxidizers in energetic formulations has been investigated. In addition, the heats of formation of the products were calculated with the program package Gaussian 09. Several detonation parameters such as the detonation pressure, velocity, energy and temperature were computed using the EXPLO5 code. Furthermore, the sensitivity towards impact, friction and electrical discharge was determined using the German Federal Institute for Materials Research and Testing (BAM) drop hammer, a friction tester as well as a small-scale electrical discharge device.

7.2 INTRODUCTION

Ammonium perchlorate (**AP**) is a widely used oxidizer in solid-rocket propellants for civil applications. Unfortunately, this readily available and cheap compound comes along with several problems for the environment, such as the formation of large amounts of hydrogen chloride gas during the combustion of a solid rocket composite.[1] Therefore, it is important to drive research towards environmental friendly chlorine free compounds and to provide a large excess of oxygen for the combustion of the used aluminum fuel. Highly nitrated CHNO compounds were found to be useful as high energetic materials because of their good oxygen content.[1a,2]

The performance of solid-rocket boosters depends on the specific impulse as one of the most important parameters. It is proportional to the reciprocal of the molecular weight of the decomposition products M and the temperature inside the combustion chamber T_c during combustion of the composite.[3] An increase of the value for the specific impulse (I_s) by 20 s leads empirically to a doubling of the usual payload.[3a] Therefore, the development of new energetic oxidizers based on CHNO compounds decomposing into small volatile molecules as well as an increase of the temperature of combustion should enhance the specific impulse of modern solid rocket motors.

On the basis of previous investigations, compounds derived from 2-fluoro-2,2-dinitroethylamine and 2,2,2-trinitroethanol might be useful as starting materials for preparing new chlorine free potential high-energy dense oxidizers, which decompose in a more environmental friendly way, even though they contain the halogen fluorine.[1a,2a-c]

The chemistry of 2,2,2-trinitroethanol is different to that of other alcohols due to the electron-withdrawing effect of the trinitromethyl group.[4] As a result the basicity of the hydroxyl group is decreased and it behaves acidic (pK_a= 6.1). At pH values above 6, the equilibrium is shifted towards the starting materials nitroform and formaldehyde.[2b,5] The amine 2-fluoro-2,2-dinitroethylamine shows also a decreased basicity due to the electron-withdrawing fluorodinitromethyl functionality (σ^* = 4.4).[6] The σ^* parameter indicates the influence of a substituent during a reaction through polar (inductive, field, and resonance) effects of organic compounds.[4,7] The most common way for synthesizing new compounds using 2,2,2-trinitroethanol as precursor is a Mannich-type reaction with amine moieties.

A detailed study of the synthesis and characterization of (2-fluoro-2,2-dinitroethyl)-2,2,2-trinitroethylnitramine and precursors is presented in this work. The compounds were

investigated as potential high-energetic oxidizers based on the starting material 2-fluoro-2,2-dinitroethylamine, which is known since the 1960ies.[8]

7.3 RESULTS AND DISCUSSION

Synthesis

The amine 2-fluoro-2,2-dinitroethylamine (**1**) was synthesized from 2-fluoro-2,2-dinitroethanol with aqueous ammonia[8a] (Scheme 1). After distillation, the amine **1** must be handled very carefully. Therefore, an unexpected sudden deflagration occurs as a neat liquid within several hours at room temperature. Storage of **1** as solution in chloroform is recommended.

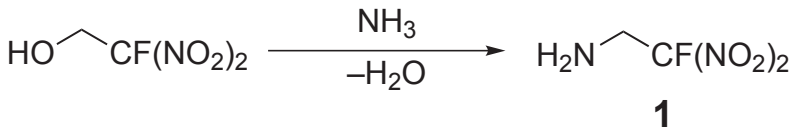

Scheme 7.1. Synthesis of 2-fluoro-2,2-dinitroethylamine (**1**).

The MANNICH-type reaction of **1** with 2,2,2-trinitroethanol leads to the mixed secondary amine (2-fluoro-2,2-dinitroethyl)-2,2,2-trinitroethylamine (**2**). The reaction was carried out in chloroform, assisted by the use of molecular sieves (4 Å). Further nitration of compound **2**, using a mixture of nitric and sulfuric acid, gave the corresponding nitramine (2-fluoro-2,2-dinitroethyl)-2,2,2-trinitroethylnitramine (**3**) in good yields (Scheme 2).

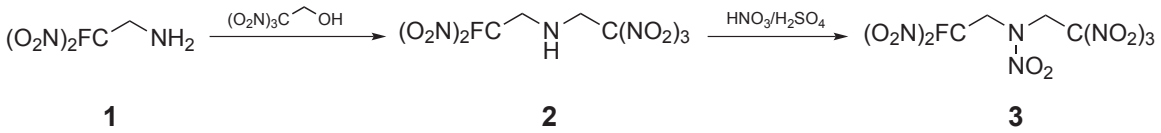

Scheme 7.2. Synthesis of compound **2** and **3** from 2-fluoro-2,2-dinitroethylamine (**1**).

Multinuclear NMR Spectroscopy

The compounds were thoroughly characterized by ^{1}H, $^{13}C\{^{1}H\}$, ^{15}N and ^{19}F NMR spectroscopy. The ^{1}H NMR spectrum of compound **1** revealed the resonance of the CH_2 group as a doublet at $\delta = 3.92$ ppm caused by the coupling with the adjacent fluorine atom ($^{3}J_{F,H} = 17.6$ Hz). The amino resonance was observed broadened at $\delta = 1.49$ ppm. In the ^{13}C NMR the resonance for the fluorodinitromethyl group was identified as a doublet at $\delta = 123.0$ ppm with a coupling constant of $^{1}J_{C,F} = 287.5$ Hz. The methylene carbon resonance occurred also as doublet at $\delta = 44.5$ ppm ($^{2}J_{C,F} = 19.6$ Hz). The amino nitrogen

resonance of 2-fluoro-2,2-dinitroethylamine was observed at $\delta = -377.2$ ppm in the ^{15}N NMR spectrum. Additionally, the nitrogen atoms of the nitro groups appeared at $\delta = -20.8$ ppm as a doublet due to the ^{2}J coupling with fluorine ($^{2}J_{15N,F} = 15.0$ Hz). The ^{19}F NMR spectrum showed a broadened resonance at $\delta = -111.1$ ppm, because of the quadrupolar influence of ^{14}N in the nitro groups.

The ^{1}H NMR spectrum of (2-fluoro-2,2-dinitroethyl)-2,2,2-trinitroethylamine (**2**) showed different resonances for the two methylene groups. The doublet at $\delta = 4.31$ ppm ($^{3}J_{H,H} = 7.8$ Hz), which was caused by a ^{3}J coupling with the adjacent NH moiety, was assigned to the trinitroethyl group of **2**. The resonance of the $CH_2CFC(NO_2)_2$ moiety appeared as a doublet of doublets at $\delta = 4.10$ ppm owing to an additional $^{3}J_{H-F}$ coupling with coupling constants of $^{3}J_{H,H} = 7.3$ Hz and $^{3}J_{H,F} = 16.6$ Hz. The N*H* resonance was observed as a quintet at $\delta = 2.55$ ppm. In the ^{13}C NMR spectrum the resonance of the trinitromethyl carbon was typically found as a broadened resonance at $\delta = 126.2$ ppm. The fluorodinitromethyl carbon resonance was found at $\delta = 121.3$ ppm as doublet with a $^{1}J_{C-F}$ coupling constant of 288.3 Hz. As expected, the resonances of the CH_2 moieties were observed as a singlet at $\delta = 52.5$ ppm [$CH_2C(NO_2)_3$], and as a doublet at $\delta = 50.8$ ppm [$CH_2CF(NO_2)_2$; $^{2}J_{C,F} = 19.2$ Hz], respectively. The ^{15}N NMR spectrum showed the nitro resonances of two different polynitromethyl moieties as a doublet of multiplets at $\delta = -22.9$ ppm [$CF(NO_2)_2$; $^{2}J_{N,F} = 14.9$ Hz] for the fluorodinitromethyl moiety and the trinitromethyl functionality as triplet a at $\delta = -32.3$ ppm [$C(NO_2)_3$; $^{3}J_{N,H} = 2.0$ Hz] ppm. The amine resonance appeared as a doublet at $\delta = -373.0$ ppm owing to the direct $^{1}J_{N,H}$ coupling with 83.0 Hz.

The resonances of the two methylene groups in the ^{1}H NMR spectrum of **3** were identified as a singlet at $\delta = 6.14$ ppm for the trinitroethyl moiety and at $\delta = 5.80$ ppm as doublet with a $^{3}J_{H,F}$ coupling constant of 9.5 Hz for the fluorodinitroethyl group. Similar to **2**, at $\delta = 124.2$ ppm a broadened singlet appears in the ^{13}C NMR spectrum for the trinitromethyl carbon and the fluorodinitromethyl carbon was identified as a doublet at $\delta = 118.6$ ppm ($^{1}J_{C,F} = 294.0$ Hz). The methylene carbon connected to the trinitromethyl moiety was found as a singlet at $\delta = 55.2$ ppm, and a doublet at $\delta = 55.0$ ppm was assigned to the second methylene group adjacent to the fluorodinitromethyl group with a $^{2}J_{C,F}$ coupling constant of 16.1 Hz. The ^{19}F NMR spectrum showed a broadened resonance appearing as triplet at $\delta = -107.1$ ppm. In the ^{15}N NMR spectrum the different polynitro moieties as well as the newly introduced nitramine functionality were detected (Figure 1). The resonance at $\delta = -22.5$ ppm was assigned to the nitrogen atoms of the

fluorodinitromethyl group. As a result of the $^{3}J_{N,H}$ = 1.7 Hz coupling with the attached methylene hydrogen and an additional $^{2}J_{N,F}$ = 15.2 Hz coupling, this resonance is split into a doublet of triplets. Owing to the $^{3}J_{N,H}$ coupling of 2.0 Hz, the resonance of the C(NO_2)$_3$ moiety was found as a triplet at δ = –33.7 ppm. The nitramine group showed two resonances, a quintet at δ = –33.4 ppm for the nitro group ($^{3}J_{N–H}$ = 3.2 Hz, coupling to four hydrogen atoms of the two methylene groups), and the amine nitrogen resonance was identified as a singlet at δ = –217.2 ppm.

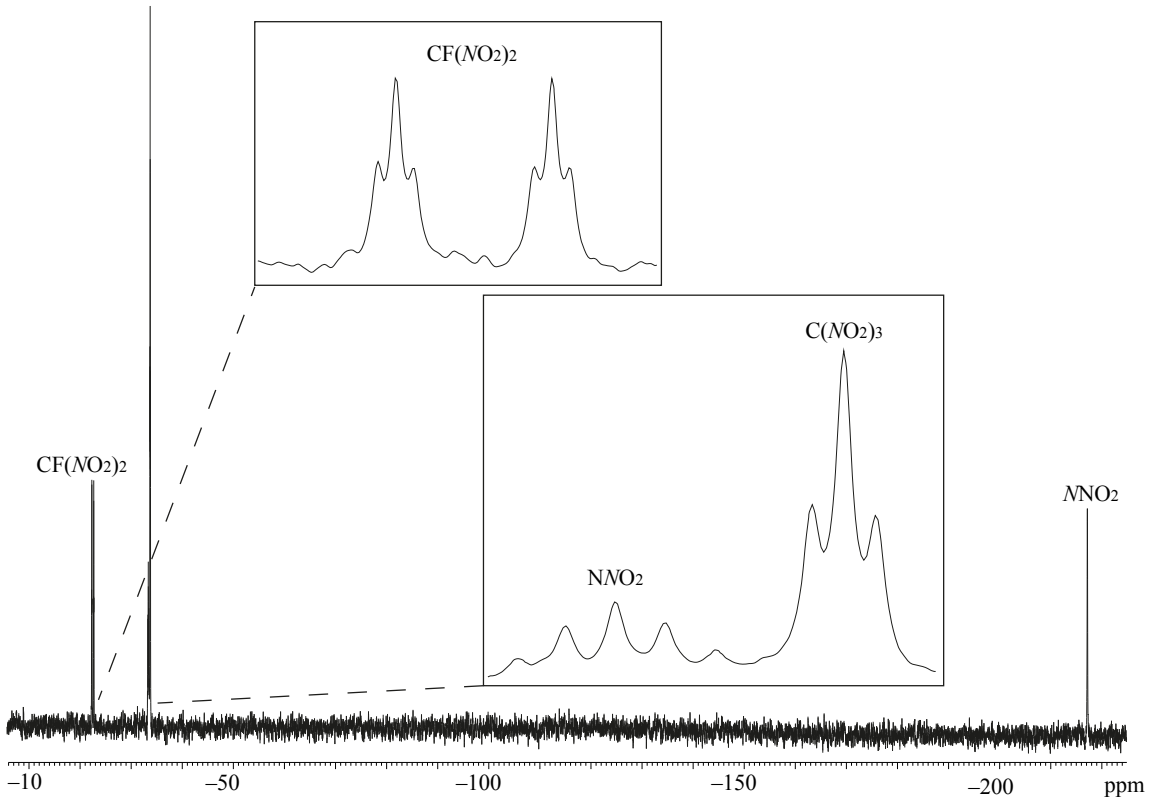

Figure 7.1. ^{15}N NMR spectrum of **3** in [D_6]acetone.

Vibrational spectroscopy

The vibrational spectra of **1**–**3** showed the characteristic asymmetric stretching vibrations $\nu_{as}(NO_2)$ in the range of 1614–1579 cm^{-1} and the symmetric stretching vibrations $\nu_s(NO_2)$ at 1316–1270 cm^{-1} (Table 1). The two different polynitro moieties (trinitromethyl/fluorodinitromethyl moiety) might cause the observed spread of the $\nu_{as}(NO_2)$ vibration energies. For compounds **1** and **2** the N–H stretching vibrations of the amine moieties were observed in the range of 3428–3361 cm^{-1}. The C–N, C–O, C–F and C–C vibrations of **1**–**3** could be observed in the typical ranges for CHFNO compounds, respectively.[9]

Table 7.1. IR and Raman bands of carbonyl and nitro groups for **1**–**3**

	1		**2**		**3**	
	IR[a]	Raman[b]	IR[a]	Raman[b]	IR[a]	Raman[b]
ν NH	3428 (w)	3361 (9)	3368 (w)	3368 (4)		
	3364 (w)					
ν_{as} NO_2	1581 (vs)	1588 (18)	1579 (vs)	1612 (23)	1591 (vs)	1614 (22)
				1601 (22)		1589 (10)
				1585 (18)		1566 (5)
ν_s NO_2	1281 (m)	1310 (18)	1305 (s)	1311 (30)	1316 (m)	1300 (16)
			1245 (m)	1247 (12)	1270 (w)	1271 (44)

[a] IR intensities in [cm^{-1}]; vs = very strong, s = strong, m = medium, w = weak. [b] Raman intensities [cm^{-1}] at 300 mW in brackets.

X-Ray Diffraction

The compounds **2** and **3** were investigated by low-temperature single-crystal X-ray diffraction. The crystal and structure refinement data of the structure determinations are given in Table 2. Suitable single crystals for X-ray diffraction measurements were obtained by slow evaporation of chloroform. The bond lengths and angles of compound **2** and **3** are comparable with previously discussed values for CHNO-compounds containing a trinitromethyl moiety.[3b,10] Additional data on intermolecular interactions of **2**–**3** are given in the Supporting Information.

The molecular structure of (2-fluoro-2,2-dinitroethyl)-2,2,2-trinitroethylamine (**2**) is shown in Figure 2. Compound **2** crystallizes in the orthorhombic space group $Pna2_1$ with eight formula units per unit cell and a density of 1.89 g cm^{-1} at 173 K. The average N–O bond lengths of the trinitromethyl and the fluorodinitromethyl moieties are 1.217 Å for the two molecules in the asymmetric unit. For the top molecule, there is a typical propeller-type orientation of the trinitromethyl moiety with C2–C1–N–O torsion angles between 31.0(3) ° and 51.7(3) °. The bottom molecule shows a comparable structure of the trinitromethyl moiety with a contrary sense of rotation [C6–C5–N–O: –55.8(3) ° to –35.5(3) °]. The orientation of the fluorodinitromethyl moieties also indicates a propeller-like structure.[9c] The C–C–N–O torsion angles of these four nitro groups [26.2(3) °/–27.5(3) °/–36.7(3) °/65.9(3) °] are within the typical range for a propeller like structure of

polynitromethyl moieties (23–67 °).[9c] Several weak intermolecular improper hydrogen bonds might be a reason for the quite high density of **2**.

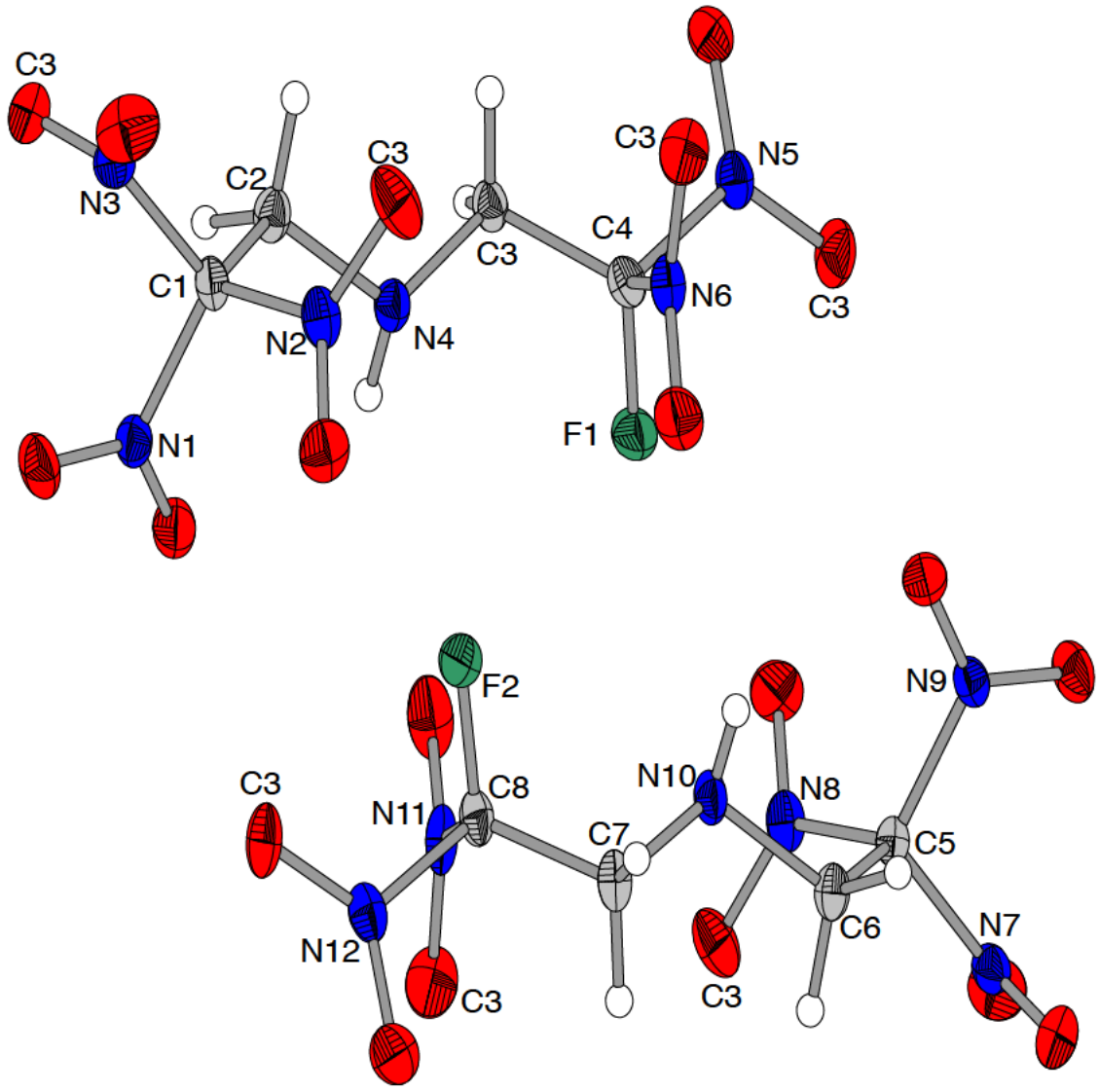

Figure 7.2. Molecular structure of **2**. Thermal ellipsoids are shown at the 50 % probability level. Selected distances [Å] and angles [°]: C1–C2 1.522(3), C2–N4 1.455(3), C3–N4 1 459(3), C3–C4 1.510(3), C4–F1 1.325(2), C1–$(NO_2)_{avg}$ 1.520, C4–$(NO_2)_{avg}$ 1.537, C5–C6 1.523(3), C6–N10 1.460(3), C7–N10 1 454(3), C7–C8 1.506(3), C8–F2 1.328(3), C5–$(NO_2)_{avg}$ 1.518(3), C8–$(NO_2)_{avg}$ 1.536, C2–N4–C3 113.1(2), C3–C4–F1 113.2(2), C6–N10–C7 113.8(2), C7–C8–F2 113.3(2), C2–C1–N1–O1 31.0(3), C2–C1–N2–O4 50.9(2), C2–C1–N3–O6 51.7(3), C3–C4–N5–O7 26.2(3), C3–C4–N6–O9 –64.9(2), C6–C5–N7–O11 –35.5(3), C6–C5–N8–O14 –55.8(2), C6–C5–N9–O15 –36.7(3), C7–C8–N11–O18 65.9(3), C7–C8–N12–O20 –27.5(3).

(2-Fluoro-2,2-dinitroethyl)-2,2,2-trinitroethylnitramine (**3**) also crystallizes in the orthorhombic space group *Pna*2_1 with four formula units in the unit cell (Figure 3). The density at 173 K was calculated with 1.95 g cm^{-1}. The average N–O bond length of the trinitromethyl moiety is 1.209 Å. The trinitromethyl moiety displays a molecular geometry with a propeller-type orientation of the nitro groups connected to C1.[9c] The twisted orientation is energetically favorable and leads to several N···O-dipolar interactions between the geminal NO_2 groups (range of 2.56–2.62 Å), which are considerably shorter than the sum of the van der waals radii for nitrogen and oxygen (ca. 2.9 Å).[9c] The shorter distances are caused by the fact that such twisting of the nitro groups reduces the intramolecular electrostatic repulsion between the oxygen atoms, while at the same time optimizing the attractive N···O interactions between the geminal NO_2 groups.[9c] The average fluorodinitromethyl moiety C1F1$(NO_2)_2$ N–O bond length [1.214(4) Å] is comparable to that of the trinitromethyl group. The C2–C1–N–O torsion angles [–37.6(2) °/38.9(2) °] are also in the typical range (23–67 °) of a propeller-type orientation of the nitro groups attached.[9c] At 1.226(3) Å, the averaged N–O distance of the nitramine moiety is slightly longer than the previously described polynitro groups. This might be caused by some shared π-electron density between the N–N bond and the N–O bonds of the nitramine moiety.[9c] The C3–N3–N4–O dihedral angles (–20.7 °/1.3 °) are in the typical range for cyclic nitramines like hexogen (RDX).[11] The C–F distance with 1.324(3) Å is comparable with a C–F single bond and typical for a fluorodinitromethyl moiety.[12]

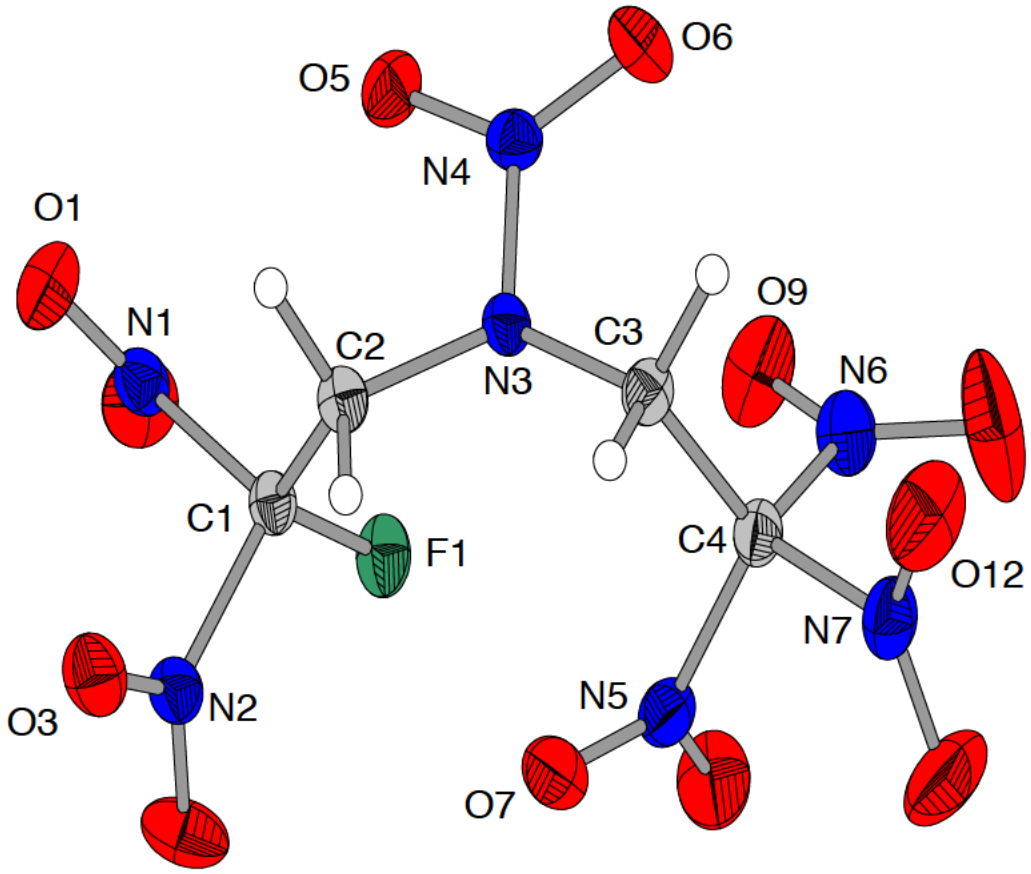

Figure 7.3. Molecular structure of **3**. Thermal ellipsoids are shown at the 50 % probability level. Selected distances [Å] and angles [°]: C1–C2 1.534(2), C1–F1 1.324(2), C1–$(NO_2)_{avg}$ 1.544, C2–N3 1.457(2), N3–N4 1.383(2), N3–C3 1.454(2), C3–C4 1.529(2), C4–$(NO_2)_{avg}$ 1.530, C2–C1–F1 114.3(1), C2–N3–N4 115.3(1), O6–N4–N3 118.2(1), C2–C1–N1–O1 –37.6(2), C2–C1–N2–O3 38.9(4), C2–N3–N4–O5 –20.7(2), C3–N3–N4–O6 1.3(2), C3–C4–N5–O7 –33.8(2), C3–C4–N6–O9 –64.2(2), C3–C4–N7–O12 –26.4(2).

Table 7.2. Crystal and structure refinement data for **2** and **3**

	2	**3**
Empirical formula	$C_4H_5FN_6O_{10}$	$C_4H_4FN_7O_{12}$
Formula mass [g mol^{-1}]	316.12	361.11
Temperature [K]	173(2)	173(2)
Crystal size [mm]	0.40 × 0.18 × 0.03	0.20 × 0.06 × 0.02
Crystal description	colorless platelet	colorless needle
Crystal system	orthorhombic	orthorhombic
Space group	$Pna2_1$	$Pna2_1$
a [Å]	18.5686(10)	16.8034(5)
b [Å]	5.9732(4)	6.1707(2)
c [Å]	20.0793(15)	11.8499(4)
β [°]	90	90
V [Å^3]	2227.1(3)	1228.70(7)
Z	8	4
ρ_{calc} [g cm^{-3}]	1.8856(3)	1.9522(1)
μ [mm^{-1}]	0.195	0.204
F(000)	1280	728
θ range [°]	4.12–30.00	4.21–30.07
index ranges	$-19 \le h \le 26$	$-23 \le h \le 23$
	$-7 \le k \le 8$	$-8 \le k \le 8$
	$-28 \le l \le 27$	$-16 \le l \le 16$
Reflections collected	14438	15575
Reflections observed	6265	3599
Reflections unique	5149	3119
$R1$, $wR2$ (2σ data)	0.0410, 0.0856	0.0346, 0.0719
$R1$, $wR2$ (all data)	0.0576, 0.0952	0.0450, 0.0778
max. / min. transmission	1.00000/0.89677	1.00000/0.93078
Data/restraints/parameters	6265/1/387	3599/0/217
GoF on F^2	1.042	1.030
Largest diff. peak/hole [e Å^{-3}]	0.310/–0.253	0.332/–0.317

Thermal and Energetic Properties

The compounds **2** and **3** are stable when exposed to air and moisture. As indicated earlier, amine **1** decomposes violently within hours as neat compound at ambient temperature. Thermal stabilities for **1**–**3** were investigated with various DSC measurements (heating rate: 5 °C min^{-1}). The melting point of compound **1** was determined roughly at –11 °C. Decomposition starts at 80 °C. The melting points were rising from 37 °C for **2** to 87 °C for **3**. Decomposition becomes significant for compound **2** at 121 °C and 162 °C for **3**. The investigated physical and chemical properties are shown in Table 7.3.

The sensitivities towards impact, friction and electrostatic discharge for **2** and **3** were determined experimentally according to standards of the Federal Institute for Materials Research and Testing (BAM)[13] and the results displayed in Table 7.4. The compounds **2** and **3** showed comparable impact sensitivity values with 6 J for **2** and 5 J for **3**, respectively. The friction sensitivity was determined with 360 N for compound **2**. Nitration to **3** decreased the stability towards friction to 144 N. Amine **1** was omitted from the determination of the sensitivities owing to its instability as neat liquid.

Predictions of the detonation parameters using the EXPLO5 code[14] were performed based on heats of formations calculated ab initio using the Gaussian 09 program package[15] at the CBS-4M level of theory. Energetic parameters are attributed to the density of the corresponding compound at ambient temperature. The resulting heats of detonation (Q_v), detonation temperatures (T), pressures (p) and velocities (D) for **1**–**3** are shown in the Table 7.4. The densities needed for the estimation of the detonation parameters with the EXPLO5 code[14] were derived from experimental determinations *via* pycnometer measurements for **2** and **3**. The calculated detonation velocities of **2** (8719 m s^{-1}) and **3** (8673 m s^{-1}) are in the range of the known value for RDX (8750 m s^{-1}), and therefore both compounds might useful as high-performing oxygen rich energetic materials.[16] The thermal stability rises from 80 °C (compound **1)** through 121 °C (compound **2**) to 162 °C for compound **3**.

The specific impulses of the compounds **1**–**3** were calculated for compositions of 70 % oxidizer, 16 % aluminum, 6 % polybutadiene acrylic acid, 6 % polybutadiene acrylonitrile and 2 % bisphenol-A ether modeled on rocket-motor compositions for solid-rocket boosters used by the NASA Space Shuttle program.[17] These impulses were compared with the calculated impulse of **AP** in an analogous composition. The chosen mixture with **AP** as oxidizer provides a specific impulse of 258 sec. The impulses for **1**–**3** were increasing with increasing oxygen content (249–266 s). Nitramine **3** shows a

superior specific impulse of 266 s relative to an analogous mixture with **AP** as oxidizer. The lesser oxygen balance of the compounds **1–3**, according to **AP**, also leads to a decreased oxygen balance for the calculated formulations that varies between –64.94 % and –46.21 %. A similar composition with **AP** as oxidizer has an oxygen balance of –30.1 %.

Table 7.3. Physical and chemical properties of **1–3**

	1	**2**	**3**
Formula	$C_2H_4FN_3O_4$	$C_4H_5FN_6O_{10}$	$C_4H_4FN_7O_{12}$
Mol mass [g mol^{-1}]	153.07	316.12	361.11
T_m [°C][a]	–11	37	82
T_d [°C][b]	80	121	162
N [%][c]	27.45	26.59	27.15
$N + O$ [%][d]	69.26	77.2	80.32
Ω_{CO} [%][e]	5.2	20.2	28.8
Ω_{CO2} [%][f]	–15.7	0	11.1
ρ [g cm^{-3}][g]	1.80	1.79	1.85
$-\Delta U°_f$ [kJ kg^{-1}][h]	1631.8	821.7	575.9
$-\Delta H°_f$ [kJ mol^{-1}][i]	264.7	287.0	238.8

[a] Melting (T_m) point from DSC measurement carried out at a heating rate of 5 °C min^{-1}. [b] Decomposition (T_d) point from DSC measurement carried out at a heating rate of 5 °C min^{-1}. [c] Nitrogen content. [d] Combined nitrogen and oxygen content. [e] Oxygen balance assuming the formation of CO. The oxygen balance of ammonium perchlorate is 34.0 % [f] Oxygen balance assuming the formation of CO_2. [g] Experimental density from pycnometer measurement. [h] Calculated energy of formation at 298 K. [i] Calculated heat of formation at 298 K.

Table 7.4. Predicted detonation and combustion parameters (using the EXPLO5 code) and sensitivity data for **1–3**

	1	**2**	**3**
$-Q_v$ [kJ kg^{-1}]	5136	5733	5210
T_{ex} [K][a]	3535	4310	4104
V_0 [L kg^{-1}][b]	750	752	748
p [kbar][c]	315	368	354
D [m s^{-1}][d]	8496	8719	8637
Impact [J][e]	n.d.	6	5
Friction [N][e]	n.d.	360	144
ESD [J][f]	n.d.	0.1	0.1
Grain size [µm][g]	liquid	< 100	< 100
Thermal shock[h]	burns	burns	burns
I_s [s][i]	249	257	266
Ω_{comp} [%][j]	–64.94	–53.96	–46.21

[a] Temperature of the explosion gases. [b] Volume of the explosion gases (assuming only gaseous products). [c] Detonation pressure. [d] Detonation velocity. [e] Impact and friction sensitivities according to standard BAM methods.[13] n.d. = not determined. [f] Sensitivity towards electrostatic discharge. n.d. = not determined. [g] Grain size of the samples used for sensitivity tests. [h] Response to fast heating in the "flame test". [i] Specific impulse for compositions with 70 % oxidizer, 16 % aluminum, 6 % polybutadiene acrylic acid, 6 % polybutadiene acrylonitrile and 2 % bisphenol-A ether at 70.0 bar chamber pressure using the EXPLO5 code[14]. The specific impulse for similar composition with ammonium perchlorate ($I_{s\ AP}$ = 258 s, $\Omega_{comp,\ AP}$ = –30.13 %) has been calculated. [j] Oxygen balance for the composition used for combustion calculations.

7.4 CONCLUSION

Two new energetic polynitro compounds containing a fluorodinitromethyl moiety derived from 2-fluoro-2,2-dinitroethylamine (**1**) with a high positive oxygen balance were synthesized and characterized using multinuclear NMR, vibrational spectroscopy, elemental analysis and mass spectrometry and single-crystal X-ray crystallography. The single-crystal X-ray structures revealed a typical propeller like orientation of the trinitromethyl moiety for both the secondary amine **2** and the nitramine **3**. A rather high crystal density for **3** was found with 1.95 g cm^{-3}, which is comparable with hexogen (RDX).[1b] The calculated detonation velocities of **2** (8719 m s^{-1}) and **3** (8673 m s^{-1}) are slightly below the literature known value for RDX (8750 m s^{-1}).[16] The thermal stability rises from 80 °C (compound **1)** through 121 °C (compound **2**) to 162 °C for compound **3**. The sensitivities of **2**–**3** with 6 J for **2** and 5 J for **3** are slightly less than pentaerythritol tetranitrate (PETN), which is a basic requirement for new compounds to be meant as potential high energy dense oxidizers.[1b,3a] Surprisingly, compound **2** turned out to be insensitive towards friction. With respect to a possible application as high-energy dense oxidizer in solid rocket boosters, the specific impulses (I_s) of **1**–**3** were calculated in formulations with fuel, oxidizer & additives. Compound **3** in particular turned out to be a quite promising oxidizer with a superior specific impulse of 266 sec relative to similar formulations with ammonium perchlorate (AP) [I_s(AP) = 258 s] and acceptable sensitivities as a neat compound. Apart from the high specific impulse of **3**, compound **2** showed a comparable value to an AP composite. This promising result makes secondary amine **2** interesting as potential precursor for further reactions in the course of developing new potential high-energy dense oxidizers.

7.5 EXPERIMENTAL SECTION

General Procedures

The syntheses and manipulation of air- and moisture-sensitive materials were performed in an inert atmosphere of dry argon (purity 5.0 Air Liquide) using flame-dried glass vessels and SCHLENK techniques.[18] Commercial available chemicals (all Sigma Aldrich) were used as received. 2,2,2-Trinitroethanol and 2-fluoro-2,2-dinitroethanol were prepared according to literature known procedures.[2b,2c,8a,10c,19]

Raman spectra were recorded with a Bruker FT-Raman MultiRAM Spectrometer equipped with a Klaastech DENICAFC LC-3/40 laser source at 300mW laser power; infrared spectra were measured with a Perkin–Elmer Spectrum BX-FTIR spectrometer equipped with a Smiths DuraSamplIR II ATR device. All spectra were recorded at ambient temperature as neat samples. Densities were determined at ambient temperature using a Quantachrome Ultrapyc1200e gas pycnometer equipped with helium (5.6 Air Liquide). NMR spectra were recorded with a JEOL Eclipse 400 instrument and chemical shifts were determined with respect to external Me_4Si (^1H, 399.8 MHz; ^{13}C, 100.5 MHz), $MeNO_2$ (^{15}N, 40.6 MHz) and CCl_3F (376.5 MHz). Mass spectrometric data were obtained with a JEOL MStation JMS 700 spectrometer (DEI+/DCI+). Analyses of C/H/N were performed with an Elementar Vario EL Analyzer. Melting points were measured with a Perkin-Elmer Pyris6 DSC using a heating rate of 5 °C min^{-1} and checked by a Büchi Melting Point B-540 apparatus; they are not corrected. The sensitivity data were performed using a BAM drophammer and a BAM friction tester.[13]

Computational Details

All ab initio calculations were carried out using the Gaussian 09 (Revision B.03) program package[15b] and visualized by GaussView 5.08.[15a] Structure optimizations and frequency analyses were performed with Becke's B3 three parameter hybrid functional using the LYP correlation functional (B3LYP). For C, H, N and O a correlation consistent polarized double-zeta basis set was used (cc-pVDZ). The structures were optimized without symmetry constraints and the energy is corrected with the zero point vibrational energy.[20]

The enthalpies (H°) and free energies (G°) were calculated and finally corrected to a temperature of 298 K using the complete basis set method (CBS-4M) on the basis of ab

initio optimized structures or X-ray diffraction data to obtain accurate values.[20a] The CBS models use the known asymptotic convergence of a pair of natural orbital expressions to extrapolate from calculations using a finite basis set to the estimated complete basis set limit. CBS-4 starts with a HF/3-21G(d) structure optimization, which is the initial guess for the following self-consistent field (SCF) calculation as a base energy and a final MP2/6-31+G calculation with a CBS extrapolation to correct the energy in second order. The used reparametrized CBS-4M method additionally implements a MP4(SDQ)/6-31+(d,p) calculation to approximate higher order contributions and also includes some additional empirical corrections.[20b,20c] The enthalpies of the gas-phase species were estimated according to the atomization energy method.[20a,21]

All calculations affecting the detonation parameters were carried out using the program package EXPLO5 V6.01.[14,22] The detonation parameters were calculated at the CJ point with the aid of the steady-state detonation model using a modified Becker-Kistiakowski-Wilson equation of state for modeling the system. The CJ point is found from the Hugoniot curve of the system by its first derivative.[22-23] The main detonation products for the calculations of the energetic parameters were assumed with N_2, H_2O, CO_2 and HF for a CHFNO-compound. In addition, compounds with a positive oxygen balance provide O_2 as combustion product. The specific impulses were also calculated with the EXPLO5 program, assuming an isobaric combustion of a composition of 70 % oxidizer, 16 % aluminum as fuel, 6 % polybutadiene acrylic acid, 6 % polybutadiene acrylonitrile as binder and 2 % bisphenol-A as epoxy curing agent.[17] A chamber pressure of 70.0 bar and an ambient pressure of 1.0 bar with frozen expansion conditions were estimated for the calculations.

X-ray Crystallography

For all compounds, an Oxford Xcalibur3 diffractometer with a CCD area detector was employed for data collection using Mo-K_α radiation (λ = 0.71073 Å). The structures were solved by direct methods (SIR97)[24] and refined by full-matrix least-squares on F^2 (SHELXL).[25] All non-hydrogen atoms were refined anisotropically. The hydrogen atoms were located in a difference Fourier map and placed with a C–H distance of 0.99 Å for CH_2 groups. ORTEP plots are shown with thermal ellipsoids at the 50 % probability level.

CCDC-946430 (for **2**) and CCDC-946431 (for **3**) contains the supplementary crystallographic data for this paper. These data can be obtained free of charge from the Cambridge Crystallographic Data Centre *via* www.ccdc.cam.ac.uk/data_request/cif.

Synthesis

CAUTION! All high-nitrogen- and -oxygen-containing compounds are potentially explosive energetic materials. In particular, 2-fluoro-2,2-dinitroethylamine (**1**) was proven to be a dangerous unstable material, when handled as neat compound. Especially with this compound, this necessitates additional meticulous safety precautions (earthed equipment, Kevlar gloves, Kevlar sleeves, face shield, leather coat, and ear plugs). In addition, 2,2,2-trinitroethanol and 2-fluoro-2,2-dinitroethylamine show significant degrees of toxicity,[26] including own recent results.[27] Particular care should be exercised in handling of those materials and derivatives.

*2-Fluoro-2,2-dinitroethylamine (**1**)*

Prepared according to the literature.[8a,28].

DSC: T_m = approx. –11 °C, T_{dec} = 80 °C. ^{1}H NMR ($CDCl_3$): δ = 3.92 [d, 2 H, CH_2CF$(NO_2)_2$, $^3J_{H,F}$ = 17.6 Hz], 1.49 (s, br, 2 H, NH_2) ppm. ^{13}C{^{1}H} NMR ($CDCl_3$): δ = 123.0 [d, *C*F$(NO_2)_2$, $^1J_{C,F}$ = 287.5 Hz], 44.5 [d, *C*H$_2$CF$(NO_2)_3$, $^2J_{C,F}$ = 19.6 Hz] ppm. ^{15}N{^{1}H} NMR ($CDCl_3$): δ = –20.77 [d, CF(*N*O$_2)_2$, $^2J_{N,F}$ = 15.0 Hz], –377.20 (s, *N*H$_2$) ppm. ^{19}F NMR ($CDCl_3$): δ = –111.1 [br. s, C*F*$(NO_2)_2$] ppm. IR ν = 3428 (w), 3364 (w), 2916 (w), 1581 (vs), 1434 (w), 1318 (m), 1281 (m), 1193 (w), 1088 (w), 1052 (w), 990 (w), 849 (w), 786 (m), 686 (w) cm^{-1}. Raman (300 mW) ν = 3361 (9), 3003 (15), 2942 (33), 2860 (4), 2202 (3), 1588 (18), 1436 (13), 1310 (18), 1190 (4), 978 (5), 852 (100), 564 (7), 504 (7), 418 (18), 381 (56), 320 (7), 282 (8) cm^{-1}. MS (DEI$^+$): m/z (%) = 154 (1) [M + H]$^+$, 106 (1) [M + H – NO$_2$]$^+$, 61 (1) [M$^+$ – 2NO$_2$]. $C_2H_4FN_3O_4$ (153.07): C 15.69, H 2.63, N 27.45; found: C 15.82, H 2.59, N 227.35

*2-Fluoro-2,2-dinitroethyl 2,2,2-trinitroethylamine (**2**)*

2,2,2-Trinitroethanol (0.59 g, 3.2 mmol) and 2-fluoro-2,2-dinitroethylamine (0.50 g, 3.2 mmol) were diluted in chloroform (10 mL) under argon. Molecular sieves (4 Å, 0.5 g) was added and the reaction mixture was stirred at ambient temperature for 24 h. The reaction mixture was filtered, and the volatile materials were removed under vacuum

yielding **2** as slightly orange colored oil. The crude product was recrystallized in chloroform giving colorless crystals of **2** (0.81 g, 78 %).

DSC: T_m = 37 °C, T_{dec} = 121 °C. ^{1}H NMR ($CDCl_3$): δ = 4.31 [d, 2 H, CH_2C$(NO_2)_3$, $^3J_{H,H}$ = 7.8 Hz], 4.10 [dd, 2 H, CH_2CF$(NO_2)_2$, $^3J_{H,H}$ = 7.3 Hz, $^3J_{H-F}$ = 16.6 Hz], 2.55 [qi, 1 H, N*H*] ppm. ^{13}C{^{1}H} NMR ($CDCl_3$): δ = 126.2 [br., *C*$(NO_2)_3$], 121.3 [d, *C*F$(NO_2)_2$, $^1J_{C,F}$ = 288.3 Hz], 52.5 [*C*H_2C$(NO_2)_3$], 50.8 [d, CH_2CF$(NO_2)_3$, $^2J_{C,F}$ = 19.2 Hz] ppm. ^{15}N NMR ($CDCl_3$): δ = –22.9 [dm, CF*N*$O_2)_2$, $^2J_{N,F}$ = 14.9 Hz], –32.3 [t, C$(NO_2)_3$, $^3J_{N,H}$ = 2.0 Hz], –373.0 (d, *N*H, $^1J_{N-,H}$ = 83.0 Hz) ppm ^{19}F NMR ($CDCl_3$): δ = –109.6 [br. t, C*F*$(NO_2)_2$, $^3J_{F,H}$ = 15.6 Hz] ppm. IR ν = 3368 (w), 2933 (w), 2895 (w), 1579 (vs), 1479 (m), 1443 (m), 1403 (w), 1371 (w), 1358 (w), 1338 (w), 1305 (s), 1243 (m), 1154 (m), 1138 (m), 1063 (w), 999 (w), 981 (w), 879 (w), 857 (w), 850 (m), 799 (m), 780 (m), 757 (m), 725 (m), 667 (w) cm^{-1}. Raman (300 mW) ν = 3368 (4), 3024 (10), 3012 (11), 2983 (16), 2937 (74), 2886 (6), 1612 (23), 1601 (22), 1585 (18), 1483 (4), 1447 (18), 1405 (12), 1373 (20), 1359 (53), 1311 (30), 1247 (12), 1148 (11), 1037 (10), 995 (7), 911 (11), 881 (9), 859 (100), 851 (27), 809 (4), 783 (5), 763 (7), 668 (5), 642 (9), 576 (9), 523 (15), 471 (8), 440 (20), 421 (48), 399 (49), 381 (65), 368 (47), 330 (26), 281 (20), 263 (35), 210 (36) cm^{-1}. MS (DEI$^+$): m/z (%) = 316.1 (1) [M^+], 269 (1) [M^+ – HNO_2], 224 (1) [$M^+ - 2NO_2$], 193 (29) [$NHCH_2C(NO_2)_3]^+$, 166 (29) [$NHCH_2CF(NO_2)_2]^+$, 115 [$C_4H_4FN_2O]^+$, 147 (29) [$NHCH_2C(NO_2)_2]^+$, 85 [$C_4H_4FN]^+$, 46 (100) [$NO_2]^+$, 30 (100) [$NO]^+$. $C_4H_5FN_6O_{10}$ (316.12): calcd. C 15.20, H 1.59, N 26.59; found: C 15.50, H 1.61, N 26.29. Impact sensitvity: 6 J; friction sensitvity: 360 N; ESD: 0.1 J; grain size: < 100 µm.

*2-Fluoro-2,2-dinitroethyl 2,2,2-trinitroethylnitramine (**3**)*

Compound **2** (0,68 g, 2.2 mmol) was added slowly into a mixture consisting of sulfuric acid (96 %, 4 mL) and nitric acid (100 %, 2 mL) at 0 °C. The reaction mixture was stirred at ambient temperature for 4 h and poured onto a large excess of ice (200 g). The colorless precipitate was filtered, washed with water and dried in vacuo to obtain a colorless powder of **3** (0.59 g, 76 %). Alternatively, crude **2** (yellow oil) is sufficient and can be used for the nitration without loss of product.

DSC: T_m = 85 °C, T_{dec} = 165 °C. ^{1}H NMR ([D$_6$]acetone): δ = 6.14 [s, 2 H, CH_2C$(NO_2)_3$], 5.80 [d, 2 H, CH_2CF$(NO_2)_2$, $^3J_{H,F}$ = 9.5 Hz] ppm. ^{13}C{^{1}H} NMR ([D$_6$]acetone): δ = 124.2 [s, *C*$(NO_2)_3$], 118.6 [d, *C*F$(NO_2)_2$, $^1J_{C,F}$ = 294.0 Hz], 55.2 [s, *C*H_2C$(NO_2)_3$], 55.0 [d, *C*H_2CF$(NO_2)_3$, $^2J_{C,F}$ = 16.1 Hz] ppm. ^{15}N NMR ([D$_6$]acetone): δ = –22.5 [dt, CF$(NO_2)_2$,

$^{2}J_{N,F}$ = 15.2 Hz, $^{3}J_{N,H}$ = 1.7 Hz], –33.4 [q, N*N*O_2, $^{3}J_{N,H}$ = 3.2 Hz], –33.7 [t, C$(NO_2)_3$, $^{3}J_{N,H}$ = 2.0 Hz], –217.2 (s, *N*NO_2) ppm. ^{19}F NMR ([D_6]acetone): δ = –107.1 [t, C*F*$(NO_2)_2$, $^{3}J_{F–H}$ = 9.1 Hz] ppm. IR ν = 3371 (vw), 2965 (vw), 2926 (vw), 1707 (w), 1591 (vs), 1492 (vw), 1465 (w), 1444 (vw), 1359 (w), 1316 (s), 1270 (w), 1229 (w), 1182 (vw), 1052 (vs), 949 (vw), 905 (w), 849 (m), 800 (s), 763 (w), 737 (m), 701 (vw), 686 (w) cm^{-1}. Raman (300 mW) ν = 3024 (24), 2978 (53), 1614 (24), 1589 (10), 1566 (5), 1439 (5), 1407 (6), 1391 (14), 1358 (50), 1340 (15), 1300 (16), 1271 (44), 1228 (3), 1128 (3), 1058 (4), 1002 (2), 978 (11), 878 (3), 868 (15), 854 (102), 804 (2), 784 (5), 755 (2), 723 (4), 626 (10), 545 (12), 442 (8), 425 (18), 402 (31), 388 (17), 369 (11), 341 (9), 324 (49), 247 (14), 221 (11), 209 (6) cm^{-1}. MS (DEI$^+$): m/z (%) = 361 (1) [M^+], 269 (1) [$M^+ – 2\ NO_2$], 211 (1) [$M^+ – C(NO_2)_3$], 118 (29) $[CH_2C(NO_2)_2]^+$, 46 (100) $[NO_2]^+$. $C_4H_4FN_7O_{12}$ (361.11): calcd. C 13.30, H 1.12, N 27.15; found: C 13.40, H 1.20, N 26.3. Impact sensitivity: 5 J; friction sensitivity: 192 N; ESD: 0.1 J; grain size: < 100 µm.

7.6 ACKNOWLEDGEMENT

Financial support of this work by the Ludwig-Maximilian University of Munich (LMU), the U.S. Army Research Laboratory (ARL) under grant no. W911NF-09-2-0018, the Armament Research, Development and Engineering Center (ARDEC), and the Office of Naval Research (ONR) under grant nos. ONR.N00014-10-1-0535 and ONR.N00014-12-1-0538 is gratefully acknowledged. The authors acknowledge collaborations with Dr. Mila Krupka (OZM Research, Czech Republic) in the development of new testing and evaluation methods for energetic materials and with Dr. Muhamed Sucesca (Brodarski Institute, Croatia) in the development of new computational codes to predict the detonation and propulsion parameters of novel explosives. We are indebted to and thank Drs. Betsy M. Rice and Brad Forch (ARL, Aberdeen, Proving Ground, MD).

7.7 REFERENCES

[1] a) T. M. Klapötke, S. F. Rest, *New Trends Res. Energ. Mater. Proc. Semin*., 13th **2010**, Pt. 2, 642–651; b) J. P. Agrawal, *High Energy Materials Propellants, Explosives and Pyrotechnics*, 1st ed., Wiley-VCH, Weinheim, Germany, **2010**.

[2] a) M. E. Hill, US3306939, **1967**; b) M. Göbel, T. M. Klapötke, *Adv. Funct. Mater.* **2009**, *19*, 347–365; c) T. M. Klapötke, B. Krumm, R. Moll, *Chem. Eur. J.* **2013**, *19*, 12113–12123; d) T. M. Klapötke, B. Krumm, R. Moll, S. F. Rest, *Spectroscopic and structural studies of nitro substituted fluoro-methanes and ethanes*, 20th International Symposium on Fluorine Chemistry (ISFC), Kyoto, Japan, **2012**; e) T. M. Klapötke, B. Krumm, R. Moll, S. F. Rest, W. Schnick, M. Seibald, *J. Fluorine Chem.* **2013**, DOI: 10.1016/j.jfluchem.2013.06.019.

[3] a) T. M. Klapötke, *Chemistry of High-Energy Materials*, 2nd Ed., de Gruyter, Berlin, **2012**; b) T. M. Klapötke, B. Krumm, R. Moll, S. F. Rest, *Z. Anorg. Allg. Chem.* **2011**, *637*, 2103–2110.

[4] J. Hine, J. W. Bailey, *J. Org. Chem.* **1961**, *26*, 2098–2099.

[5] T. N. Hall, *Tetrahedron* **1963**, *19*, 115–120.

[6] H. G. Adolph, *J. Org. Chem.* **1975**, *40*, 2626-2630.

[7] a) C. K. Ingold, *J. Chem. Soc. (Resumed)* **1930**, 1032-1039; b) L. A. Kaplan, H. B. Pickard, *J. Org. Chem.* **1970**, *35*, 2044-2045.

[8] a) H. G. Adolph, M. J. Kamlet, *J. Org. Chem.* **1969**, *34*, 45–50; b) L. V. Kustova, Y. I. Rubtsov, E. P. Kirpichev, L. T. Eremenko, R. G. Gafurov, A. G. Korepin, *Zh. Fiz. Khim.* **1976**, *50*, 1903–1904.

[9] a) A. B. Sheremetev, I. L. Yudin, *Mendeleev Commun*. **2005**, *15*, 204–205; b) G. Socrates, *Infrared and Raman Characteristic Group Frequencies: Tables and Charts*, 3rd ed., Wiley, Chichester, UK, **2004**; c) Y. Oyumi, T. B. Brill, A. L. Rheingold, *J. Phys. Chem.* **1985**, *89*, 4824–4828.

[10] a) M. Göbel, B. H. Tchitchanov, J. S. Murray, P. Politzer, T. M. Klapötke, *Nat. Chem.* **2009**, *1*, 229–235; b) M. Göbel, T. M. Klapötke, *Z. Anorg. Allg. Chem.* **2007**, *633*, 1006–1017; c) M. Göbel, T. M. Klapötke, *Acta Crystallogr. Sect. C* **2007**, *63*, o562–o564; d) M. Göbel, T. M. Klapötke, P. Mayer, *Z. Anorg. Allg. Chem.* **2006**, *632*, 1043–1050; e) S. K. Bhattacharjee, H. L. Ammon, *Acta Crystallogr. Sect. B* **1982**, *38*, 2503–2505.

[11] a) D. I. A. Millar, I. D. H. Oswald, C. Barry, D. J. Francis, W. G. Marshall, C. R. Pulham, A. S. Cumming, *Chem. Commun.* **2010**, *46*, 5662-5664; b) C. S. Choi, *Acta Crystallogr. Sect. B* **1972**, *28*, 2857–2862.

[12] a) H. L. Ammon, S. K. Bhattacharjee, *Acta Crystallogr. Sect. B* **1982**, *38*, 2718–2721; b) H. L. Ammon, S. K. Bhattacharjee, S. R. Hall, B. Skelton, *Acta Crystallogr. Sect. C* **1983**, *39*, 1565–1568; c) H. L. Ammon, S. K. Bhattacharjee, *Acta Crystallogr. Sect. C* **1984**, *40*, 487–490.

[13] Laying down test methods pursuant to Regulation (EC) No 1907/2006 of the European Parliament and of the Council on the Evaluation, Authorisation and Restriction of Chemicals (REACH), ABl. L 142, **2008**.

[14] M. Sućeska, *EXPLO5 V6.01*, Brodarski Institute, Zagreb, Croatia, **2012**.

[15] a) R. Dennington, T. Keith, J. Millam, GaussView, Version 5, Semichem Inc., Shawnee Mission KS, **2009**; b) M. J. Frisch, G. W. Trucks, H. B. Schlegel, G. E. Scuseria, M. A. Robb, J. R. Cheeseman, J. A. Montgomery Jr., T. Vreven, K. N. Kudin, J. C. Burant, J. M. Millam, S. S. Iyengar, J. Tomasi, V. Barone, B. Mennucci, M. Cossi, G. Scalmani, N. Rega, G. A. Petersson, H. Nakatsuji, M. Hada, M. Ehara, K. Toyota, R. Fukuda, J. Hasegawa, M. Ishida, T. Nakajima, Y. Honda, O. Kitao, H. Nakai, M. Klene, X. Li, J. E. Knox, H. P. Hratchian, J. B. Cross, V. Bakken, C. Adamo, J. Jaramillo, R. Gomperts, R. E. Stratmann, O. Yazyev, A. J. Austin, R. Cammi, C. Pomelli, J. W. Ochterski, P. Y. Ayala, K. Morokuma, G. A. Voth, P. Salvador, J. J. Dannenberg, V. G. Zakrzewski, S. Dapprich, A. D. Daniels, M. C. Strain, O. Farkas, D. K. Malick, A. D. Rabuck, K. Raghavachari, J. B. Foresman, J. V. Ortiz, Q. Cui, A. G. Baboul, S. Clifford, J. Cioslowski, B. B. Stefanov, G. Liu, A. Liashenko, P. Piskorz, I. Komaromi, R. L. Martin, D. J. Fox, T. Keith, M. A. Al-Laham, C. Y. Peng, A. Nanayakkara, M. Challacombe, P. M. W. Gill, B. Johnson, W. Chen, M. W. Wong, C. Gonzalez, J. A. Pople, *Gaussian 09*, Rev. B.03, Gaussian, Inc., Wallingford CT, **2003**.

[16] P. W. Cooper, *Explosives Engineering*, 1st ed., Wiley-VCH, New York, **1996**.

[17] a) NASA, Space Shuttle News Reference, 2–20–22–21, http://de.scribd.com/doc/17005716/NASA-Space-Shuttle-News-Reference-1981; b) NASA, press release: STS-122 The Voyage of Columbus, 2008, 82–84, http://www.nasa.gov/pdf/203212main_sts122_presskit2.pdf.

[18] D. F. Shriver, M. A. Drezdzon, *The Manipulation of Air-Sensitive Compounds*, 2nd ed., Wiley, New York, **1986**.

[19] a) H. Feuer, T. Kucera, *J. Org. Chem.* **1960**, *25*, 2069–2070; b) V. Grakauskas, A. M. Guest, *J. Org. Chem.* **1978**, *43*, 3485–3488; c) H. Adolph, *J. Org. Chem.* **1972**, *37*, 747–751; d) N. S. Marans, R. P. Zelinski, *J. Am. Chem. Soc.* **1950**, *72*, 5329–5330.

[20] a) T. M. Klapötke, J. Stierstorfer, Phys. *Chem. Chem. Phys.* **2008**, *10*, 4340–4346; b) J. J. A. Montgomery, M. J. Frisch, J. W. Ochterski, G. A. Petersson, *J. Chem. Phys.* **2000**, *112*, 6532–6542; c) J. W. Ochterski, G. A. Petersson, J. J. A. Montgomery, *J. Chem. Phys.* **1996**, *104*, 2598–2619.

[21] a) E. F. C. Byrd, B. M. Rice, *J. Phys. Chem. A* **2005**, *110*, 1005–1013; b) B. M. Rice, S. V. Pai, J. Hare, *Combust. Flame* **1999**, *118*, 445–458; c) L. A. Curtiss, K. Raghavachari, P. C. Redfern, J. A. Pople, *J. Chem. Phys.* **1997**, *106*, 1063–1079.

[22] M. Sućeska, *Propellants, Explos. Pyrotech.* **1991**, *16*, 197–202.

[23] T. M. Klapötke, B. Krumm, F. X. Steemann, K. D. Umland, *Z. Anorg. Allg. Chem.* **2010**, *636*, 2343–2346.

[24] a) A. Altomare, M. C. Burla, M. Camalli, G. L. Cascarano, C. Giacovazzo, A. Guagliardi, A. G. G. Moliterni, G. Polidori, R. Spagna, *J. Appl. Crystallogr.* **1999**, *32*, 115–119; b) A. Altomare, G. Cascarano, C. Giacovazzo, A. Guagliardi, A. G. G. Moliterni, M. C. Burla, G. Polidori, M. Camalli, R. Spagna, *SIR97*, **1997**.

[25] a) A. L. Spek, *Acta Crystallogr. Sect. D* **2009**, *65*, 148–155; b) G. M. Sheldrick, *Acta Crystallogr. Sect. A 2008*, *64*, 112–122; c) L. J. Farrugia, *J. Appl. Crystallogr.* **1999**, *32*, 837–838; d) G. M. Sheldrick, *SHELX-97*, University of Göttingen, Göttingen (Germany), **1997**.

[26] a) A. L. Fridman, O. B. Kremleva, V. S. Zalesov, Z. V. Platonova, F. A. Gabitov, L. A. Rubinshtein, A. N. Plaksina, *Pharm. Chem. J.* **1977**, *11*, 64–67; b) M. B. Frankel, G. L.; Grant, L. R.; Kistner, R. L.; Lecce, J. V.; Wilson, E. R.; Woolery, D. O. I., *Process studies on nitroform and related compounds*, Final report for period January 30, **1984** – March 31, **1987**, UCRL-15908, Rockwell International Corp., Rocketdyne Division, Canoga Park, CA (USA), **1987**, 1–66.

[27] R. Scharf, T. M. Klapötke, Private communication, LMU Munich September **2012**.

[28] M. B. Frankel, G. L. Rowley, US3544630A, **1970**.

8. SUMMARY

Various polynitro containing molecules were synthesized, characterized and investigated during the progress of this work aiming a positive oxygen balance of the target molecules. Therefore, the synthesized materials belong to the class of *high energy dense oxidizers* (HEDO). In addition, the accumulated intermediate compounds were also fully characterized and the energetic purposes were investigated. The most promising compounds from chapter 2–7 of this dissertation are shown in Figure 8.1 and selected properties are summarized in Table 8.1.

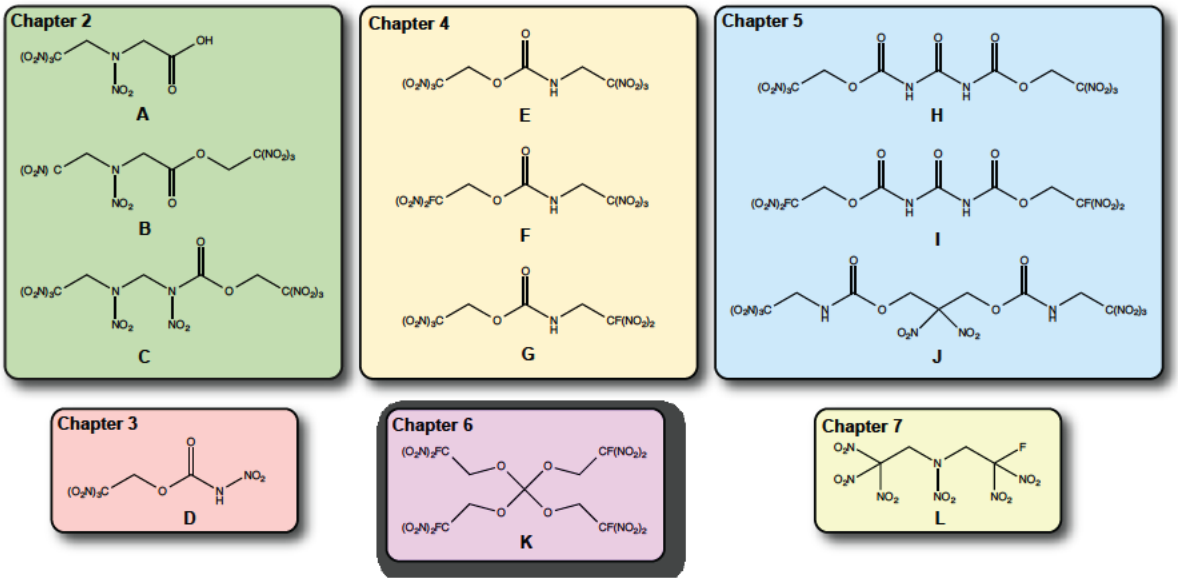

Figure 8.1. Abridgement of the most promising compounds of chapter 2–7.

Table 8.1. Properties of the most promising compounds of chapter 2–7

	A	**B**	**C**	**D**	**E**	**F**	**G**	**H**	**I**	**J**	**K**	**L**
formula	$C_4H_5N_5O_{10}$	$C_6H_6N_8O_{16}$	$C_6H_6N_{10}O_{18}$	$C_3H_3N_5O_{10}$	$C_5H_5N_7O_{14}$	$C_5H_5FN_6O_{12}$	$C_5H_5FN_6O_{12}$	$C_7H_6N_8O_{17}$	$C_7H_6F_2N_6O_{13}$	$C_9H_{10}N_{10}O_{20}$	$C_9H_8F_4N_8O_{20}$	$C_4H_4FN_7O_{12}$
T_d / C [a]	167	183	161	153	186	191	191	169	211	169	193 (boiling)	162
Ω_{CO} /% [b]	19.8	25.1	28.5	+32.7	+26.9	+22.2	+22.2	+23.6	+15.2	+16.6	23.1	28.8
Ω_{CO2} /% [c]	–2.83	3.59	9.48	+14.87	+6.2	0.0	0.0	0	–11.4	–8.3	0	11.1
ρ /g cm^{-3} [d]	1.82	1.87	1.90	1.73	1.90	1.83	1.86	1.90	1.88	1.83	1.84	1.95
D /m s^{-1} [e]	8351	8518	8491	7541	8661	8517	8553	8363	7620	8050	8440	8637
impact /J [ ]	15	3	2	10	4	3	3	7	10	3	9	5
friction /N [f]	144	64	120	96	96	360	360	288	240	160	192	144
ESD /J [g]	0.036	0.25	0.035	0.10	0.4	0.4	0.4	0.1	0.18	--	0.25	0.1
gr. size /µm [h]	100–500	<100	<100	500-1000	100–500	<100	<100	<100	<100	100–500	100–250	< 100
I_s /sec [i]	250	258	262	257	257	248	249	249	230	223	246	266

a) Decomposition (T_d) point from DSC measurement carried out at a heating rate of 5 °C min^{-1}. b) Oxygen balance assuming the formation of CO. The oxygen balance of ammonium perchlorate is 34.0% c) Oxygen balance assuming the formation of CO_2. d) Experimental density from pycnometer measurement. e) Detonation velocity. f) Impact and friction sensitivities according to standard BAM methods. g) Sensitivity towards electrostatic discharge. h) Grain size of the samples used for sensitivity tests. i) Specific impulse for compositions with 70% oxidizer, 16% aluminum, 6% polybutadiene acrylic acid, 6% polybutadiene acrylonitrile and 2% bisphenol-A ether at 70.0 bar chamber pressure using the EXPLO5 code.

The readily available simple amino acid glycine, accompanied with 2,2,2-trinitroethanol, was the starting material for an interesting reaction cascade including eight intermediates and three new potential high energy dense oxidizers, described in chapter 2. Compound **A** turned out to be an interesting precursor for the development of new potential high energy dense materials. The synthesis is simple, and low sensitivities make manipulation and handling less dangerous. At the end of the reaction cascade described in chapter 2, the potential material 2,2,2-trinitroethyl 2-(nitro-(2,2,2-trinitroethyl)amino)acetate2,2,2-Trinitroethyl 2-(nitro-(2,2,2-trinitroethyl)amino)acetate (**B**) was prepared. The compound showed a thermal stability above 180 °C, moderate sensitivities towards mechanical stimuli and a satisfying oxygen balance $\Omega(\mathbf{B})_{CO}$ = 25.1 %. Furthermore starting from A, in another reaction pathway including a CURTIUS rearrangement, the resulting 2,2,2-trinitroethyl (nitro-(2,2,2-trinitroethyl)amino)methyl nitrocarbamate (**C**) showed an improved oxygen balance of 28.5 % (calculated to CO) compared with **B**.

In chapter 3, the synthesis and the characterization of 2,2,2-trinitroethyl-N-nitrocarbamate (**D**) is presented in addition with a new synthesis route of the precursor 2,2,2-trinitroethyl chloroformate. Compound **D** shows an oxygen balance with $\Omega(\mathbf{D})_{CO}$ = 32.7 % really close to ammonium perchlorate (**AP**) $\Omega(\mathbf{AP})$ = 34.0 %. Along with the oxygen balance, the moderate sensitivities make the compound a quite promising candidate for future use as high energy dense oxidizer.

Furthermore, the carbamate as well as the carbonate group as a quite stable conjunction for polynitro containing moieties was investigated in chapter 4. Several carbamates/carbonates containing a 2,2,2-trinitroethyl and/or a 2-fluoro-2,2-dinitroethyl group were prepared and characterized successfully (**E**–**G**). All of the compounds presented in this part, turned out to be temperature stable above 180 °C in addition with impact sensitivities around 3–4 J.

Knowing the improved thermal stability of a carbamate conjunction, chapter 5 investigates with the reactions of the very reactive starting material carbonyl isocyanate with 2,2,2-trinitroethanol or 2-fluoro-2,2-dinitroethanol, yielding the corresponding carbonyl-biscarbamates (**H**–**I**). The resulting materials show improved sensitivities in addition with thermal stabilities comparable with the final products showed in chapter 3. Furthermore, the polynitro compounds 2,2-dinitropropane-1,3-diyl bis(2,2,2-

trinitroethylcarbamate) (**J**) and 2,2-dinitropropane-1,3-diyl bis(2,2,2-trinitroethyl) dicarbonate, derived form 2,2-dinitropropane-1,3-diol were investigated for future applications as HEDO.

After introducing the 2-fluoro-2,2-dinitroethyl moiety (compare chapter 4 and 5), tetrakis(2-fluoro-2,2-dinitroethyl) orthocarbonate (**K**) as well as tris(2-fluoro-2,2-dinitroethyl) orhoformate were synthesized and characterized in chapter 6. The compound **K** turned out to be as powerful as **PETN** and less sensitive. Compared with tetrakis(2,2,2-tinitroethyl) orthocarbonate, a phase transition in the range of –22 °C was also observed during the investigation of the compound.

During our investigations, the starting material 2-fluoro-2,2-dintroethylamine was used for the Mannich type of reaction with 2,2,2-trinitroethanol yielding the secondary amine 2,2,2-trinitroethyl-2-fluoro-2,2-dintroethylamine. Further nitration leads to the corresponding nitramine 2,2,2-trinitroethyl-2-fluoro-2,2-dintroethylnitramine (**L)** with an oxygen balance of 28.8 % (assuming CO as decomposition product). The compound showed interesting energetic properties and turned out to be more powerful than **PETN**. The whole work is described in chapter 7.

9. APPENDIX

9.1 SUPPORTING INFORMATION FOR MULTIPLY NITRATED HIGH-ENERGY DENSE OXIDIZERS DERIVED FROM THE SIMPLE AMINO ACID GLYCINE

A strong classical intermolecular hydrogen bond with covalent character occurs at the carboxylic group with the following distances and angles: O1–H5···O2 (1.836(1) Å), O1···O2 2.688(1) Å and O1–H5···O2 176(2)°. This leads to a dimer structure of **3** (Figure 9.1).

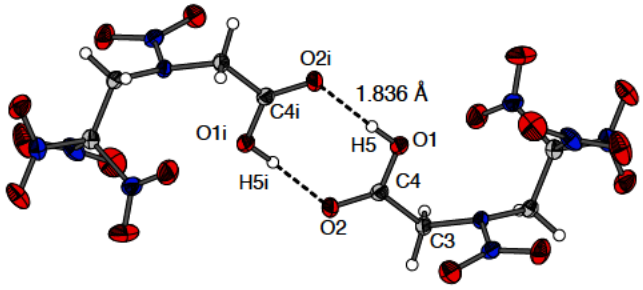

Figure 9.1. Dimer of **3** with strong hydrogen bonds. Symmetry: i = 2–x; –y; 2–z.

The disordered strucutre of ethyl 2-(nitro-((2,2,2-trinitroethoxy)carbonyl)amino) acetate (**10**) is shown in Figure 9.2. The disorder of the trinitromethyl moiety is displayed in the supplementary information. Such disorders of the crystal structure are not uncommon for compounds containing a trinitromethyl moiety. Nevertheless, both conformations A and B show the typical propeller type arrangement of the trinitromethyl moiety, with averaged C6–C7–N(A/B)–O(A/B) torsion angles of 38.1(4)° for A and –38.3(4)° for B.

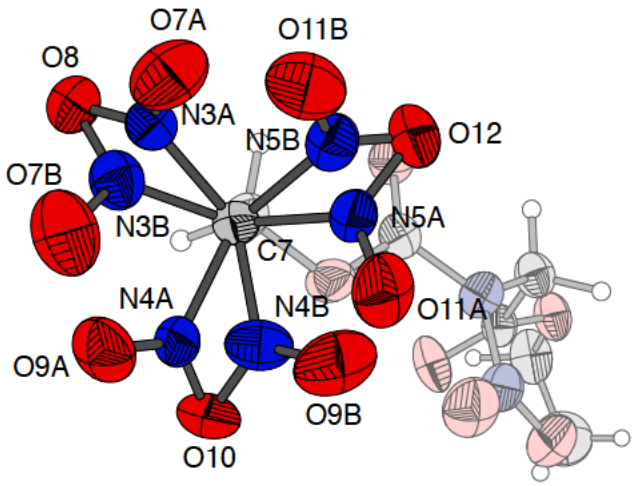

Figure 9.2. Disordered trinitromethyl moiety of **10**. Selected distances [Å] and angles [°]:C7–$(NO_2)A_{av}$ 1.545(4), C7–$(NO_2)B_{av}$ 1.507(4), N3A–C7–N3B 28.1(2), N4A–C7–N4B 34.8(2), N5A–C7–N5B 32.6(2), N4A–O8–N4B 44.8(3), N5A–O10–N5B 40.7(4), N3A–O12–N3B 35.3(3), C6–C7–N4A–O10 39.6(3), C6–C7–N4B–O10 –45.6(3), C6–C7–N5A–O12 40.9(3), C6–C7–N5B–O12 –36.6(4), C6–C7–N3A–O8 33.7(4), C6–C7–N3B–O8 –32.8(4).

9.2 SUPPORTING INFORMATION FOR ASYMMETRIC FLUORODINITROMETHYL DERIVATIVES OF 2,2,2-TRINITROETHYL N-(2,2,2-TRINITROETHYL) CARBAMATE

Selected weak improper hydrogen bonds for compounds **1**–**5.**

The hydrogen atoms were located in a difference Fourier map and placed with a C–H distance of 0.99 Å for CH_2 groups and a N–H distance of 0.88 Å for NH groups.

Table 9.1: Hydrogen bonds of S-ethyl N-(2,2,2-trinitroethyl)thiocarbamate (**1**)

symmetry operation		distances [Å] und angels [°]	
i	x, 0.5–y, –0.5+z	H1–N4	0.880(2)
ii	x, 0.5–y, 0.5+z	H2–N8	0.881(2)
iii	1–x, 1–y, 1–z	H2A–C2	0.989(2)
		H2B–C2	0.990(2)
		H4A–C4	0.990(3)
		H7B–C7	0.990(2)
		H1···O7(i)	2.122(2)
		H2···O14(i)	1.957(2)
		H2A···S1(ii)	2.811(2)
		H4A···O3(ii)	2.520(2)
		H7B···O6(iii)	2.497(2)
		H2B···O10	2.418(2)
		C2···O10	3.109(3)
		C2···S1(ii)	3.769(2)
		C4···O3(ii)	3.449(4)
		C7···O6(iii)	3.430(3)
		N4···O7	2.883(2)
		N8···O14	2.826(2)
		C2–H2A···S1(ii)	163.3(1)
		C2–H2B···O10	126.4(1)
		C4–H4A···O3(ii)	156.2(2)
		C7–H7B···O6(iii)	156.9(1)
		N4–H1···O7(i)	144.4(1)
		N8–H2···O14(i)	168.9(1)

Table 9.2: Hydrogen bonds of 2,2,2-trinitroethyl 2,2,2-trinitroethylcarbamate (**2**)

symmetry operation		distances [Å] und angels [°]	
i	x, y, 1+z	H2A–C2	0.967(2)
ii	0.5+x, 1.5–y, 0.5+z	H2B–C2	0.970(1)
		H2A···O6(ii)	2.745(1)
		H2B···O5(i)	2.480(1)
		C2···O5(i)	3.350(2)
		C2···O6(ii)	3.092(2)
		C2–H2A···O6(ii)	101.8(1)
		C2–H2B···O5(i)	149.6(1)

Table 9.3: Hydrogen bonds of 2-fluoro-2,2-dinitroethyl 2,2,2-trinitroethylcarbamate (**3**)

symmetry operation		distances [Å] und angels [°]	
i	2–x, –y, 1–z	H2B–C2	0.991(2)
ii	1–x, –y, –z	H3–N4	0.880(2)
		H2B···O7(i)	2.379(2)
		H3···O9(iI)	2.338(2)
		C2···O7(i)	3.350(2)
		N4···O9(ii)	3.092(2)
		C2–H2B···O7(i)	140.2(1)
		N4–H3···O9(ii)	144.3(1)

Table 9.4: Hydrogen bonds of 2,2,2-trinitroethyl 2-fluoro-2,2-dinitroethylcarbamate (**4**)

symmetry operation		distances [Å] und angels [°]	
i	x, 0,5–y, 0.5+z	H1–N4	0.880(1)
ii	x, 0,5–y, –0.5+z	H2B–C2	0.990(2)
iii	X, –1+y, z	H4A–C4	0.990(2)
		H1···O8(i)	2.175(1)
		H2B···O5(ii)	2.470(1)
		H4A···O9(iii)	2.583(1)
		C2···O5(ii)	3.219(2)
		C4···O9(iii)	3.127(2)
		N4···O8(i)	3.050(2)
		C2–H2B···O5(ii)	132.1(1)
		C4–H4A···O9(iii)	114.58(9)
		N4–H1···O8(i)	172.74(9)

Table 9.5: Hydrogen bonds of 2-fluoro-2,2-dinitroethyl 2,2,2-trinitroethyl carbonate (**5**)

symmetry operation		distances [Å] und angels [°]	
i	–0.5+x, 1–y, –0.5+z	H2A–C2	0.991(3)
ii	0.5+x, 1–y, –0.5+z	H2B–C2	0.991(3)
iii	1+x, y, z	H4B–C4	0.990(3)
iv	–1+x, y, z		
		H2A···O5(i)	2.471(2)
		H2B···O4(iii)	2.391(2)
		H2B···O6(ii)	2.607(2)
		H4B···O10(iv)	2.597(3)
		C2···O4(iii)	3.296(3)
		C2···O5(i)	3.341(3)
		C2···O6(ii)	3.330(4)
		C4···O10(iv)	3.425(4)
		C2–H2A···O5(i)	146.4(2)
		C2–H2B···O4(iii)	151.5(2)
		C2–H2B···O6(ii)	129.9(2)
		C4–H4B···O10(iv)	141.3(2)

9.3 SUPPORTING INFORMATION FOR POLYNITRO CONTAINING ENERGETIC MATERIALS BASED ON CARBONYLDIISOCYANATE AND 2,2-DINITROPROPANE-1,3-DIOL

Selected weak improper hydrogen bonds for compound **1**–**3**.

The hydrogen atoms were located in a difference Fourier map and placed with a C–H distance of 0.99 Å for CH_2 groups.

Table 9.6: Hydrogen bonds of bis(2,2,2-trinitroethyl) carbonyl-N,N-dicarbamate (**1**)

symmetry operation		distances [Å] und angels [°]	
i	–1+x, y, z	H2A–C2	0.991(3)
ii	–1+x, 1+y, z	H2B–C2	0.990(4)
iii	1+x, –1+y, z	H6A–C6	0.990(3)
iv	1+x, y, z	H6B–C6	0.990(3)
v	1–x, 1–y, –z	H9A–C9	0.989(3)
vi	2–x, 1–y, –z	H13B–C13	0.991(2)
vii	x, –1+y, z	H16A–C16	0.990(4)
viii	x, 1+y, z	H16B–C16	0.990(4)
		H20–N4	0.74(4)
		H20A–C20	0.991(4)
		H20B–C20	0.990(3)
		H22–N12	0.75(4)
		H23–N13	0.83(3)
		H23A–C23	0.990(2)
		H23B–C23	0.990(3)
		H25–N21	0.83(3)
		H26–N28	0.67(3)
		H27A–C27	0.990(5)
		H27B–C27	0,991(4)
		H2A···O27	2.569(2)
		H2B···O20	2.497(4)
		H6A···O46	2.553(3)
		H6B···O25(iv)	2.432(2)
		H9A···O10(i)	2.250(2)
		H13B···O17	2.544(2)
		H13B···O18	2.551(3)
		H16A···O43(v)	2.605(3)
		H16B···O61(ii)	2.238(4)
		H20···O60	2.23(4)
		H20A···O63(viii)	2.444(5)
		H20B···O59(viii)	571(2)
		H22···O1	2.60(3)
		H23···O32(v)	2.35(3)
		H23···O43	2.51(4)
		H23A···O22(v)	2.454(3)
		H23A···O37(vii)	2.681(3)
		H23B···O44(vii)	2.620(2)
		H25···O26	2.14(3)
		H26···O9(vi)	2.27(3)
		H27A···O42(iii)	2.618(3)
		H27B···O33(iii)	2.555(2)

C2···O20	3.362(6)
C2···O27	3.409(3)
C6···O25(iv)	3.173(4)
C6···O46	3.326(5)
C9···O10(i)	3.230(3)
C13···O17	3.494(3)
C13···O18	2.971(5)
C16···O43(v)	3.514(5)
C16···O61(ii)	3.162(5)
C20···O59(viii)	3.469(3)
N4···O60	2.908(3)
C20···O63(viii)	3.407(6)
N12···O1	3.083(3)
N13···O32(v)	3.136(5)
N13···O43	3.032(3)
C23···O22(v)	3.182(4)
C23···O37(vii)	3.493(4)
C23···O44(vii)	3.486(3)
N21···O26	2.941(3)
N28···O9(vi)	2.893(3)
C27···O42(iii)	3.365(6)
C27···O33(iii)	3.348(5)
C2–H2A···O27	142.6(2)
C2–H2B···O20	145.8(2)
C6–H6A···O46	143.9(2)
C6–H6B···O25(iv)	131.2(2)
C9–H9A···O10(i)	170.7(2)
C13–H13B···O17	160.6(2)
C13–H13B···O18	105.4(2)
C16–H16A···O43(v)	152.6(2)
C16–H16B···O61(ii)	154.6(2)
N4–H20···O60	152(5)
C20–H20A···O63(viii)	163.8(2)
C20–H20B···O59(viii)	150.8(2)
N12–H22···O1	125(3)
N13–H23···O32(v)	133(3)
N13–H23···O43	139(3)
C23–H23A···O22(v)	130.0(2)
C23–H23A···O37(vii)	147.4(2)
C23–H23B···O44(vii)	146.1(2)
N21–H25···O26	156(4)
N28–H26···O9(vi)	156(4)
C27–H27A···O42(iii)	132.3(2)
C27–H27B···O33(iii)	136.9(2)

Table 9.7: Hydrogen bonds of bis(2-fluoro-2,2-diinitroethyl) carbonyl-N,N-dicarbamate (**2**)

symmetry operation		distances [Å] und angels [°]	
i	–x, 1–y, 1–z	H2–N4	0.76(4)
ii	–1+x, y, z	H2A–C2	0.990(3)
iii	2–x, 2–y, 2–z	H2B–C2	0.989(3)
iv	1–x, 1–y, 1–z	H6A–C6	0.990(3)
v	x, y, 1+z	H6B–C6	0.990(3)
		H2···O7(iii)	2.10(4)
		H2A···O6(ii)	2.467(2)
		H2B···O11(v)	2.531(3)
		H6A···O3(i)	2.571(3)
		H6B···O10(iv)	2.605(3)
		C2···O6(ii)	3.455(4)
		C2···O11(v)	3.361(4)
		C6···O3(i)	3.420(4)
		C6···O10(iv)	3.481(4)
		N4···O7(iii)	3.847(4)
		C2–H2A···O6(ii)	176.7(2)
		C2–H2B···O11(v)	141.4(2)
		C6–H6A···O3(i)	144.8(2)
		C6–H6B···O10(iv)	147.5(2)
		N4–H2···O7(iii)	167(4)

Table 9.8: Hydrogen bonds of 2,2-dinitropropane-1,3-diyl bis(2,2,2-trinitroethylcarbamate) (**3**)

symmetry operation		distances [Å] und angels [°]	
i	–1+x, y, z	H2A–C2	0.990(2)
ii	–x, –y, –z	H2B–C2	0.990(2)
iii	1–x, –y, –z	H3–N4	0.85(3)
iv	1+x, y, z	H4B–C4	0.990(3)
v	–x, 1–y, –z	H6A–C6	0.990(3)
		H6B–C6	0.990(3)
		H8A–C8	0.990(2)
		H8B–C8	0.990(2)
		H2A···O1(i)	2.469(2)
		H2A···O10(ii)	2.620(3)
		H2B···O14(iii)	2.375(2)
		H3···O15(v)	2.28(3)
		H4B···O7(iii)	2.546(2)
		H6A···O7(iii)	2.451(2)
		H6B···O11(iv)	2.559(2)
		H8A···O4(iii)	2.503(2)
		H8B···O3(ii)	2.595(2)
		H8B···O20(i)	2.490(3)
		C2···O1(i)	3.386(3)
		C2···O10(ii)	3.044(4)
		C2···O14(iii)	3.252(3)
		N4···O15(v)	3.113(3)
		C4···O7(iii)	3.300(4)
		C6···O7(iii)	3.246(4)
		C6···O11(iv)	3.368(3)
		C8···O4(iii)	3.463(3)
		C8···O3(ii)	3.122(3)
		C8···O20(i)	3.438(3)
		C2–H2A···O1(i)	154.1(1)
		C2–H2A···O10(ii)	105.9(2)
		C2–H2B···O14(iii)	147.3(1)
		N4–H3···O15(v)	167(3)
		C4–H4B···O7(iii)	132.8(2)
		C6–H6A···O7(iii)	136.9(2)
		C6–H6B···O11(iv)	138.8(2)
		C8–H8A···O4(iii)	163.1(2)
		C8–H8B···O3(ii)	113.3(2)
		C8–H8B···O20(i)	160.2(2)

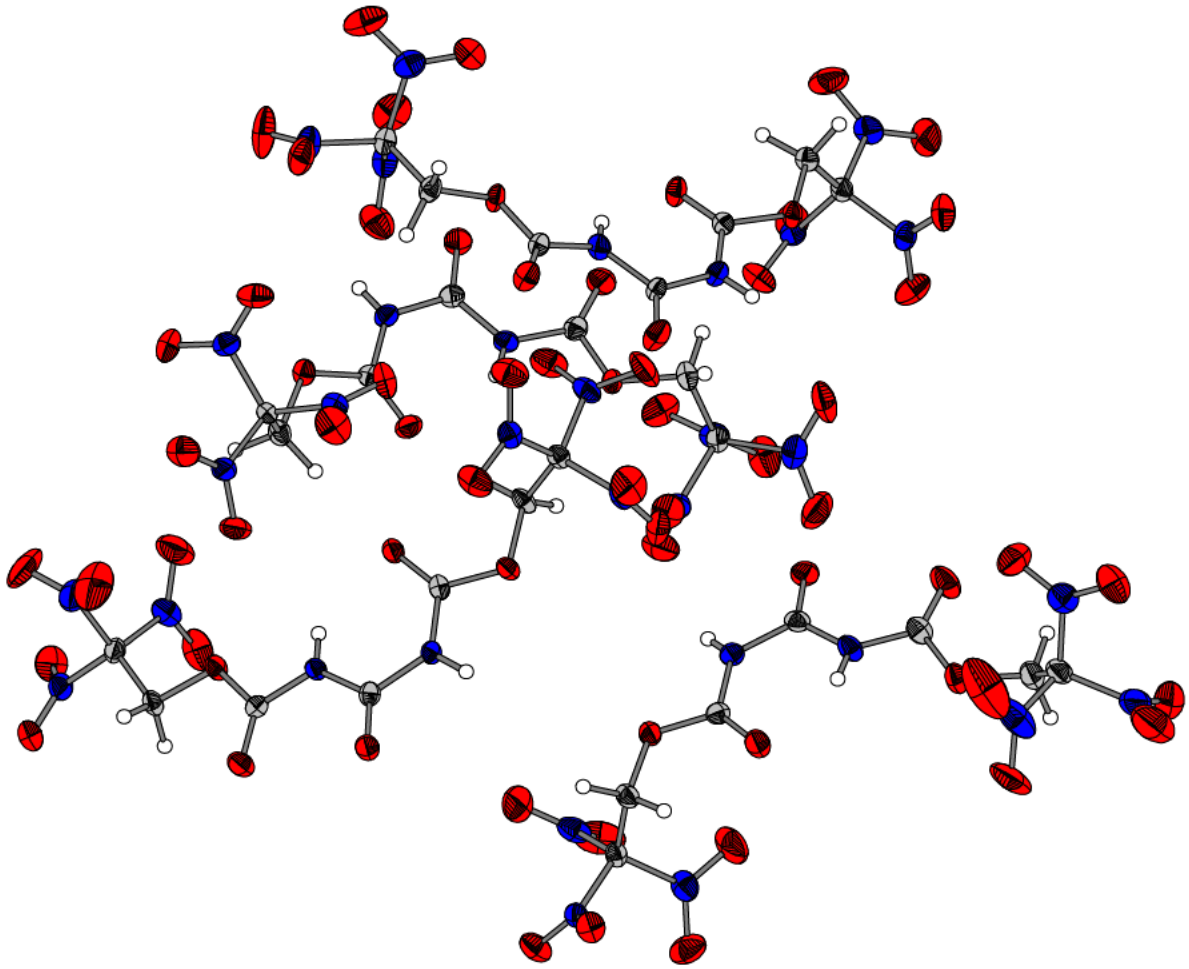

Figure 9.3. Molecular structure of Bis(2,2,2-trinitroethyl) carbonyl-N,N-dicarbamate (**1**). The complete asymmetric unit is displayed.

9.4 SUPPORTING INFORMATION FOR 2-FLUORO-2,2-DINITROETHYL 2,2,2-TRINITROETHYLNITRAMINE, A POSSIBLE HIGH ENERGY DENSE OXIDIZER

Selected weak improper hydrogen bonds for compounds **2** and **3.**

The hydrogen atoms were located in a difference Fourier map and placed with a C–H distance of 0.99 Å for CH_2 groups.

Table 9.9: Hydrogen bonds of 2-fluoro-2,2-dinitroethyl 2,2,2-trinitroethylamine (**2**)

symmetry operation		distances [Å] und angles [°]	
i	1–*x*, –*y*, 0.5+*z*	H2–N10	0.831(3)
ii	0.5–*x*, 0.5+*y*, 0.5+*z*	H2B–C2	0.991(2)
iii	*x*, –1+*y*, *z*	H3A–C3	0.989(2)
iv	1–*x*, –*y*, –0.5+*z*	H3B–C3	0.990(2)
v	0.5–*x*, 0.5+*y*, –0.5+*z*	H6A–C6	0.989(2)
vi	*x*, 1+*y*, *z*	H7A–C7	0.990(2)
		H7B–C7	0.991(2)
		H2···O10	2.588(3)
		H2B···O20(*i*)	2.485(2)
		H3A···O12(*ii*)	2.480(2)
		H3B···O4(*iii*)	2.364(2)
		H6A···O6(*iv*)	2.578(2)
		H6A···O7(*v*)	2.558(2)
		H7A···O14(*vi*)	2.463(2)
		H7B···O6(*iv*)	2.414(2)
		N10···O10	3.327(3)
		C2···O20(*i*)	3.260(3)
		C3···O12(*ii*)	3.457(3)
		C3···O4(*iii*)	3.155(3)
		C6··O6(*iv*)	3.483(3)
		C6···O7(*v*)	3.302(3)
		C7···O14(*vi*)	3.169(3)
		C7···O6(*iv*)	3.347(3)
		N10–H2···O10	148.8(1)
		C2–H2B···O20(*i*)	134.8(1)
		C3–H3A···O12(*ii*)	169.2(1)
		C3–H3B···O4(*iii*)	136.2(1)
		C6–H6A···O6(*iv*)	152.2(1)
		C6–H6A···O7(*v*)	131.9(1)
		C7–H7A···O14(*vi*)	127.9(1)
		C7–H7B···O6(*iv*)	156.9(1)

Table 9.10: Hydrogen bonds of 2-fluoro-2,2-dinitroethyl 2,2,2-trinitroethylnitramine (**3**)

symmetry operation		distances [Å] und angles [°]	
i	–0.5+*x*, –0.5–*y*, *z*	H2A–C2	0.990(2)
ii	0.5–*x*, –0.5+*y*, 0.5+*z*	H3A–C3	0.990(2)
		H2A···O11(*i*)	2.543(2)
		H3A···O2(*ii*)	2.482(1)
		C2···O11(*i*)	3.373(2)
		C3···O2(*ii*)	3.179(2)
		C2–H2A···O11(*i*)	141.2(1)
		C3–H3A···O2(*ii*)	127.1(1)

Additionally a short dipolar N···O interaction was observed between the nitramine nitrogen N4 with oxygen O4 of a neighbored nitro group. The distance N4···O4 with 2.912(2) Å is shorter than sum of the VAN DER WAALS radii of nitrogen and oxygen (3.07 Å).[a]

a. Bondi, *J. Phys. Chem.* **1964**, 68, 441.